Characterization of apoptosis induced by BH3-containing hepatitis B virus proteins

Lu, Yi Wei

2007

Lu, Y. W. (2007). Characterization of apoptosis induced by BH3-containing hepatitis B virus proteins. Doctoral thesis, Nanyang Technological University, Singapore.

https://hdl.handle.net/10356/35759

https://doi.org/10.32657/10356/35759

Characterization of Apoptosis Induced by BH3-Containing Hepatitis B Virus Proteins

Lu Yi Wei

School of Biological Sciences

A thesis submitted to the Nanyang Technological University
in fulfilment of the requirement for the degree of Ph.D

2007

To my family and friends

Acknowledgements

I would like to express my sincere appreciation to my supervisor A/P W.N. William Chen, for his continuous guidance, enthusiasm, inspiration and great efforts to explain things clearly. Through out my thesis writing period, he provided encouragement, advice, good teaching, lots of good ideas and prompt help. I would have been lost without him.

I gratefully acknowledge the financial support of the Nanyang Technological University, without which I could not have undertaken this study.

I am grateful to my colleagues for their support during the time we shared there, particularly: Dr. Lee PengFu for teaching and fruitful discussions, Mr. Tan TuanLin for his useful advice, and Mr. Sui JianJun and Mr.s PanHong for their kind help.

I am grateful to my family and friends for their support and understand at my frequent non-attendance on so many occasions.

Finally, but not least, I would like to thank my parents and my wife. They support me, teach me and love me. To them, I dedicate this thesis!

Abstract

CHARACTERIZATION OF APOPTOSIS INDUCED BY BH3-CONTAINING HEPATITIS B VIRUS PROTEINS

Lu YiWei
SBS, NTU, Singapore

2006
Submitted for the degree of D.Phil

The smallest protein of hepatitis B virus (HBV), HBx, has been implicated in the development of liver diseases by interfering with normal cellular progresses. Its role in cell proliferation has been unclear as both pro-apoptotic and anti-apoptotic activities have been reported. We showed molecular evidence that HBx induced apoptosis in HepG2 cells. A Bcl-2 Homology Domain 3 (BH3) was identified in HBx, which interacted with anti-apoptotic but not pro-apoptotic members of the Bcl-2 family of proteins. HBx induced apoptosis when transfected into HepG2 cells, as demonstrated by both flow cytometry and caspase-3 activity. However, HBx protein may not be stable in apoptotic cells triggered by its own expression as only its mRNA or the fusion protein with the glutathione-S-transferase was detected in transfected cells. These results suggested that HBx behaved as a pro-apoptotic protein and was able to induce apoptosis.

Similar BH3 motif was also identified in HBSP, a spliced mRNA generated protein. We showed that transfection of mammalian cells with a replicative HBV genome caused extensive cytopathic effects, leading to the death of infected cells, while results from flow cytometry suggested that apoptosis played a major role in this HBV-induced cell death. HBSP is a spliced viral protein previously shown to be able to induce apoptosis and associated with HBV pathogenesis. HBSP expressed at early stage of our cell-based HBV replication. After transfection into HepG2 cells, HBSP leaded to apoptosis in a caspase-3 dependent manner. Further investigation by using HBSP mutant in BH3 abrogated the apoptotic effects caused by HBSP. A deletion, the POL-N containing the BH3 remained the ability to induce apoptosis. Immunoprecipitation of the POL-N with HepG2 cell extracts identified an autophagy related protein which provided possibility involving the autophagic cell death.

Taken together, our results suggested a direct involvement of HBV viral proteins in cellular apoptosis and revealed the possible molecular mechanism through the BH3 domain.

Contents

Lu, Y. W., and Chen, W. N. (2005) Human hepatitis B virus X protein induces apoptosis in HepG2 cells: Role of BH3 domain. Biochem Bioph Res Co, *338*, 1551-1556.

Lu, Y. W., Tan, T. L, Vincent, C., and Chen, W. N. (2006) The HBSP gene is expressed during HBV replication, and its coded BH3-containing spliced viral protein induces apoptosis in HepG2 cells. Biochem Bioph Res Co, *351*, 64-70.

Tan, T. L., Feng, Z. Q., **Lu, Y. W.**, Vincent, C., and Chen, W. N. (2006) Adhesion Contact Kinetics of HepG2 Cells during Hepatitis B Virus Replication: Involvement of SH3-binding Motif in HBX. Biochem Bioph Acta, *1762*, 755-766.

Xu, J. L., Khor, K. A., **Lu, Y. W.**, Chen, W. N., and Kumar, R. (Under revision) Osteoblast Interactions with Various Hydroxyapatite Based Biomaterials Consolidated Using a Spark Plasma Sintering Technique.

Abbreviations

ATP	adenosine triphosphate
bp	base pair (s)
BSA	bovine serum albumin
cDNA	complementary DNA
dNTP	3'-deoxynucleotide triphosphate
dATP	3'-deoxyadenosine triphosphate
dCTP	3'-deoxycytidine triphosphate
dGTP	3'-deoxycytidine triphosphate
dTTP	3'-deoxythymidine triphosphate
DMSO	dimethyl sulphoxide
DNA	3'-deoxyribonucleic acid
DTT	dithiothreitol
ECL	enhanced chemiluminescence
EDTA	ethylene-diamine-tetraacetic acid
ELISA	enzyme linked immunosorbant assay
FACS	fluorescence activated cell sorting
FBS	fetal bovine serum
FCS	fetal calf serum
FITC	fluorescein isothiocyanate
h	hour (s)
HBV	hepatitis B virus

HEPES	N-[2-hydroxyethyl]piperazine-N'[2-ethanesulphonic acid]
IP	immunoprecipitation
kbp	kilobase pair (s)
kD	kilodaltons
mAb	monoclonal antibody
min	minute (s)
MOPS	3-[N-morphoplino]propanesulphonic acid
MTT	3-[4, 5dimethyliazol-2-yl]-2,5-diphenyltetrazolium bromide
OD	optical density
PAGE	polyacrylamide gel electrophoresis
PBS	phosphate buffered saline
PCR	polymerase chain reaction
PMFS	phenylmethysulphonyl fluoride
rpm	revolutions per minute
RT	room temperature
SD	standard deviation
SDS	sodium dodecyl sulphate
sec	second (s)
TEMED	N,N,N',N'-tetramethylethlenediamine
Tm	melting point
Tris	2-amino-2-(hydroxymethyl)-1,3-propanediol
UV	ultraviolet
v/v	volume per volume

w/v	weight per volume

The single letter and triplet codes for amino acid residues are used. Restriction enzymes are referred to by their three letter names. Other abbreviations are defined in the text when first used.

Chapter One: Introduction

1.1 INTRODUCTION

Viral infection remains one of the threats to human health. Besides the HIV, newly-emerged SARS-corona virus and avian influenza virus, the Hepatitis B virus (HBV) is all the time one of the threatening viruses (Zuckerman, 1999). HBV, the leading pathogen of hepatitis B, is a global health problem with vast infection and considerable morbidity. Despite significant progresses in vaccination and antiviral therapy development, over 400 million people are currently chronically infected, with 1~2 million death per year being directly caused as a consequence of the infection (Zuckerman, 1999; Blumberg *et al.*, 1975).

HBV is a double-stranded DNA virus with a circular genome composed of 3215 nucleotides (Carman *et al.*, 1993). It is the smallest virus infectious to human and usually leads to a wide range of liver diseases, including viral hepatitis and hepatocellular carcinoma (HCC). Viral hepatitis is characterized by an inflammatory reaction in the infected liver cells and is associated with cell damage and death (Lau *et al.*, 1998; Jaeschke *et al.*, 2002). On the other hand, inhibition of cell death and uncontrolled cell growth has been shown to be present in HCC (Natoli *et al.*, 1995; Higaki *et al.*, 1996). Cell death is therefore a key modulator for the outcome of HBV infection. Apoptosis, one of the typical processes of cell death, is considered to be mechanism of host defense against viral infections (Baell *et al.*, 2002). In the counteraction against host immune system, viruses have evolved strategies to either

prevent or promote apoptosis in order to maximize the production of virus progeny and facilitate their spread to neighboring cells. The roles of two HBV viral proteins, HBV X protein (HBx) and HBV splice-generated protein (HBSP), in regulating apoptosis were investigated. In the case of HBx, evidence has suggested its importance in regulating gene expression and development of apoptosis-related affairs in infected liver cells. However, both transforming ability and pro-apoptosis events were reported, leaving the role of HBx still controversial (Chen *et al.*, 2000; Takada *et al.*, 1999; Rakotomahanina *et al.*, 1994; Soussan *et al.*, 1999). HBSP, an RNA splice-generated protein, was reported to be associated with viral replication and liver fibrosis. Furthermore, it was also suggested to induce apoptosis in liver or liver cancer derived cell line (Soussan *et al.*, 2000; Soussan *et al.*, 2003). Thus, the study of HBx and HBSP in apoptosis was carried out in this study.

1.2 MOLECULAR VIROLOGY OF HBV

Hepatitis B is caused in humans by HBV. The viral hepatitis is commonly characterized by jaundice on the skin and in eyes, malaise, loss of appetite, right upper quadrant pain, and raised serum levels of liver enzymes, aspartate aminotransferase (AST) and alanine aminotransferase (ALT) (Viral hepatitis prevention board, 1997). Chronic HBV infection can lead to chronic hepatitis, cirrhosis, and even HCC. HBV belongs to genus *orthohepadnavirus*, family *Hepadnaviridae*. It is a virus with high affinity towards liver cells (Purcell *et al.*, 1994). As the pathogen of hepatitis B, HBV was so far known to cause cell damage in infected liver. However, this is not directly caused by the viral proteins (Alexander,

1990). Instead, infected hepatocytes are attacked and killed by the immune system, especially in a cytotoxic T cell (CTL) dependent way. Clinical symptoms therefore reflected to a large extent the influence of the immune mechanism of the host (Chisari and Ferrari, 1995; Grob, 1995; Grob, 1998).

During the course of chronic infection, three types of viral particles can be found in human serum (Pugh and Bassendine, 1990). Complete and infectious viron, initially named as Dane particles, has a size of 42 nm in diameter (Dane *et al.*, 1970). This viron has an outer envelope and an inner core particle containing viral DNA. Incomplete viral particles can exist in two forms: spherical viral particles with diameter of 20 nm and tubular forms of variable length. These two particles do not contain viral genome DNA and thus are unable to infect other liver cells (Verheyen *et al.*, 1998).

1.2.1 Genotypes and Serotypes

Genotype is generally defined as the constitution of the genetic information of an organism or cell while serotype is defined as components that can be separated by serological characterization. In the case of HBV, a number of serotypes have been described. The existence of the common *a* determinant of HBsAg and the two mutually exclusive determinants, *d* or *y*, and *w* or *r*, lead to various combinations: *adw, adr, ayw,* and *ayr.* They are distributed differentially around the world and thus are evaluated as epidemiology markers (Grob, 1998). Genetic analysis has, however, revealed these mentioned serotypes do not correspond with single genotype (Grob,

1998; Ohba *et al.*, 1995). At present, eight HBV genotypes (A-H) and nine serotypes have been defined (Hideaki, 2004). The *a* determinant is of the greatest importance since it is the dominant epitope cluster. Besides, it is also highly conserved among all the HBV serotypes (Magnius and Norder, 1995).

The *a* determinant is localized in the major hydrophilic region (MHR) of HBsAg. Its tertiary structure was shown to be important for the viral antigenicity. It consists of 23 amino acids, from 124 and 147, forms two loops that are exposed to the outside environment from the envelope of the virus (Carman *et al.*, 1990). Most antibodies derived from vaccines recognize nine amino acids of *a* determinant, from 139 to 147. On the other hand, aa 120-124 was reported to interfere with aa 139-147. As a consequence, antibodies used in routine diagnosis are raised against HBsAg *a* determinant (Carman *et al.*, 1997).

1.2.2 Viral Genetics

HBV is the only DNA virus among the human hepatitis viruses. It is the smallest DNA virus infectious to people (Carman *et al.*, 1993). The circular DNA genome is not completely but partly double-stranded (ds). Once entered in the liver cells the single-stranded DNA is synthesized to ds before viral replication by the viral DNA polymerase (Sumers *et al.*, 1975; Kaplan *et al.*, 1973). During the replication, a full length plus-strand RNA intermediate (pregenome) is transcribed using the minus-strand DNA as template (Feiteson, 1994). Subsequently, the minus-stand HBV DNA genome is reversely transcribed from the RNA intermediate by the viral

polymerase. In this process, the HBV behaves like a retrovirus (Lee, 1997). The pregenomic RNA also serves as templates for translation of some other viral proteins, as shown in figure1.1 (Pugh and Bassendine, 1990).

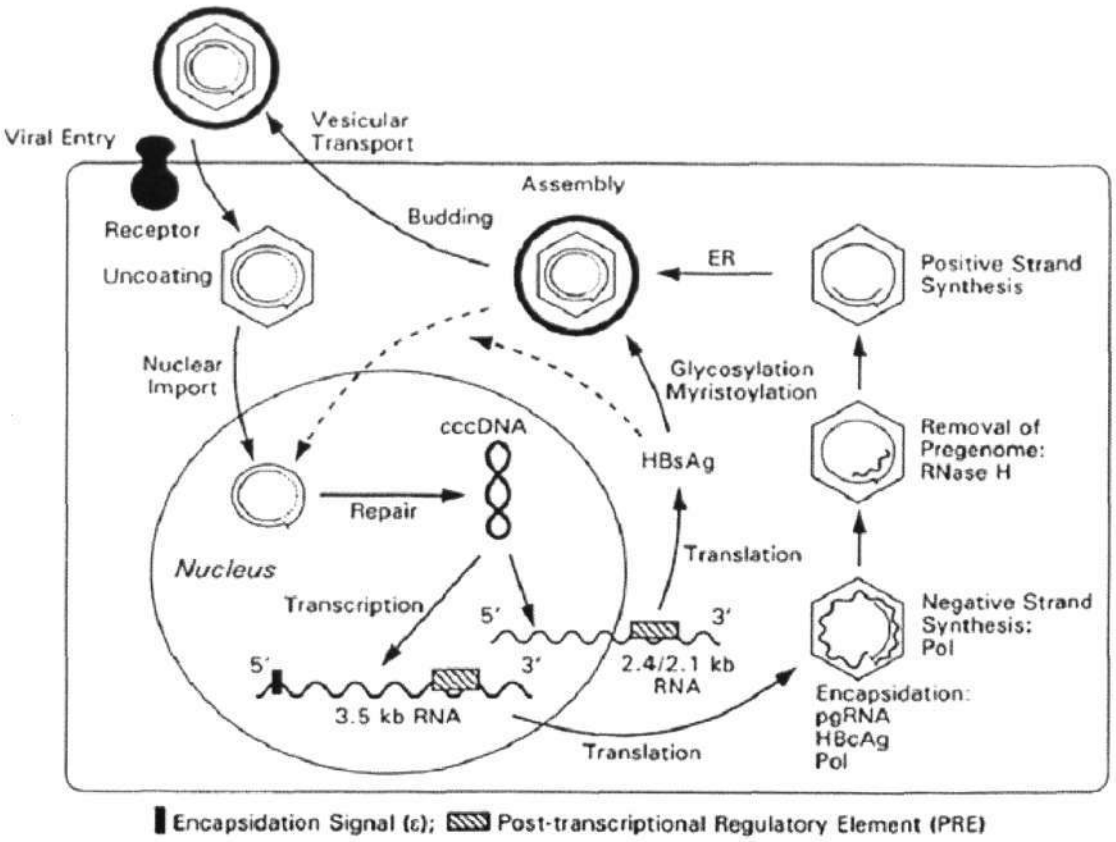

------cited from *L.Johnson et al., 1998*

Figure 1.1: HBV life cycle. Replication cycle is discussed in the text. During initiation of infection the viral genome is converted into cccDNA. The cccDNA is template for transcription of all viral mRNAs. The 3.5kb pregenome is the mRNA for core protein and the viral polymerase. The polymerase binds to the 5' end of its own mRNA template, and they are packaged into nucleocapsids. When the double-stranded DNA is produced, nucleocapsids acquire an outer envelope in the ER. Some of these nucleocapsids migrate to the nucleus to serve as cccDNA. Accumulation of viral envelope proteins reversely inhibits excessive cccDNA formation.

The viral genome consists of different translation start sites (ATG) and forms four overlapping open reading frames (ORFs), as shown in Fig 1.2. They are defined as surface (S), core (C), polymerase (P), and HBx (X) genes (Lee, 1997). The P gene is

the longest and encodes the viral polymerase. The S gene is completely located in P gene, albeit at a different reading frame. PreS1-PreS2-S encodes large (L), middle (M), and small (S) HBsAg degressively. The core protein serving as viral nucleocapsid is encoded by C gene. A by-product E antigen (HBeAg) is encoded by Pre-C and C genes which are in frame and share the same promoter. The smallest X gene encodes the HBx (Seeger and Mason, 2002).

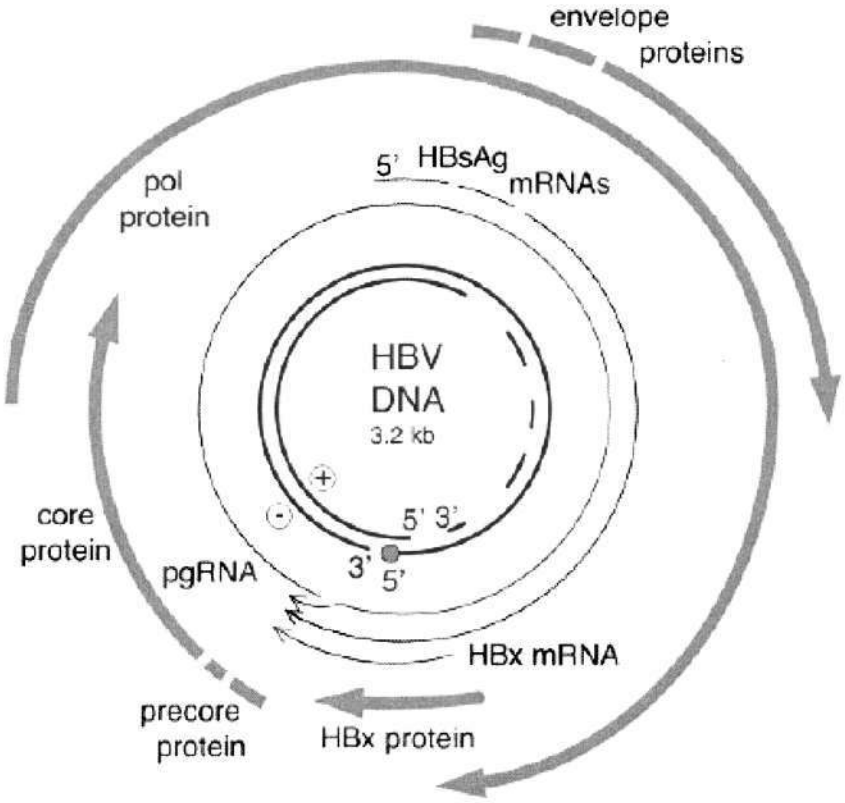

------cited from M.J.Bouchard *et al., (J.Virology, 2004)*

Figure 1.2: A diagrammatic representation of the HBV genome. The inner circle represents the virion genomic DNA that is packaged within viral particles in the cytoplasm of infected cells, and the dashes indicate the region of the genome which is incompletely synthesized. The thick arrows represent open reading frames corresponding to core, envelope (surface antigen), polymerase (POL), and HBx proteins. The thin lines represent HBV RNAs.

1.2.3 Life Cycle

The life cycle of HBV is characterized by the synthesis of its viral genome. The synthesis involves in a reverse transcription process through the viral polymerase which also displays an RNA reverse transcriptase activity (Figure 1.1). The mechanism of reverse transcription has been well characterized through genetic and biochemical studies as well (Ganem *et al.*, 1994). On the contrary, early events of the viral life cycle, including entry into cells, uncoating of nucleocapsids, and delivery of the viral genome into the cell nucleus, is not well understood currently.

1.2.3.1 Attachment

Hepatocytes or liver cells are the primary cell type for HBV infection. Similarity to other viruses is believed that this specificity is due to the existence hepatocyte-specific receptor. In fact, a variety of studies suggested a selectivity of the virus in only a few specific cell types (Jilbert *et al.*, 1987; Tagawa *et al.*, 1987). But by far the receptor has not been identified, thus the study on early steps of its life cycle remains limited. Although HBV is a robust infective pathogen to human, due to the absence of specific receptor, tissue culture cells are curiously unsensible to HBV infection (Gripon *et al.*, 2002; Cooper A *et al.*, 2003). There are many reports describing the early stages of Duck HBV (DHBV) because a tissue culture system has been established for DHBV infection. However, the information from research in DHBV attachment and entry might not be relevant to HBV due to the fact that the human HBV envelop polypeptides are N-glycosylated whereas the DHBV envelop polypeptides are non-N-glycosylated.

The HBV surface protein antigens (HBsAg) are composed of three proteins. They are L, M, and S HBsAg (Stibbe and Gerlich, 1983). They are encoded by the PreS1-PreS2-S gene in frame from N-terminus degressively as shown in Figure 1.3 (Heermann *et al.*, 1984). They played different roles in the viral intake and release.

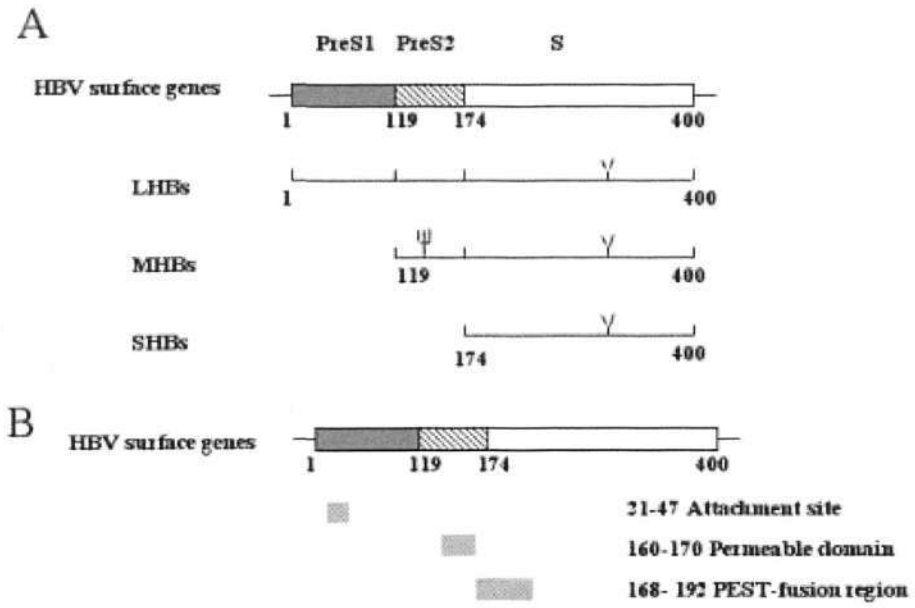

------*adapted from T. Block et al., 2004*

Figure 1.3: Schematic representation of HBsAg composition. HBV surface gene encodes proteins, the L, M, and S proteins. They share the same C-terminus but differ in N-terminus (A). aa 121-47 was critical for the viral attachment to host cell.

The LHBsAg has been suggested in viral attachment to liver cells (Glebe *et al.*, 2003). The attachment site was defined within in the PreS1 by anti-PreS1 antibody which prevented the viral infection to liver cells (Neurath *et al.*, 1986; Neurath *et al.*, 1989). The attachment site was more precisely described to be aa 21-47 in Pre-S1 from synthetic peptides study (Figure 1.3) (Paran *et al.*, 2001). Moreover, the QLDPAF sequence within this region was found to be crucial for viral attachment (Paran *et al.*,

2001). The involvement of MHBsAg in the viral infection has not been clear (Ferholz *et al.*, 1993; Pollicino *et al.*, 1997).

SHBsAg is the most abundant portion in surface proteins (Bruss and Ganem, 1991). SHBsAg was proved able to bind specifically to several human cells instead of other species cells (Leenders *et al.*, 1990). Furthermore, the SHBsAg was sufficient to bind to and be internalized into liver cells by endocytosis (Bruin *et al.*, 1995).

1.2.3.2 The receptor

In fact the exact receptor for HBV attachment is still unclear. Gp180 was the first discovered promising receptor which could be co-precipitated by DHBV (Kuroki *et al.*, 1994; Kuroki *et al.*, 1995). It was further identified to be the carboxypeptidase D which also exists in human hepatocyte (Li *et al.*, 1996). Despite the precise preS1 as the attachment site was verified, the exact receptor for HBV binding was not found. Non-infectable liver cell lines and limited availability of primary liver cells are the major problems (Petit *et al.*, 1992). There are some unconvincing results claiming as the receptor. However, the full understanding of the HBV attachment and its receptors could not be fulfilled unless a successful system or model established for researching and testing.

1.2.3.3 Fusion and proteolysis

Following the viral attachment is the host cell in-take involving fusion and proteolysis. Viral fusion is dependent on fusion motif which is normally composed of

hydrophobic amino acids (Gerlich *et al.*, 1993; Hughson, 1995). HBV was reported to contain a conservative region LFLGLLAG in its N-terminus of S protein, (Gerlich *et al.*, 1993; Lu *et al.*, 1996; Jason and Scheller, 1997; White, 1992). The fusogenic ability of this sequence was confirmed by using synthesized peptides to induce the fusion of bio-membranes *in vitro* (Rodriguez *et al.*, 1999).

1.2.3.4 Internalization

Most knowledge about HBV internalization is from investigation on DHBV. Normally there are two kind of methods by which viruses enter host cell. One is direct fusion with the host cell membrane, the other is endocytosis. DHBV was proved to enter host cell by endocytosis (Breiner and Schaller, 2000).

As for HBV, the study was based on HepG2 cells which were somehow different with primary hepatocytes. HepG2 is capable of supporting viral replication but refractory to infection. It has been proved HBV is uptaken by endocytosis in liver cells (Qiao *et al.*, 1994).

1.2.3.5 cccDNA formation

Following the internalization, the viral genome converts to covalently-closed-circular DNA (cccDNA) and starts to replicate. The partial ds DNA is firstly repaired to be complete ds DNA by the viral polymerase (Moraleda *et al.*, 1997). Inevitably, the host cellular DNA repair may also contribute to this process. The cccDNA thus serves as template for replication and the transcription of all the viral mRNAs.

1.2.3.6 Gene expression

There are totally 4 viral mRNA transcribed as shown in figure 1.4.

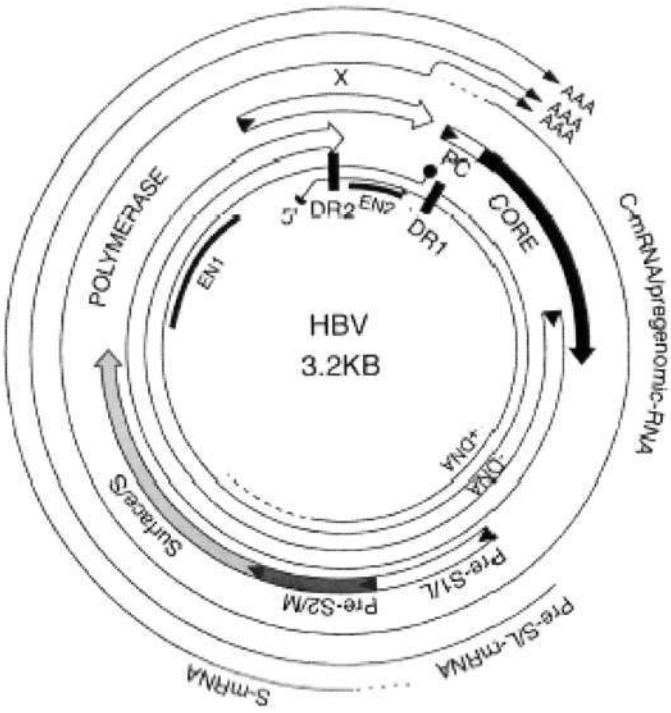

------adapted from *C.Seeger et al., (Microbiol. Mol. Biol Rev, 2000)*

Figure 1.4: Gene map of HBV. The inner circle represents the rcDNA. The direct repeats, DR1 and DR2, as well as the enhancers, EN1 and EN2, are indicated. The outer circle shows the 3.5kb pregenomic mRNA, 2.4kb, 2.1kb mRNA, and the 0.8kb mRNA. The four ORFs are shown in the middle.

The control of gene expression was first emphasized to define or analyse their promoters and enhancers. There are two enhancers and four promoters in HBV. They have been obtained primarily by expression studies in liver derived cell lines. For the 3.5kb pregenomic RNA and 2.4kb mRNA, a positive effect of transcription sequence (PET) was reported to control their normal transcription (Huang *et al.*, 1994). Another regulating sequence, negative effecter of transcription (NET) was reported for

termination of the mRNA transcription (Beckel and Summers, 1997). Regulation of viral gene expression also occurs at translation level. The pregenomic RNA serves as template for both core protein and viral polymerase which starts at an AUG located in the core gene (Chang *e .al.*, 1989; Ou *et al.*, 1990). The expression of polymerase is much lower than core protein due to the distally located starting site. However, the ratio of core protein to polymerase at 240: 1 is enough for viral replication. Therefore, such regulation is reasonable (Bartenschlager and Schaller, 1992; Crowther *et al.*, 1994).

1.2.3.7 Viral proteins

HBV genome encodes for seven proteins. The core protein is essential for nucleocapsids. Polymerase is necessary for viral DNA replication. Three surface proteins are major component of viral envelope. Another two proteins expressed during natural infection are HBx and HBeAg. HBeAg is not necessary for *in vivo* infection (Yaginuma *et al.*, 1987; Blum *et al.*, 1992). HBx is required of infection *in vivo* but dispensable for virus replication (Chen *et al.*, 1993; Zoulim *et al.*, 1994). Besides, HBx is involved in cellular signal transmitting and apoptosis.

The core protein forms dimmer before the assembly of icosahedral viral nucleocapsid (Chang *et al.*, 1994). The structure of core protein was resolved by X-ray crystallography (Wynne *et al.*, 1999) which indicated the protein was folded into four α-helices. The structure revealed regions necessary for dimmerization of core monomers (Konig *et al.*, 1998; Zlotnick *et al.*, 1998).

The polymerase which is translated from pregenomic mRNA consists of four major domains. The N-terminal domain, termed as terminal protein (TP) plays an important role in the packaging of pregenomic mRNA and priming of minus strand DNA. The domain following TP is the Spacer which separates the TP and the third domain Polymerase. The polymerase is a multifunction protein serving as reverse transcriptase, DNA polymerase. It is the most important protein involved in viral replication. The C-terminal domain is Rnase H domain and digests pregenomic mRNA when the reverse transcriptation completes.

HBV expresses three envelope components, the L, M, and S HBsAg. All the three envelope components are glycosylated, type II transmembrane proteins. They are major component of viral envelope. As a indicator, they can accumulate to a very high concentration in the serum of patients. Antibodies to S protein are sufficient to protect against HBV infection.

The unique regulatory protein HBx is a multi-functional protein. With diverse involvement in various aspects of cellular processes, HBx and a spliced generated protein HBSP will be discussed in detail in the following text.

1.2.3.7 Assembly and reverse transcription

Based on genetic experiments, it has been inferred that translation of the polymerase and packaging of pregenomic mRNA into viral nucleocapsids are tightly relevant, the

polymerase is esentitial for pgRNA package happening (Bartenschlager *et al.*, 1990; Hirsch *et al.*, 1990; Junker *et al.*, 1990). It was discovered that reverse transcriptase is required for RNA packaging and the packaging occurs in *cis*. It is now well understood that the polymerase triggers the packaging by binding to a RNA stem-loop structure named epsilon at the 5' end of pgRNA (Pollack and Ganem, 1993; Wang *et al.*, 1994) (figure 1.5). Epsilon is also important in DNA synthesis acting as a RNA primer (Lanford *et al.*, 1995; Tavis and Ganem, 1993; Wang and Seeger, 1992). The DNA synthesis starts at the Epsilon (Pollack and Ganem, 1994; Wang and Seeger, 1993). The reaction only synthesizes four nucleotides as primer before termination, then it transferred the nascent DNA from epsilon to the 3' end of the pgRNA to bind to their complementary sequence (Fig 1.5). Due to the lack of information about conformation of the nucleic acids and polymerase inside the core particles, the mechanism of this transfer remains unclear. Following the complementary sequence, the DNA primer, the minus strand is synthesized later on by the polymerase.

Like the minus-strand priming, the plus-strand priming is also involved in a transfer reaction. In contrast to a DNA primer, an RNA primer is involved (Seeger *et al.*, 1986). The RNA primer is probably the remaining segment of the pgRNA when it is being digested by Rnase H activity of the polymerase. The RNA primer is annealed to its complementary sequences at the acceptor site (figure 1.5). Following the normal synthesis, the plus-stranded DNA is synthesized. However, it is shorter than the minus-strand due to the length occupied by the RNA primer. This process produces a genome with two modified 5' ends and an incomplete plus-strand DNA.

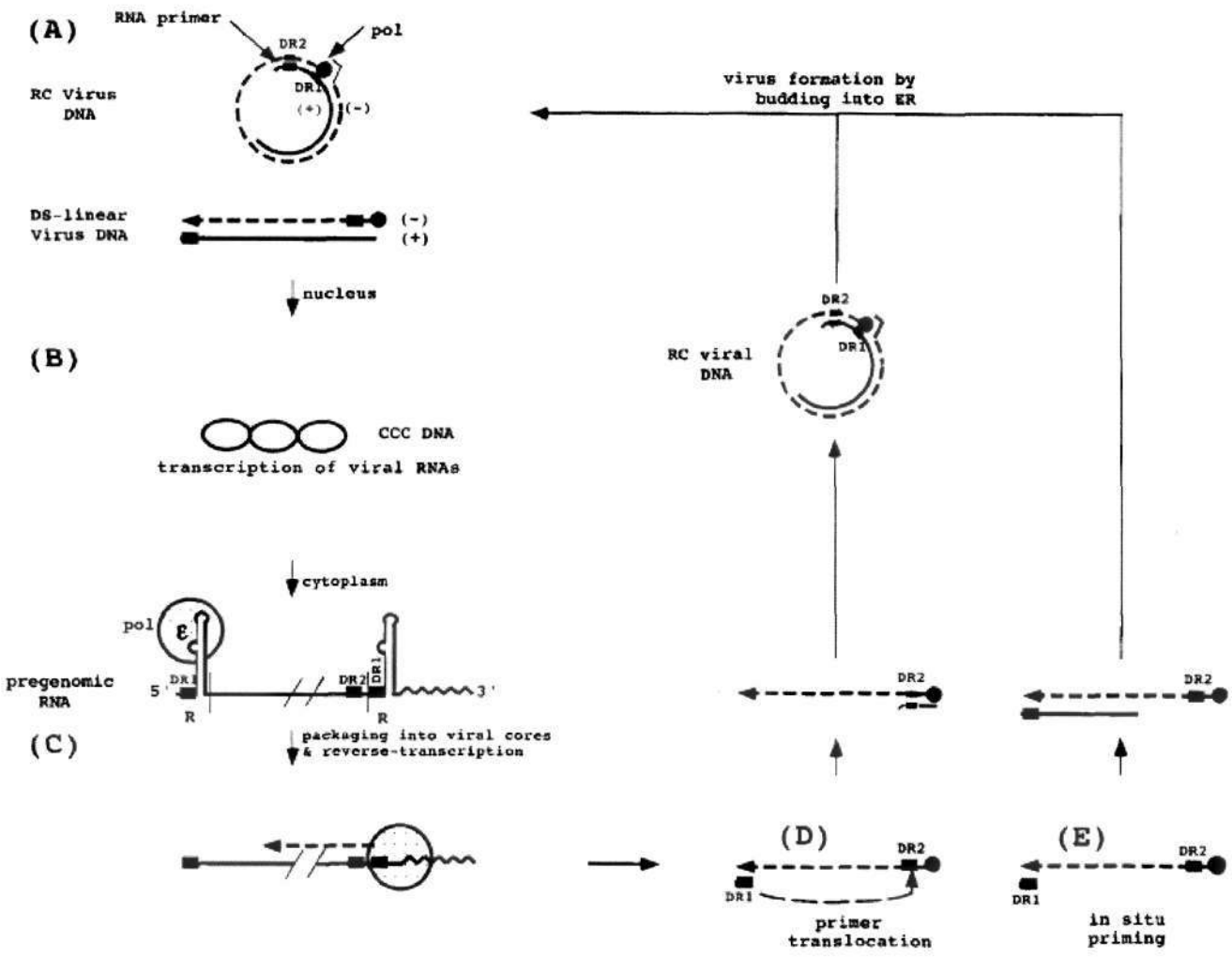

------adapted from *C.Seeger et al., (Microbiol. Mol. Biol Rev, 2000)*

Figure 1.5: HBV DNA replication. (A) Virus particles contain predominantly DNA with a complete minus strand and a partial plus strand. (B) During initiation of infection, viral DNA is converted to cccDNA which serves as template. The polymerase binds to the epsilon structure near the 5' end of its own mRNA to initiate reverse transcription with a protein primer, utilizing a tyrosine located near the N-terminus of the polymerase. (C) Following the synthesis of 4 bases, the polymerase moves to the 3' end of the RNA template, where the 4 bases can anneal with complementary sequences. (D) The remaining fragment from Rnase digestion serves as the primer for plus-strand synthesis. A third translocation occurs when the plus strand reaches the 5' end of the minus strand. The plus strand is not completed prior to virion release; a repair reaction to produce a fully double stranded DNA occurs during initiation of a subsequent round of infection. (E) A fraction of the virion has linear genomes because priming of plus-strand DNA synthesis occurs in the absence of primer translocation.

1.2.3.8 cccDNA amplification and virus production

The regulation of cccDNA synthesis is one of the most intriguing steps during the HBV replication cycle. Cytoplasmic rcDNA is much higher that cccDNA during the DHBV infection. Amplification of cccDNA takes place in the first few days following viral infection (Tuttleman *et al.*, 1986; Summers *et al.*, 1990; Summers *et al.*, 1991). The overwhelming accumulation of cccDNA could lead to a toxic level in infect cells in the absence of envelope proteins (Summers *et al.*, 1991; Lenhoff *et al.*, 1998). Thus, envelope proteins are quite possible to regulate the cccDNA synthesis. There is a direct indication that the cccDNA amplification occurs when the envelope proteins are in low concentration. Once the surface proteins increase in concentration, core particles containing cccDNA bind to surface proteins and the mature viron is secreted. But the exact molecular signals between the core protein and surface proteins remain unknown. The phosphorylation of core proteins may play a role in this interaction (Pugh *et al.*, 1989). The core particles bind to surface proteins and get across the ER membrane. Enveloped core particles are proved to transport to the Golgi complex (Huovila *et al.*, 1992) where some modification take place. When the assembly completes, the mature virions are secreted into the bloodstream and start a new lifecycle.

1.3 HBV INFECTION AND APOPTOSIS

HBV infection is closely associated with liver diseases worldwide, including viral hepatitis and hepatocellular carcinoma (HCC). Viral hepatitis is a kind of inflammation in infected liver cells and is characterized by cell damage and death

(Lau *et al.*, 1998). Epidemiological study has also revealed a relationship between persistent HBV infection and the development of HCC (Hearath *et al.*, 2006). In the case of HCC, inhibition of cell death and uncontrolled cell growth has been reported (Motola-Kuba *et al.*, 2006). Thus cell death is a key modulator for the outcome of HBV infection.

Apoptosis is commonly known as programmed cell death (Adams and Cory, 1998). It is widely accepted that apoptosis is one key mechanism of host defense against viral infection during which a CTL-related effect is involved (Baell and Huang, 1998). Thus, the early response will interrupt viral replication by eliminating infected cells before the viron matures. On the other hand, to counteract the host defense, viruses have developed strategies to delay apoptosis such that they could complete replication process, produce viral progeny, and promote spreading to healthy host cells.

In the case of HBV, a lot of research findings have suggested a role of Fas ligand and HBx protein in development of hepatitis (Kondo *et al.*, 1997; Hayashi *et al.*, 1999; Schneider *et al.*, 1997; Chirillo *et al.*, 1997). Recent reports also pointed to the involvement of the mitochondria-dependent apoptotic pathway which is governed by the Bcl-2 family of proteins in the development of liver diseases (Chen et *al.*, 1997; Ehrmann *et al.*, 2000). The role of HBx in the Bcl-2 mediated apoptotic pathway might give an explanation (Tanaka *et al.*, 1999; Schuster *et al.*, 2000; Pollicino *et al.*, 1998). However, little is known on the viral proteins in this pathway at molecular level.

Characterizing the Bcl-2 mediated apoptosis in HBV-related hepatitis lies in the fact that viral proteins might either block or induce apoptosis. Delay of apoptosis would leads to the virus survival, whereas induction of apoptosis by viral proteins might result in spread of infectious viral particles in apoptotic bodies (membraned small vesicles after the cell undergoes apoptosis). Actually it is known that some viruses also induce apoptosis in host cell at late stages of their infection (Teodoro *et al.*, 1997). The spreading of viral particles in apoptotic bodies helps them to escape host immune response as well as protecting these hidden virus particles from host antibodies.

In the last two decades, understanding of the mechanism of apoptosis involved in liver diseases has dramatically increased. Increasing evidence suggested that liver cell apoptosis can be induced by viral proteins. (Nayashi *et al.*, 1999). CTL and Fas system-mediated apoptosis was indicated as one of the major mechanisms (Kondo *et al.*, 1997). The HBx was also suggested to play an important role in the apoptosis (Chen *et al.*, 2001). In the case of HCC, a down-regulated apoptosis was observed (Wang *et al.*, 2004). That includes decreased Fas expression, defect in caspase expression, and tolerance to p53 gene regulation (Shin *et al.*, 1998; Alshatwi *et al.*, 2006).

1.3.1 Apoptosis in Viral Hepatitis

Viral hepatitis is known to be related to liver cell damage and cell loss. Apoptosis is

defined as a protection mechanism of host cells against viral infection (Teodoro and Branton, 1997). In viral hepatitis, this is believed to be effected by CTL and through Fas/FasL system as well (Smyth *et al.*, 1995; Lowin *et al.*, 1994; Kagi *et al.*, 1994). Cytokines such as tumor necrosis factor-alpha (TNF-α) may also be involved through TNF receptors. In acute hepatitis, portal and lobular inflammatory infiltration, liver cell degeneration and regeneration could be observed. In this progress, hepatocytes undergo two types of changes. The first is cytoplasm swelling and the second is formation of acidophilic hepatocytes. These acidophilic cells undergo fragmentation, a characteristic of apoptosis (Patel and Gores, 1995). It was reported that Fas was found to be expressed at high level on cell membrane during a study of fulminant hepatitis. Furthermore, DNA fragmentation by terminal transferase mediated dUTP-biotin nick end-labeling assay (TUNEL) was observed in cells undergoing these changes (Ryo *et la.*, 1995). These are all characteristic of apoptosis.

In chronic hepatitis the pathways involved in apoptosis induced in hepatocytes may include FasL/Fas, perforin/granzyme B, TNF, insulin-like growth factor-II (ILGF-II), and transforming growth factor-β1 (TGF-β1) (Patel *et al.*, 1995; Yang *et al.*, 1996). Further more, several other cellular pathways may be implicated (Williams and Smith, 1993). For example, a role of immune response was suggested based on clinical observation (Lau and Wright, 1993). There are a lot of data showing both CD4+ and CD8+ T lymphocytes are involved in the pathogenesis of chronic hepatitis B (Chisari, 1995; Chisari 1995). As for Fas/FasL, experiments in transgenic mice have revealed their role in the CTL-related apoptosis. Significant liver disease was

not seen which suggested that Fas is required for the CTL mediated apoptosis (Nakamoto *et al.*, 1997). In another study, FasL was shown to be important to induce hepatitis. Neutralization of FasL by Fas protects liver cells (Kondo *et al.*, 1997). Taken together, the Fas/FasL system is possible to be important in the CTL-mediated apoptosis.

On the other hand, TNF-α expression was shown to be higher in chronic HBV patient than healthy individuals (Sheron *et al.*, 1991; Fang *et al.*, 1996). In addition, the TNF-α receptor was also proved to be increased in hepatocytes in infected patients (Lau *et al.*, 1991). TNF-α has been shown to have antiviral activity and is able to induce apoptosis through receptor-mediated pathway (Fang *et al.*, 1996). Some cell lines containing replicating HBV were more sensitive to apoptosis induced by TNF-α than normal cells do (Guihot *et al.*, 1996), and the HBx was shown to regulate this process (Su *et al.*, 1997). Thus, TNF-α may play a role in contributing to apoptosis caused in HBV chronic infection.

The expression of TGF-β1 in liver has been shown to be increased in patients with chronic hepatitis B (Castrilla *et al.*, 1991). It is known to be a signal for hepatocyte apoptosis in liver, which may assist in the elimination of HBV-infected cells (Patel and Gores, 1995).

Besides the above mentioned, several cellular genes have also been proved important in inducing or inhibiting apoptosis in chronic hepatitis B. p53 has been extensively

investigated. It was reported to suppress the expression of HBx (Takada *et al.*, 1996). On the contrary, HBx was observed to either induce p53 mediated apoptosis (Chirillo *et al.*, 1997) or abrogate it (Wang *et al.*, 1995), or have no effect (Puisieux *et al.*, 1995). Such different effects of HBV genes on apoptosis may depend on the different physiological status of the cells.

Thus, the exact role of apoptosis as a host defense, an effecter mechanism in CTL response, and as a viral induced phenomenon, is still largely undefined in hepatitis B. The regulatory role of HBV genes on the apoptotic pathways remains to be investigated.

1.3.2 Apoptosis Induced by Viral Proteins

The role of viral proteins in modulating apoptosis has become an important feature (Pafeletal *et al.* 1999). To prolong their survival and facilitate the spreading of progeny particles, viruses have developed diverse mechanisms for the modulation of apoptosis (Lau *et al.*, 1998). Induction of apoptosis observed in chronic HBV carriers may be due to activation of p53, up-regulation of Fas and TNF receptor, or alternation in TNF/Fas pathways. Apoptosis in response to a viral infection most likely involves the interaction of both host and viral factors. Host factors include CTL and pro-apoptotic cytokines such as TNF-α and FasL, or even viral factors may include proteins such as the HBx and HBcAg. Clearly, the host CTL response is involved in apoptosis. The involvement of Fas and FasL is suggested by the correlation of their expression with the degree of liver pathology and inflammation. On the other hand,

HBx has variable effects in apoptosis and may sensitize cells to TNF, induce apoptosis, or abrogate effects of TNF (Wang *et al.*, 2004; Chen *et al.*, 2001).

1.4 SIGNALING PATHWAY OF APOPTOSIS:

Programmed cell death, or apoptosis, is one of the hottest areas of current research. It is characterized by the coordinated effort of a cell, including membrane blebbing, reduction in cell size, chromatin condensation and DNA degradation followed by ingestion of apoptotic bodies by neighbouring cells. There are two distinct apoptotic pathways, namely the death receptor pathway which includes the TNF receptor leading to caspase-8 activation, and the mitochondrial pathway which involves the Bcl-2 family of proteins leading to caspase-9 activation (Brechot, 2004). The death receptors belong to the TNF-receptor superfamily, including TNFR-1, Fas, TRAMP, and TRAIL. The receptors are characterized by an intracellular region also known as the death domain (DD), which transmits the cytotoxic signal to inside of the cell. Activation of these receptors by ligand binding results in movement of an adaptor protein to the DD. The adaptor protein then binds to a caspase nearby. For example, the caspase-8 to activate the caspase signaling cascade (Schulze *et al.*, 1998). The Bcl-2 family of proteins consists of both repressors (anti-apoptotic) and activators (pro-apoptotic) of apoptosis. Many of them can interact with each other in a combination of homodimers and heterodimers. The relative ratios of pro- and anti-apoptotic members determine the outcome of cell function (Douglas and John, 1998). Four conserved domains within the Bcl-2 family of proteins have been identified through their sequence similarity and named as Bcl-2 homology (BH)

domain 1-4 (Kelekar and Thomson, 1998). Anti-apoptotic members normally possess BH1-3 or BH1-4. In the case of pro-apoptotic members, they at least possess the BH-3 domain, which is needed for inducing apoptosis (Huang and Strasser, 2000). BH-3 only proteins function after the formation of heterodimer with anti-apoptotic Bcl-2 related protein. The heterodimer formation may occur on the outer membrane of mitochondria where the anti-apoptotic proteins are located to safeguard the membrane potential. Neutralizing of Bcl-2 and Bcl-xl by their association with pro-apoptotic members leads to the loss of membrane potential and release of cytochrome C (Cyt C). Cyt C then activates caspase-9 and apoptosis (Douglas and John, 1998).

1.4.1 Signaling by Death Receptors

Apoptosis-inducing activity has also been reported for a number of receptors: tumor necrosis factor receptor 1 (TNF-R1), CD95 (Fas), TNF-related apoptosis-mediated protein (TRAMP), and TNF-related apoptosis-inducing ligand receptor (TRAIL-R. Each of them possesses two to four cystine rich domains in their extracellular region, whereas all of them have one similar intracellular death domain, as shown in Figure 1.6. For most of them their natural ligands have been identified, such as TNF, FasL, lymphotoxin-α, and TRAIL (Beutler and Huffel, 1994; Wiley *et al.*, 1995). A similar mechanism of receptor recognition and triggering has been implied by the structural similarities for both the receptors and ligands. It is likely that all ligands are composed of identical subunits and trigger the activation of their receptors by the process of oligomerization (Jones *et al.*, 1992).

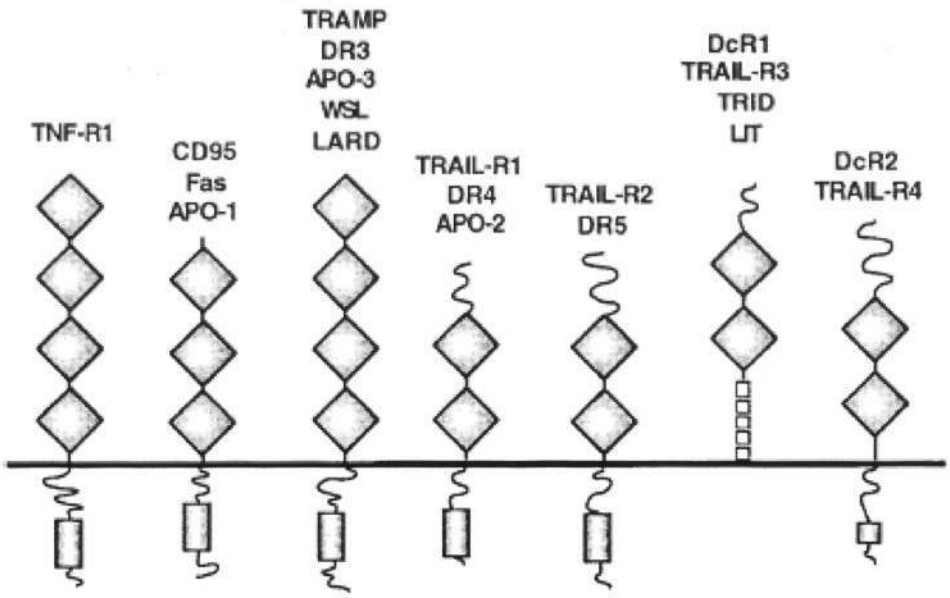

------ adapted from *S. Osthoff et al. (Eur: J.Biochem. 254)*

Figure 1.6: Schematic representation of the death receptors. Members of the TNF receptor superfamily are characterized by the intracellular death domain, depicted as a gray box. The boxes in the extracellular part represent Cys-rich domains.

1.4.1.1 Death receptors in apoptosis

TNF was isolated and named based on its killing ability towards tumor cells and cause necrosis in mice. TNF plays a crucial role in various inflammations (Vassalli, 1992; Bazzoni and Beutler, 1996). Foe example, TNF is mostly produced from activated macrophages, NK cells and other cells in the lymphatic system (Vasalli *et al.*, 1992). TNF activities are mediated by TNF-R1 (Tartaglia *et al.*, 1991). The CD95 (Fas) was identified originally as a cell surface receptor implicated in cell detach (Trauth *et al.*, 1989). Agonistic antibodies to Fas were able to inhibit tumor growth in nude mice (Trauth *et al.*, 1989). Fas is also reported to be involved in the suppression of immune response and plays a role for tumor cells to escape the surveillance of host

immune system (Hahne *et al.*, 1996; Chervonsky *et al.*, 1997). TRAMP is mainly expressed in thymocytes and lymphocytes. It is related to the TNF receptors at both structural and functional levels. However, the ligand for TRAMP still remains to be identified. TRAIL and its different receptors were identified as ligand/receptor complex. TRAIL has also been reported to induce cellular apoptosis in transformed cells (Lee *et al.*, 2006; Lin *et al.*, 2006).

1.4.1.2 Death receptor associated proteins

One key regulator of death receptor signaling pathway was death domain (DD). It is an intracellular region consisting of about 80 amino acids (Figure 1.6). Alignment of DD-like amino acid sequence not only helped in the identification of new death receptors but also facilitated the identification of new adaptor molecules (Huang *et al.*, 1996). The DD can self-bind and bind to other DD containing proteins. Following self-association, the DD of the receptors recruits other DD-containing adaptors in the signaling cascades (figure 1.7).

Among the characterized cellular proteins, TNF-associated death domain (TRADD), Fas-associated death domain (FADD), and Receptor-interacting protein (RIP) were identified DD-containing adaptor proteins. As a consequence of TNF-R1 activation, TRADD is bound firmly to DD of TNF-R1. Interestingly, the DD of TRADD, Fas and RIP could interactively bind to each other, which suggested a potential communication of the different receptor signaling pathways. For FADD, there is a death effector domain (DED) in the N-terminal which is sufficient to cause apoptosis

(Chinnaiyan *et al.*, 1995). RIP contains a kinase domain at its N-terminus and a DD domain at its C-terminus (Stanger *et al.*, 1995). It is crucial to the NF-κB activation by TNF-R1 (Hsu *et al.*, 1996; Ting *et al.*, 1996).

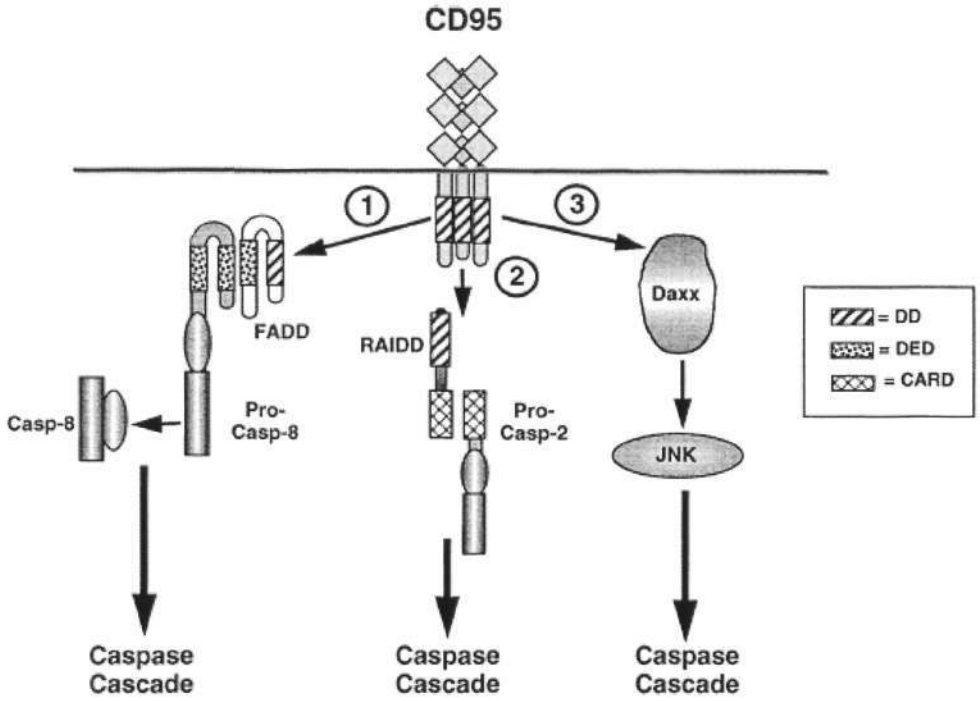

------ adapted from *S. Osthoff et al. (Eur: J.Biochem. 254)*

Figure 1.7: CD95 proximal signal transduction. Example of CD95 activation pathway. The death effector domain (DED) of FADD in turn recruits and activate procaspase-8. An alternative pathway may activate caspase-2 through RAIDD. RAIDD contains a DD and a caspase recruitment domain (CARD). A third pathway may recruit Daxx to the DD of CD95. This pathway involves JNK activation. However, the physiological relevance of the latter two pathways is rather unknown.

As for FasL/Fas system activation, FADD was dhown to bind to Fas following stimulation. Together with the receptor and FADD, the proteins complex with the receptors and FADD formed the death-inducing signaling complex (DISC). Co-IP also resulted in identification of an important protein in the downstream of FADD,

the FLICE or caspase-8 (Muzio *et al.*, 1996). After receptor activation, FADD and caspase-8 are recruited to Fas. Association of pro-caspase 8 to with triggers a structural change leading to caspase-8 activation. The active subunits p10 and p18 from caspase-8 are released into the cytoplasm to exert their apoptotic activity (Muzio *et al.*, 1997).

In TNF-R1 pathway, activation of TNF-R1 recruits TRADD. Subsequently TRADD recruits FADD upon binding of DD (Chinnaiyan *et al.*, 1996). TRAMP is a TNF-R1-like receptor and able to recruit TRADD, FADD and caspase-8, leading to apoptosis (Chinnaiyan *et al.*, 1996). TRAIL binds to two apoptosis signaling receptors, TRAIL-R1 and TRAIL-R2. In contrast to caspase-8, TRAIL activates caspase-10 (Pan *et al.*, 1997). But whether the FADD is involved in TRAIL-R mediated apoptosis remains to be investigated.

1.4.2 Signaling by Bcl-2 Family of Proteins

Bcl-2 family of proteins has shown their increasing prominance in apoptosis. Members of this family are highly conserved in sequence, known as Bcl-2 homology (BH) domains. BH domains can play opposing role in the proteins in cell death and survival. Recently the emergence of the BH3 domain as a potent death domain and a BH-3 only subgroup has been reported (Kelekar and Thompson, 1998). These proteins function at the mitochondria outer membrane and determine the cell fate by controlling the release of cytochrome C (Cyto C) which activate pro-caspase 9 (Tsujimoto and Shimizu, 2000).

1.4.2.1 Classification of the Bcl-2 family

Bcl-2, was identified originally as a proto-oncogene but mainly in helping cells to survive under unfavorable conditions (Bakhshi *et al.*, 1985). Nowadays, a number of Bcl-2 related proteins have been identified. Some are anti-apoptotic to delay cell death like Bcl-2 and Bcl-xl, others are facilitators of apoptosis like Bad and Bax. Pro-apoptotic members include Bcl-2, Bcl-xl, Bcl-w, Mcl-1, A-1, adenoirus E1B19K, EBV BHRF1 and CED-9. Death promoters include Bax, Bak, Bad, Bik, Bid, Bim, Hrk and Blk et al (Kelekar and Thompson, 1998). These proteins share the Bcl-2 homology 1-4 and could be divided into three categories based on this domain organization (figure 1.8). Anti-apoptotic members such as Bcl-2, Bcl-xl contain all the four BH domains. Pro-apoptotic members such as Bax, Bak, and Bad share sequence homology in BH 1-3. While the BH-3 only proteins Bik, Bid, Bim, Hrk, and Blk, share sequence homology only in BH-3. The family members are able to interact with one another to form heterodimers and homodimers to function.

.

The three-dimensional structure of one family member, Bcl-xl, which was solved in 1998, may help to understand the structure of the Bcl-2 homologies (Sattler *et al.*, 1997). It demonstrates two central hydrophobic α–helices, α-5 and α-6, surrounded by five amphipathic helices, α 1-4 and 7. The BH1-3 regions form an hydrophobic cleft, whereas the BH4 domain forms an amphipathic helix (Muchmore *et al.*, 1996). Between the BH4 and BH3, lies a loop region in 60 residues' length containing a caspase proteolytic site (figure 1.8). BH4 is necessary for the anti-apoptotic members (Hunter *et al.*, 1996). The transmembrane (TM) domain renders some of the proteins

to be anchored to intracellular membranes. Bcl-2 and Bcl-xl are targeted to the outer membrane of mitochondrial, ER membrane and nuclear membrane. Bad and Bid, which lack a TM domain, exhibit a diffuse distribution in cytoplasm (Nguyen *et al.*, 1993).

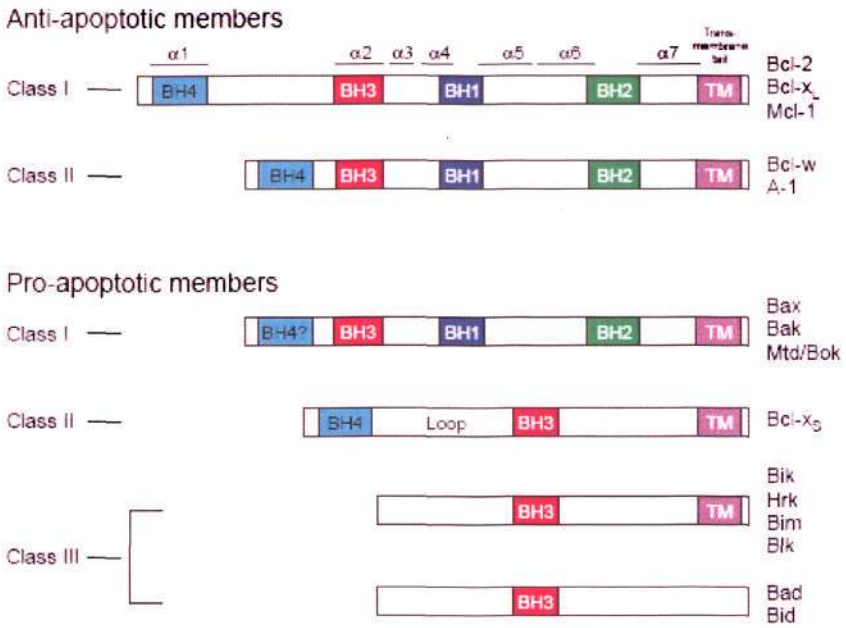

------adapted from A. Kelekar *et al., (Trends in Cell Biology, 1998)*

Figure 1.8: Classification of the Bcl-2 family. The general representation of the proteins is shown (not to scale); Bcl-2 homology (BH) domains and transmembrane (TM) domains are labelled. A-1, Bax and Bak exhibit weak homology to Bcl-2 in the BH4 region. The predicted α-helical segments are indicated on the Bcl-2/Bcl-xL prototype. α-helices 5 and 6 are predicted to participate in channel formation.

1.4.2.2 BH1 and BH2 domains

The BH1 and BH2 domains have been repoted in all anti-apoptotic members (Figure 1.8). Amino acid residues in the BH1 and BH2 domains are essential for the survival function of the death suppressors and for their association with pro-apoptotic members (Sedlak *et al.*, 1995; Yin *et al.*, 1994). Mutation of a conserved glycine within BH1, inhibits Bcl-2 function and blocks its interaction with Bax (Yin *et al.*,

1994; Sattler *et al.*, 1997). The lack of BH1 and BH2 of Bcl-2 leads to a splice variant Bcl-xs which is pro-apoptotic (Minn *et al.*, 1996). With the BH1 and BH2, Bcl-2, Bcl-xl and Bax were confirmed to insert into lipid bilayers and form ion-conducting channels (Minn *et al.*, 1997; Schlesinger *et al.*, 1997; Schendel *et al.*, 1997). In crystal structure of Bcl-xl, BH1 and BH2 domains flank the hydrophobic core helices, α–5 and α–6 (Muchmore *et al.*, 1997). The BH1 and BH2 may regulate different ion-selectivity and conductance in the heterodimer of Bcl-2 and Bax. At neutral PH, Bcl-2 and Bcl-xl are more selective to cations, whereas at lower PH, Bax channels exhibit a preference to anions (Minn *et al.*, 1997; Schlesinger *et al.*, 1997; Antonsson *et al.*, 1997). Thus, in the case of cytochrome C release, Bax induces this release, whereas Bcl-2 and Bcl-xl prevent it (Rosse *et al.*, 1998).

1.4.2.3 BH3 domain

The BH3 domain was introduced as a 16 amino acids motif in Bak (Sattler *et al.*, 1997; Chittenden *et al.*, 1995). BH3 are found in many Bcl-2 family of proteins, and it is functionally important only in death promoting. For the BH3-only proteins, existence of BH3 is especially independent. Figure 1.9 shows an alignment of the BH3 domains from some known Bcl-2 family members, with the core residues highlighted. Solution structure of a complex between Bcl-xl and the BH3 domain of Bak revealed that this domain forms an amphipathic α–helix that binds with high affinity to the hydrophobic pocket created by the BH1, BH2 and BH3 of Bcl-xl through both hydrophobic and electrostatic interactions (Sattler *et al.*, 1997). Mutations in Bak BH3 affect both heterodimerization with the Bcl-xl and its capacity

to induce cell death (Sattler *et al.*, 1997). In Figure 1.9, the well conserved leucine and aspartic acid residues were defined as the crucial residues in both heterodimerization and death promotion, by solution structure and functional studies (Sattler *et al.*, 1997).

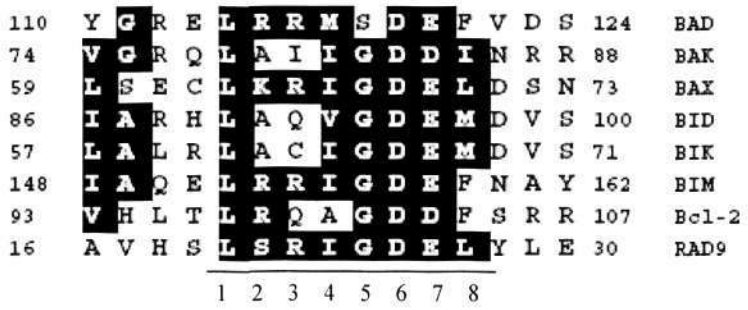

------adapted from A. Kelekar *et al., (Trends in Cell Biology, 1998)*

Figure 1.9: Alignment of BH3 domains. Core residues 1-8 are indicated. Numbers on the left denote amino acid positions in the context of full-length protein. Boxes indicate the most conserved residues

1.4.2.4 BH3-only Proteins

These proteins share no homology with Bcl-2 except the BH3 domain (figure 1.8). They are able to induce apoptosis by heterodimerization with anti-apoptotic members, whereas unable to form homodimers. Bad was the first discovered such protein (Yang *et al.*, 1995). It does not possess a C-terminal transmembrane domain, thus is generally found in the cytosol. When heterodimerized with Bcl-2 or Bcl-xl, Bad becomes membrane associated and therefore exert its pro-apoptotic activity (Kelekar *et al.*, 1997). Bid, which also lacks a C-terminal TM domain, is predominantly cytosolic and also could be found membrane associated. It could bind to Bcl-2 and Bcl-xl to abrogate their anti-apoptotic function. However, Bid was also reported to bind to Bax and induce apoptosis via a caspase-dependent manner (Wang *et al.*,

1996).

The remaining known BH3-only proteins all contain C-terminal TM domain, thus localize on intracellular membranes individually. These proteins also bind to Bcl-2 and Bcl-xl by their BH3 domain. Bik is additionally able to complex with E1B 19K and EBV BHRF (Boyd *et al.*, 1995). Bim has three isoforms, Bim-EL, Bim-L, and Bim-S. Bim-S is the strongest death promoter, whereas the other two maybe regulate the Bim-S (O'Connor *et al.*, 1998). HRK is expressed in lymphoid tissure. Blk is structurally related to Bik but more restrictly expressed in liver and kidney (Hegde *et al.*, 1998). They all induce apoptosis by heterodimerizing with anti-apoptotic members.

1.4.2.5 BH3 domain functions:

Bcl-2 and Bcl-xl maintain mitochondrial homeostasis while BH3-only proteins could abrogate their protective function by heterodimerizing with them, thus creating dysfunctional pore. Alternatively, heterodimerization could lead to conformational change in Bcl-2 and Bcl-xl to abolish their ability inserting in the membrane. Bax or Bax homodimers could also form channels but on the contrary they lead the cell to apoptotic degradation. The point that commits the cell to apoptosis is the release of Cyt.C into the cytosol (figure 1.10). Cytosolic Cyt.C form a complex with Apaf-1, pro-caspase-9 in which pro-caspase 9 is activated to caspase 9. (Li *et al.*, 1997). Bcl-2 and Bcl-xl function to block the release of Cyt.C from mitochondria (Kluck *et al.*, 1997; Yang *et al.*, 1997), whereas pro-apoptotic members neutralize them and thus

abrogate such block. Current research indicates that release of Cyt.C is result of the mitochondrial swelling and outer membrane rupture (Vander Heiden *et al.*, 1997). Alternatively, a BH3 protein might displace a protein from a complex with Bcl-2 or Bcl-xl. In the complex with Bcl-xl (figure 1.10), Apaf-1 could be displaced by BH3 proteins. On the other hand, BH3 domain alone is proved sufficient to induce Cyt.C release and caspase activation as supported by BH3 peptide assay showing promoted apoptosis in cell-free system based on *Xenopus* egg extracts (Cosulich *et al.*, 1997).

An examination of the BH3 domain alignment in Figure 1.9 to compare residues between pro- and anti-apoptotic proteins suggests some possible functional difference. Core position 1 and 6 are crucial for the interaction between members. Residues at position 4 might serve to set the pro and anti-apoptotic members apart. Though all the position 4 residues are nonpolar, only Bcl-2 has it as alanine. Replacement of the position 4 in a Bak BH3 peptide with alanine decreased its affinity for Bcl-xl significantly (Sattler *et al.*, 1997). The minor difference the BH3 domains of Bcl-2 family of proteins might therefore cause differences in relative binding affinity hierarchy. By this reason, the BH3 domain of Bcl-2 and Bcl-xl does not function as pro-apoptotic. This might be explained on structure study that BH3 buried in the hydrophobic pocket is unavailable to bind with anti-apoptotic proteins of similar tertiary structure (Sattler *et al.*, 1997).

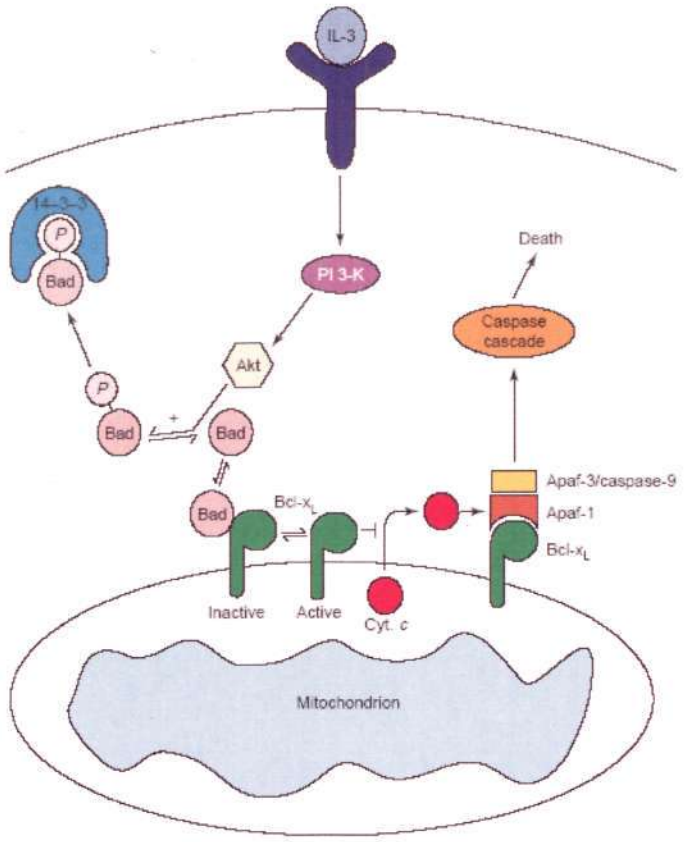

------adapted from A. Kelekar *et al., (Trends in Cell Biology, 1998)*

Figure 1.10: Example of Bad regulation. Cell survival factor interleukin 3 (IL-3) activated receptor mediates the activation of phosphoinositide 3-kinase (PI3-K) and Akt who phosphorylate Bad at Ser136. Phosphorylated Bad is inactivated by being sequestered with phosphoserine-binding protein 14–3–3. In the absence of IL-3 receptor occupation, Bad is in active form hypophosphorylated and binds to Bcl-xl,. Inactive Bcl-xl thus fail to block the release of Cyt.C into the cytosol. Cyt.C activates the caspase cascade through Apaf-1 and caspase-9.

1.4.3 Autophagic Cell Death

Autophagy is responsible for protein trafficking in cells. In autophagy process, undesired cytoplasmic materials are segregated into vesicles and they are degraded in the lysosomes (Eskelinen 2005). This is a short-term stress response of cells when they are starvation conditions like nutrient-limited or deficiency. Through the degradation of cytoplasmic materials cells could survive by making use of the

material for metabolism. On the other hand, autophagy also plays an important role in autophagic cell death as known the programmed cell death type II (Tsujimoto and Shimizu, 2005). Autophagy was observed to take place when Bax and Bak knocked out fibroblast cells were under death stress. Bcl-xl was also reported to play a role in the signaling of autophagic cell death (Shimizu *et al.*, 2004). Beclin1, an autophagy inducing gene, was reported to be negatively regulated by Bcl-2. This regulation inhibited Beclin1 depedent autophagy (Pattinre and Levine, 2006). Bnip3 is a BH3 only pro-apoptotic protein existing in heart cells. During ischemia/reperfusion of heart, Bnip3 was inhibited by autophagy (Hamacher *et al.*, 2006). Thus, there is relationship between apoptosis and autophagy. The exact mechanism remains to be investigated.

1.5 HBx

HBx is a very important regulator protein of the HBV during its infection, replication, pathogenesis, and carcinogenesis. It is encoded by the X gene and translated from a 0.8 kb mRNA under the HBx promoter (figure 1.2) (Guo *et al.*, 1991; Sugata *et al.*, 1994). The name of X protein implied its unknown function and no similarity with known proteins in the start. HBx is no doubt naturally expressed during HBV infection (Levrero *et al.*, 1990). It consists of 154 amino acids with molecular weight of 17 kD. HBx's structure still remains unknown due to its insolubility. Its amino acid sequence is highly conserved in different species, including α-helix in both N-terminus and C-terminus (Colgrove *et al.*, 1989). HBx was reported to be phosphorylated when expressed in HepG2 cells (Schek *et al.*, 1991).Acetylation was

also observed when it was over expressed in insect cells (Urban *et al.*, 1997). HBx amino acids 52 to 148 were proved essential for various functions (Yen, 1996). There is some evidence that HBx may form dimers (Ganem *et al.*, 2001). In the case of subcellular localization, most studies indicate that it is located largely in the cytoplasm but also detectable on mitochondrial and in nucleus (Dandri *et al.*, 1996; Dandri *et al.*, 1998; Takada *et al.*, 1998). Recently HBx was reported to be nuclear located at low levels, however to convert to cytosolic distribution when expression increases (Henkler *et al.*, 2001; Kim *et al.*, 2003). Crm-1 was reported to be involved in HBx shuttling between the nucleus and the cytoplasm (Forgues *et al.*, 2001)

1.5.1 A Multiple Function Protein

1.5.1.1 Importance for HBV life cycle

HBx was reported to augment HBV replication and persistence of infection in hybrid animals raised from HBx-expressing mice crossed with HBV-expressing mice (Xu *et al.*, 2002). An important but nonessential role of HBx in HBV has been demonstrated in HepG2 cells in tissue culture (Bouchard *et al.*, 2001; Melegari *et al.*, 1998). Controversially, in cell culture of Huh7, the influence of HBx expression on HBV replication was not obvious (Blum *et al.*, 1992).

1.5.1.2 Transcriptional activator

HBx was reported to moderate many different viral and cellular transcription elements (Yen, 1996), including NF-κB, AP-1, AP-2 c-EBP, CREB, and NF-AT (Faktor and Shaul, 1990; Lara-Pezzi *el al.*, 1999; Levrero *et al.*, 1990; Lucito and

Schneider, 1992; Maguire *et al.*, 1991; Mahe *et al.*, 1991; Williams *et al.*, 1995). HBx also activates RNA pol I- and pol III-dependent promoters. HBx exhibits its capacity not by binding to DNA directly, but by protein-protein interaction with nuclear transcription components and cytosolic signal transduction pathway components. HBx was shown to associate with some basal transcription elements, like TFIIB, TFIIH, and the TATA-binding protein (TBP) (Haviv *et al.*, 1998; Lin *et al.*, 1997; Qadri *et al.*, 1996). However, these studies are based on over expression experiments and lack of viral infection.

1.5.1.3 Cytoplasmic signal transduction pathways

It was reported that the HBx is mostly localized in the cytoplasm of cells (Dandri *et al.*, 1996; Dandri *et al.*, 1998). The potential of HBx to stimulate cytoplasmic signaling pathways has been investigated by a lot of studies. HBx has been shown to stimulate various signaling pathways (Figure 1.11). HBx was proved to activate the extracellular signal-regulated kinases (ERKs), and the stress-activated protein kinases (SAPK) (Benn *et al.*, 1996; Tarn *et al.*, 2001). Moreover, HBx activation of mitogen-activated protein kinases (MAPKs) was demonstrated in mouse (Nijhara *et al.*, 2001). HBx also stimulate Ras-Raf-MAP kinase signal transduction when expressed with replicating HBV in primary mouse hepatocytes (Klein and Schneider, 1997; Nijhara *et al.*, 2001). However, no direct interaction has been found between HBx and any of these protein kinases. It has now been shown that HBx activates some signaling pathways by activating several non-receptor tyrosine kinases (Tarn *et al.*, 2002; Lee and Yun, 1998). HBx also promotes alternation of cellular junctions

(Lara-pezzi *et al.*, 2001). HBx was demonstrated to activate focal adhesion kinase (FAK) and the proline-rich kinase (Pyk2) (Bouchard *et al.*, 2001; Rao *et al.*, 1997). In NF-κB activation, evidence shows that HBx activates the protein Inhibitor of κB Kinase (IKK) to inactivate another protein Inhibitor of κB-α and -β (IKB-α and -β) by phosphorylation, leading to the release of NF-κB and translocation to nucleus (Weil *et al.*, 1999). Besides these, HBx is also largely involved in apoptosis pathways.

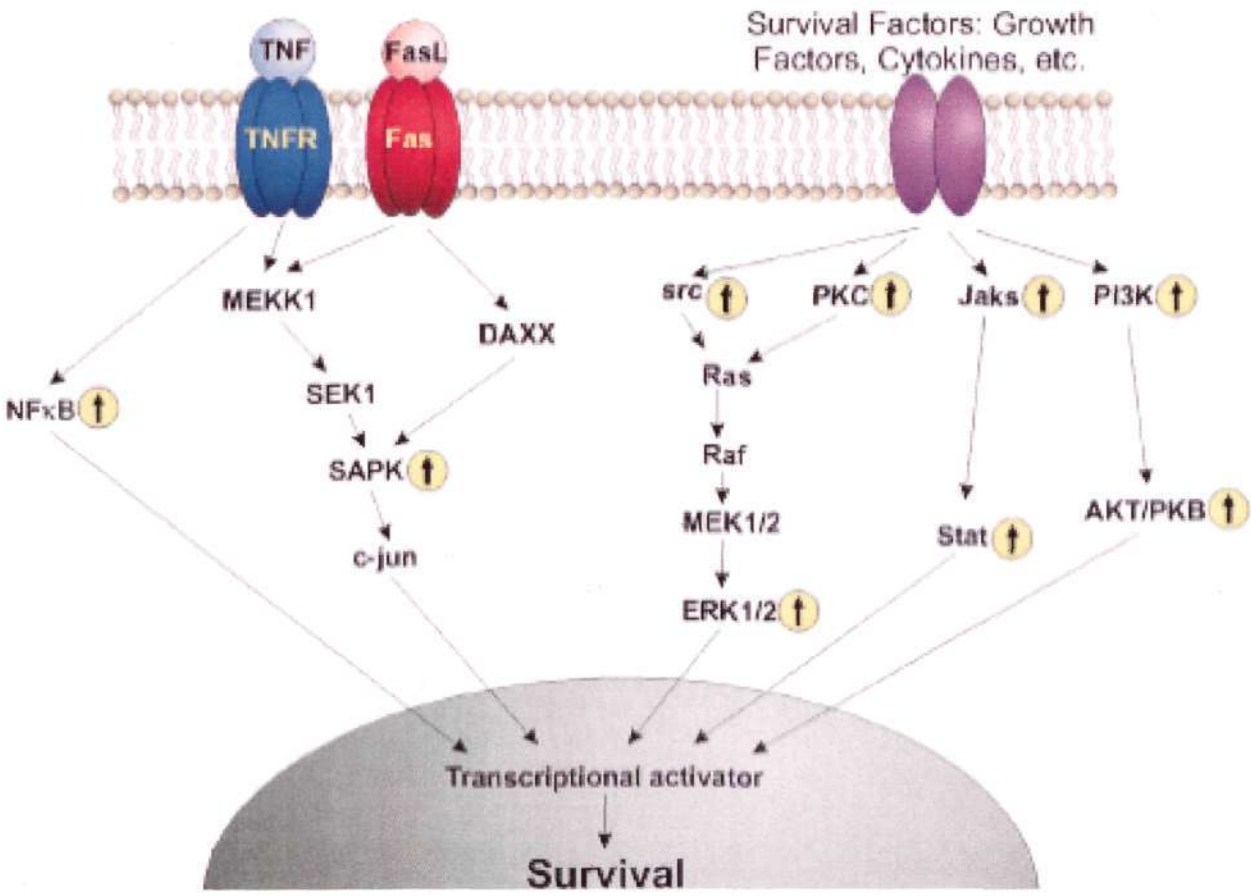

------adapted from J. Diao *et al., (Cytokine & Growth Reviews 2001)*

Figure 1.11: Effect of HBx signal transduction pathways. Vertical arrow pointing upward denotes increased activity in the presence of HBx. HBx also upregulates the activity of the NF-κB transcription factor.

1.5.2 Effect on apoptotic pathways

In order to survive in host cells and therefore spread the virus progeny, many viruses regulate host cell apoptosis. Normally viruses produce proteins to interact with cellular components regulating apoptosis. HBx is such a viral protein. Infected hepatocytes are more sensitive to factors that can lead to apoptosis during HBV infection. Apoptotic factors include DNA damage, immune attack by CTL, and toxic effects of cytokines (Chisari and Ferrari, 1995; Chisari, 1995). HBx has been reported to lead to cell death, especially in some HBx over expression cases. However, in some other cases, it was implicated as a survival factor.

It was reported that HBx expression in the mouse liver was associated with increased hepatocyte apoptosis in a p53 independent way (Terradillos *et al.*, 1998). It was shown that expression of HBx is associated with increased apoptosis in liver cells from two transgenic mouse lines. In transient transfection experiments, over-expression of HBx in hepatocyte cell line MMHD3 and HepG2 lead to apoptosis in dose-dependent manner (Pollicino *et al.*, 1998). Further investigation revealed HBx was able to abolish the protective effect of Bcl-2 and restore the cell sensitivity to the Fas death signal in Bcl-2 over-expressed mouse hepatocyte. A downstream Cyt.C release from mitochondria and activation of caspase-3 were demonstrated. But no direct interaction of HBx and Bcl-2 was detected (Terradillos *et al.*, 2002). This link between Fas death signal and Bcl-2 could be understood that the t-Bid resulted from death receptor pathway could be located to mitochondria and bind to Bcl-2. In cultured cell lines, its pro-apoptotic activity was also reported. HBx significantly

increased apoptosis independent of p53 in mouse liver cell line (Terradillos *et al.*, 1998). However, some other group showed that HBx interacted with the p53 and inhibited its entry into the nucleus (Ueda *et al.*, 1995). In focus formation assay, expression of HBx completely abrogated the focus-forming ability of Ha-*ras*, v-*src*, v-*myc*, v-*fos*, and E1a in NIH3T3 cells. Moreover, the inhibition effect could be reversed by transfection of Bcl-2, suggesting that the observation is regulated by mitochondrial pathway of apoptosis (Kim *et al.*, 1998). A stable cell line Chang-HBx was reported to grow slower in soft agar than normal Chang liver cell line. HBx also caused the induction of G1 phase arrest of cell growth in early infection of HBV (Wang *et al.*, 2004). In HepG2 cells, HBx was demonstrated to induce Fas ligand expression (Shin *et al.*, 1999).

Recent studies have reported that HBx may acts on the mitochondrial outer membrane as the potential mechanism for HBx regulated apoptosis. Yeast two-hybrid assays, *in vitro* labeling and *in vivo* co-immunoprecipitation studies indicated that HBx might interact with the human voltage-dependent anion channel (HVDAC) on mitochondria (Rahmani *et al.*, 2000). In addition, over-expression of HBx in transfected cells showed a co-localization of HBx with mitochondria at the periphery of nucleus that lead to cell apoptosis (Takada *et al.*, 1999). Heat shock protein 60 (Hsp60) was identified as a novel HBx-binding protein by affinity purification and mass spectrometry. It was shown that HBx and Hsp60 were co-localized on mitochondria and Hsp60 facilitated HBx-induced apoptosis (Tanaka *et al.*, 2004). It was also reported that HBx interacted with c-FLIP and abrogated its

apoptosis-inhibition function (Kim *et al.*, 2003). Moreover, HBx expressed from a replicating HBV genome in cell culture induced hypersensitivity of the cells to TNF (Su and Schneider, 1997). This observation was confirmed by others' investigation (Kim *et al.*, 2003).

1.6 HBSP

1.6.1 Spliced-Generated Transcripts in HBV

HBV encode capsid, surface, polymerase and HBx proteins. They are all identified to be translated from unspliced mRNAs (Ganem and Varmus, 1987). However, singly and doubly spliced HBV mRNA transcripts have been identified both *in vivo* and in *in vitro*. Splice generated proteins were also found abundant in replicative HBV transfected HepG2 culture (Wu *et al.*, 1991). HBV-spliced transcripts generated from the pregenomic RNA have been found to be present as 30% of the pregenomic RNAs (Wu *et al.*, 1991). Spliced RNA transcripts were also detected in hepatitis virus infected woodchuck (Ogston and Razman, 1992; Hantz *et al.*, 1992). Non-infective HBV particles were demonstrated to contain a 2.2 kb RNA complementary to a singly spliced RNA in chronical patients (Rosmorduc e*t al.*, 1995; Gunther *et al.*, 1997). Advantage of defective viral particles is to neutralize the immune protection and thus facilitate the infection of HBV (Rosmorduc e*t al.*, 1995). Defective particles are secreted with help of wild-type virus (Terre *et al.*, 1991). These findings indicate the role of these defective HBV particles and the significance of spliced mRNA and their translation proteins.

1.6.2 HBV Splice-Generated Protein (HBSP)

Expression of the singly spliced 2.2 kb RNA leads to accumulation of the HBcAg in cell and to an increased secretion of HBeAg (Rosmorduc e*t al.*, 1995). Interestingly, it encodes a novel open reading frame which encodes an HBV splice-generated protein (HBSP). This protein consists of 93 amino acids. It starts at the polymerase N-ternimus and includes the first 46 amino acids of the polymerase following by another 47 amino acids corresponding to a new sequence generated by the frame-shift (figure 1.12). *In vivo*, HBSP was demonstrated to be detectable in liver tissue from chronic patients. Anti-HBSP antibodies also occurred in some sera samples from chronic HBV carriers. *In vitro*, the over-expression of HBSP was shown to induce cell apoptosis (Soussan *et al.*, 1999).

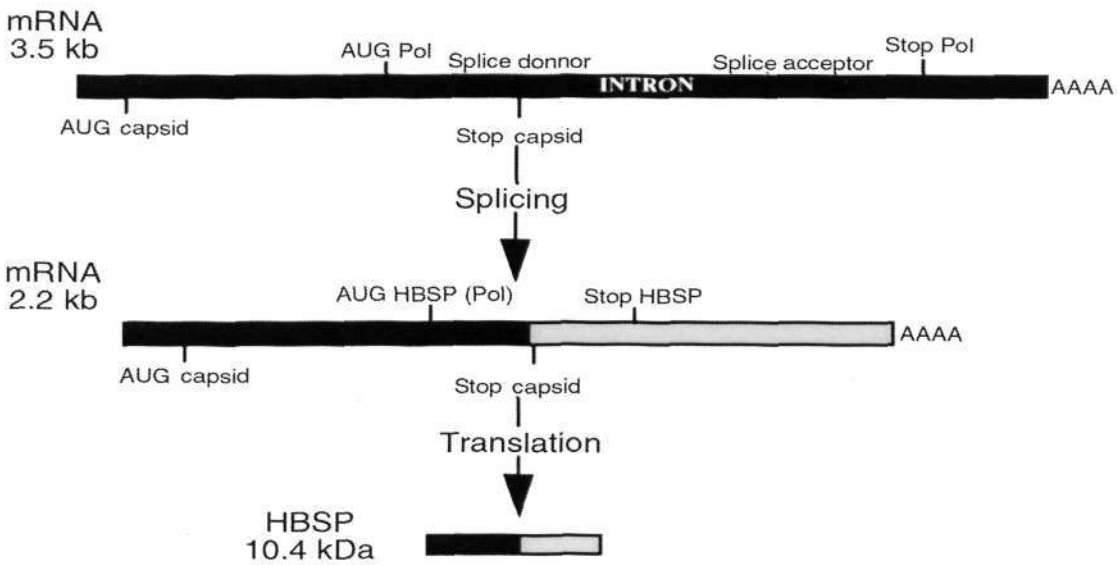

------adapted from P.Soussan et al., (J.Clinic Investigation, 2000)

Figure 1.12: Schematic representation of HBSP production. The HBSP begins at the polymerase start codon and includes the first 46 amino acids of the polymerase, followed by the 47 amino acids corresponding to a new HBV amino acid sequence generated by the frameshift.

It was considered that spliced proteins were not necessary for *in vitro* viral replication (Wu *et al.*, 1991). However, a spliced RNA and its protein have been shown to be indispensable for viral replication in DHBV (Obert *et al.*, 1996). Another important issue concerning spliced RNAs is that they might help in the viral life cycle as demonstrated for human foamy virus and cauliflower mosaic virus (Giron *et al.*, 1998; Kiss-Laszlo *et al.*, 1995). It have also been reported that HBV spliced RNAs can encode for a polymerase and surface fusion protein. The latter may influence the viral entry into host cell *in vitro* (Huang *et al.*, 2000). In the case of HBSP, anti-HBSP antibody prevalence in HBV chronic carriers was about 46%. With respect to HBV-related liver disease, an association was observed between the liver fibrosis and HBSP. Moreover, HBSP was proposed to independently increase the viral replication and elevate TNF-α secretion which may attribute to hepatocyte apoptosis (Soussan *et al.*, 2003). Taken together, these findings support the hypothesis that spliced RNAs and their encoded proteins may be involved in the pathogenesis of HBV infection.

1.7 PROJECT AIMS

The general aim of this study is to elucidate the mechanism by which apoptosis is induced in HBV infected cells at molecular level. Viral proteins are most possibly responsible for the observed apoptosis. Based on sequence alignment among HBV proteins and Bcl-2 family of proteins, a death-triggering BH3-like domain was identified in HBx and HBSP. This might give a reasonable explanation to the apoptosis induced by HBV at molecular level. This study aims to analyze the pro-apoptotic activity of HBx and HBSP by biochemical assays. Furthermore, by

specific mutation of critical amino acid in BH3 domain, the significance of BH3 like domain was analyzed.

It is also important to know their interacting proteins with the presumable apoptosis inducer, as well as their structures to understand their function further completely. Interaction with other proteins may reveal new mechanism related to apoptosis. While the importance of structure is that it could exactly display conformational feature of proteins and confirm hypothesis.

Chapter Two: Materials and methods

2.1 GENERAL REAGENTS

General reagents and solvents were obtained from Amersham Pharmacia Biotech, Amersham International Plc., Amresco Company Ltd., BD Clontech, BDH Chemicals Ltd., Becton & Dickinson Company, Bio-Rad Laboratories, Cole-Parmer Company Ltd., Difco Laboratories, Fisher Scientific, Flowgen Ltd., Fluka Chemie Gmbh, FMC Bioproducts Gibco-BRL Ltd., ICN Biomedicals, Invitrogen Corporation, Merck KGaA, PIERCE, Promega Corporation, Q.Biogene Company Ltd., Rose Chemicals Ltd., and Sigma-Aldrich Chemie Gmbh. Other reagents, and their sources, are listed below. Solutions were sterilized when required by autoclaving at 120°C for 20 minutes or by passing through a 0.22 μm filter (Millipore, Sartorius).

2.1.1 Enzymes

Restriction endonucleases, Taq DNA Polymerase, Pfu DNA polymerase, T4 DNA ligase, Proteinase other enzymes were purchased from Amersham International Plc., Amersham Pharmacia Biotech, Bethesda Research Laboratories, New England biolabs Inc., and Promega Corporation, unless otherwise stated, and were used according to the supplier's recommendations.

2.1.2 Radioactive Reagents

[S -^{35}] dATP at 10 mCi/ml Amersham Int.

2.1.3 Commercially Available Kits

QIAprep® Spin Miniprep Kit	QIAGEN Ltd.
QIAprep® Spin Midiprep Kit	QIAGEN Ltd
QIAprep® Spin Maxiprep Kit	QIAGEN Ltd
QIAQuick® Gel Extraction Kit	QIAGEN Ltd
QIAQuick® PCR Purification Kit	QIAGEN Ltd
RNeasy® Mini Kit	QIAGEN Ltd
Effectene® Transfection Reagent	QIAGEN Ltd
ECL™ Western Bloting Analysis System	Amersham Pharmacia Biotech
Protein A and G Beads	Amersham Pharmacia Biotech
ApoAlert™ Annexin V-FITC Apoptosiskit	BD-Bioscience Clontech
ApoAlert™ Caspase-3 Fluorescent Assay Kit	BD-Bioscience Clontech
Titanium® One-Step RT-PCR Kit	BD-Bioscience Clontech
Annexin-V-Fluos Staining Kit	Roche Diagnostics Corp.
QuikChange® Site-Directed Mutagenesis Kit	Stratagene
CheckMate™ Mammalian Two-Hybrid System	Promega Corp.
Dual-Luciferase® Reporter Assay System	Promega Corp.
TnT® Coupled Wheat Germ Extract System	Promega Corp.
MasterTag Kit	Eppendorf
Mycoplasma Hoechst Staining Kit	Mp Biomedicals

2.1.4 DNA Vectors

pBIND	Promega Corp.

pACT	Promega Corp.
pEGFP-C1	BD-Bioscience Clontech
pCDNA3.1(+)	Invitrogen Corp.
pGEX-5X-1	Amersham Int.
pXJ-40	From Dr S.M. Tan (SBS, NTU)

2.1.5 cDNA Clones

HBV Polymerase-N	From A/P W.N.Chen William (SCBE, NTU)
HBX	From A/P W.N.Chen William (SCBE, NTU)
HBSP	From A/P W.N.Chen William (SCBE, NTU)
Bcl-2	From A/P Y.H.Sup Joe (SBS, NTU)
Bcl-xl	From mRNA Library
Bad	From mRNA Library
Bak	From mRNA Library
Bid	From mRNA Library
Bim	From mRNA Library

2.1.6 Cell Lines

E.coli strain DH-5	Stratagene

E.coli strain BL21	Stratagene
Huh7 cells	From ATCC
HepG(2) cells	From ATCC
293T cells	From ATCC

2.1.7 Antibodies

HA-Probe	Anti-HA	From Santa Cruz Biotechnology
β-Actin	Anti-β-Actin	From Santa Cruz Biotechnology
$Bcl\text{-}_{xl}$	Anti- $Bcl\text{-}_{xl}$	From Santa Cruz Biotechnology
$Bcl\text{-}_2$	Anti- $Bcl\text{-}_2$	From Santa Cruz Biotechnology
Goat Anti-Rabbit		From PIERCE
Goat Anti-Mouse		From PIERCE
Goat Anti-Mouse-FITC		From PIERCE

2.2 SOLUTIONS, BUFFERS AND MEDIA

2.2.1 Laboratory Stocks

20 mg/ml Ampicillin	20 mg/ml in 1 M $NaHCO_3$, pH 8.4, filterd (0.22 μM) and stored at -20°C
10 m/ml BSA	Stored at -20°C
0.1 M DTT	Stored at -20°C
1 M DTT	Stored at -20°C
0.5 M EDTA, pH 7.5	Stored at RT
0.1 M EDTA, pH 7.5	Stored at RT

0.1% ethidiom bromide	Stored at 4°C
Glycerol loading dyes	30% glycerol, 5 mM EDTA pH 7.5, 0.1% bromophenol, 0.1% xy lene cyanol FF
1 M HEPES, pH 7.4	Stored at 4°C
1 M M_gCl_2	Stored at RT
3 M NaAc, pH 6.0	Stored at RT
3 M NaAc, pH 4.8	Stored at RT
3 M NaCl	Stored at RT
5 M NaCl	Stored at RT
50 mM $NaHCO_3$, pH 9.0	Stored at RT
Phenol chloroform	Equal volumes of Biophenol-Tris and chloroform were mixed and stored at 4°C
2x protein solubilisation buffer	0.16 M T ris pH 8.0, 8 M Urea, 1.6% SDS, 0.08% bromophenol blue
10% (w/v) SDS	Stored at RT
100 mM spermidine	Stored at -20°C
10x TBE	0.89 M Tris pH 8.0, 0.89 M Boric acid, 25 mM EDTATE buffer, pH 8.0
	10 mM Tris pH 8.0, 0.1 mM EDTA
1 M Tris-HCl, pH 8.0	Stored at RT
1.5 M Tris-HCl, pH 8.8	Stored at RT

1 M Tris-HCl, pH 6.8	Stored at RT
Iso-propanol	Stored at RT
1X PBS	Stored at RT
Commassie Blue Staining Buffer	50% methanol, 10% glacial acid, 40% H_2O, 0.25g Brilliant Blue in 1 Litre Stored at RT
Commassie Blue Destaining Buffer	30% methanol, 10% glacial acid, 60% H_2O, Stored at RT

2.2.2 Media for Bacterial Culture

LB medium	1% (w.v) Bacto-tryptone (BD), 0.5 (w/v) Yeast (BD), 1% (w/v) NaCl (Merck)
LB agar	LB medium plus 1.5% (w/v) Bacto-agar(BD)
LB plates (amp^r)	LB agar plates of 100μg/ml ampicillin
LB plates ($kana^r$)	LB agar plates of 50 μg/ml kanamycin

2.2.3 Solutions for Making Competent Bacteria

$CaCl_2$	1 M, 4°C
$MgCl_2$-$CaCl_2$	0.1 M 4°C

2.2.4 Solutions for Tissue Culture

Minimum Essential Medium (MEM)	Gibco, Invitrogen Corp., 10% FBS, 100 μg /ml antibiotics/antimycotics
	Phosphate Buffered Saline, pH 7.2 Gibco, Invitrogen Corp.
Cell freezing mixture	10% DMSO in FBS
Trypsin-EDTA	Gibco, Invitrogen Corp., (0.25% Trypsin, EDTA·4Na) (1X)
RPMI/HEPES	RPMI 1640, FBS, HEPES 10 mM, pH 7.4

2.2.5 Solutions for the FITC labeling of Cells

Wash Buffer	0.1% BSA in PBS
Fixative	1% formaldehyde in PBS
Annexin-V-FITC	BD Bioscience./Roche Diagnostics.
Prodium iodide (PI)	BD Bioscience./Roche Diagnostics.

2.2.6 Solutions for Cell Lysates and Immunoprecipitation (IP) Buffers

IP buffer	10 mM Tris pH 8.0, 150 mM NaCl, 2.5 mM EDTA, 1% (w/v) NP40, 1mg/ml BSA, 0.02% (w/v) sodium azide
100 mM PMSF	Prepared fresh in ethanol

100 mM Iodoacetamide	Prepared fresh in PBS
1 mg/ml Sulfo-NHS-biotin	Prepared fresh in PBS
0.1% BSA in PBS	Prepared from 10% stock solution
IP-PI buffer	IP buffer, 0.5 mM PMSF, 2.5 mM Iodoacetamide
IP-PIA buffer	IP-PI buffer with 75 μg/mlaprotonin
Sucrose cushion	30% (w/v) sucrose in IP buffer, stored at 4°C

2.2.7 Buffers for SDS-PAGE

10x Running buffer	0.25 M Tris, 1.9 M Glycine, 1%(w/v) SDS
4x Separating gel buffer	1.5 M Tris, 0.4% (w/v) SDS, pH8.8
4x Stacking gel buffer	0.5 M Tris, 0.4% (w/v) SDS, pH6.8
Sample loading buffer	0.01% (w/v) bromophenol blue, 2% (w/v) SDS, 8 M urea, 0.2 M Tris pH 8.0

2.2.8 Protein Blotting Buffers

Blotting buffer	12.5 mM Tris pH 8.0, 96 mM glycine, 10% (w/v) ethanol
Blocking buffer	3% dried milk, 0.05% Tween® 20 in PBS
Washing buffer	0.1% (v/v) Tween® 20 in PBS

2.3 METHODS

2.3.1 General Methods for DNA Manipulation

Many of the methods used, unless otherwise stated, are modifications of methods described by Molecular Cloning 3rd Version. (Sambrook et.al 2001)

2.3.1.1 Phenol/Chloroform and Chloroform Extraction

This procedure was used to remove contaminating proteins from DNA. Phenol:chloroform were added in an equal volume to a DNA solution, mixed by vortexing for 30s and centrifuged for 2 mins at 12,000 rpm in a bench microfuge at room temperature(Sartorius, Sigma). The top aquatic layer was carefully transferred to a fresh tube, avoiding the precipitated protein at the interface. Traces of phenol were removed by repeating this process by adding an equal volume of chloroform.

2.3.1.2 Ethanol precipitation of DNA

DNA was precipitated by the addition of NaAc, pH 6.0, to a final concentration of 0.3 M, plus 2.5 times the combined volume of absolute ethanol. This solution was kept at -70 4°C for 45 min, or in dry ice/ethanol for 15 min. Following centrifugation at 12,000g for 10 min at 4°C the DNA pellet was washed with chilled 70% (v/v) ethanol to remove contaminating salt. The pellet was dried briefly on the bench and redissovled in TE buffer or sterile Mili-Q water.

2.3.1.3 Isopropanol precipitation of DNA

DNA was precipitated by the addition of 7/10 volume of isopropanol pre-equilibrated to RT. Following centrifugation at 12,000 g for 30 min at 4°C the DNA pellet was washed with chilled 70% (v/v) ethanol to remove contaminating salt. The pellet was dried briefly on the bench and redissolved in TE buffer or sterile Mili-Q water.

2.3.1.4 Quantitation of DNA

The concentration of DNA was determined by its absorbance at a wavelength of 260 nm (using a SHIMAZHU BioSpec-Mini digital ultravaiolet spectrophotometer) based on the calculation: 50 μg/ml double-stranded DNA gives an OD_{260} of 1. The OD_{280} was also read and the purity of the DNA was estimated using the ratio of OD_{260}/OD_{280}.

2.3.1.5 Restriction endonuclease digestion

Restriction endonuclease digestions were usually carried out in 20~100 μl volume reactions, where 2~5 units of enzyme were used for up to 500 ng of DNA, for 4~18 hours at an appropriate tempreture. Commercially available 10x buffers were used according to the manufacturer's instructions. In case where the supplied reaction buffer was not used, reaction buffers were prepared (10mM Tris pH 8.0, 10 mM $MgCl_2$, 10 mM DTT with the recommended concentration of NaCl). 5 mM spermidine was usually included except when the reaction buffer contained no NaCl. Where buffer requirements were incompatible for a multiple enzyme digestion, restriction digestion were performed sequentially with a column purification (QIAGEN) between each.

2.3.1.6 Synthesis and purification of oligonucleotides

Oligonucleotides were purchased from reputable suppliers (Proligo). The design of the oligonucleotides varied according to their intended use. For example, those intended for use as PCR primers were matched for melting/annealing temperature (Tm), the temperature at which half of the molecules will be dissociated from a complementary DNA strand. Tm is calculated according to the formula:

$$Tm = 4(G+C) + 2(A+T)$$ (Wallace and Miyada, 1987)

Alternatively the following formula derived from EMBL (Heidelberg, Deutschland) was used:

$$Tm = 64.9 + 41x\ (G+C-16.4)/(A+G+C+T)$$

For PCR, the oligonucleotides were commonly used 20 bases long, with a Tm around 60°C. Stocks were stored at -20 °C.

2.3.1.7 "End Filling" of DNA fragments with recessed 3' end

The Klenow Fragment of *E.coli* DNA polymerase together with nucleotides was used to prepare DNA fragments with recessed 3' end for blunt ended ligations. Depengding on the composition of the 5' overhang the DNA fragment was incubated in a 150 µl reaction containing 10 mM Tris pH 8.0, 5 mM $MgCl_2$, 0.1 mM DTT, 0.05 mg/ml BSA, 50 µM of nucleotides (dATP, dTTP, dGTP, dCTP). The reaction was left for 40 min at RT before heat inactivation at 65 °C for 20 min. The DNA fragment was purified by agarose gel electrophoresis before subsequent ligations.

2.3.1.8 Separation by agarose gel electrophoresis

A 0.8% Bio-Rad agarose gel was normally used for anyalysis of 0.3 ~ 8.0 kb DNA fragments. To improve the resolution of DNA fragments < 0.1 kb a 1.5% Bio-Rad agarose gel was used. Agarose (Bio-Rad) was melted in 1x TAE, cooled to 55 °C and ethidium bromide was added to a final concentration of 1 μg/ml before casting. The gel was allowed to set at RT for at least 20 min or at 4 °C for 10 min. Electrophoresis was carried out in a horizontal tank with the gel submerged in 1x TAE at < 100 mA. DNA samples were loaded with glycerol loading dyes and a standard DNA ladder (100 bps ladder or 1 kb ladder, 20 ng/μl, Ferments and New England Laboratories) was used to estimate the size of the DNA fragments. DNA fragments were visualized by fluorescence under a UV light in Gel Dock and recorded (Syngene, Evolve Science Pte Ltd.)

2.3.1.9 Purification of DNA fragments by agarose gel electrophoresis

Gel slices containing the DNA fragments to be purified were cut from the gel using a scalpel blade and avoided exposure to the UV light. DNA was extracted using a QIAquick Gel Extraction Kit (QIAGEN Ltd.)

2.3.1.10 Alkaline phosphatase treatment of DNA fragments

DNA fragments were treated with alkaline phosphatease to reduce self ligation or ligation with other alkaline phosphatase treated DNA fragments. Alkaline phosphatase (Ferments, 1 unit per 50 pmol 5' DNA molecules) was added to the DNA mix at the time of endonuclease digestion. No alternative buffer conditions were

necessary. After an incubation of 1~4 h the reaction mix was heated to 65 °C for 10 min to inactivate the enzyme. The DNA was purified for ligation, by using a QIAQuick PCR Purification Kit (QIAGEN Ltd.)

2.3.1.11 DNA ligation

DNA fragments with complementary ends to be ligated were prepared by restriction enzyme digestion and where necessary treated with alkaline phosphatase and/or purifed using agarose gel electrophoresis to reduce background ligations. Vector DNA (~10 ng) and insert DNA (20~40 ng) were ligated using 1 unit if T4 DNA ligase in a 10 µl reaction mixture containing 1mM ATP, 50 mM Tris-HCl pH 8.0, 10 mM $MgCl_2$, 20 mM DTT, 50 µg/ml BSA and incubated at 16 °C overnight. As controls, a reaction with insert DNA and a reaction without both insert DNA and T4 DNA ligase were included in the experiment. The ligation reaction was used directly to transform competent cells or stored at -20 °C.

2.3.1.12 Preparation of *E.coli* competent cells

Competent cells of *E.coli* strain DH-5α and BL-21 were routinely used for plasmid transformation. The bacteria were streaked out a LB agar plate (amp^r) and incubated at 37 °C for ~18 h. A single clony was used to inoculate 20 ml LB broth in a 250 ml flask and incubated at 37 °C with constant shaking for 3 h (OD_{600} of 0.35). The culture was transferred into a 50ml polypropylene tube (Falcon) and cooled down to 0 °C by leaving on ice for 10 min. The bacteria were sedimented by centrifugation at 4100 rpm for 10 min at 4 °C and resuspended in 150 ml pre-chilled 0.1 M

$CaCl_2$-$MgCl_2$ (80 mM $MgCl_2$, 20 mM $CaCl_2$) solution. The bacteria were pelleted by centrifugation at 4100 rpm for 10 min at 4°C and resuspended in 10 ml pre-chilled 0.1 $CaCl_2$M solution. The competent bacteria were divided into 600 µl alquots in pre-chilled microfuge tubes, flash frozen in liquid nitrogen and stored at -70°C.

2.3.1.13 Transformation of *E.coli* with plasmid DNA

Competent *E.coli* cells were thawed on ice. 100 µl competent cells were mixed with 5 µl of a ligation mix, or with 5 ng plasmid DNA, in a pre-chilled 1.5 ml microfuge tube and incubated on ice for 30 min and then heated to 42 °C for 2 min. 200 µl LB was added and the cells were allowed to recover at 37°C for 1 h. The cells were pelleted by a flash centrifugation and resuspended in 50 µl LB. 5 µl and 45 µl were routinely plated on separated plates for each transformation mixture. Plates were incubated at 37°C for 18 h. Transformation efficiency could be estimated using uncut plasmids.

2.3.1.14 Bacterial cell stocks

10 µl of overnight culture was mixed with 30 µl glycerol and 260 µl LB broth and stored at -70°C.

2.3.1.15 Purification of plasmid DNA

For small scale purification of plasmid DNA 5 ml LB broth was inoculated with a single clony from an agar plate or a glycerol cell stock and incubated at 37°C with constant shaking for ~16 h. For sequencing plasmid DNA was prepared using a

Plasmid Mini Kit (QIAGEN Ltd.) according to the manufacturer's instructions.

For large scale purification of plasmid DNA of trasfection quality, a Plasmid Midi Kit or Plasmid Maxi Kit (QIAGEN, Ltd) was used according to the manufacturer's instructions.

2.3.1.16 Polymerase chain reaction (PCR)

DNA fragments between two oligonucleotide primers were amplified by PCR through repeated cycles of three incubation steps at different tempretures for denaturation of the template, annealing of the oligonucleotide primers to the template and the extention of the oligonucleotide primers by DNA polymerase (Saiki et al., 1988) respectively. A typical cycle included denaturation at 94°C for 1 min, annealing for 30 sec at a temperature 5–10°C below the lower Tm of the two primers and an extension at 72°C for an appropriate period of time (normally 1 min per kb)

2.3.1.17 Standard PCR protocol

PCR was routinely performed in a 20 µl reaction volume containing 1 µl template DNA (~0.2 µg), 1 µM each oligonucleotide primer, 200 µM each dNTP, 2 µl 10x reaction buffer (supplied with enzyme) and 1 unit of DNA polymerase. *Pfu* DNA polymerase (Stratagene) was used for high fidelity DNA synthesis. *Tag* DNA polymerase (Promega) was used for PCR colony screening.

2.3.1.18 Combinatorial PCR

When the products of two separate PCR reactions had an overlapping sequence of at

least 15 bp at the end, they could be combined using PCR. Both PCR products to be combined were separated from their original templates and oligonucleotide primers and were purified by agarose gel electrophoresis. The combination PCR reaction used the two purified products from the original reactions as template amd the two outside oligonucleotide primers. After denaturation the two PCR products from the original reactions could anneal to each other after denaturation via their overlapping sequence. The annealed 3' ends were extended via PCR to give a combined PCR product (Higuchi, 1989). This combined product was then amplified using the outside primers. This method was employ to generate gene of HBSP.

2.3.1.19 Identification of colonies that contain recombinant plasmid of interest

Colonies of interest were identified using either PCR screening or restriction endonuclease digestion depending on the availability of suitable PCR primers for screening and the degree of background indicated by the control plates. Each colony to be tested was used to inoculate 20 μl LB broth in a 0.5 μl Eppendorf tube using a sterile pipette tip. 10 μl of this inoculated LB broth was layered by paraffin oil to the top and heated to 98°C for 10 min before cooling down on ice for 10 min. Pellete was sedimented by centrifugation at 13, 2000 rpm for 10 min and discarded. The supernatant containing plasmid beneath paraffin oil was pipetted out and added to a PCR reaction as template. A negative control and, where possible, a positive control were included in the experiment. Colonies containing the correct recombinant clone of interest were indentified by the size of their PCR products ising agarose gel electrophoresis.

Positives from PCR screening were routinely confirmed by using restriction endonuclease digestion. The colonies inoculated to LB broth corresponding to those screened by PCR were cultured in a 5 ml LB broth overnight at 37°C for a DNA mini prep and subsequent restriction endonuclease digestion.

2.3.1.20 Sequencing of double-stranded DNA templates

DNA sequencing was performed by the dideoxy chain-termination method (Sanger *et al.* 1977) using the T7 sequencing kit™ (Pharmacia) following the manufacture's instructions. Briefly, the double-stranded DNA template was denatured using NaOH at a final concentration of 0.4 M at 37 °C for 30 min. The denatured DNA templates were precipitated by ethanol and resuspended in 10 µl H_2O. 2 µl of 10 µM oligonucleotide primer and 2 µl of the supplied Annealing Buffer were mixed with the template and incubated at 37 °C for 20 min and RT for a further 10 min. the extension and labeling with [α-S^{35}]dATP of the annealed template-primer and termination of the reactions were carried out using the T7 DNA polymerase and dideoxynucleotides and other reagents orivided in the kit.

2.3.1.21 Denaturing polyacrylamide gel electrophoresis of sequencing reaction

Denaturing polyacrylamide gel electrophoresis was used to separate single-stranded DNA fragments for the analysis of sequencing reactions. A suitable volume of 6% polyacrylamide gel was prepared according to the size of plates to be used by combining Sequagel® -6 Ready-to-use 6% Sequencing Gel Solution (National

diagnostics) and Sequagel™ buffer reagent (National Diagnostics) at a 4:1 ratio with 0.8% (v/v) of 10%(w/v) ammonium persulphate. The gel mix was immediately poured between the two glass plates with the notched one had been siliconised prior to taping the other together (Bio-Rad). A shark's tooth comb was inserted to form flat base for sample loading wells and the plates were tightly clipped together with bulldog clips.

Gels were allowed to set for at least 1 h at RT before use. Samples were preheated to 85 °C for 5 min before loading at 2.5 µl per lane. Electrophoresis was carried out in vertical gel apparatus in 1x TAE buffer at 30 mA. The gel was usually preheated, by running for 30 min immediately prior to sample loading, in order to ensure that the samples ran at a consistent temperature for the whole period of running. This was important if more than one loading was being used on a single gel.

Following electrophoresis the siliconised plate was removed and the gel was fixed by soaking in 10 % acetic acid, 10 % methanol for 30 min and then rinsed in water. The gel was transferred onto 3M Watman paper and dried in a Model 583 Ger Dryer (Bio-Rad) and exposed directly to Kodak X-OMAT film at RT for 18 h, or longer if necessary. Films were developed in a Kodak X-OMTA ME-1 processor.

2.3.1.22 Automated sequencing

Sequencing was also carried out by commercial company. Briefly, primers were extended on template DNA using the BigDye® dideoxynucleotide chain termination

method. Following precipitation to remove unincorperated dye, t he samples were analysed on ABI 377XL Prism DNA sequencers.

2.3.1.23 mRNA extraction from mammalian cells

Mammalian cells were collected by centrifugation at 2000rpm for 3 min. Cell pellete was use to extract mRNA by using a RNeasy® Mini Kit (QIAGEN Ltd.) according to the manufacturer's instruction. mRNA was stored at -70 °C.

2.3.2 Cell Culture Methods

Cell lines were cultured in 5 % CO_2/air at 37 °C in a humidified tissue culture incubator using Nunc or TPP tissure culture flasks (Life Tech.)

2.3.2.1 Cell storage in liquid nitrogen

Cells were dedimented at 300g, resuspending in freezing mixture (1-5x 10^6 cells/ml for HepG2 cell lines and 1-7x 10^6 cell/ml for 293T cells) and aliquotted into Cryo Vials (Greiner Lab.). Cells were frozen in a Nalgene™ Cryo 1 °C freezing container (Nalgene) for 24 h at -70 °C, to achieve a 1 °C/min rate of cooling, after which the vials were transferred to liquid nitrogen.

2.3.2.2 Cells' recovery from liquid nitrogen

Cells were removed from the liquid nitrogen, quickly brought to 37 °C, and washed in 10 ml of culture media. The cells were sedimented at 300 g, resuspended in 10 ml of growth media, and transferred to 50 ml flask for growth.

2.3.2.3 Culture of HepG2 and 293T cells

Cells were maintained in a fast growing, logarithmic state. When ~95% confluency was erached they were washed in PBS, without Ca^{2+}/Mg^{2+}, lifted by covering with 0.25% Trypsin (Gibco) for 5 min, followed by tapping of each flask. Media was added to dilute the cells as required (~4-8 dilution) for propagation or seeding for transfections (1.5-2 dilution). Cells were propagated indefinitely without any adverse effect on transfection efficiency.

2.3.2.4 Transfection of HepG2 and 293T cells by calcium phoshate and Effectene®

Effectene® reagent (QIAGEN Ltd.) was used to transfect HepG2 cells for the transient expression of viral protein according to supplier's instruction. For transfection in 6-well plate, 50% confluency was reached 16~24 h after cells were seeded. Cells were washed once by PBS (Gibco) before adding Effectene® reagent. A starting mixture which contained 0.4 μg of plasmid and 3.2 μl enhancer in a final volume of 100 μl in EC buffer was prepared and left at RT for 5 min with occasional swirling. 10 μl Effectene® reagent was added into the mixture and left at RT for 10 min. The mixture was added into cells evenly. Cells were incubated at 37 °C, 5% CO_2 and media was changed 2~3 h after. Cells were returned to the 37 °C incubator in complete media.

The Calcium Phosphate method of cell transfection (Graham and Van der Eb, 1973)

was used in 293T cells. For 60 mm dish, cells were seeded to reach ~50% confluentcy before transfection. One hour prior to the transfection, media was changed to contain 25μM chloroquine. A mixture containing 2~8 μg plasmid DNA, 360 μl H_2O, 55 μl $CaCl_2$ (2M) and 430 μl HBS (2x) was added into cells. Media was changed 8~11 h later and cells were returned to incubation in fresh media.

2.3.2.5 Harvesting of transfected cells

20~72 h after transfection the cells were washed in PBS (without Ca^2+/Mg^2+) and detached in 2~5 ml 0.25% trypsin by incubating at 37 °C for 2~8 min. 5~8 ml media containing FBS was added to the detached cells to neutrolise the trypsin. Cells were aliquotted depending on the type of assay to be carried out.

2.3.3 Experiment Assays

Some of the assays used are modified from methods described by Molecular Cloning 3rd Version. (Sambrook et.al 2001) Many of the commercially available kits are used according to manufactures' instructions, unless otherwise stated.

2.3.3.1 *In vitro* expression of proteins

To express proteins *in vitro*, a TnT® coupled wheat germ extract system was used. A standard reaction mixture contains 25 μl wheat germ extract, 2 μl 2x reaction buffer, 1 μl T7 RNA polymerase, 1 μl amino acid mixture (1mM, minus methionine), 1 μl [S^{35}]methionine (1000ci/mmol at 10mCi/ml), 1 μl ribonuclease inhibitor (40 u/μl) and 1 μg DNA template in a final volume of 50 μl with nuclease-free water. The

mixture was incubated at 30 °C for 1 h for transcription and translation. A small volume of mixture was loaded onto SDS-PAGE and run 200V for 1 h. The gel was fixed in methanol/acetic acid solution and dried using a gel dryer at 65 °C for 1 h. Kodak X-OMATS film was used to detect the radiation. Films were developed in a Kodak X-OMAT ME-1 processor.

2.3.3.2 Mammalian two-hybrid interaction analysis

Mammalian two hybrid system (Promega) was used to detect *in vivo* interaction between proteins. The pBIND contained a GAL4 binding domain in fusion with our viral protein coding reagion and an internal controlling *Renilla* Luciferase and served as pBD. The pACT contained a VP16 domain in fusion with interested proteins (Bcl-$_2$, Bcl-$_{xl}$, Bad, Bak, Bid, Bim) and served as pAD. pBIND, pACT and a reportor vector pG5*luc* which contained a firefly luciferase were co-transfected into HepG2 cells using Effectene® reagent. Media was changed 2~3 h after and cells were returned to incubation for 48 h in fresh midia.

2.3.3.3 Dual-luciferase® reporter assay for mammalian 2-hybrid system

Dual-luciferase® reporter assay system (Promega) was used to detect the mammalian 2-hybrid assay result. Cells were harvested by trysinization and sedimented by centrifugation at 2000 rpm for 5 min. Cell pellete was resuspended in suitable volume of lysis buffer and left on ice for 30 min. The total lysate was centrifuged at 15000 rpm for 15 min at 4 °C. 20 µl Supernatant was added to 100 µl predispensed Luciferase Assay Reagent (LAR) and mix by pipetting 2 or 3 times. A Sirius

luminoteter (Sirius Designs, Germany) was programmed to perform a 2-second premeasurement delay and followed by a 10-second measurement period for each reporter assay. The LAR mixture tube was then placed in the luminometer and initiated to read firefly luciferase activity. After reading, 100 µl Stop & Glo® reagent was added into the reagent to stop the firefly luciferase and initiate *renilla* luciferase reading which served as pBIND internal control. All the readings were recorded by the luminometer automatically. The ratio of firefly/*renilla* luciferase readings were calculated and compared to positive and negative readings.

2.3.3.4 Cell viability assay using MTT

After transfection, cells were harvested and counted in order to add $2x10^4$ cells/well in 100 µl of resuspended cells in a 96-well plate. Cells were aliquotted onto a fresh plate to be used to calculate the total cells on the assay plate before washing. Both plates were incubated at 37 °C for 48 h before being washed by fresh media and filled up with 100 µl media. 20 µl freshly prepared MTT (5 mg/ml in PBS, filtered through 0.22 µm filter) was added to each well, including those on the "total cells" plate. The plates were incubated at 37 °C for 3 h, during which the MTT was taken up by the living cells and cleaved intracellularly to an insobluble formazan product (Mosmann, 1983). The plates were centrifuged at 1000 g and the supernatant was removed by aspiration using a fine needle. The formazan crystals were dissolved in 200 µl DMSO per well and the absorbance was read at 562 nm using an ELISA plate reader (FL600, Bio-Tek, USA).

2.3.3.5 Caspase-3 fluorescent assay

Caspase-3 is an active cell-death protease involved in the execution phase of apoptosis. This assay aimed to detect the caspase-3 activity in cells. 293T Cells were transfected by plasmids containing viral protein coding region using calcium phosphate method. After an incubation period of 48 h, Cells were harvested by gentle trypsinization and sedimented by centrifugation at 2000 rpm for 5 min. Cell pellet was resuspended in PBS and washed for 1 time. After centrifugation, cell pellet was resuspended in 50 µl of prechilled lysis buffer and incubate on ice for 30 min. Cell lysate was centrifuged at 15000 rpm for 10 min at 4 °C to precipitate cellular debris. The supernatant was added to 50 µl 2x reaction buffer which contained 50 µM of caspase-3 substrate (DEVD-AFC). Incubate the reaction mixture at 37 °C for 3 h after which the mixture was tranfered to a 96-well plate and read in an ELISA plate reader (FL600, Bio-Tek, USA). The samples were read through an endpoint protocol set as for 400-nm excitation and 505-nm emission. The results were recorded automatically and analysed by comparing to positive and negative controls' readings.

2.3.3.6 Flow cytometric analysis

FACS analysis was used to detect externalization of phosphotidylserine (PS) during apoptosis in viral protein transfected cells. Harvested cells were sedimented at 300 g and resuspended in a suitable volume of wash buffer. After wash cell were sedimented and resuspended in 200µl 1x binding buffer. 5 µl of Annexin-V-FITC and 10 µl Propidium Iodide were added into the cells. Incubate cells at RT for 15 min in the dark before using binding buffer to bring the reaction volume to at least 500 µl for

BD FACS analysis using a single laser emitting excitation light at 488 nm.

2.3.3.7 Analysis of flow cytometric data

Externaliztion of PS was primarily characterized using dotblot. Additionally statistics were calculated using the function of the Cell Quest software (Becton Dickinson). Gates were set to include the most fluorescent 95% of the cells using the cell diameter and granulity. This gate was used to calculate the percentage of cells that were positive or negative. Cells were divided into 4 quadrants depending on the dual staining of FITC and PI and quadrant statics were calculated automatically.

2.3.3.8 Polyacrylamide gel electrophoresis in sodium dodecyl sulphate (SDS-PAGE)

Gels containing 5% polyacrylamide were made as stacking gel and gels containing 12% polyacrylamide were made as separating gel according to the method of leammli (1970). Proteins were reduced prior to electrophoresis by incubating in an equal volume of sample and SDS-loading buffer (2x) containing a final concentration of 20 mM DTT for 5 min at 100 ^{o}C. Presained Hig Range Molecular Weight Protein Markers were denatured similarly and loaded in the same volume as the test samples. Electrophoresis was carrie out at a constant voltage of 100 V (~2 h), according to the migration of the prestained markers.

2.3.3.9 Western blot assay

Proteins separated by SDS-PAGE were transferred onto PVDF membrane (Rio-Rad)

by western blotting. The PVDF membrane was prepared according to the manufacturer's instructions: Pretreated in ethanol for 10 sec, washed in water until miscible and washed in blotting buffer for 5~10 min. The SDS-PAGE gel was agitated in blotting buffer for a minimum of 15 min. Blotting was carried out in semi-dry western blotting apparatus (Bio-Rad) in blotting buffer at 21~25 V for 30~45 min. The PVDF membrane was then transferred to blocking buffer and agitated at RT for 1 h.

2.3.3.10 ECL detection of protein blotted onto PVDF membrane

The PVDF membrane was removed from blocking buffer and agitated in 1:5000 dilution of primary antibody for 1 h at RT. It was then washed three times in PBS-T for 15 min each at RT. The membrane was agitated in 1:5000 dilution of secondary antibody which was labelled with Horseradish Peroxidase (HRP) in PBS-T for another 1 h at RT, followed by three 15 min washes in PBS-T. An ECL kit (Amersham) was used to detect the protein by exposure to Kodak X-OMATS film at RT for 10 sec – 4 h as necessary. Films were developed in a Kodak X-OMAT ME-1 processor.

2.3.3.11 DNA fragmentation detection

Nuclear DNA fragmentation, a hallmark of apoptosis was detected based on the terminal deoxynucleotidyl transferase-mediated dUTP nick-end labeling (TUNNEL) method (Lazebnik, et al. 1994). HepG2 cells growing on chamber slides (Lab-Tek) were transfected with plasmids by Effectence® reagent and changed media 2 h later.

After 48 h of induction slides were washed twice by PBS before fixing the cells using 4% formaldehyde/PBS at 4 °C for 25 min. Cells were immersed in PBS for another 3 times to remove formaldehyde trace before being penetrated by 0.2% Triton X-100 for 5 min on ice. After that, the slide was washed by PBS for 2 times and immersed in 100 µl of equilibration buffer to equilibrate at RT for 10 min. TdT incubation buffer containing fluorescent nucleotide mix and TdT enzyme was added onto the slide and covered by a piece of coverslip to evenly spread the liquid. To perform the tailing reaction, place the slide into 37 °C 5% CO_2 incubator for 1 h. After incubation terminating buffer was added onto the slide and incubated for 15 min at RT. The slide was washed twice by PBS and added a drop of anti-fade reagent and viewed as soon as possible under confocal microscope using a standard fluorescein filter set (520+_20 nm).

2.3.3.12 Indirect immunofluorescence detection of viral proteins

HepG2 Cells were grown on chamber slide (Lab-Tek) and transfected with plasmid DNAs using Effectene® reagent. After 48 h's induction, cells were washed by PBS and fixed by 4% formaldehyde/PBS at RT for 15 min. Incubation with 0.2% Triton X-100/PBS at RT for 10 min was used to penetrate cells before they were rinsed thrice by PBS. Mono-specific antisera were diluted to 1:50 in PBS and incubated with cells for at least 1 h at RT. Cells were then subjected to three washes with PBS and incubated with anti-mouse IgG conjugated to FITC (Sigma) or TRITC (Sigma) diluted in PBS (1:30~ 1:50) for at least 1 h at 4 °C. After three washes with PBS, cells were mounted with glass coverslips using a fluorescence mounting demium

containing 15 mM NaN_3 (Dako). Slides were subjected to con-focal microscope. The green (FITC) or red (TRITC) fluorescence could be detected using respective filters at appreciate wavelength according to the microscope settings.

2.3.3.12 Protein expression and purification in *E.coli*

pGEX-5X-1 containing gene of interest was used to express protein in fusion with Glutathione S Transferase (GST) in *E.coli* strain BL21. Cells were grown on LB agar plate at 37 °C overnight. Innoculate one colony into 5 ml LB broth and shake for 10 h before being poured into 2ml LB broth. When the cells grew to an $O.D_{600}$=0.6~0.8 2 h after, IPTG was added into the broth to a final concentration of 0.5~1mM. The broth was incubated at 16 °C with constant shaking at 220 rpm overnight. Cells were harvested by centrifugation at 5500 rpm for 10 min at 4 °C. Cell pellete was resuspended in 30 ml PBS and subjected to a sonicator with 5-sec on 3-sec off protocol (22% amplitude). A small volume of cell lysate was reserved for SDS-PAGE while most of the total lysate was applied to a centrifugation > 20,000 g at 4 °C for 30min. The cell debris was decarded and the supernatant was mixed with GST beads (Amersham) while a small volume was reserved for SDS-PAGE. The mixture was put on a roller mixter at 4 °C for 1 h's incubation. The mixture was then poured in a purification column (Amersham) and went through. Flow through fluid was kept for further usage and the beads were washed by PBS. Elution buffer was add to the clean beads and went through. A small volume of elution fluid was selected to SDS-PAGE while most of them were stored at 4 °C. A SDS-PAGE was run and stained by Commasie Blue to tell the protein expression and purification efficiency. Based on the

gel result, the elution fluid contains the purified protein. If needed, a following FPLC separation was carried out to remove adulterated protein. The purified protein could be identified by mass spectrometry.

Chapter Three: cDNA Constructs

3.1 INTRODUCTION

This chapter describes the strategies used to generate Bcl-2 family of proteins cDNAs, HBV viral protein cDNAs and to introduce point mutation into the HBV polymerase, HBx and HBSP. Bcl-2 family of proteins cDNAs were derived from mRNA extracted from mammalian cells. HBV viral proteins cDNAs were amplified from pcDNA3.1-HBV Genome (Genotype A) provided by A/P W.N. Chen William (SCBE, NTU, Singapore)

Cloned PCR fragments were sequenced to ensure the presence of inserted genes and correctness. The strategies for cloning cDNAs into vectors for transient expression are also described in this chapter. The rationale of the choice of point mutations included in this investigation, and their subsequent analysis will be described in following chapters. To avoid confusion, all of the text in this chapter will be shown together, followed by figures and tables in the order they are referred.

3.2 GENERATION OF Bcl-2 FAMILY OF PROTEINS AND VIRAL PROTEINS

All the cDNAs of Bcl-2 family of proteins used were amplified from mRNA extracted from tumor cell lines (HepG2, Huh7, COS7) using *reverse transcriptase* RCR method. Viral proteins cDNAs were amplified from an infective HBV genome A by normal PCR. The spliced variant HBSP cDNA was amplified as two parts and joined using a combinatorial PCR reaction. All these cDNAs were confirmed after

amplification. Their sequences were shown in figure 3.1.

Bcl-2:

MAHAGRTGYDNREIVMKYIHYKLSQRGYEWDAGDVGAAPPGAAPAPGIFSSQPGHTPHPAASRDPVART
SPLQTPAAPGAAAGPALSPVPPVVHLALRQAGDDFSRRYRGDFAEMSSQLHLTPFTARGRFATVVEELFRD
GVNWGRIVAFFEFGGVMCVESVNREMSPLVDNIALWMTEYLNRHLHTWIQDNGGWDAFVELYGPSMRP
LFDFSWLSLKTLLSLALVGACITLGAYLSHK

Bcl-xl:

MSQSNRELVVDFLSYKLSQKGYSWSQFSDVEENRTEAPEGTESEMETPSAINGNPSWHLADSPAVNGATA
HSSSLDAREVIPMAAVKQALREAGDEFELRYRRAFSDLTSQLHITPGTAYQSFEQVVNELFRDGVNWGRIV
AFFSFGGALCVESVDKEMQVLVSRIAAWMATYLNDHLEPWIQENGGWDTFVELYGNNAAAESRKGQER
FNRWFLTGMTVAGVVLLGSLFSRK

Bax:

MDGSGEQPRGGGPTSSEQIMKTGALLLQGFIQDRAGRMGGEAPELALDPVPQDASTKKLSECLKRIGDEL
DSNMELQRMIAAVDTDSPREVFFRVAADMFSDGNFNWGRVVALFYFASKLVLKALCTKVPELIRTIMGWT
LDFLRERLLGWIQDQGGWDGLSYFGTPTWQTVTIFVAGVLTASLTIWKKMG

Bad:

MFQIPEFEPSEQEDSSSAERGLGPSPAGDGPSGSGKHHRQAPGLLWDASHQQEQPTSSSHHGGAGAVEIRS
RHSSYPAGTEDDEGMGEEPSPFRGRSRSAPPNLWAAQRYGRELRRMSDEFVDSFKKGLPRPKSAGTATQM
RQSSSWTRVFQSWWDRNLGRGSSAPSQ

Bak:

MASGQGPGPPRQECGEPALPSASEEQVAQDTEEVFRSYVFYRHQQEQEAEGVAAPADPEMVTLPLQPSST
MGQVGRQLAIIGDDINRRYDSEFQTMLQHLQPTAENAYEYFTKIATSLFESGINWGRVVALLGFGYRLALH
VYQHGLTGFLGQVTRFVVDFMLHHCIARWIAQRGGWVAALNLGNGPILNVLVVLGVVLLGQFVVRRFF
KS

Bik:

MSEVRPLSRDILMETLLYEQLLEPPTMEVLGMTDSEEDLDPMEDFDSLECMEGSDALALRLACIGDEMD
VSLRAPRLAQLSEVAMHSLGLAFIYDQTEDIRDVLRSFMDGFTTLKENIMRFWRSPNPGSWVSCEQVLLA
LLLLLALLLPLLSGGLHLLLK

HBV Polymerase:

MPLSYQHFRKLLLLDXXXEAGPLEEELPRLADEGLNRRVAEDLNLGNLNVSIPWTHKVGNFTGLYSSTV
PIFNPEWQTPSFPHIHLQEDIINRCQQYVGPLTVNEKRRLKLIMPARFYPNLTKYLPLDKGIKPYYPEHAVN
HYFKTRHYLHTLWKAGILYKRETTRSASFCGSPYSWEQELQHGRLVFQTSTRHGDESFCSQSSGILSRSPV
GPCVRSQLKQSRLGLQPQQGSLARGKSGRSGSIRARVHPTTRRSFGVEPSGSGHIDNSASSTSSCLHQSAV
RKTAYSHLSTSKRQSSSGHAVELHNIPPSSARPQSEGPILSCWWLQFRNSKPCSDYCLTHIVNLLEDWGPC
TEHGEHNIRIPRTPARVTGGVFLVDKNPHNTTESTLVVDFSQFSRGSTHVSWPKFAVPNLQSLTNLLSSNL
SWLSLDVSAAFYHIPLHPAAMPHLLVGSSGLPRYVVCLSSTSKNINYQHGTMQ

DLHDSCSRNLYVSLFLLYKTFGRKLHLYSHPIILGFRKIPMGVGLSPFLLAQFTSAICSVVRRAFPHCLAFS
YMDDVVLGAKSVQHLESLFTSITNFLLSLGIHLNPNKTKRWGYSLNFMGYVIGCWGTLPQEHIVLKIKQC
FRKLPVNRPIDWKVCQRIVGLLGFAAPFTQCGYPALMPLYACIQSKQAFTFSPTYKAFLCKQYLNLYPVA
RQRSGLCQVFADATPTGWGLAIGHRRMRGTFVAPLPIHTAELLAACFARSRSGAKLIGTDNSVVLSRKYT
SFPWLLGCAANWILRGTSFVYVPSALNPADDPSRGRLGLYRPLLHLPFRPTTGRTSLYAVSPSVPSHLPDR
VHFPSPLHVAWRPP

HBV Polymerase N-terminal:

MPLSYQHFRKLLLLDXXXEAGPLEEELPRLADEGLNRRVAEDLNLGNLNVSIPWTHKVGNFTGL

HBx:

MAARVCCQLDPARDVLCLRPVGAESRGRPVSGPFGPLPSPSASAVPANHGAHLSLRGLPVCAFSSAGPCA
LRFTSARRMETTVNAHQVLPKVLYKRTLGLSAMSTTDLEAYFKDCLFKDWEELGEEIRLKVFVIGGCRH
KLVCSPAPCNFFTSA

HBx C-Ternimal:

RTLGLSAMSTTDLEAYFKDCLFKDWEELGEEIRLKVFVIGGCRHKLVCSPAPCNFFTSA

HBSP:

MPLSYQHFRKLLLLDXXXEAGPLEEELPRLADEGLNRRVAEDLNLGQDQQQPVRDHAKPARLLLKATLC
FPHVAVQNLRMEIAPVFPSHRPGL

Figure 3.1: Amino acid sequence of Bcl-2 family of protein and viral proteins. As indicated are Bcl-2, Bcl-xl, Bax, Bad, Bak, Bik, HBV Polymerase, POL-N, HBx, HBx-C and HBSP. All the sequences are displayed by one-letter amino acid abbreviation.

3.3 SUBCLONING INTO EXPRESSION VECTORS

The modified viral proteins POL, POL-N, HBX and HBX-C were cloned into expression vector pACT (Promega Corp.). The hypothesized interacting Bcl-2 family of proteins was cloned into the expression vector pBIND (Promega Corp.). This pair of vectors was selected because: they are suitable for use in HepG2 transient transfection, they contain convenient enzyme restriction sites in the polylinker, they are relatively small and thus easy to manipulate by molecular cloning techniques, they have a high copy number for growth in *E.coli* thus facilitating the large scale preparation of DNA for transfection studies, and most importantly they are designed

suitable to investigate protein-protein interation in mammalian two-hybrid system. The selected HBX, HBSP and POL-N cDNAs were cloned into prokaryocyte expression vector pGEX-5X-1 (Amersham Int.) to be in frame with a GST coding gene. The GST-viral proteins were then modified and subcloned into expression vector pXJ-40 provided by Dr S.M. Tan (SBS, NTU) (Fig. 3.1b). Besides the benefits stated before, this 2-step cloning facilitated the viral proteins with a GST to stabilize their expression and easy to be detected with a HA tag at the N-terminal. The multiple cloning sites region and main features of vectors are shown in figure 3.2a~3.2e

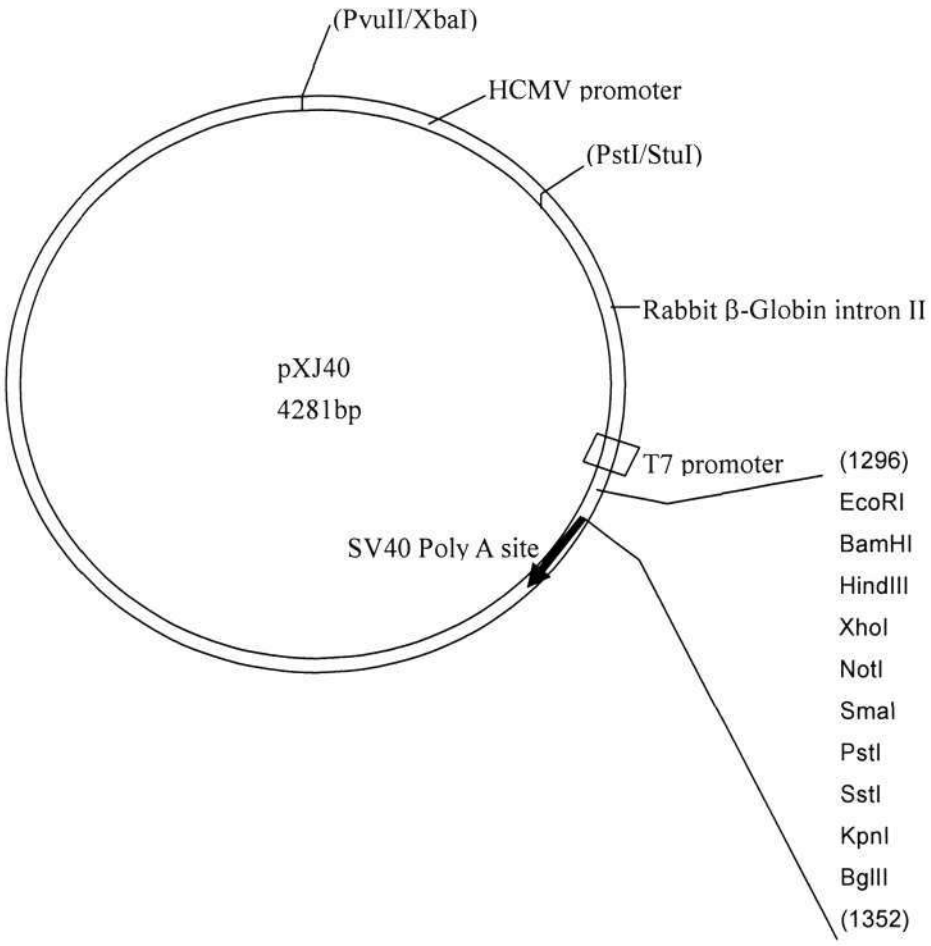

Figure 3.1b: pXJ-40 Vector circle map and MCR

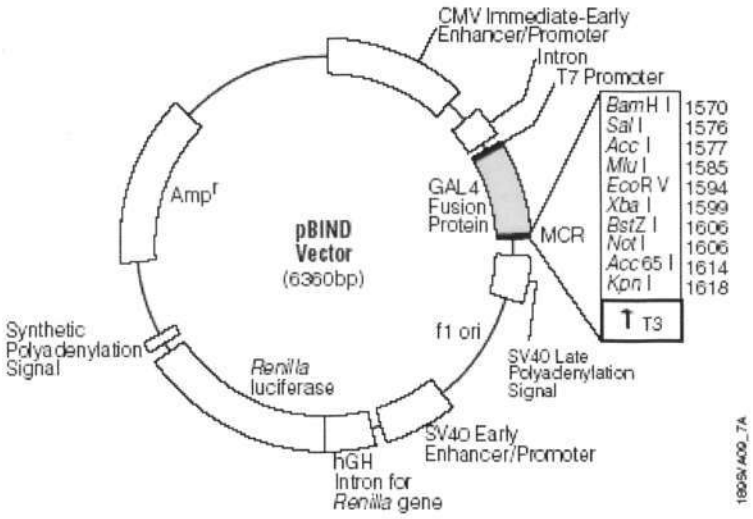

pBIND Vector sequence reference points:

CMV immediate-early enhancer	1–659
CMV immediate-early promoter	669–750
chimeric intron	890–1022
T7 EEV sequencing primer binding site	1053–1074
T7 RNA polymerase promoter (–17 to +2)	1067–1085
GAL4 fusion protein	1116–1556
multiple cloning region (MCR)	1570–1619
T3 RNA polymerase promoter (–16 to +3)	1639–1657
SV40 late polyadenylation signal	1666–1887
phage f1 origin of replication	1982–2437
SV40 early enhancer/promoter	2527–2872
SV40 minimum origin of replication	2770–2835
hGH intron for *Renilla* gene	2924–3183
Renilla luciferase gene coding region	3208–4143
synthetic polyadenylation signal	4201–4249
β-lactamase (Amp^r) coding region	4668–5528

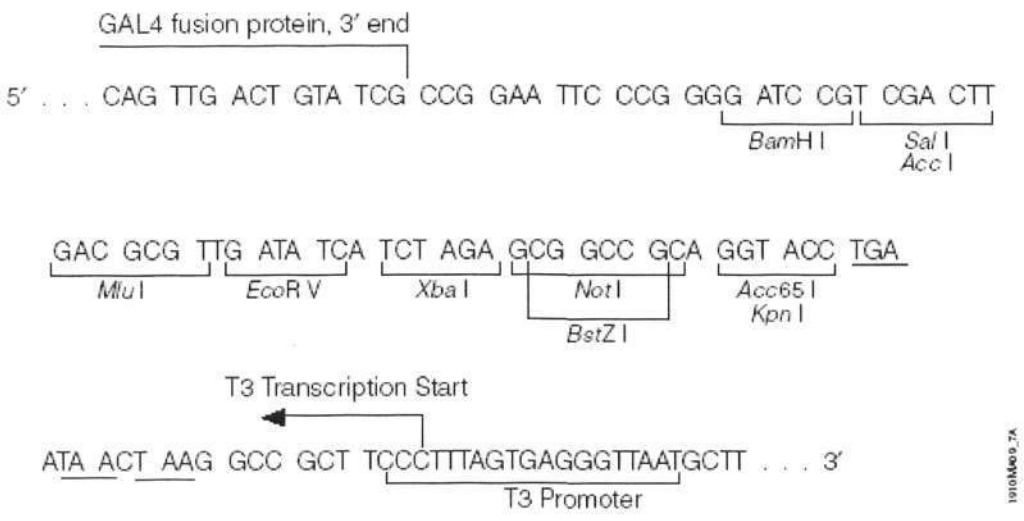

Figure 3.2a: pBIND Vector circle map, sequence reference points and MCR

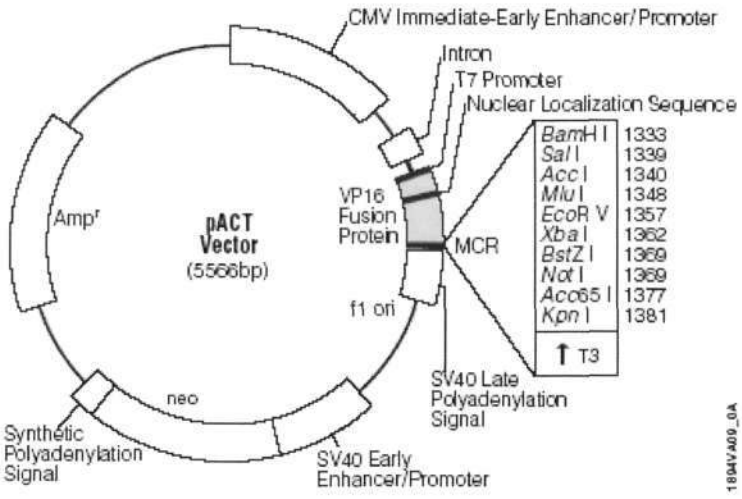

pACT Vector sequence reference points:

CMV immediate-early enhancer	1–659
CMV immediate-early promoter	669–750
chimeric intron	890–1022
T7 EEV sequencing primer binding site	1053–1074
T7 RNA polymerase promoter (–17 to +2)	1067–1085
GAL4 1–11 amino acids	1116–1148
VP16 fusion protein	1188–1325
multiple cloning region	1333–1382
T3 RNA polymerase promoter (–16 to +3)	1402–1420
SV40 late polyadenylation signal	1429–1650
phage f1 origin of replication	1693–2148
SV40 early enhancer/promoter	2181–2526
SV40 minimum origin of replication	2424–2489
neomycin (neo) phosphotransferase coding region	2571–3365
synthetic polyadenylation signal	3429–3477
β-lactamase (Ampr) coding region	3874–4734

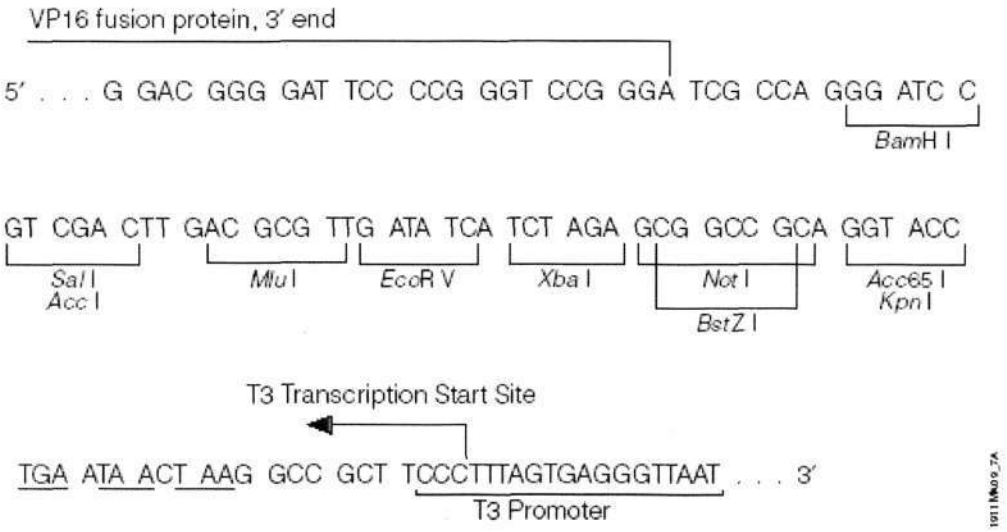

Figure 3.2b: pACT Vector circle map, sequence reference points and MCR

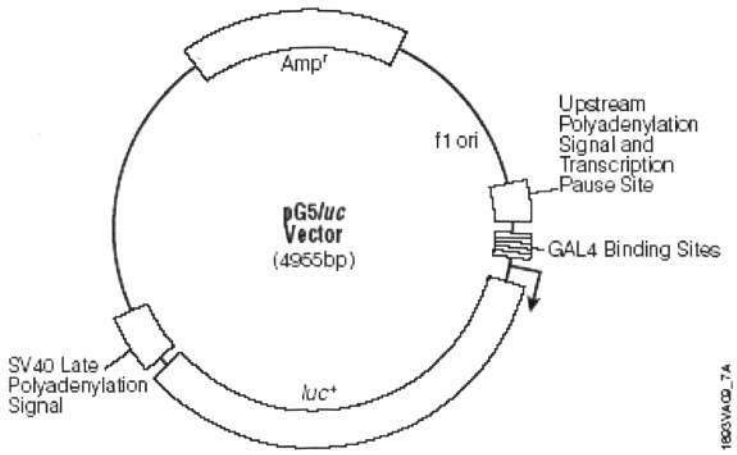

pG5*luc* Vector sequence reference points:

five GAL4 binding sites	18–120
major late promoter of adenovirus	132–172
predicted transcriptional start site	168
luciferase (*luc*+) gene	225–1877
SV40 late polyadenylation signal	1909–2130
β-lactamase (Amp^r) coding region	4077–3217
phage f1 origin of replication	4209–4664
upstream polyadenylation signal and transcriptional pause site	4795–4948

Figure 3.2c: pG5luc vector circle map and sequence reference points

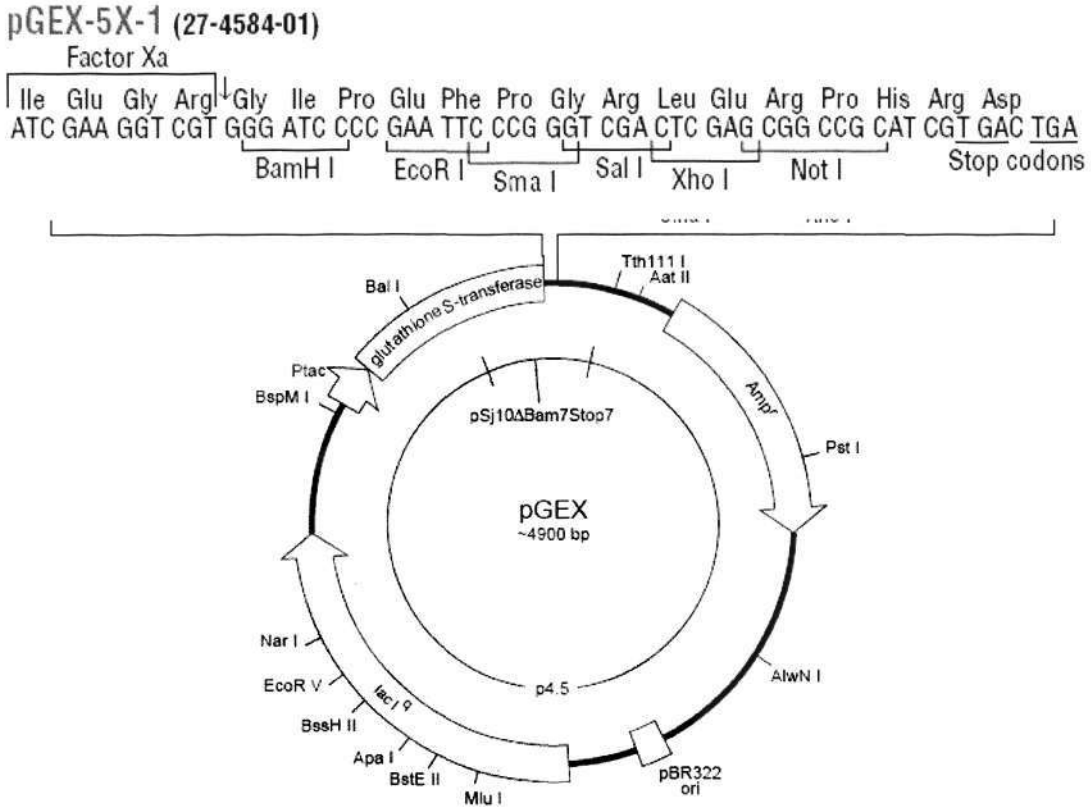

Figure 3.2d: pGEX-5X-1 vector circle map and MCR

3.4 GENERATION OF ALANINE MUTANTS

The aim of this section of the project was to elucidate the role of the BH3 domain in inducing apoptosis. It has previously been shown that the conserved α-helix is required for the formation of heterodimer with the cleft formed by BH1~3 from other family members. The critical residues' mutation to alanine did affect expression levels and the activity of the resultant heterodimers (Sattler *et al.*, 1997). The mutations were introduced into viral proteins' cDNA using the combinatorial PCR method from expression vectors containing wild type proteins. All the mutants were generated and confirmed by automated sequencing. The mutated residues and the nomination of the mutants are showed in figure 3.3a and 3.3b.

HBV Pol wt:	**----------LEEELPRLADEGLNR----------**
HBV Pol L21A:	**----------AEEELPRLADEGLNR----------**
HBV Pol L25A:	**----------LEEEAPRLADEGLNR----------**
HBV Pol A29R:	**----------LEEELPRLRDEGLNR----------**
HBV pol D30A:	**----------LEEELPRLAAEGLNR----------**
HBV pol E31A:	**----------LEEELPRLADAGLNR----------**
HBV Pol-N wt:	**----------LEEELPRLADEGLNR----------**
HBV Pol-N L21A:	**----------AEEELPRLADEGLNR----------**
HBV Pol-N L25A:	**----------LEEEAPRLADEGLNR----------**
HBV Pol-N A29R:	**----------LEEELPRLRDEGLNR----------**
HBV pol-N D30A:	**----------LEEELPRLAAEGLNR----------**
HBV pol-N E31A:	**----------LEEELPRLADAGLNR----------**
HBSP wt:	**----------LEEELPRLADEGLNR----------**
HBSP L25A:	**----------LEEEAPRLADEGLNR----------**

Figure 3.3a: Mutants of HBV polymerase, POL-N and HBSP in BH3 domain. Point mutations were introduced into the BH3 domain at the 5 critical amino acids position. All the sequences were confirmed by automated sequencing.

```
HBx wt:        ----------VFKDWEELGEEIRLK----------
HBx V116A:     ----------AFKDWEELGEEIRLK----------
HBx W120A:     ----------VFKDAEELGEEIRLK----------
HBx G124R:     ----------VFKDWEELREEIRLK----------
HBx E125A:     ----------VFKDWEELGAEIRLK----------
HBx E126A:     ----------VFKDWEELGEAIRLK----------

HBx-C wt:      ----------VFKDWEELGEEIRLK----------
HBx-C V20A:    ----------AFKDWEELGEEIRLK----------
HBx-C W24A:    ----------VFKDAEELGEEIRLK----------
HBx-C G28R:    ----------VFKDWEELREEIRLK----------
HBx-C E29A:    ----------VFKDWEELGAEIRLK----------
HBx-C E30A:    ----------VFKDWEELGEAIRLK----------
```

Figure 3.3b: Mutants of HBx and HBx-C terminal in BH3 domain. Point mutations were introduced into the BH3 domain at the 5 critical amino acids position. All the sequences were confirmed by automated sequencing.

Chapter Four: Apoptosis Induced by HBx

4.1 INTRODUCTION

This chapter describes that HBx induced apoptosis in HepG2 cells: role of the BH3 domain. HBV infection leads to a wide range of liver diseases, including viral hepatitis. Viral hepatitis is characterized by a host immune response to infected liver cells and associated with cell damage and death. Apoptosis is one of the typical processes of cell death. Apoptosis can be initiated by either external or internal stimuli and two distinct pathways have been defined. These include the death receptor pathway involving the TNF receptors and caspase-8 activation, and the mitochondrial pathway involving the Bcl-2 family of proteins with caspase-9/caspase-3 activation.

In the case of HBV infection, some evidence has suggested a role of Fas ligand and HBx protein in the development of apoptosis-related hepatitis (Kondo *et al.*, 1997; Hayashi *et al.,* 1999; Su *et al.,* 1997; Chirillo *et al.,* 1997). Recent reports have also pointed to the involvement of the mitochondrial-dependent apoptotic pathway in the development of liver diseases (Chen *et al.*, 2001; Ehrmanm *et al.,* 2000). This appears to be supported by the pro-apoptotic role of HBx in the Bcl-2 mediated apoptotic pathway (Tanaka *et al.,* 1999; Schuster *et al.,* 2000; Pollicino *et al.,* 1998). This apoptosis process may result in the dissemination of viral particles with minimum host immune response as well as protecting progeny viral particles from host neutralizing antibodies, since apoptotic cells are usually vacuolated and endocytosed by neighboring cells. However, little is known on the mechanism of HBV viral

proteins in this pathway at molecular level. Based on a multiple alignment of HBV viral proteins and related Bcl-2 family of proteins, a BH3-like domain in HBx was defined. The function of the BH3-containing HBx was investigated and shown to be pro-apoptotic.

4.2 IDENTIFICATION OF BH3 DOMAIN IN HBx

The conserved BH3 like regions of pro-apoptotic Bcl-2 family of proteins are critical for their induction of cell death and for their interactions with anti-apoptotic proteins including the prototype Bcl-2. To investigate whether any of the HBV viral proteins is directly involved in apoptosis, a BH3 motif was screened in all HBV viral proteins including HBx. A distantly related BH3 motif was identified in HBx (amino acid 116-130 in an overall 154 residues). A multiple alignment of the BH3 motif among HBx and some Bcl-2 family of proteins (including Bcl-2, BAD, BAK, BAX, BID, BIK, BIM and RAD9) is shown in figure 4.1.

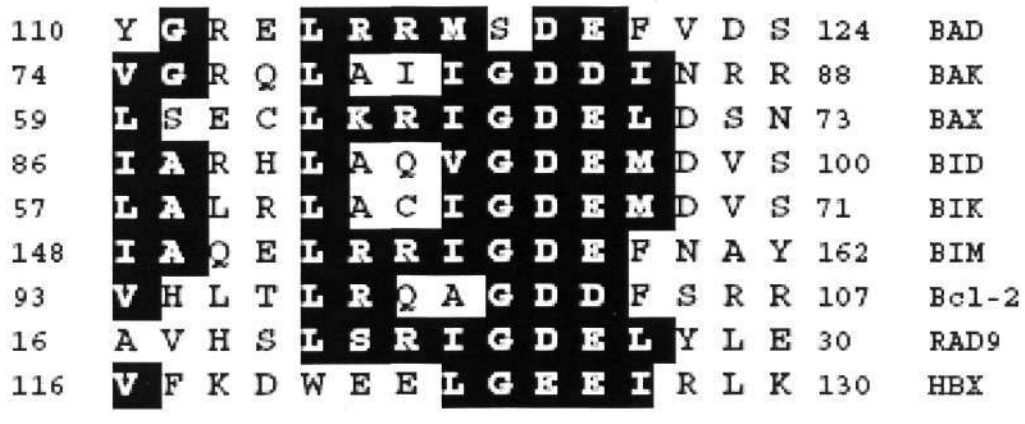

Figure 4.1: Alignment of amino-acid residues in the BH3-homology regions of Bcl-2 family members and HBX. Comparison of the BH3-like regions in HBX and Bcl-2 family members (HBX GenBank accession number CAA49453; human BAD, AF021792; human BAK, U23765; human BAX L22474; human BID, CAG30275; human BIK, U34584; human BIM, AF032457; human Bcl-2, P10415; human RAD9, U53174). Amino acids that match the BH3 consensus (accession number PS01259) are darkly shaded.

Conserved amino acids are darkly shaded. Although HBx has been reported to associate with various pathways of apoptosis and possess pro-apoptotic activity, this finding provided a molecular clue on its action.

4.3 MAMMALIAN TWO-HYBRID ASSAY BETWEEN HBx AND BCL-2 FAMILY OF PROTEINS

It has been shown that interactions among members of the Bcl-2 family of proteins can be analyzed in the yeast two-hybrid system (Sato *et al.*, 1994). To determine the significance of the distantly related BH3 motif identified in HBx, its interaction with Bcl-2 family of proteins was carried out in a mammalian cell-based system similar to the yeast two-hybrid. Specifically, the coding regions of both full length HBx and HBx-C terminal were amplified by PCR and cloned in-frame with the DNA binding domain of GAL4 in the pBIND vector from CheckMate system. A missense mutant HBx (E125A) was generated using the pBIND-HBx as template. On the other hand, the coding regions for six members of the Bcl-2 family of proteins, namely Bcl-2 and Bcl-xl (anti-apoptotic), Bad, Bak, Bik, and Bax (pro-apoptotic), were amplified from extracted mRNA and cloned in-frame with the GAL4 activation domain in the pACT vector. As the luciferase activity results from the gene expression in the nucleus, the interaction between HBx and the Bcl-2 related proteins containing a transmembrane domain (Bcl-2, Bcl-xl, Bax, Bak, Bik) may not be properly reflected using such an assay. For this reason, the coding regions of these four Bcl-2 members excluding their transmembrane domain were amplified and cloned in this study.

Transient transfection of HepG2 cells was carried out with an equal amount of the three plasmids, the bait (HBx and HBx-C), prey (Bcl-2 related proteins), and the pG5*luc* reporter which encodes the firefly luciferase. The interaction between bait and prey was then read as raw data showing the firefly luciferase activity (interaction reporter) and *Renilla* luciferase activity (encoded in pBIND and served as an internal control efficiency of transfection). The ratio of firefly luciferase activity to *rennilla* luciferase activity was normalized comparing to positive control supplied by the manufacturer. Results from the independent transfections for each combination are shown in table 4.1a~b and figure 4.2a~b.

Proteins	(+)	Bcl-2 Bad	(-)	Bcl-xl	Bcl-2	Bad	Bak	Bik	Bax
Firefly Luc	51512	28425	1620	11542	17569	4111	2250	2740	3219
	54088	25021	1417	14605	16952	4232	2138	2961	3310
	45980	27968	1498	11863	20589	3813	2446	2873	3440
Average	50800	27138	1510	12670	18370	4052	2278	2858	3323
Renilla Luc	12159	16205	11579	11728	14505	10998	12500	13322	15777
	14582	12110	17205	15393	15631	10504	11447	15118	18052
	10117	11300	6880	15491	13988	12551	12998	15087	12977
Average	12286	13205	11888	14204	14708	11351	12315	14509	15602
Firefly/renila	4. 11	2. 05	0. 127	0. 892	1. 249	0. 357	0. 185	0. 197	0. 213
Percentage	100%	50%	3. 10%	21. 70%	30. 40%	8. 70%	4. 52%	4. 80%	5. 20%

Data unit: relative fluorescence unit (RFU)

Table 4.1a: Raw data of HBx interaction with Bcl-2 family of proteins. pBIND-ID and pACT-MyoD was set as positive control. pBIND and pACT was set as negative control. Three independent experiments were carried out for each pair of interaction. The average was calculated and thereading was compared to the reading of positive control and displayed as percentage. HBx interaction with Bcl-xl and Bcl-2 resulted in 21.7% and 30.4%, respectively. HBx interaction with other members remained lower than 8.70%.

Proteins	(+)	Bcl-2 Bad	(-)	Bcl-xl	Bcl-2	Bad	Bak	Bik	Bax
Firefly Luc	51512	28425	1620	1855	2122	2759	3315	2860	2158
	54088	25021	1417	1742	2235	2642	3025	2631	2042
	45980	27968	1498	1404	3023	3122	2714	3380	2496
Average	50800	27138	1510	1667	2460	2841	3018	2957	2232
Renilla Luc	12159	16205	11579	11404	15815	15626	12156	15762	11058
	14582	12110	17205	12131	12111	11315	11425	14325	11222
	10117	11300	6880	14079	12038	14237	20159	14949	16894
Average	12286	13205	11888	12538	14556	13726	14580	15012	13058
Firefly/renila	4.11	2.05	0.127	0.133	0.169	0.207	0.213	0.197	0.171
Percentage	100%	50%	3.10%	3.25%	4.12%	5.05%	5.20%	4.80%	4.17%

Data unit: relative fluorescence unit (RFU)

Table 4.1b: Raw data of HBx-C interaction with Bcl-2 family of proteins. Interaction between pBIND-ID and pACT-MyoD was set as positive control. pBIND and pACT was set as negative control. Three independent experiments were carried out for each pair of interaction. The average was calculated and the reading was compared to the reading of positive control and displayed as percentage. HBx-C interaction with all Bcl-2 family of proteins remained lower than 5.20%.

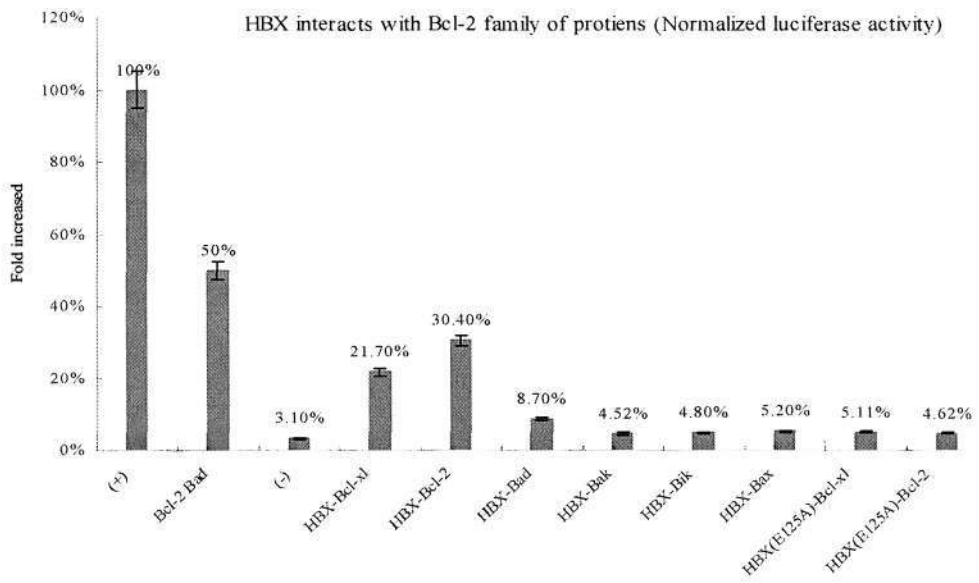

Figure 4.2a: Interaction of HBX with Bcl-2-related proteins by luciferase activity. The coding region of HBX and the missense mutant HBX (E125A) was amplified and cloned in-frame with a GAL4 DNA binding domain in-pBind vector. The coding regions of six members of Bcl-2 family proteins, including Bcl-2, Bcl-xl, Bad, Bak, Bik, and Bax but excluding their transmembrane region, were amplified and cloned in-frame with a VP16 transcription activation domain in pACT vector. Luciferase activity was measured from HepG2 cells transfected with constructs of HBX and one of the Bcl-2-related genes (see Materials and methods). Values obtained were normalized with the levels of *Renilla* luciferase absorbance in which pBind acted as an internal control of protein expression. The results represent means ± SE from three independent experiments. *Statistically significant at $p < 0.05$ in luciferase activity.

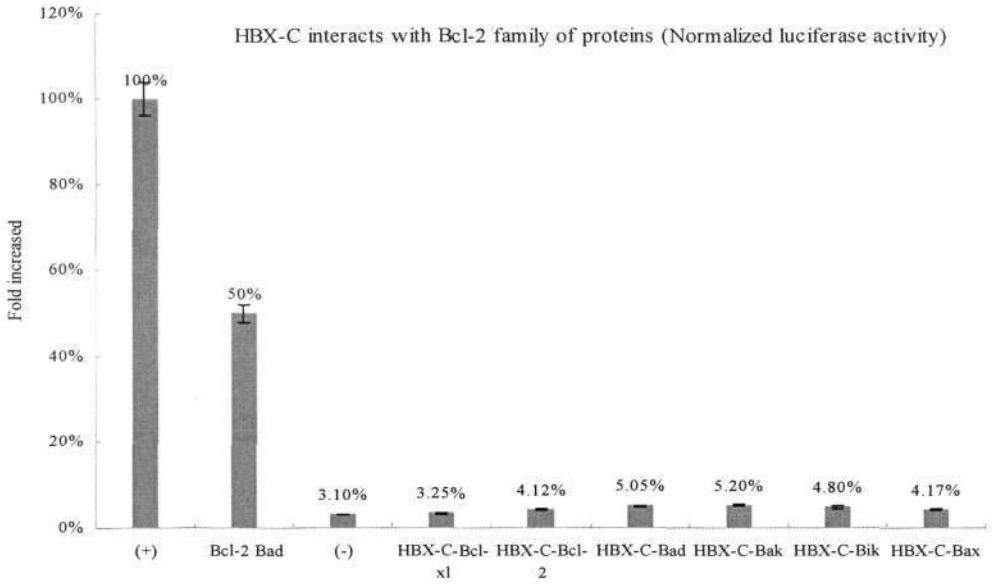

Figure 4.2b: Interaction of HBX-C with Bcl-2-related proteins by luciferase activity. The coding region of HBX-C was amplified and cloned in-frame with a GAL4 DNA binding domain in-pBind vector. The coding regions of six members of Bcl-2 family proteins, including Bcl-2, Bcl-xl, Bad, Bak, Bik, and Bax but excluding their transmembrane region, were amplified and cloned in-frame with a VP16 transcription activation domain in pACT vector. Luciferase activity was measured from HepG2 cells transfected with constructs of HBX-C and one of the Bcl-2-related genes (see Materials and methods). Values obtained were normalized with the levels of *Renilla* luciferase absorbance in which pBind acted as an internal control of protein expression. The results represent means ± SE from three independent experiments. *Statistically significant at $p < 0.05$ in luciferase activity.

The positive control between pBIND-Id and pACT-MyoD gave out a normalized ratio of 4.11 and was set as 100%. The negative control between pBIND and pACT showed 3.10% activity comparing to the positive control. The internal control readings of *Renilla* luciferase activity during the whole experiment was mostly bracketed between 10,000 and 20,000. As indicated in figure 4.2a, it showed that Bad interacted with Bcl-xl with a 50% activity as expected between pro-apoptotic and anti-apoptotic Bcl-2 related proteins. Interestingly, HBx interacted with anti-apoptotic proteins Bcl-2 and Bcl-xl with 30.4% and 21.7% activity, respectively, whereas HBx did not interact with pro-apoptotic proteins such as Bad (8.7%), Bak (4.52%), Bik

(4.80%) and Bax (5.20%). To further prove the significance of the interaction between HBx and anti-apoptotic members, a missense mutant HBx (E125A in BH3 domain) and HBx-C which was considered as deletion containing the BH3 domain were applied to the experiment. HBx (E125A) was co-transfected with Bcl-2 and Bcl-xl, respectively. The decreased luciferase activity (4.62% for Bcl-2 and 5.11% for Bcl-xl) significantly supported the hypothesis that HBx interacted with Bcl-2 and Bcl-xl throught the BH3 domain. However, the luciferase activity of HBx-C with Bcl-2 and Bcl-xl was 4.12% and 3.25%, not consistant with what HBx did with Bcl-2 and Bcl-xl. HBx-C also did not interact with other members such as Bad (5.05%), Bak (5.20%), Bik (4.17%) and Bax (4.80%). The mechanism why HBx-C didn't interact with Bcl-2 and Bcl-xl remains to be investigated.

4.4 MTT ASSAY OF HBx IN HepG2 CELLS

It has been proved that HBx but not HBx-C was able to interact with Bcl-2 and Bcl-xl through its BH3 domain. HBx was applied to HepG2 cells and followed by MTT assay. MTT [3-(4,5-dimethylthiazol-2-yl)-2,5-diphenyltetrazolium bromide] assay is based on the ability of a mitochondrial dehydrogenase enzyme from viable cells to cleave the tetrazolium rings of the pale yellow MTT and form a dark blue formazan crystals which is largely impermeable to cell membranes, thus resulting in its accumulation within healthy cells. Solubilisation of the cells by the addition of a detergent results in the liberation of the solubilized crystals. The number of surviving cells is directly proportional to the level of the formazan product created. The color can then be quantified using a simple colorimetric assay (Mosmann *et al.*, 1983).

To determine the quantitive relationship of HBx and cell viability, a series of HBx plasmid (0.4μg, 0.8μg, 1.2μg and 1.6μg) was transfected in equal starting amount HepG2 cells. After 48h incubation, cells were treated in 5mM MTT for 3h and solubilized in lysis buffer. Results were read by a microplate reader under a wave length 505nm. The normal cells treated with transfection reagent were set as negative control while the cells treated with UV irradiation for 15min were set as positive control to modulate the killing effect. Three independent experiments were carried out at same condition and results were presented. As shown in table 4.2, normal cells showed an average reading of 0.545 (100%) and UV treated cells resulted in an average of 0.310 which meant 56.9% of living cells survived relatively. According to the increasing plasmid amount transfected, HBx transfected cells gave out a series of decreasing readings: 0.406, 0.379, 0.378 and 0.316 which indicated 74.50%, 69.54%, 69.35% and 57.98% of living cells survived. From figure 4.3, an approximate extent of cell-killing effect was seen between the UV treated cells and 1.6 μg HBx transfected cells. So, it could be confirmed that HBx induced cells death in dose-dependend manner.

MTT assay	Normal Cells	Cells (UV)	HBX 0.4ug	HBX 0.8ug	HBX 1.2ug	HBX 1.6ug
Experiments	0.566	0.342	0.499	0.389	0.39	0.342
	0.505	0.343	0.334	0.319	0.349	0.297
	0.565	0.246	0.385	0.43	0.396	0.31
Average	0.545	0.31	0.406	0.379	0.378	0.316
Cell viability%	100%	56.90%	74.50%	69.50%	69.30%	58.00%

Measurement: relative absorbance at 505nm

Table 4.2: Results of HBx MTT assay. Three independent experiments were carried out for each sample. The original data for each reading was displayed in this table. The average of the three readings was applied to analysis. Normal cells acted as negative control as 100% living cell while the UV treated cells acted as (+) control.

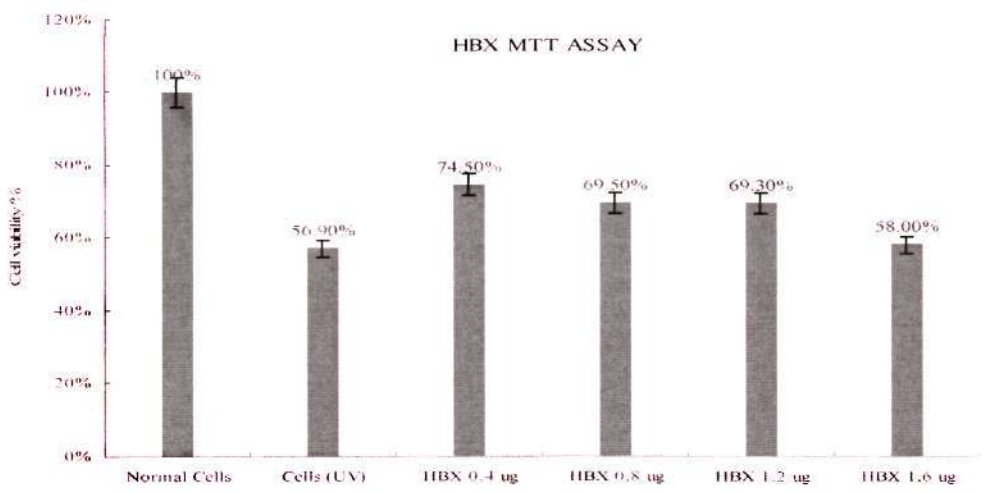

Figure 4.3: HBX MTT Assay. HBX was transfected into HepG2 cells for 48h before collection. Cells were treated in 5mM MTT and lysed after 3h's incubation at 37°C. Results were read by a microplate reader under a wave length of 505nm. The normal cells (100%) and UV treated cells (56.9%) were set as negative and positive controls .It showed HBX transfected cells received a decrease in cell viability (74.5%~58.0%) depending on HBX dose increasement (0.4μg~1.6 μg).

4.5 SUBLOCALIZATION IN HepG2 CELLS

HBx is known to be a multiple functional protein to transactivate a number of viral and cellular genes (Spandau *et al.*, 1998). Some reports suggested that HBx was found in the cytoplasm around the nuclear periphery (Benn *et al.*, 1994). HBx was also indicated associated with abnormal aggregated mitochondrial structure around the nuclear periphery (Takada *et al.*, 1999). On the other hand, mitochondrion is the exact place where Bcl-2 family of proteins form heterodimers to decide the fate of cell.

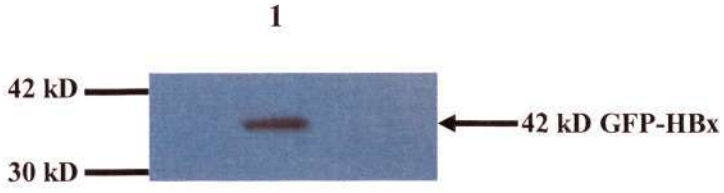

Figure 4.4a: Expression of EGFP-HBX. Western blot assay of the GFP-HBX was carried out in transfected cells. The lane 1 displayed the fusion protein of 42 kD.

Figure 4.4b: Detection of EGFP-HBX in HepG2 cells. HepG2 cells were transfected with pEGFP-HBX and incubated at 37° for 48h. The EGFP-HBX was then detected directly under fluorescence microscope.

Due to the conflicting specificity of the commercially available antibodies for HBx, the subcellular localization of HBx was analyzed using the enhanced green fluorescent protein (EGFP) tag. The pEGFP-HBx was transfected into HepG2 cells for 48h and detected directly under fluorescence microscope. Result of western blot analysis using transfected cell lysate, as shown in figure 4.4a, indicated the expected molecular weight of EGFP-HBx (42kD). This detection suggested that the observed subcellular localization was reflective of the EGFP-HBx expression. In contrast to the diffuse fluorescence signal throughout the cytoplasm and nucleus of EGFP, spotty perinuclear fluorescence was observed in cells transfected with EGFP-HBx, as shown in figure 4.4b. This was identical to the reported HBx localization that was associated with abnormally aggregated mitochondrial structures around the nuclear periphery.

This result supported a possibility that HBx might interact with Bcl-2 or Bcl-xl on the mitochondia.

4.6 APOPTOSIS INDUCED BY HBx IN HepG2 CELLS

From the results obtained above it remains to be determined whether: 1) the cell death caused by HBx was apoptosis or necrosis and 2) the apoptosis was consistant to HBx expression level. To address these questions the HBx was generated as described in Chapter 3. The pXJ-HBx was transfected into HepG2 cells and measured by flow cytometry and fluorescence reading. The HBx expression was determined by Western blot analysis.

4.6.1 Flow Cytometric Analysis of Phosphatidylserine Externalization

One of the apoptotic natures of the apoptotic cells is the phosphatidylserine (PS) translocation from inner face of the plasma membrane to the cell surface which then becomes detectable by Annexin-V (S.J. Martin *et al* 1995). To investigate the effect of HBx in liver cells, HepG2 cells were transfected with either HBx at two different amounts (1.0 μg and 2.0 μg) or empty pXJ-40 vector. Cells treated with 50 μM cisplatin were used as positive control. The labeling of cells was by Annexin-V-FITC (FL1-H) and Propidium Iodide (PI, FL2-H) and was analyzed by flow cytometry.

As shown in figure 4.5a, the bottom left square indicates the number of total living cells, the bottom right square the number of apoptotic cells, and top squares the number of necrotic cells. As apoptotic cells remain membrane integrity and necrotic

cells membrane were disintegrated, they could be discriminated by the PI staining which is specific to nucleus. The results indicated there were 12.27% and 15.27% apoptotic cells in cells transfected with 1.0 and 2.0 μg of the pXJ-HBx construct, respectively (Fig 4.5a, panel C and D). This was significantly higher than cells transfected with empty pXJ-40 vector (3.53%, Fig 4.5a, panel A) which was set as negative control, but lower than the positive control with cells treated by 100 μM cisplatin for 16h (30.93%, Fig 4.5a, panel B). Our results indicated that HBx induced apoptosis when over-expressed in HepG2 cells.

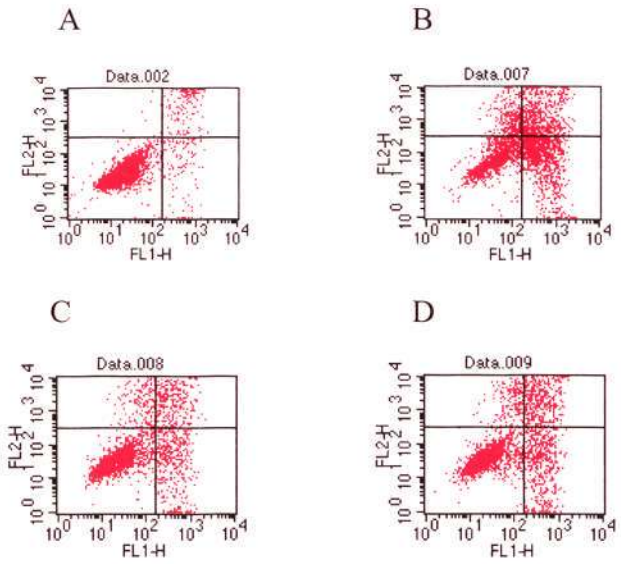

Figure 4.5a: Apoptotic effect of HBX in HepG2 cells by flow cytometry analysis. HepG2 cells were transfected with either HBx at two different amounts (C and D) or empty pXJ-40 vector (A). Cells treated with cisplatin were used as positive control. The labeling of cells was by Annexin-V-FITC (FL1-H) and propidium iodide (FL2-H) (see Materials and methods). The bottom left square indicates the number of total living cells, the bottom right square the number of apoptotic cells, and top squares the number of necrotic cells. The percentage of apoptotic cells was, respectively, 3.53% (empty pXJ-40 as negative control, A), 30.93% (cisplatin treated cells as positive control, B), 12.27% (1.0 μg HA-HBX transfected cells, C), and 15.27% (2.0 μg HA-HBX transfected cells, D).

4.6.2 Analysis of Caspase-3 Acitivity

Caspase-3, the hallmark of apoptosis as downstream executive proteinase, cleaves a variety of cellular substrates after aspartic acid residues. It is synthesized in the cytosol of mammalian cells as inactive zymogen form and is activated through intracellular cascades (Cohen, 1997). To further examine the apoptotic activity of HBx, a caspase-3 substrate conjugate DEVD-AFC (7-amino-4-trifluoromethyl coumarin) was used. The DEVD-AFC usually emits blue light (λ_{max}=400 nm), however, cleavage of the substrate by caspase-3 liberates AFC, which fluoresces yellow-green (λ_{max}=505 nm).

To this end, HepG2 cells transfected with 2 μg of pXJ-HBx were analyzed at different time points. As shown in figure 4.5b, cells transfected with the empty pXJ-40 showed caspase-3 activity (cleavage of DEVD-AFC substrate) of 2254 as negative control. Those cells treated with 100 μM cisplatin showing caspase-3 activity of 31766 was set as positive control. For cells transfected with pXJ-HBx construct, the caspase-3 activity was 1688 (24h), 1917 (36h), 4633 (48h), 7147 (60h) and 3998 (72h), respectively. There was a significant increase of caspase-3 activity in HBx transfected cells from 48-72 h, with the peak at 60 h. the decrease of caspase-3 activity as observed at 72 h may be due to the decrease in the number of apoptotic cells. This indicated a time dependent effect of apoptosis inducing ability of HBx. Our results further supported the evidence of HBx-induced apoptosis as shown in the flow cytometry analysis.

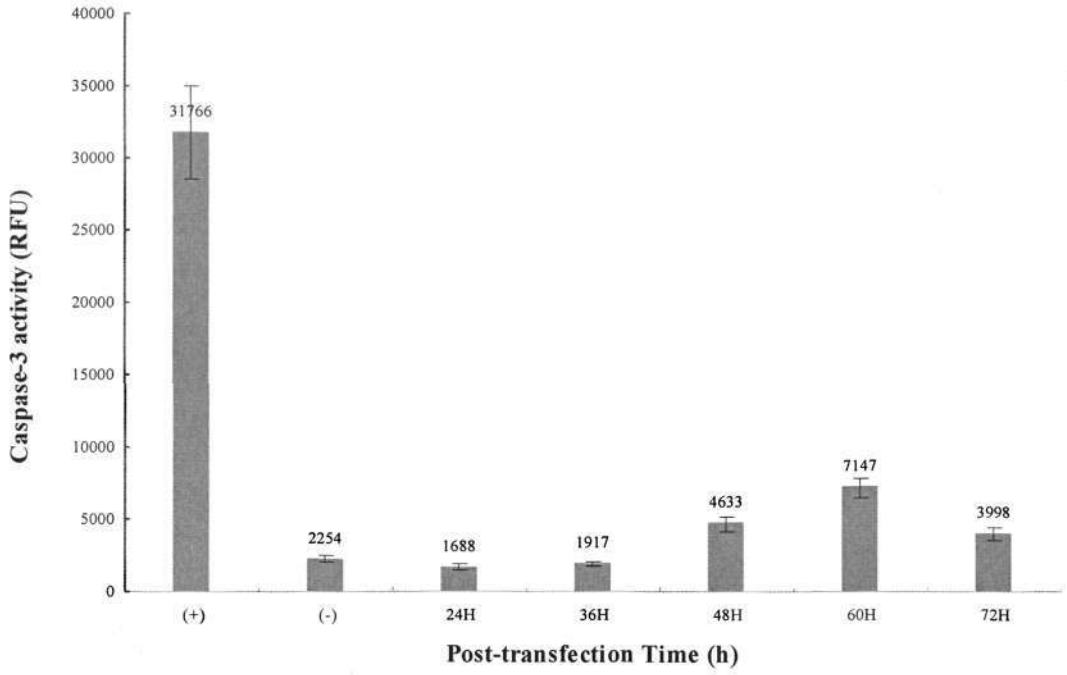

Figure 4.5b: Apoptotic effects of HBX in HepG2 cells by caspase-3 activity. HepG2 cells were transfected with HA-HBX construct and analyzed for caspase-3 activity at different time points (see Materials and methods). A similar analysis was carried out on cells treated with cisplatin (+) and those transfected with the empty pXJ-40 plasmid (-). The results represent means ± SE from three independent experiments.

4.6.3 Analysis of HBx Half-life on Apoptotic Effect

To correlate the expression level of HBx in HepG2 cells with the observed apoptotic effects, Western blot analysis was carried out in HepG2 cells transfected with pXJ-HBx construct using anti-HA antibody. However, no protein band was observed. This could be due to the fast onset of apoptosis in cells expressing HBx protein, leading to the absence of detectable HBx protein in our Western blot analysis. To confirm this hypothesis, expression of HBx mRNA in HepG2 transfected with pXJ-HBx was examined by reverse transcription PCR. As shown in figure 4.5c, the band of expected size for HBx (462 bps) was detected in HBx transfected HepG2 cells (lane 2) but not in the non-transfected control HepG2 cells (lane 3). To further

explore this possibility, the same pXJ-HBx construct was transfected into the epithelial cell line 293T which generally yields a higher protein level compared with HepG2 cells. No protein band was observed in the 293T cell extract in Western blot analysis. To determine if HBx could be more stable when fused with a different protein as reported by other investigators (A.T.Lee *et al.*, 2005), HBx was cloned in-frame with the glutathione-S-transferase (GST) gene together with the HA tag in the same pXJ-40 vector (see Materials and methods). Another cell line, the epithelial 293T cells, was used in the transfection and the subsequent Western blot analysis. Results shown in figure 4.5d indicate that the fusion protein HA-GST-HBX was expressed in 293T cells and expressed in a dose-dependent manner. However, no apoptotic activity was detected in 293T cells expressing the fusion protein HA-GST-HBx by either flow cytometry or caspase-3 activity. Our results were consistent with the hypothesis that HBx protein may not be stable in apoptotic cells triggered by its own expression, while the fusion HA-GST-HBx may be more stable and therefore detectable by Western blot analysis.

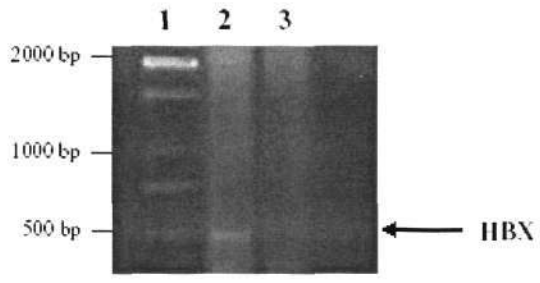

Figure 4.5c: Expression of HBX mRNA in transfected HepG2 Cells. Total RNA was extracted from HepG2 and HBX transfected HepG2 cells after 48 hrs, respectively. Reverse transcription-PCR was carried out using HBX specific primers (see Materials and methods). Lane 1, 100 bp DNA ladder. Lane 2, HBX transfected HepG2 cells. Lane 3, non-transfected HepG2 cells.

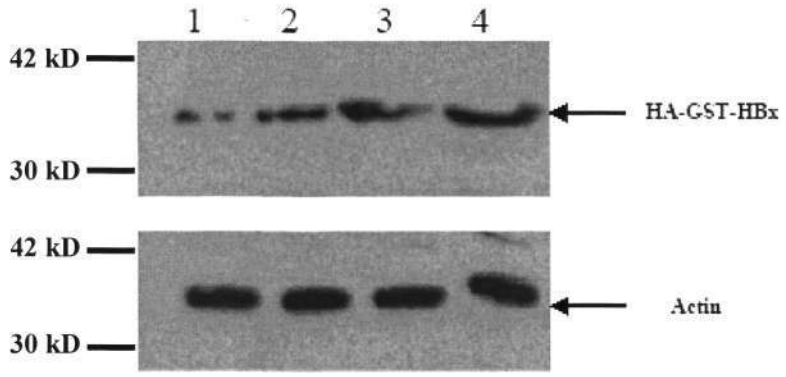

Figure 4.5d: Western blot analysis of HA-GST-HBX in 293T cells. Cells were transfected with different amount of the fusion construct HA-GSTHBX, 0.5 ug (lane 1), 1 ug (lane 2), 2 ug (lane 3), and 4 ug (lane 4), respectively. Western blot analysis was carried out on cell extracts using anti-HA and anti-actin antibodies (see Materials and methods).

4.7 CONCLUSION

In conclusion, we report the identification of a pro-apoptotic BH3 domain in HBx. Significance of this BH3 domain was supported by the interactions of HBx with anti-apoptotic members of the Bcl-2 family of proteins, but not with those pro-apoptotic members. The apoptotic activity of HBx was further supported by molecular analyses including flow cytometry and caspase-3 activity. Importantly, the identified BH3 motif in HBx matches the domain mediating its previously reported pro-apoptotic activity. Our results therefore have provided the first molecular evidence of apoptosis conferred directly by HBx.

Chapter Five: HBSP induces Apoptosis

5.1 INTRODUCTION

It has been shown in the preceding chapter that HBx was found to contain a BH3-like motif and decrease cell viability. HepG2 cells transiently transfected with HBx was sensitized to apoptosis. That was detected by the externalization of Phosphotidylserine (PS) from the inner face of plasma membrane to the cell surface and confirmed by activation of caspase-3 in transfected HepG2 cells. In this chapter, the effect of HBV infection in HepG2 cells and the role of a HBV spliced mRNA generated protein (HBSP) involved in HBV induced apoptosis will be explained.

A number of related studies have previously reported that Hepatitis B is characterized by an inflammatory reaction in the infected liver cells and death (Lau *et al.,* 1998). As wildly known, the host immune response to viral proteins expressed by infected hepatocytes, but not the direct cytopathic effects of virus, was regarded as main reason of hepatocyte damage (Brechot *et al.,* 2004). To investigate the HBV infection effect on HepG2 cells, a cell-based system for HBV replication was generated (Chen *et al.*, 2000). HBV genome was transfected into HepG2 to analyze the effect. The ImX technique (An Elisa method detecting the soluble HBsAg) was applied to detect the viral replication. As a consequence, HBV was found to replicate and induce cell death in HepG2 cells.

To explain the molecular mechanism of HBV induced cell death, the viral proteins

were investigated. A screen of BH3 motif was carried out in all HBV viral proteins including HBx which was mentioned in chapter four, and the polymerase. Results revealed a BH3motif in the N-terminus of HBV DNA polyermase, spanning from residue 21 to 35. HBSP was reported detectable in patients' sera in nature status and was able to induce liver cell apoptosis when transiently expressed *in vivo*. It was further proved to increase the HBV replication in a system by increasing the viron production (Sooussan *et al.*, 2000). Surprisingly, the HBSP shares the first 46 amino acids with HBV polymerase with the N-terminus. Taken together, there was reason to investigate the role of BH3 motif in apoptosis induced by HBV.

HBSP cDNA was generated and cloned into expression vector pXJ-40. The effect of HBSP on HepG2 cell viability was analyzed by using flow cytormetry and fluorescence reader. Transient expression in HepG2 cells was analyzed by Western blot assay. The results confirmed the pro-apoptotic activity of HBSP. To further describe the function of the BH3 motif, a missense mutant HBSP (L25A) was generated and its function was analyzed. A deletion excluding the C-terminus of HBSP was also created and expressed to investigate the function of the BH3 motif in the N-Terminus. BH3 motifn, one of the four Bcl-2 homology domains, is the unique characteristic of pro-apoptotic members of Bcl-2 family of proteins (Kelekar *et al.*, 1998). Most of the BH3-only pro-apoptotic proteins appear to function essentially as transdominant inhibitors by binding to anti-apoptotic Bcl-2 family proteins and neutralizing their ability to prolong cell survival (Huang *et al.*, 2000). The N-terminus of HBSP (POL-N) was then applied to a mammalian two-hybrid system to check the

interaction of BH3 motif with other members of Bcl-2 family. Results indicated there was positive interaction between the POL-N and Bcl-2 or Bcl-xl.

5.2 APOPTOSIS INDUCED IN HBV REPLICATION

Infective HBV genome was cloned in pcDNA3.1 and transfected into HepG2 cells. The replication of HBV was determined through detecting the excreted HBsAg by using an ImX technique as mentioned above. The infected HepG2 cells were analyzed under confocal microscope and were found to display features of apoptosis. PS externalization was also detected from infected HepG2 cells by flow cytometry.

5.2.1 Analysis of HBsAg in HBV Transfected HepG2 cells

To generate a cell-based system for HBV replication, a linearised form of HBV genome has been constructed in the mammalian expression vector pcDNA3.1 (Chen *et al.,* 2000). The linear HBV genome contained the viral promoter at its 5' end and the region for termination of transcription at its 3' end. The ability of this genome in behaving as a replicative virus after its transfection in HepG2 cells was investigated.

ID	HBsAg Rate
Positive	166.9
Negative	4.1
12H	107.6
24H	120.3
36H	278.7
48H	259.6

Data unit: relative fluorescence unit (RFU)

Table 5.1: HBsAg production in HBV-infected HepG2 cells. The HBsAg was detected by ImX technique. Positive and negative readings were supplied by the manufacturer. Samples were treated according to the requirement by the instruction. Results showed the readings of different time point incubation HBV transfected cells.

In our study, HepG2 cells were transfected with 2.0 μg HBV genome plasmids and incubated for 12h, 24h, 36h and 48h, respectively. Medium of each experiment was collected and applied to ImX machine to detect the HBsAg expression (Abbott Laboratories). As shown in table 5.1, the positive and negative controls supplied by the system were 166.9 and 4.1. The medium samples were read as 107.6, 120.3, 278.7 and 259.6 for 12h, 24h, 36h and 48h incubated HepG2 cells. An increase in the amount of HBsAg was apparent. The replicating ability of this HBV genome was positive comparing to the controls and therefore confirmed the previous reports. This system was chosen to analyze the effect of HBV replication on the cells.

5.2.2 Apoptosis Assays in HBV Transfected Cells

HBV replication effect on cells was analyzed under con-focal and normal microscopes. The morphological abnormities were regarded as cell death. Biochemical analysis further confirmed the cell death was apoptosis.

5.2.2.1 Membrane blebbling

In contrast to the widely accepted non-cytopathic nature of HBV, recent reports have suggested a direct role of the HBx in apoptosis during the infection of HBV (Lee *et al.*, 2005). HepG2 cells transfected by linear HBV genome and likely undergoing by the onset of viral replication showed typical apoptotic and cytopathic effects (CPE), *i.*e. membrane blebbing, rounding up, detachment of cells from the culture dish, and eventually cell lysis and death. Careful examination of infected cells under

microscopy showed characteristic signs of apoptosis during the infection process. As shown in figure 5.1, under con-focal microscope observation, membrane blebbing was visible 150 min after the transfection of HBV genome in HepG2 cells (panel B). This characteristic of apoptosis was neither detected in cells 5 min after transfection (panel A), nor in cells transfected with the empty vector pcDNA3.1 for 5 min and 150 min (panel C and D).

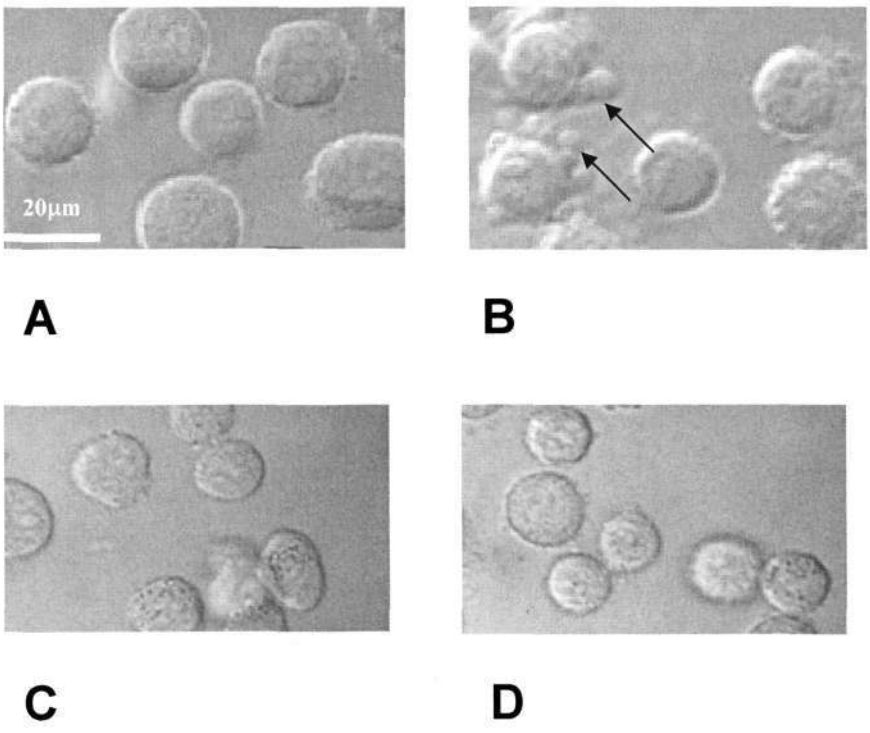

Figure 5.1 Confocal microscope analysis of membrane blebbing of HepG2 cells transfected with HBV. Panel A and B, HepG2 cells transfected with replicative HBV genome at 5 and 150 min respectively after cell seeding on collagen-coated substrates (scale bar: 20 μm). Panel C and D, HepG2 cells transfected with transfected empty vector pcDNA3.1 at 5 and 150 minutes respectively after cell seeding on collagen-coated substrates. Membrane blebbing (arrow heads) was observed in panel B (HBV-replicating cells at 150 min after cell seeding).

5.2.2.2 Detachment from culture dish

To see whether the transfection of HBV genome caused cell death in the whole

population, a series of transfection were carried out. As the incubation time after transfection prolonged, the number of dead cells which were detached from the culture dish increased. With the longer infection times at 12, 24, 36 and 48 h, more and more cells were found to round up and detach from culture dish (Panel C, D, E and F, respectively), as shown in figure 5.2. The morphological abnormalities observed in these cells were not detected in HepG2 cells 48h after their transfection with empty plasmids which served as negative control (Panel A). Interestingly, the morphological changes in HBV-infected cells at the 48h time point approched to the effect of HepG2 cells treated with 50 μM cisplatin, a known chemical that causes apoptosis (Panel B).

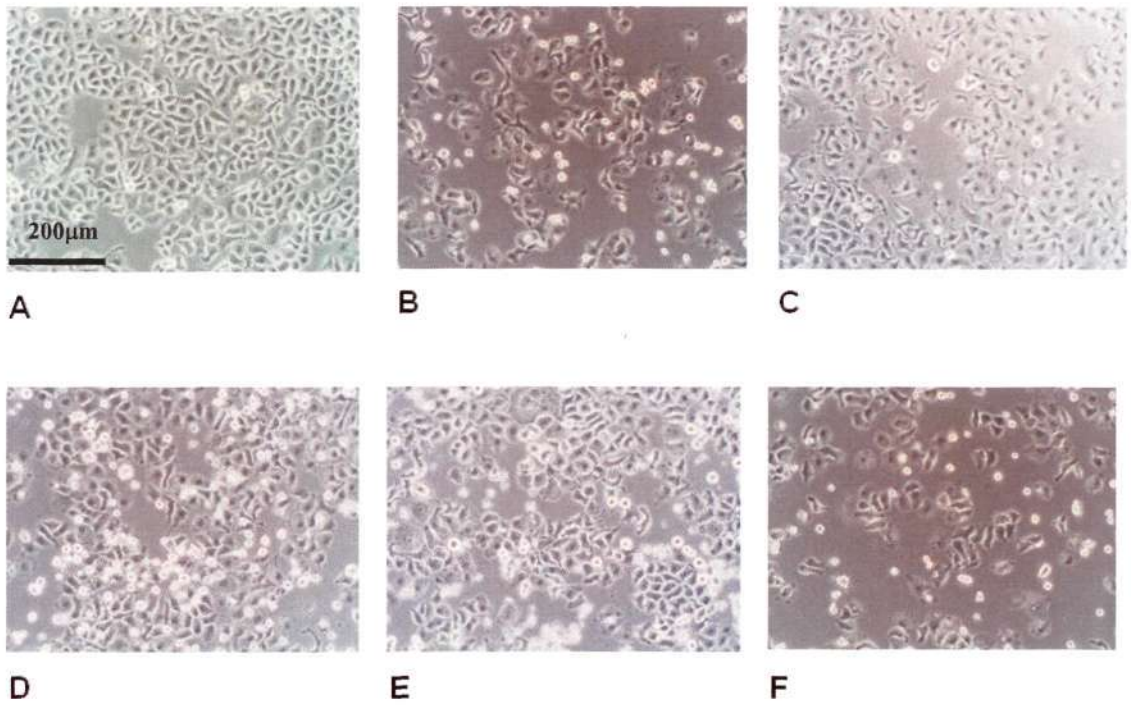

Figure 5.2: Analysis of morphology of HBV-replicating HepG2 cells. A series of phase contrast images of HepG2 cell transfected with replicative HBV genome and incubated at 6 hr (panel C), 12 hr (panel D), 24 hr (panel E) and 48 hr (panel F). HepG2 cells transfected with empty vector pXJ40 vector (after 48 hr) were shown in panel A. Cells treated with cisplatin, an agent inducing apoptosis, were shown in panel B. Detachment of cells and their rounding up were observed in panel B, and progressively from panel C to F.

5.2.2.3 Flow Cytometric Analysis of PS Externalization

This is a biochemical analysis to determine whether apoptosis was involved in the observed HBV-induced cell death process. Flow cytometry (FACS) was carried out by using an ApoAlert Annexin V Apoptosis kit which is based on the observation that apoptotic cells would translocate the membrane PS from the inner face of the plasma membrane to the cell surface. Typically, the proportion of apoptotic cells would reflect in the bottom-right square of the FACS profile. In this study, HBV-infected HepG2 cells were collected at time points same with the detachment experiment and were double-stained with Annexin-V-FITC and Propidium Iodide (PI).

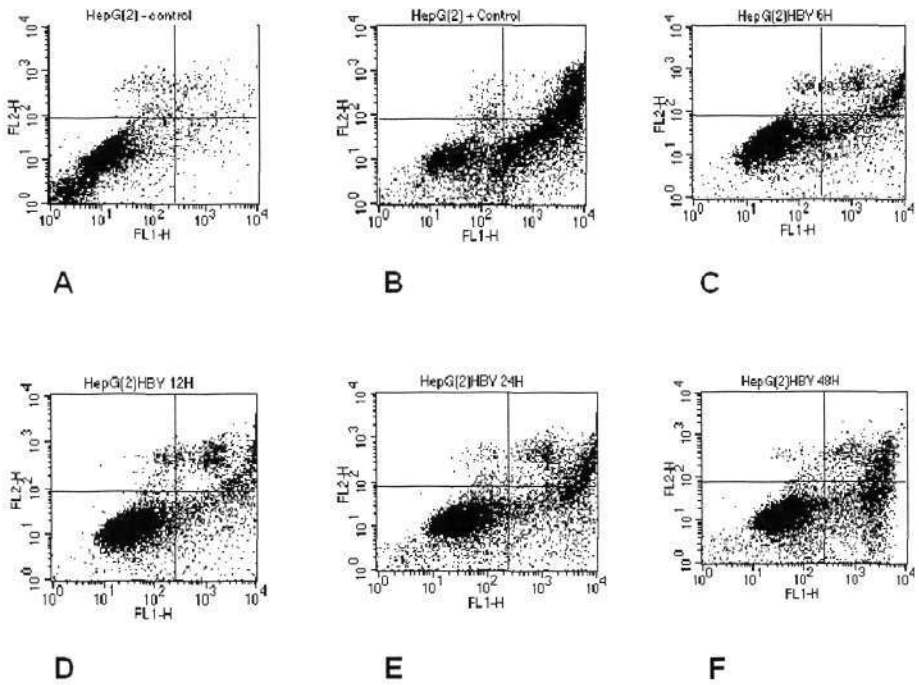

Figure 5.3: Flow cytometry analysis of apoptotic effect of HBV replication in HepG2 cells. HepG2 cells were transfected with either replicative HBV genome and incubated at different time points (6, 12, 24, and 48hrs) or empty pXJ40 vector [(-) 3.53%]. Cells treated with 50 μM cisplatin were used as positive control. The labeling of cells was by Annexin-V-FITC (FL1-H) and Prodium Iodide (FL2-H). In each panel, the bottom left square indicated the number of total cells, the bottom right square the number of apoptotic cells and top right square the number of necrotic cells.

Results shown in figure 5.3 indicated there was an increased apoptotic cells portion when the infection time prolonged. Specifically, 10.07% of apoptotic cells were detected 6 h after the onset of HBV infection (panel C), while the proportion of such cells were at 14.85%, 20.75% and 28.83% for 12 h, 24 h and 48 h, respectively (Panel D, E and F). It was significantly higher than the negative control, HepG2 cells transfected with empty pcDNA3.1 (+) (Panel A). But it was lower than the positive control in which cells were treated by 50 μM cisplatin for 20 h (36.12% panel B).

To investigate the involvement of necrosis in the HBV-induced cell death, the proportion of necrotic cells reflected in the top two squares of the FACS profile was analyzed. As shown in figure 5.3, the necrotic cells remained approximately the same around 14% for all the time points selected in this study. These data therefore indicated that apoptosis was likely to be the main mechanism of HBV-induced cell death.

5.3 APOPTOSIS INDUCED BY HBSP

To investigate the molecular mechanism of HBV-infection induced apoptosis, amino acid sequences of HBV proteins for pro-apoptotic motif were screened and aligned. HBSP and HBx were found to posess a BH3-like motif. HBSP was proved to express during HBV infection and transfected into HepG2 cells to study its effect. Results showed HBSP was capable to induce apoptosis which is consistent with other researchers' report.

5.3.1 Identification of BH3 Domain

To investigate whether HBV viral proteins were directly involved in the observed apoptosis, their sequences were screened for pro-apoptotic motif. Results from a multiple alignment among HBv proteins and Bcl-2 family of proteins revealed a BH3 motif in the N-terminus of the HBV DNA polymerase, spanning from the aa 21-35, which included conserved and critical residues found in the BH3 motifss of all Bcl-2 family of proteins, as shown in figure 5.4.

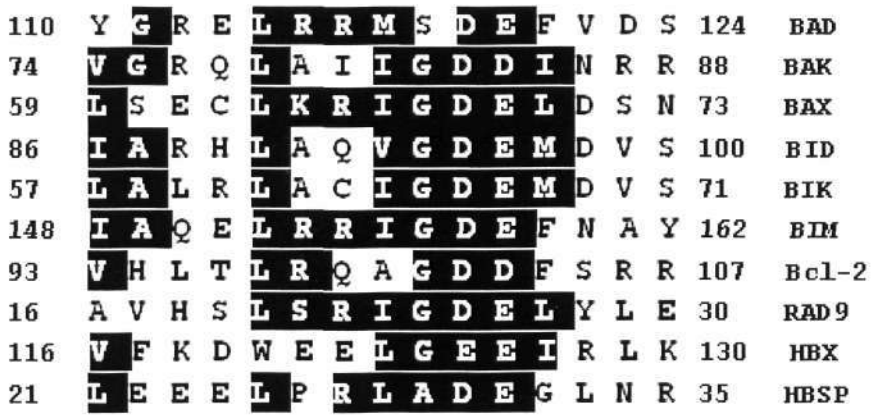

Figure 5.4: Alignment of BH3-homology regions of Bcl-2 family members and HBSP. Comparison of the BH3-like regions in HBSP and Bcl-2 family members (HBV Polymerase, GenBank accession number AAP06643; human BAD, AF021792; human BAK, U23765; human BAX L22474; human BID, CAG30275; human BIK, U34584; human BIM, AF032457; human Bcl-2, P10415; human RAD9, U53174). Conserved amino acids are shaded.

Interestingly, the BH3 motif was shared by HBSP, the spliced mRNA generated protein consisting of the first 46 amino acid residues at the N-terminus of HBV DNA polymerase and 47 amino acid residues created by the new reading frame (Soussan *et al.,* 2000). HBSP was reported to cause apoptosis through a hitherto unknown mechanism (Soussan *et al.,* 2000, Soussan *et al.,* 2003). The identification of the BH3 motif may therefore provide molecular insights on its apoptotic effect. The

hydrophobicity of HBSP was also analyzed as shown in figure 5.5 that the N-terminal part is more hydrophilic, whereas the C-terminus is more hydrophobic. The location of the hypothetic BH3 motif in the hydrophilic N-terminus supports the characteristic of BH3 domain as an amphipathic α-helix as described by others (Sattler *et al.*, 1998).

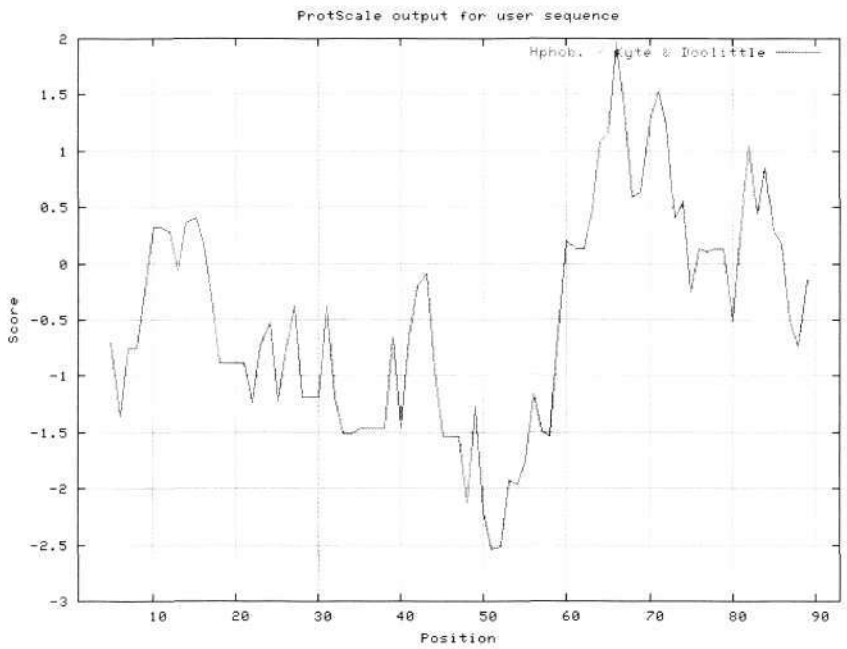

Figure 5.5: Hydrophobicity Plot of HBSP. The hydrophobicity plot of HBSP was generated by ProtScale. The N-terminal region containing 1-60 aa is hydrophilic, whereas the C-terminus is hydrophobic. The BH3 domain locates in 21-37 aa in the N-terminus.

5.3.2 Expression in HBV Replication

Although HBSP was found in HBV infected liver tissue and anti-HBSP antibody could be detected in sera of chronic HBV carriers (Soussan *et al.,* 2000), its expression during HBV replication has not been characterized. Results from such an analysis would be particularly relevant to the observed apoptosis following HBV replication in HepG2 cells. To this end, HepG2 cells transfected with HBV genome

were collected at various time points (6, 12, 24, 36, 48and 60h). mRNAs extracted from cells at each time point were analyzed as templates for reverse transcriptase PCR. Results shown in figure 5.6 indicated that the 297 bps HBSP gene was expressed in HBV transfected cells at 6, 12 and 24 h, but not thereafter. In the case if HBSP was not expressed or samples were contaminated with the parent plasmid, there should be no bands generated or the 1000 bps bands occurred.

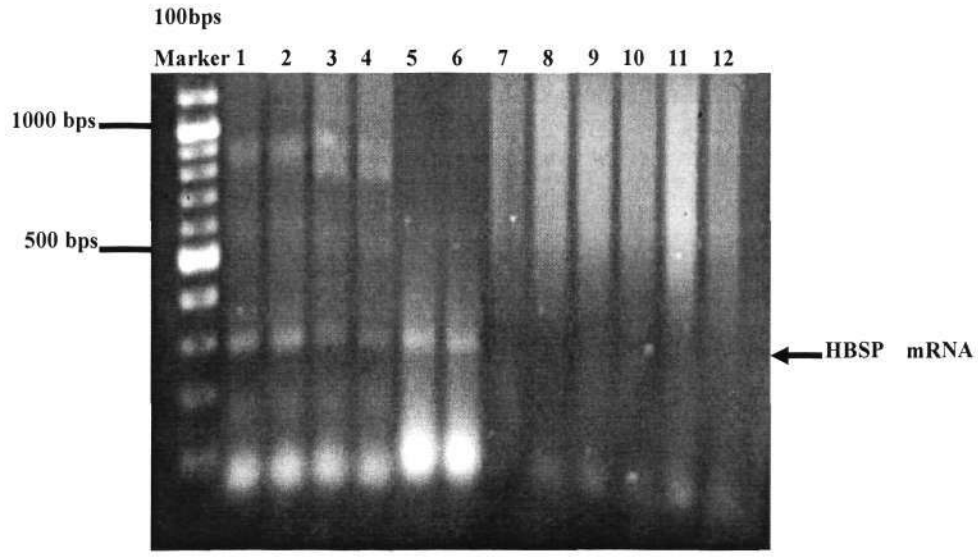

Figure 5.6: Expression of HBSP gene by RT-PCR analysis. mRNA was extracted from HepG2 cells transfected with replicative HBV genome, and used as template for RT-PCR analysis using primers encompassing the coding region of HBSP. Duplicate samples were analyzed for each of the following time points after transfection: 6, 12, 24, 36, 48, and 60hr. HBSP expression was detected up to 24 hr after transfection (arrow head).

The results therefore proved that HBSP was expressed during the HBV replication and may contribute directly to the observe apoptotic effect following HBV replication.

5.3.3 MTT Assay

To investigate the effect on HepG2 cell viability, HBSP was transfected into HepG2

cells and applied to MTT assay as described in Chapter four. To determine the quantitive relationship of HBSP and cell viability, a series of HBSP cDNA (0.4μg, 0.8μg, 1.2μg, 1.6μg and 2.0μg) was transfected in equal starting amount HepG2 cells. Three independent experiments were carried out at same condition and results were presented.

MTT assay	Normal Cells	Cells (UV)	HBSP 0.4ug	HBSP 0.8ug	HBSP 1.2ug	HBSP 1.6ug	HBSP 2.0ug
Experiments	0.589	0.322	0.423	0.385	0.421	0.342	0.373
	0.572	0.311	0.412	0.461	0.371	0.376	0.374
	0.545	0.303	0.497	0.391	0.388	0.427	0.342
Average	0.568	0.312	0.444	0.412	0.393	0.381	0.363
Cell viability%	100%	54.90%	78.20%	72.50%	69.30%	67.20%	63.90%

Data unit: relative fluorescence unit (RFU)

Table 5.2: MTT assay of HBSP transfected HepG2 cells. Three independent experiments were carried out for each sample. The original data for each reading was displayed in this table. The average of the three readings was applied to analysis. Normal cells acted as negative control as 100% living cell while the UV treated cells acted as positive control.

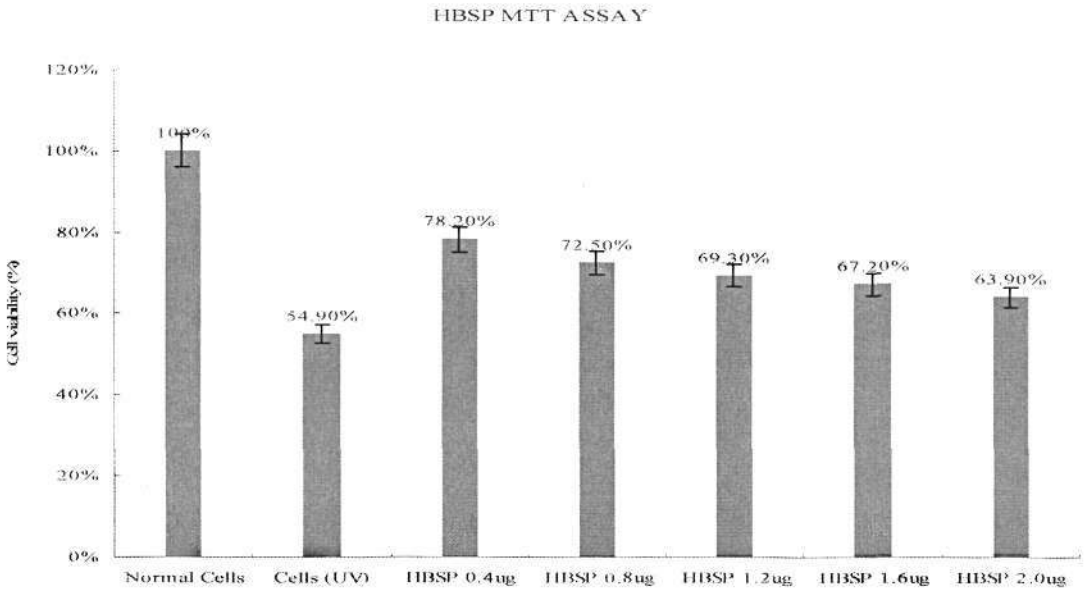

Figure 5.7: MTT assay of HBSP transfected HepG2 cells. HBSP was transfected into HepG2 cells for 48h before collection. Cells were treated by 5mM MTT and lysed after 3hrs incubation at 37°C. Results were read by a microplate reader under a wave length of 505nm. The normal cells and UV treated cells were set as negative and positive controls. The result showed a dose-dependent manner (0.4μg~1.6 μg).

As shown in table 5.2, normal cells treated by tranfection reagents showed an average reading of 0.568 which was regarded as 100% viability while UV treated cells resulted in an average of 0.312 (54.9%) was set as positive control. When the transfected HBSP increased from 0.4μg to 2.0 μg, the cells gave out a series of decreasing readings: 0.444, 0.412, 0.393, 0.381 and 0.363 indicating 78.2%, 72.5%, 69.3%, 67.2% and 63.9% of living cells survived. From figure 5.7, the decreasing cell viability could be clearly observed consistently when the HBSP increased, although not to the extent that UV killed the cells. It could be explained as HBSP induced cells death by a dose-dependent manner.

5.3.4 Analysis of Caspase-3 Activation

To investigate the molecular basis of HBSP-induced apoptosis, HepG2 cells transfected with pXJ40-GST-HBSP were analysed by caspase-3 protease assay, a hallmark of apoptosis. To this end, HepG2 cells were transfected with increasing amount of HBSP at 2 μg, 4 μg, 6 μg and 8 μg, incubated for 48 hr and analyzed for the caspase-3 protease activity.

Capase-3 assay	(+)	(-)	HBSP 2ug	HBSP 4ug	HBSP 6ug	HBSP 8ug	(L25A) 2ug	(L25A) 4ug	(L25A) 6ug	(L25A) 8ug
Experiments	32091	3409	6290	12980	11250	14329	1876	6851	7929	2786
	29558	2876	5385	9867	12393	15663	1763	7154	5366	4208
	31282	3591	3913	8740	10329	15809	2469	5690	6592	3680
Average	30987	3292	3292	10529	11324	15267	2036	7053	6629	3558

Units for all data: relative fluorescence units (RFU)

Table 5.3: Analysis of caspase-3 activation by HBSP and HBSP (L25A). All the samples were applied to three independent experiments. The raw data were presented and the averages were picked up for analysis. Positive and negative controls were 30987 RFU and 3292 RFU, respectively.

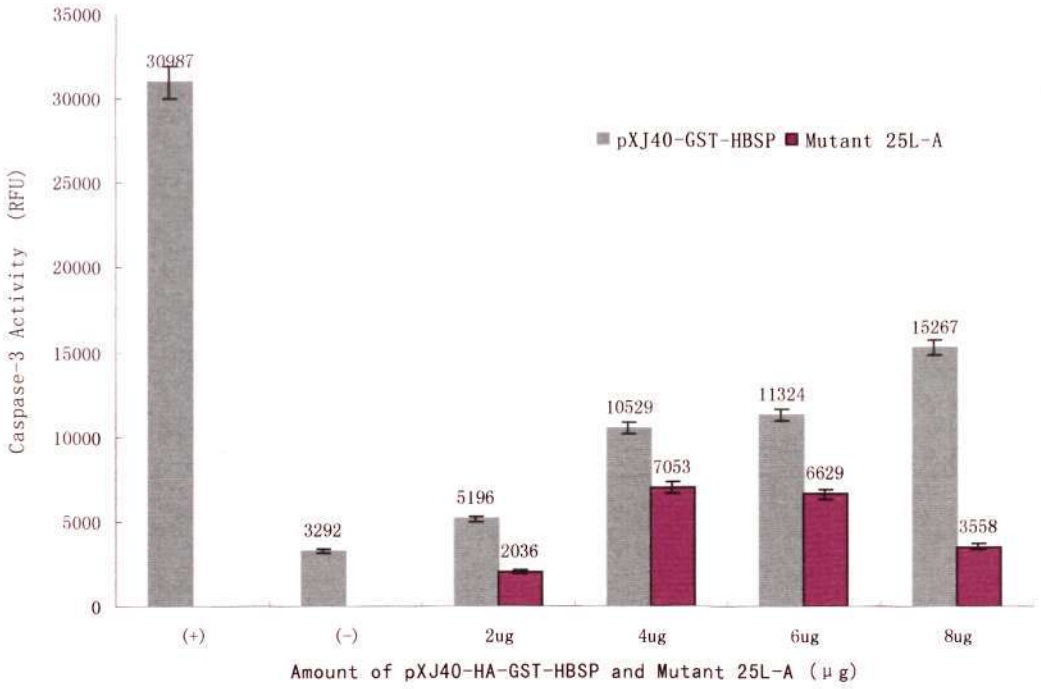

Figure 5.8: Apoptotic Effects of HBSP in HepG2 Cells by Caspase-3 Activity. HepG2 cells were transfected with increasing amounts of either wild type pXJ40-GST-HBSP or mutant pXJ40-GST-HBSP (25A) and analyzed for caspase-3 activity. Similar analysis was carried out on cells treated with cisplatin (+) and those transfected with pXJ40-GST (-). Caspase-3 activity was measured as relative fluorescence units (RFU) in three independent transfections for each amount of plasmid used in this study.

As shown in table 5.3, the caspase-3 activity was measured in three independent transfections as relative fluorescence units (RFU) for each dose of HBSP applied in this study. The average was thereafter calculated to represent each experiment and summarized in figure 5.8. The caspase-3 activity (cleavage of DEVD-AFC substrate) of 3292 RFU was found in cells transfected with pXJ40-GST (negative control), whereas the cells treated by 50 μM cisplatin (positive control) displayed the caspase-3 activity of 30987. In cells transfected with different dose of HBSP, the caspase-3 activity was of 5196, 10529, 11324 and 15627 for 2 μg, 4 μg, 6 μg and 8 μg, respectively. There was therefore a significant increase of caspase-3 activity in HBSP transfected cells, in a dose-dependent manner.

To correlate the expression level of HBSP in HepG2 cells with the observed caspase-3 activity, Western Blot assay was carried out in the total lysate of HepG2 cells by using anti-HA antibody. Results shown in figure 5.9 indicated that an increased intensity of the expected molecular weight of HA-GST-HBSP (38 kD, panel A) was detected, consistent with the increased amount of pXJ40-GST-HBSP used in experiments. On the other hand, only the 26 kD GST protein was detected in cells transfected with pXJ40-GST. A constant intensity of the endogenous actin protein (42 kD, panel B) was observed by using anti-β actin antibody.

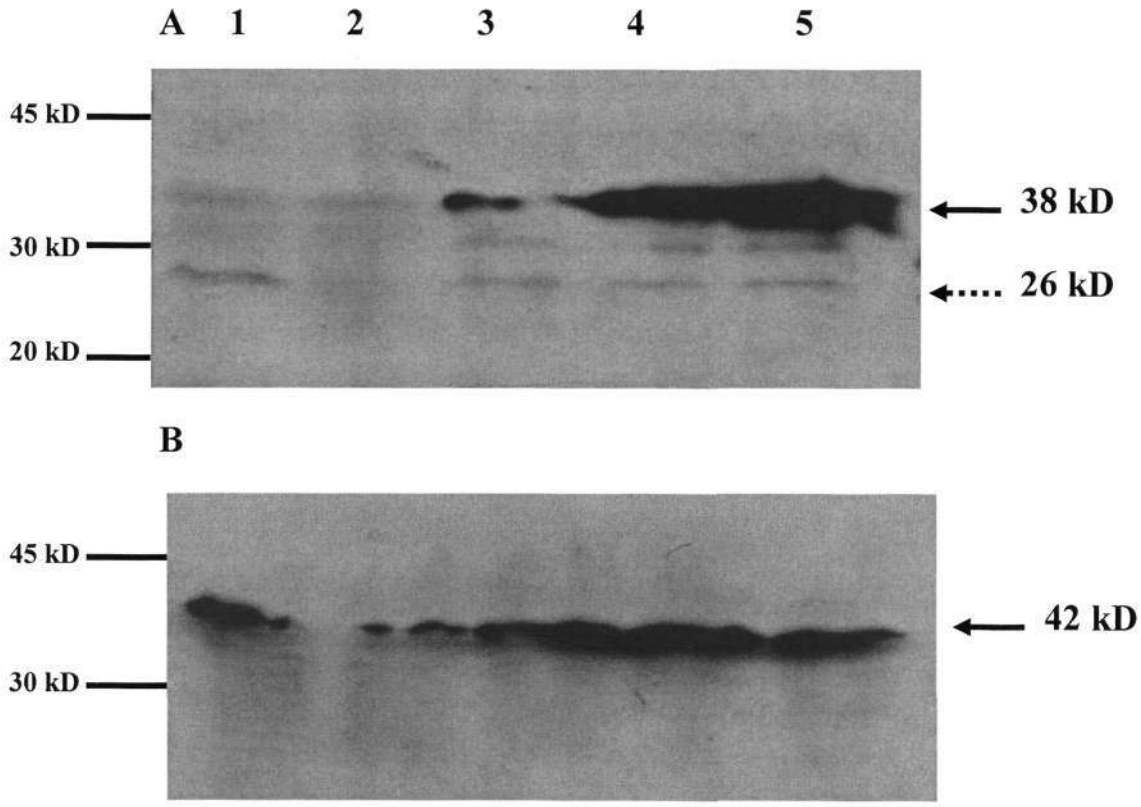

Figure 5.9: Western Blot Analysis of HA-GST-HBSP in HepG2 Cells. Cells were transfected with the different amount of the wild type pXJ40-GST-HBSP (panel A): 2 μg (lane 2), 4 μg (lane 3), 6 μg (lane 4) and 8 μg (lane 5) respectively. HepG2 cells transfected with pXJ40-GST were used as negative control (lane 1, panel A). Endogenous actin was used as an internal control. Antibodies used were anti-HA (panel A) and anti-actin (panel B) respectively. Panel A, solid arrow head indicated the fusion HA-GST-HBSP protein at 38 kD. The discontinued arrow head indicated the 26 kD GST protein in cells transfected with pXJ40-HA-GST (lane 1, panel A). Panel B, arrow head indicated the endogenous action protein at 42 kD.

5.3.5: Analysis of Nuclear Fragmentation

One of the most special characteristics of apoptotic cell is the fragmented nucleus. To further determine the apoptotic effect of HBSP, HBSP was co-transfected with pEGFP into HepG2 cells, followed by nuclear staining using Hochest after 24 h incubation. As shown in figure 5.10, the two neighbouring cells were found to undergo nuclear condensation and fragmentation comparing to other cells (Panel A). Meanwhile, these two cells expressed EGFP which indicated HBSP was also expressed in them due to the same efficiency of two plasmids when co-transfected (Panel B). One cell undergoing typical nucleus fragmentation was shown as positive control (Panel C), while normal cells were stained to show normal nucleus as negative control (Panel D).

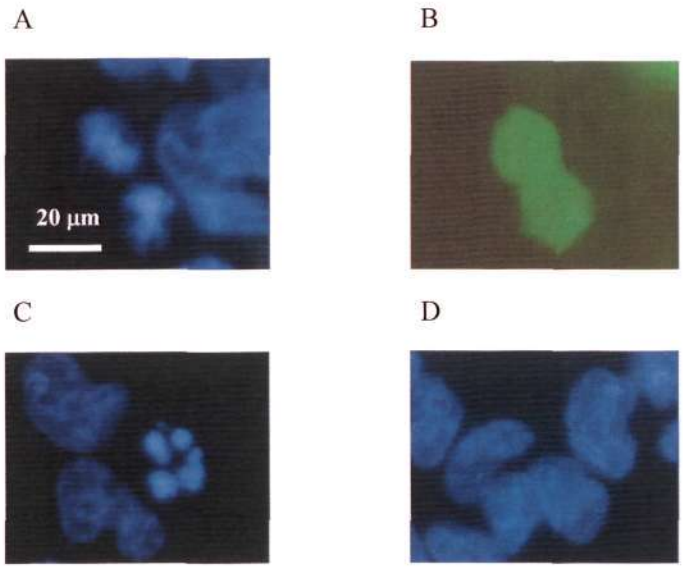

Figure 5.10: Nuclear Fragmentation Effect of HBSP Panel A: DNA Fragmentation in HBSP transfected cells. Panel B: Green fluorescence protein expressed in HBSP transfected cells. (pEGFP co-transfected with HBSP) Panel C: Positive control by cisplatin treated cells. Panel D: negative control of cells with normal nucleus

5.3.6: TUNEL Assay on HBSP and HBSP (L25A)

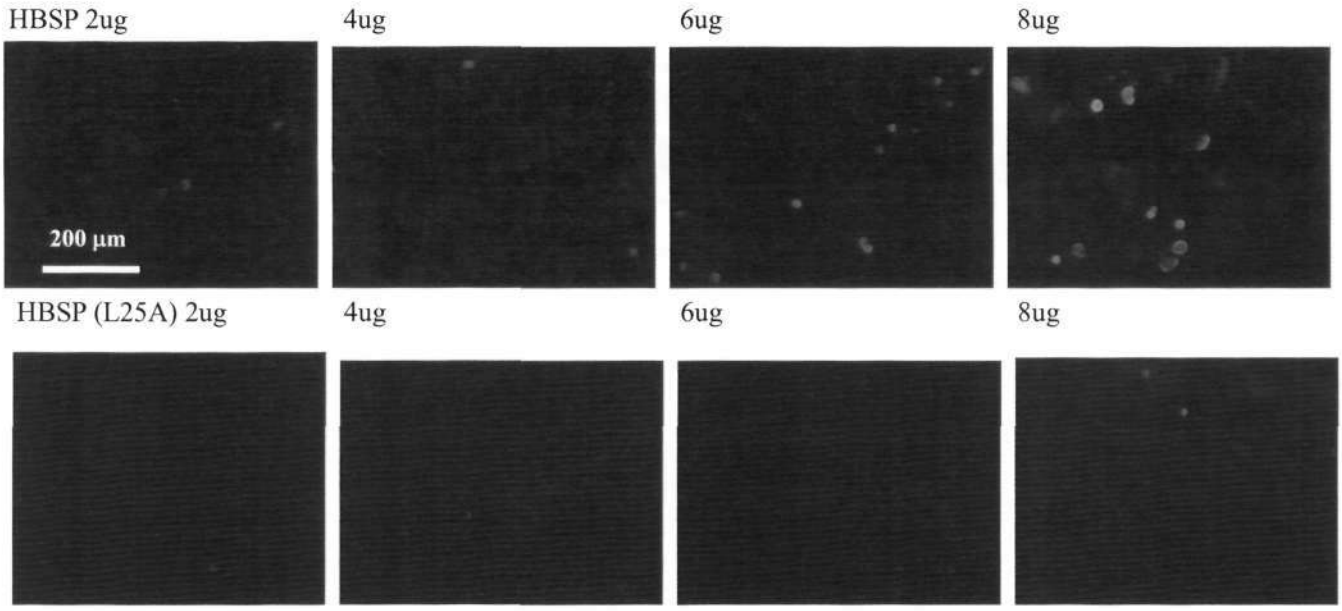

Figure 5.11: TUNEL Assay of HBSP and HBSP (L25A). HepG2 cells were transfected with HBSP and HBSP (L25A) from 2 to 8 μg. After 24 h incubation, cells were subjected to TUNEL assay and observed under fluorescent microscope. The wt HBSP showed an increasing effect of positive TUNEL labeled cells and reached the peak at 8 μg HBSP transfected cells, whereas the mutant HBSP drastically reduced the apoptotic effect at all the four concentrations.

To calculate the apoptotic effect of HBSP on nucleus quantitively, TUNEL assay was carried out. 2, 4, 6, 8 μg of HBSP were transfected into HepG2 cells and subjected to TUNEL labeling after 24 h incubation. Observed under fluorescent microscope, the wide type HBSP showed an increasing effect of positive TUNEL labeled cells and reached the peak at 8 μg HBSP transfected cells (figure 5.11). On the contrary, to specify the BH3 motif of HBSP in inducing apoptosis, a deletion and a mutant of HBSP were generated. The mutation was generated by mutation of the conserved residue lysine to alanine (L25A) which was reported to impact on the pro-apoptotic activity of BH3 containing proteins (Sattler *et al.,* 1997). The mutant was transfected into HepG2 cells in the same dose manner and analyzed by TUNEL assay. Comparing to the wt HBSP, the mutant HBSP drastically reduced the positive apoptotic cells

portion in the total cells. There was no increasing effect of apoptotic cells observed when the mutant dose increased (Figure 5.2H). These results indicated that the wt HBSP could lead to apoptosis, whereas the mutant spoiled the effect.

5.3.7 Analysis of Caspase-3 Activation by HBSP (L25A)

HepG2 cells were transfected with 2, 4, 6, 8 μg HBSP (L25A) and subjected to caspase-3 activity assay. Three independent experiments were carried out and the data was presented in table 5.3. As shown in figure 5.8, in cells transfected with different amount of HBSP (L25A), the caspase-3 activity was at 2036, 7053, 6629 and 3558 for 2 μg, 4 μg, 6 μg and 8 μg mutants, respectively. There was a significant reduction of caspase-3 activity in HBSP (L25A) transfected cells comparing to wt HBSP. In addition, the expression level of HBSP mutant detected in each set of the tranfected HepG2 was shown in figure 5.12.

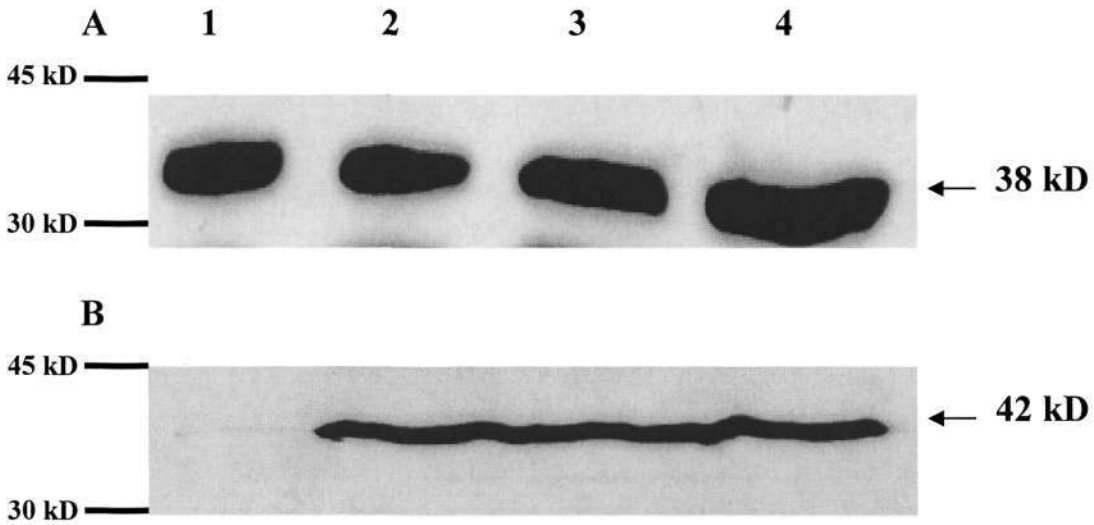

Figure 5.12: Western Blot Analysis of HA-GST-HBSP (L25A) in HepG2 Cells. Cells were transfected with the different amount of the wild type pXJ40-GST-HBSP (L25A) (panel A): 2 μg (lane 1), 4 μg (lane 2), 6 μg (lane 3) and 8 μg (lane 4) respectively. Endogenous actin was used as an internal control (Panel B). Antibodies used were anti-HA (panel A) and anti-actin (panel B) respectively. Panel A, arrow head indicated the fusion HA-GST-HBSP (L25A) protein at 38 kD. Panel B, arrow head indicated the endogenous action protein at 42 kD

The 38 kD HBSP (L25A) was strongly expressed, consistent with the plasmid amount used in the experiments (panel A). Constant intensity of the endogenous actin protein was also observed (42 kD, panel B). These results further suggested that the observed decrease in caspase-3 activity was due to the mutant HBSP, but not the absence of the mutant protein.

5.3.8 Analysis of PS Externalization by HBSP and HBSP (L25A)

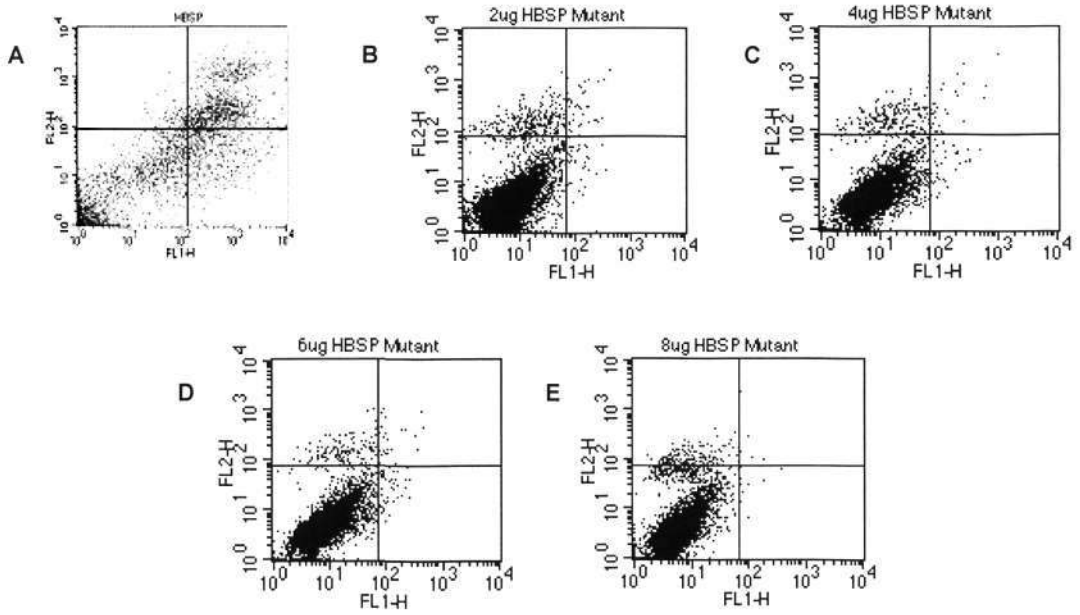

Figure 5.13: FACS analysis of apoptotic effect in HBSP and its mutant in HepG2 cells. HepG2 cells were transfected with HBSP and HBSP mutant in different concentration. The labeling of cells was by Annexin-V-FITC (FL1-H) and Prodium Iodide (FL2-H). In each panel, the bottom right square indicates the number of apoptotic cells and top right square the number of necrotic cells. A.LR: 11.22%, B.LR: 0.22%, C.LR: 0.23%, D.LR: 0.27%, and E.LR: 0.13%

The HBSP and mutant HBSP (L25A) were also transfected into HepG2 cells to test the effect on externalization of PS. Consistent with the analysis apoptosis induced by HBV replication, cells after transfection were subjected to FACS analysis. As shown in figure 5.13, HBSP induced 11.22% apoptotic cells (panel A) while there was no

significant apoptotic cells observed in HBSP mutant transfected cells (Panel B, C, D, and E, below 0.4% for the four experiments)

5.4 Apoptosis Induced by POL-N

As described, HBSP containing the BH3 motif was proved to be pro-apoptotic. The function of the viral polymerase which also contains the BH3 motif remained to be investigated. On the other hand, the 46 amino acid residues at the N-terminus of polymerase shared by HBSP was also generated and nominated as POL-N. These two proteins were cloned and transfected into liver cells to study their function.

5.4.1 Mammalian Two-Hybrid Assay

To investigate the BH3 motif identified in polymerase and POL-N, their interaction with Bcl-2 family of proteins was examined by transient transfection into Huh7 cells. Huh7 cell is another liver derived cell line with high expression and high sensitivity to transfection. On the other hand, identical results come from different cell lines further support the protein's function. The results were obtained from three independent experiments.

As shown in figure 5.14, the results of interaction between HBV POL and Bcl-2 family of proteins did not show significant difference between pro- and anti-apoptotic members. The interaction between POL and Bcl-2 family of proteins was 5.5%, 3.2%, 7.3%, 3.2%, 3.8% and 4.2% with Bcl-xl, Bcl-2, Bad, Bak, Bik and Bax. There was no distinct augment in relative luciferase activity.

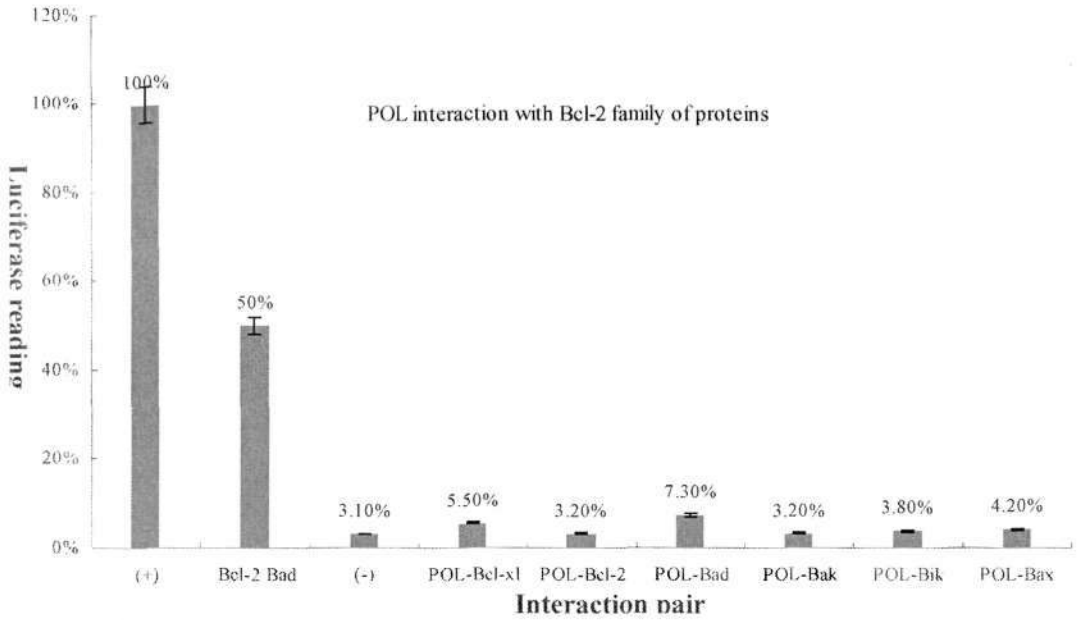

Figure 5.14: Interaction of HBV POL with Bcl-2 Proteins. HBV Polymerase was carried out in mammalian two-hybrid system to detect the interaction with Bcl-2 family of proteins. The results indicated no significant interaction detected.

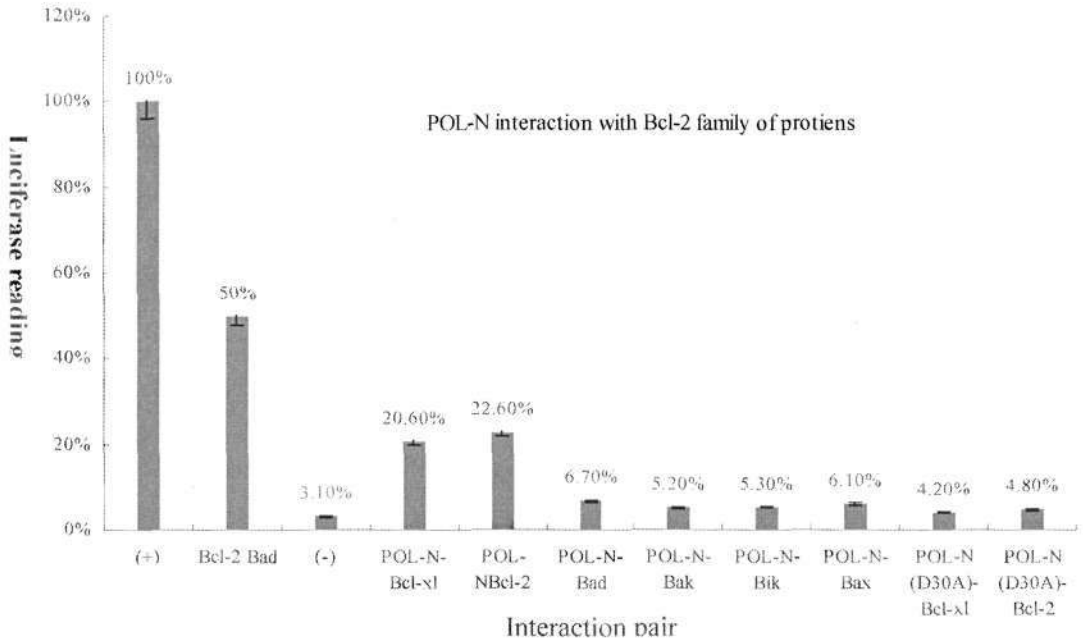

Figure 5.15: Interaction of POL-N with Bcl-2 Proteins. The mammalian two-hybrid assay revealed the relatively high interaction of POL-N with Bcl-2 and Bcl-xl than other Bcl-2 family of proteins. The reading was 20.60% and 22.60 % with Bclxl and Bcl-2 comparing to the 50% of Bcl-2 with Bad.

In the case of POL-N, the increased luciferase activity was observed between POL-N and Bcl-2 or Bcl-xl. As shown in figure 5.15, the results obtained from repeating experiments using POL-N as the bait displayed a significant increased interaction between Bcl-2 and Bcl-xl. The luciferase activity was 20.6% and 22.6% with Bcl-xl and Bcl-2, respectively. However, the interaction of POL-N with the pro-apoptotic proteins remained at 6.7%, 5.2% 5.3% and 6.1% with Bad, Bak, Bik and Bax, respectively. Furthermore, one mutant POL-N (D30A) did not interact with Bcl-xl and Bcl-2, the readings drastically dropped to 4.2% and 4.8%, respectively.

Thus, it was POL-N but not the polymerase showed stronger interaction with the anti-apoptotic Bcl-xl and Bcl-2.

5.4.2 MTT Assay

Based on the interaction results, POL-N was chosen to test its effect on HepG2 cells. Because POL-N shares the same N-terminus with HBSP, it acted as a deletion construct to further confirm the role of BH3 motif as described in HBSP. POL-N was transfected into HepG2 cells and applied to MTT assay as described in Chapter four. To determine the quantitive relationship of POL-N on cell viability, a series of POL-N cDNA (0.4μg, 0.8μg, 1.2μg and 1.6μg) was transfected in equal starting amount HepG2 cells. Three independent experiments were carried out at same condition and results were presented.

As shown in table 5.4, normal cells treated by tranfection reagents showed an average

reading of 0.568 which was taken as 100% viability while UV treated cells resulted in an average of 0.312 (54.9%) as positive control. When the plasmids increased from 0.4μg to 1.6 μg, the cells showed a series of decreasing readings: 0.527, 0.353, 0.347 and 0.305 indicating 96.2%, 64.8%, 63.6% and 56.1% of cells survived. From figure 5.3c, the decreasing cell viability could be clearly observed consistently with the POL-N increasing. It could be explained as POL-N induced cells death by a dose-dependent manner.

Measurement: relative absorbance at 505nm.

MTT assay	Normal Cells	Cells (UV)	POL-N 0.4ug	POL-N 0.8ug	POL-N 1.2ug	POL-N 1.6ug
Experiments	0.566	0.342	0.449	0.373	0.467	0.283
	0.505	0.343	0.622	0.366	0.247	0.313
	0.565	0.246	0.511	0.321	0.327	0.321
Average	0.545	0.311	0.527	0.353	0.347	0.305
Cell viability%	100%	56.90%	96.70%	64.80%	63.60%	56.10%

Table 5.4 MTT assay of POL-N transfected HepG2 cells. Three independent experiments were carried out for each sample. The original data for each reading was displayed in this table. The average of the three readings was applied to analysis. Normal cells acted as negative control as 100% living cell while the UV treated cells acted as positive control.

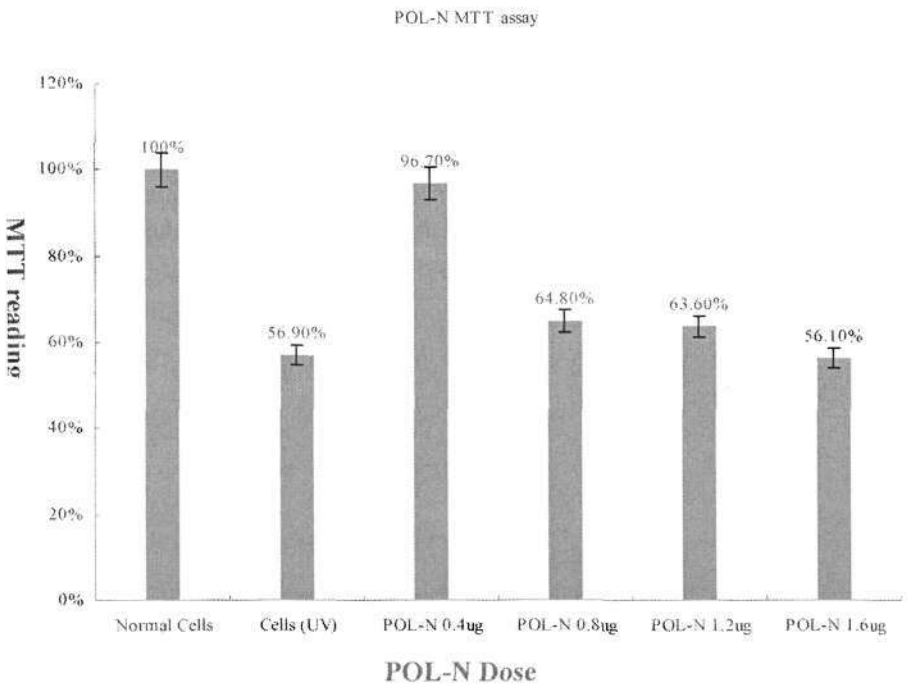

Figure 5.16: MTT assay of POL-N. POL-N decreased the cell viability when the transfection dose increased. The 1.6μg reached 56.1% living cells while the UV treated cells serving as positive control was 56.9%

5.4.3 Analysis of PS Externalization

POL-N was therefore subjected to a biochemical analysis to investigate whether it caused apoptosis. FACS using the ApoAlert Annexin V Apoptosis kit was carried out to detect the externalization of PS. In this study, POL-N transfected HepG2 cells were collected at 12h, 24h, 36h and 48h. Results shown in figure 5.17 indicated there was an increase in the number of apoptotic cells as the transfection time prolonged. 12h after the onset of POL-N transfection, 2% of apoptotic cells were detected. The proportion of such cells was at 10.6% and 15.17% at 24h and 36h after transfection, respectively. Specifically, it reached 22.87% at 48h after transfection. It was significantly higher than the negative control, HepG2 cells transfected with empty plasmid. But it was lower than the positive control in which cells were treated by 100 μM cisplatin for 16h (30.93%).

A set of dose-dependent experiments was also carried out to check the PS externalization. POL-N was transfected in to HepG2 cells from 0.1 μg to 1.2 μg and incubated for 48h. As shown in figure 5.18, the 0.1 μg to 1.2 μg POL-N showed 1.64%, 1.32%, 3.49%, 11.73% and 12.12% of apoptotic cells in the whole fraction. This is correlated to the pro-apoptotic inducing ability of HBSP.

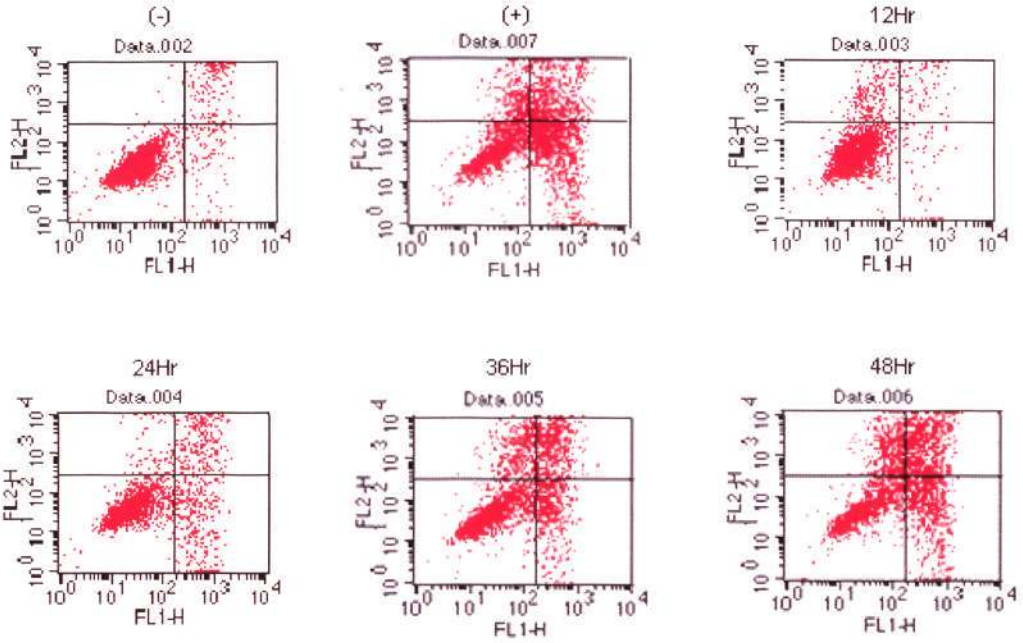

Figure 5.17: POL-N induced externalization of PS by time course. POL-N was transfected into cells and collected at different time points and applied to FACS analysis. The Lower Right (LR) quadrant represents the apoptotic cell percentage. The 36 hr (data 005) and 48 hr (data 006) POL-N transfection reached a reading of 15.17% and 22.87% apoptotic cells while the positive control (data 007) is 30.93%. Normal cells (data 002) as negative control was 3.53%, Negative control was set as 1 μg empty plasmid transfection.

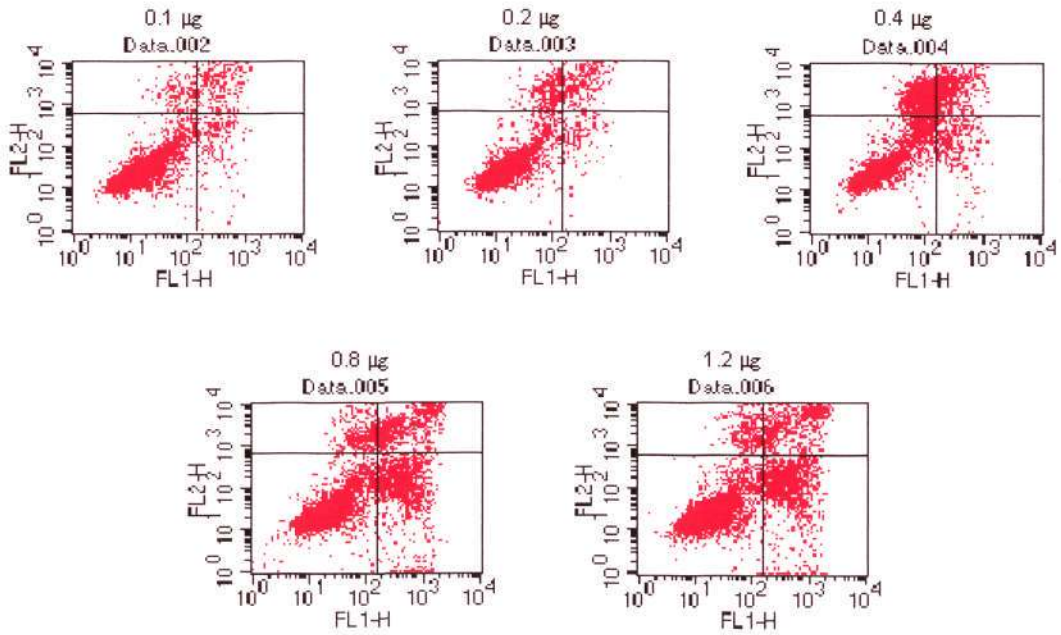

Figure 5.18: POL-N induced PS externalization by dose increasement. POL-N induced cell death by dose dependent manner. Different dose POL-N was tranfected into cells and collected at 48 h. The Lower Right (LR) quadrant represents the apoptotic cell percentage. The 0.8 μg (data 005) and 1.2 μg (data 006) was 11.73% and 12.12% respectively. Controls refer to Figure 5.17.

5.4.4 Analysis of Caspase-3 Activation

Since POL-N helps to investigate the molecular basis of HBSP-induced apoptosis, HepG2 cells transfected with pXJ40-GST-POL-N were analysed by caspase-3 protease assay. To this end, HepG2 cells were transfected with increasing amount of HBSP at 2 μg, 4 μg, 6 μg and 8 μg, incubated for 48 h and analyzed for the caspase-3 protease activity as measured by relative fluorescence units (RFU).

Caspase-3 assay	(+) control	(-) control	POL-N 2ug	POL-N 4ug	POL-N 6ug	POL-N 8ug
Experiments	34870	4383	15735	14480	16126	19718
	30520	4410	11450	15635	18137	24662
	31928	4500				
Average	32439	4431	13592	15057	17131	22190

Units for all data: relative fluorescence units (RFU)

Table 5.5 Caspase-3 assay of POL-N transfected HepG2 cells. All the samples were applied to three independent experiments. The raw data were presented and the averages were picked up for analysis as relative fluorescence units (RFU). Positive and negative controls were 32439 and 4431, respectively.

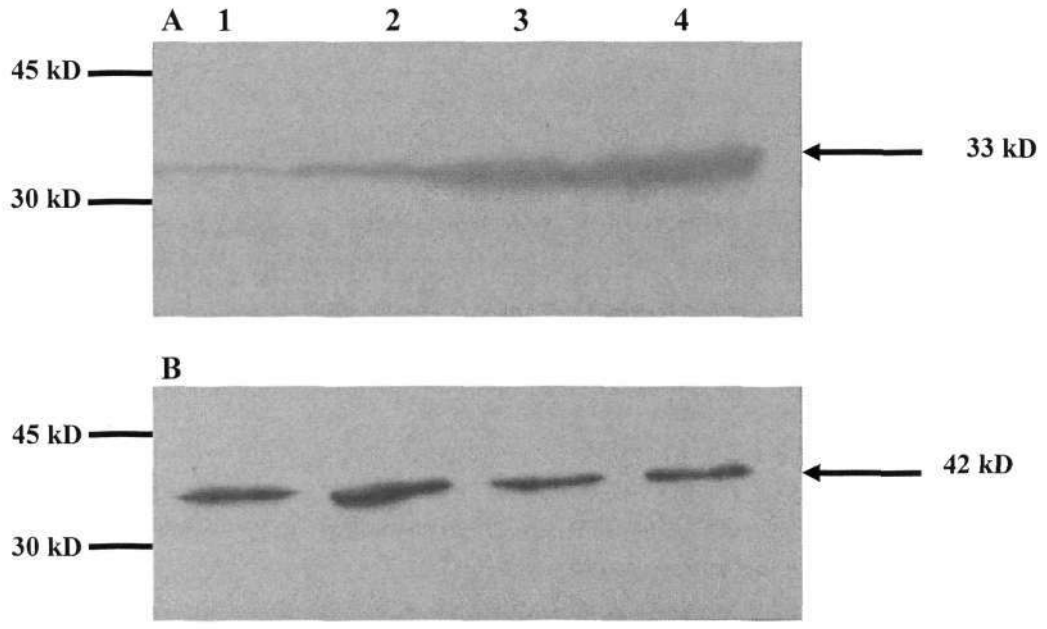

Figure 5.19: Expression of HA-GST-POL-N in caspase-3 assay. Panel A are the dose-dependent expression of the 33 kD GST-POL-N, Lane 1,2,3,4 showed the 2,4,6,8 μg GST-POL-N. Panel B showed the internal control of β–actin at the size of 42 kD.

As shown in table 5.5, the caspase-3 activity was measured as relative fluorescence units (RFU) in two independent transfections for each amount of plasmid used in this study. The average was thereafter calculated to represent each experiment. The caspase-3 activity (cleavage of DEVD-AFC substrate) of 4431 was found in cells transfected with pXJ40-GST (negative control), whereas those cells treated by 50 μM cisplatin (positive control) displayed the caspase-3 activity of 32439. In cells transfected with different amount of POL-N, the caspase-3 activity was at 13592, 15057, 17131 and 22190 for 2 μg, 4 μg, 6 μg and 8 μg, respectively. There was therefore a significant increase of caspase-3 activity in POL-N transfected cells, in a dose-dependent manner.

To correlate the expression level of POL-N in HepG2 cells with the observed caspase-3 activity, Western blot analysis was carried out in the total lysate of HepG2 cells by using anti-HA antibody. Results shown in figure 5.19 indicated an increased intensity of the expected molecular weight of HA-GST-POL-N (33 kD) was detected, consistent with the increased amount of pXJ40-GST-POL-N used in the experiments. A constant intensity of the endogenous β–actin protein (42 kD, panel B) was observed by using anti-β actin antibody.

5.4.5 Purification of GST and GST-POL-N

To further investigate possible signaling pathways of the cell death induced by POL-N, pulldown analysis was carried out. pGEX-POL-N was transformed into E.coli strain BL21 for expressing GST-POL-N. Induction by IPTG of 1 mM and

incubation at 16°C for 24 h were applied in this experiment. pGEX which express GST was set as negative control. Purified proteins were shown in figure 5.20. Panel A showed the 33 kD GST-POL-N, while panel B showed the purified 26 kD GST. Both of them were purified through a column and therefore suitable for the pull down assay.

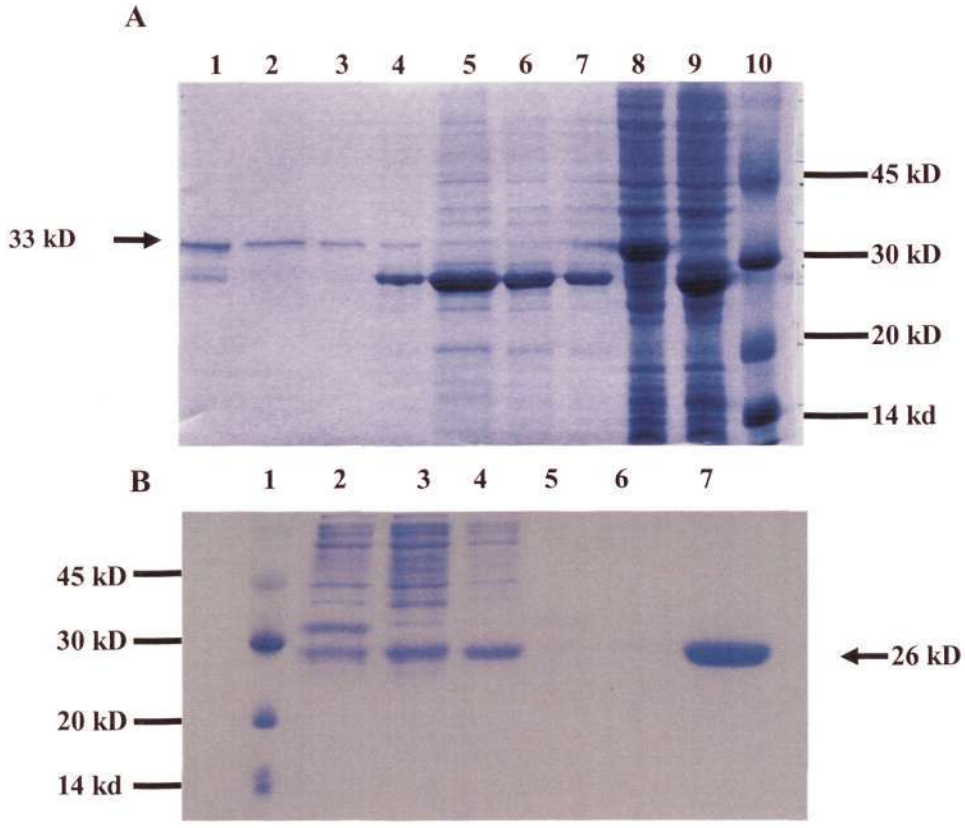

Figure 5.20: Expression and purification of GST and GST-POL-N. pGEX and pGEX-POL-N were transformed into *E.coli* strain BL21 and cultured in LB broth for 2~3 hours before the $O.D_{600}$ arrived 0.6~0.8. IPGT was added into the culture to a final concentration of 1mM before the culture was shaking incubated for 24 hours at 16°C. Bacteria were collected by a short while of centrifugation and lysed by supersonic wave. Supernatant from the total lysis after high speed centrigfugation was applied to GST-Beads column for affinity purification. The purification was repeated once. Elusion samples were checked by SDS-PAGE and Commassie Blue staining. Panel A shows the purified GST-POL-N with MW 33 kD. Panel B shows the purified GST protein, 26 kD.

5.4.6 Pull down of GST-POL-N with HepG2 Cell Extract

HepG2 cells harvested from three flasks of 150 cm^2 were applied to the pull down assay. Supernatant from the total cell lysis after high speed centrifugation was incubated with purified GST-POL-N and GST for 2 h at 4°C. The mixture was then mixed with GST-beads and incubated for another 1 h before applied to column. The binding mixture in columns was washed by PBS·T (0.1% Tween 20) for three times and eluted by GST elution buffer. Elusion samples were checked by SGS-PAGE and stained with Commassie Blue. The results revealed the different protein bands pulled down by GST or GST-POL-N as indicated in figure 5.21. In this gel, the purified GST (lane 2, G 26 kD), GST-Pull down (lane 3, G 26 kD) and GST-POL-N pull down (lane 4, N 33 kD) was displayed respectively. The bands due to GST-POL-N pull down of different size and concentration was indicated by arrows (A, B, and C). They were cut down from the gel, digested by trypsine and sent for LC/MS (Mass Spectrometry) analysis.

A number of proteins have been identified by MS. One of them which showed significant level of expression was the Spliced iso-form 4 of autophagy- related protein 16-1.

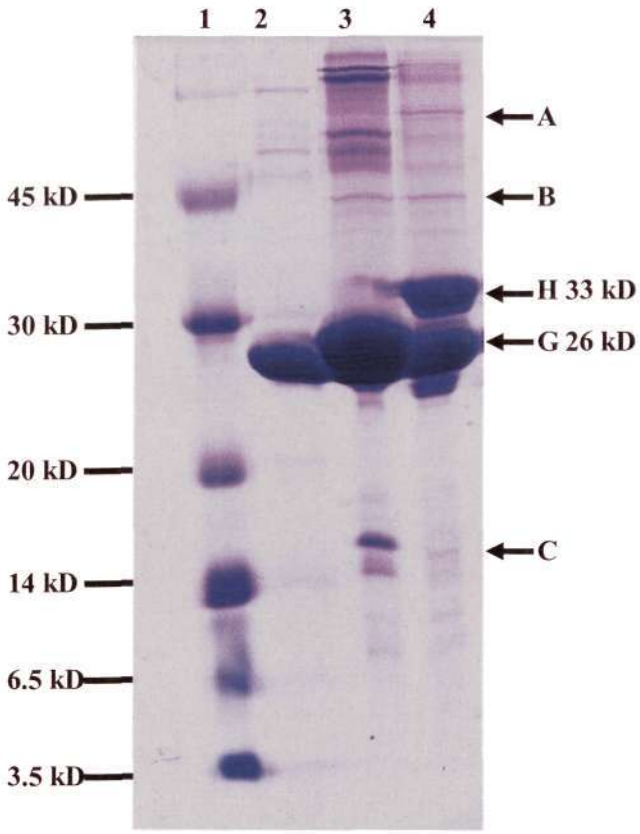

Figure 5.21: GST-POL-N Pull Down Assay. The purified GST and GST-POL-N were immobilized on GST column and incubated with supernatant from HepG2 cell extract, all in large scale. After 2 hrs binding at 4°C, the columns were washed by PBS·T (0.1% Tween 20) for three times and then washed by GST-elusion buffer. Elusion samples were applied to SDS-PAGE and stained with Commassie Blue. Results show the different protein bands pulled down(A, B, and C) by GST (Lane 2 and 3, G 26 kD) and GST-POL-N (Lane 4, N 33 kD) as indicated by arrows. The protein bands were cut down from the gel and sent for Mass Spectrometer analysis.

5.5 CONCLUSION

In conclusion, we reported the identification of a pro-apoptotic BH3 domain in HBSP. The significance of apoptosis caused by replicative HBV genome was contributed by the expression HBSP and HBx. HBSP interacted with Bcl-2 and Bcl-xl through its BH3 domain. The pro-apoptotic activity of HBSP was further supported by nuclear

fragmentation assay, TUNEL assay, FACS assay and caspase-3 assay. Furthermore, the deletion containing the BH3 domain remained able to induce apoptosis and immunoprecipitated an autophagy related protein which involved a possible role of autophagic cell death. Thus, our results have provided the molecular mechanism of apoptosis induced by HBSP.

Chapter Six: Discussion

6.1 DISCUSSION ABOUT HBx RESULTS:

6.1.1 BH3-Like Domain in HBx:

The multiple alignment of BH3 motif involving HBx and related Bcl-2 family of proteins revealed some consensus existing in them. The minimal region of BH3 required to function normally consists of 15~16 amino acids and forms an amphipathic α-helix in solution. The structure of Bcl-xl and Bak peptide complex revealed that the BH3 motif binded in a hydrophobic cleft formed by the BH1, BH2, and BH3 regions of Bcl-xl. The hydrophobic side chains of the BH3 motif pointed into the hydrophobic cleft and stabilized the heterodimerization. In addition, the charged side chains of BH3 motif were close to oppositely charged residues of Bcl-xl and stabilized the binding through electrostatic force. Binding affinity assays using alanine mutants of BH3 motif revealed that the well conserved Val, Gly, and Asp were critical for the BH3 motif activity. Substitution of these residues with alanine drastically increased the dissociation constant of the complex (Sattler *et al.,* 1997). As shown in figure 4.1, the darkly shaded residues were mostly conserved in the BH3 consensus. BH3 motif of HBx contains the hydrophobic residues (Val^{116}, Leu^{123}, and Ile^{127}) and charged residues (Glu^{125}, Glu^{126}). These residues may contribute to hydrophobic and electrostatic interaction to other anti-apoptotic members. In the case of the three most conserved residues, HBx matches the Gly^{124}, mimics the Asp with Glu^{125}, whereas has a Trp^{120} but not Val. The substitution of Asp by Glu^{125} might be reasonable while Glu is also acid residue and able to interact with basic amino acids.

6.1.2 Interaction Assay with Bcl-2 Family of Proteins

In this experiment, Bcl-2 family of proteins was excluded their transmembrane domain which will lead to their subcellular localization on organelles' membrane. The VP-16 in frame with Bcl-2 family of proteins would localize the fusion protein into nucleus without interference. On the other hand, the bait vector pBIND contains an internal control luciferase to reflect the bait protein expression. Thus, Western blotting assay was not carried out through the analysis. One mutant of HBx (E125A) was constructed to further determine the important of the critical residue Glu^{125}. Results from this experiment showed HBx had a relatively higher interaction with Bcl-2 and Bcl-xl than other pro-apoptotic members, while the basic internal control reading of *Renila* luciferase remained almost same. This supported that HBx interacted with the two anti-apoptotic members. The reading of HBx with Bad, interestingly pointed to 8.7%, a bit higher than other pro-apoptotic members. There might be some weak association between two proteins, whereas could not be as strong as interacting proteins. Whether it indicated HBx was anti-apoptotic remained to be investigated. When the alanine mutant of HBx (E125A) replaced the bait wild type HBx, it decreased the interaction of HBx with Bcl-2 and Bcl-xl to a low extent. Alanine does not occupy charged side chains, its substitution spoiled the electrostatic interaction between the aspartic acid and basic residues supposed to exist in Bcl-2 and Bcl-xl. This result supported that the interaction between BH3-like motif of HBx and Bcl-2 or Bcl-xl involved the electrostatic interaction.

On the other hand, a deletion of HBx, the HBx-C did not interact with Bcl-2 or Bcl-xl. The binding of BH3 to Bcl-xl necessitate a conformational change in the Bak protein to expose the hydrophobic surface of α2 helix. The rotation of the α2 helix needed two highly flexible loops flanked on both ends that could allow such a rotation. The deletion of N-terminus might have chopped such a flexible loop near the BH3-like motif of HBx, thus leaded to inhibition of the BH3 motif. However, the three dimensional structure of HBx has not been dissolved yet. Thus, the hypothesis remained to be determined.

6.1.3 Apoptosis Induced by HBx

The MTT assay confirmed that transfection of HBx could kill HepG2 cells in a dose-dependent manner. Whether the effect was apoptosis or necrosis was investigated by checking the externalization of phosphatidylserine (PS). PS externalization is one of the characteristics of apoptotic cell due to the loss of membrane integrity thus its detection by Annexin-V could sort out the apoptotic cells. Results from flow cytrometry of 1 μg and 2 μg pXJ-HBx transfected HepG2 cells showed 12.27% and 15.27% apoptotic cells, respectively. These two numbers represented the low-right area cell percentage. The high reading in Annexin-V-Fitc and low reading in PI indicated these cells were not stained by PI but stained by Annexin-V-FITC, thus the cell were apoptotic but not necrotic. However, the effect HBx was relatively lower than the positive control (cisplatin treated cells). Because the apoptotsis-inducible cisplatin is a known compound instead of a protein, such strong effect was reasonable. The normal cells transfected by empty plasmid pXJ

showed 3.53% apoptotic cells in overall. This might be caused by the transfection method or by the plasmid. Anyway, it served as a good negative control to discriminate the effect of the HBx with the background.

Since HBx induced apoptosis in HepG2 cells, it was decided to detect the caspase-3 activity which could further improve the truth. The results of a series of time course from 2 μg HBx transfected HepG2 cells showed an apparently high reading at 48 h and 60 h. That the caspase-3 activity at 48 h and 60 h was higher than negative control, 16 h, and 24 h might be due to the HBx protein expression difference at different time point and accumulated apoptotic cell gross. The decrease of caspase-3 activity as observed at 72 h might be caused by the decrease in the number of apoptotic cells while the time was too long. On the other hand, the difference between these readings and the positive control was not according to the scale as described in the PS externalization assay. It was because that the two experiments detected different aspects of the apoptotic cells, caspase-3 activity and double-staining. Further more, the reading of caspase-3 was acquired as fluorescence emitting numerical value which was quite indirect to some degree, whereas the PS externalization assay was calculated as single cell. After all, this assay did give out some evidence that HBx could increase caspase-3 activity during its transient expression. It further confirmed that the cell death caused by HBx was apoptosis.

6.1.4 Apoptotic Effects of HBx and Its Half-life

Western blotting assay of the pXJ-HBx transfected cells failed to detect HA-HBx in

HepG2 cells. This may be caused by the fast onset of apoptosis in cells expression HBx or due to unfavored codon to the host cell. Fusion of HBx with GST or GFP, however, could be detected by Western blotting assay and thus excluded the possibility of codon preference of host cell. Result from RT-PCR indicated HBx mRNA was expressed in transfected cells. This provided the evidence that HBx was expressed during the experiments. To further explore the hypothesis, HBx was fused with GST and applied to apoptosis assay and Western blotting assay. The results that GST-HBx was detected by Western blotting assay but did not induce apoptosis were consistent with the hypothesis that HBx protein may not be stable in apoptotic cells triggered by its own expression, whereas the fusion protein which did not induce cell death remained more stable and therefore detectable by Western blotting assay.

In contrast to the widely reported cytoplasmic localization (F.Henkler *et al.,* 2001), our previous investigation revealed a perinuclear localization of HBx when it was expressed as a fusion protein with the green fluorescent protein (GFP) (W.N.Chen *et al.,* 2001). It remains possible that the tagging of HBx with the larger GST protein alters the stability of HBx by affecting its subcellular localization, which in turn may abolish the apoptotic activity observed in our study. While our findings were consistent with recent reports on the pro-apoptotic activity by HBx (N.Lin *et al.,* 2005), HBx may be involved in the process of apoptosis by other mechanisms including its interaction with tumor suppressor p53 and inhibition of DNA repair (Lee *et al.*, 2005, Kim *et al.,* 2005). The difference in these two distinct mechanisms as reported in this and other studies may be reflective of the expression level of HBx and

its stability in transfected cells. Nevertheless, it is possible that HBx may utilize either one of these two, or both, mechanisms to induce apoptosis in infected host cells.

6.2 DISCUSSION ABOUT HBSP RESULTS:

6.2.1: Apoptosis Induced by HBSP

The generated HBV genome was proved able to replicate in transfected HepG2 cells. Detection of excreted HBsAg in culture medium showed a time-dependent augmentation. As a wildly accepted diagnosis method, detection of HBsAg applied here was fast and easy though there are some other methods to detect the existence of HBV, such as HBV DNA detection by Southern Blotting assay and pgRNA detection by Northern Blotting assay. That the HBV replication rose to the peak around 36~48 h accorded with the nature of HBV replication.

HBV genome transfected HepG2 cells showed membrane blebbing as observed under confocal microscope. Membrane blebbing is an important feature in early stage of apoptosis. The observed small vesicles protruding out the cell significantly indicated that it was undergoing apoptosis after transfection of HBV genome. Additionally, cell round up and detachment from culture surface were observed in a time-dependent manner. These two features are important in late stage of apoptosis which further confirmed the cell death caused was apoptosis. That the effect of 36 and 48 h incubation was close to that of cisplatin significantly indicated the intensity increased with accordance to HBV replication at 36 and 48 h.

Interestingly, PS externalization assay of HBV transfected HepG2 cells showed an increasing apoptotic cell proportion when the incubation time prolonged. The results indicated apoptosis was the main causation of the cell death caused by HBV transfection. However, some necrotic cells were detected during the whole experiment. With the fact that cells transfected with empty plasmids also gave similar necrotic cells proportion (about 14%) it was reasonable to regard this as the effect caused by the transfection reagent. It may also caused by some other reason which was not known by far. The apoptosis effect reached 20.75% and 28.83% at 36 h and 48 h which also reflected the pinnacle of HBV replication. The results were higher than that was caused by HBx. This may be due to the difference of experiment setting or the possibility that there was some other mechanism which increased the apoptotic effect (2 μg HBx, 48 h, 15.27%; 2 μg HBV, 48 h, 28.83%). Actually the HBSP identified afterwards did substantiate the possibility.

6.2.2: BH3 Domain and Expression in HBV Replication

The screen of BH3 motif in HBV proteins revealed the presence of a BH3 motif in N-terminus of the viral DNA polymerase, spanning from residue 21-35. However, the polymerase was not able to induce apoptosis in liver derived cell lines (data not shown). Interestingly, the HBSP consists of the N-terminal 46 residues of the polymerase, and thus is involved in the study. The BH3 motifs in Bcl-2 family of proteins are conserved and have some important residues defined as described above. The newly identified BH3 motif in HBSP (as shown in figure 5.4) has the most conserve Leu^{25} and Asp^{30}, which are identical to other known BH3 motifs. Leu^{25} was

considered to form hydrophobic interaction with the cleft in Bcl-xl, while the Asp^{30} was supposed to interact with oppositely charged residues of Bcl-xl by electrostatic force. The hydrophobicity plot of HBSP showed the protein was more hydrophilic in its N-terminus and the region spanning residue 21-35 was amphipathic. This result matches the requirement of BH3 motif as an amphipathic α-helix. The existence of BH3 motif in viral protein is consistant with other viruses capable of inducing apoptotis.

HBSP was proved to express during nature viral infection and anti-HBSP was detectable in patients' sera (Soussan *et al.,* 2000). The detection of HBSP mRNA proved its expression during HBV replication. The mRNA was detectable in early stage (6~24 h) but not late stage (36~60 h) of the HBV replication after transfection. Mechanism of the HBSP mRNA absence remains to be investigated. If there was anti-HBSP IgG, detection of HBSP by Western blotting assay would be more convincible.

6.2.3: Apoptosis in Mammalian Cells

HBSP caused cell death in HepG2 cells in a dose-dependent manner as indicated by MTT assay. Transfection of HBSP indicated this cell death was related to caspase-3 activation and thus was apoptosis. The reading of caspase-3 increased when the transfected dose of HBSP increased at 48 h. Expression of HBSP correlated with the extent of caspase-3 activation in a dose-dependent manner. Additionally, the nuclear fragmentation and condensation during the apoptosis induced by HBSP were

observed in the HBSP transfected cells. TUNEL assay, an important detective method of apoptosis, also indicated a positive role of HBSP in inducing apoptosis. These results further confirmed some characteristics of apoptosis induced by HBSP and were accordant with the property of HBSP to induce apoptosis without cell-cycle block as reported (Soussan *et al.*, 2000).

A conserved residue leucine was reported to impact on the pro-apoptotic activity of BH3 motif, thus a mutant of HBSP (L25A) was generated to replace the Leu^{25} with alanine. HBSP (L25A) induced the activation of caspase-3 not as what HBSP did. However, the activation of caspase-3 in 4 μg and 6 μg HBSP (L25A) transfected cells were still higher than negative cells which were transfected with empty plasmid. This result implied the pro-apoptotic activity of HBSP was to some degree inactivated by the mutant L25A. PS externalization assay and TUNEL assay of HBSP (L25A) tranfected cells did not show significant apoptosis. Therefore, HBSP (L25A) was proved not able to promote cell death as same as HBSP due to the mutation of BH3 motif. Thus, the BH3 motif was essential for HBSP to induce apoptosis.

6.2.4: Effects of POL-N

HBV polymerase was proved not able to induce apoptosis and interact with Bcl-2 or Bcl-xl. As a C-terminus deletion of HBSP, POL-N which contained the BH3 motif interacted with Bcl-2 and Bcl-xl. Mutation of another conserved critical residue aspartic acid to alanine (POL-N D30A) significantly decreased the interaction of POL-N with those anti-apoptotic members. These results made it convincible that

BH3 was the key motif to induce apoptosis while the conserved aspartic acid was one of the critical residues. That the viral polymerase did not function on apoptosis may be due to the large size of it at the C-terminus which executed other important functions for the virus such as reverse transcriptase, polymerase and RNase H. Like the HBSP induced apoptosis in transfected cells, POL-N caused apoptosis in cells by activating caspase-3 and inducing PS externalization, too. This accordance further proved the BH3 was the main cause of apoptosis induced by these proteins.

6.2.5 POL-N and Autophagic Cell Death

One of the pulled down proteins by POL- N was the Splice isoform 4 of autophagy-related protein 16-1. Autophagy is the intracellular system responsible for protein trafficking (degradation and recycling). Rescent research has reported autophagy might both promote cell survival and cell death (Eskelinen, 2005). During the ischemia/reperfusion process of heart, increased autophagy protect the cells from Bnip3 (a BH3 only death promoting protein) induced apoptosis (Hamacher et al., 2006). On the other hand, autophagy was defined as another way of programmed cell death dependent of autophay proteins (Tsujimoto and Shimizu, 2005). Beclin1, an autophagy gene product, interacts with Bcl-2 and negatively regulates its function (Pattingre and Levine, 2006). The interaction of POL-N with autophagy related protein 16-1 might regulate the function of autophagy, thus affect the destiny of the cell.

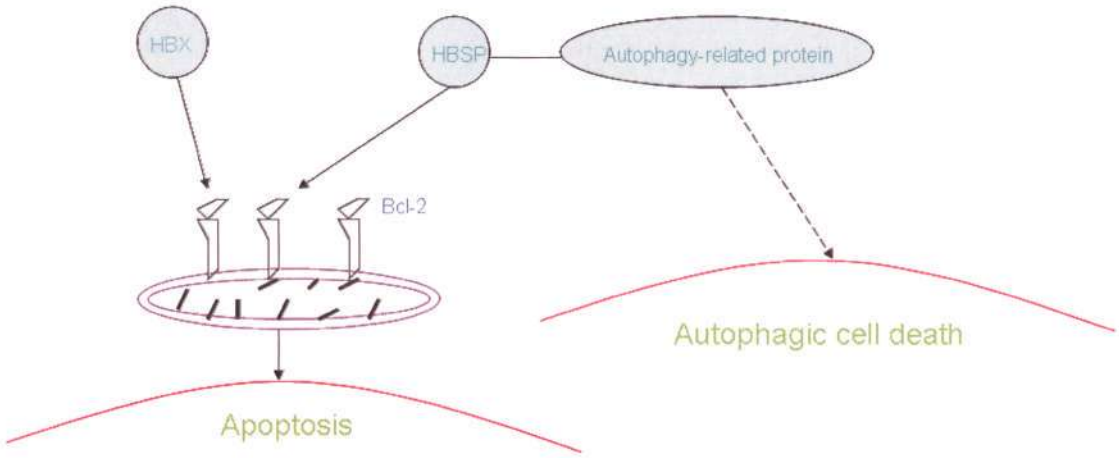

Figure 6.1 Imaginatory function of HBx and HBSP. HBx and HBSP interact with Bcl-2 and/or Bcl-xl on the outer membrane of mitochondria. The interaction is through the BH3 domain binding and leads to apoptosis due to the mitochondria collapse. HBSP interacts with another autophagy-related protein which might lead to autophagic cell death when apoptosis was not available.

Taken together, the results indicated that HBSP induced apoptosis when over-expressed in mammalian cells and may have a direct involvement in apoptosis associated with HBV replication. These findings may also point to a direct involvement of HBV viral proteins in the viral pathogenesis unrelated to the host immune response. Despite a compact genome with overlapping coding region, evidence of alternative spliced variants has been documented in HBV carriers. One of these, HBSP which has been shown to induce apoptosis and to be associated with HBV pathogenesis, contained a BH3 motif identified in this study. On the other hand, many viruses synthesize viral proteins that induce apoptosis by enhancing the various constitutive apoptotic mechanisms of the hosts. Actually apoptotic cells usually are vacuolized and endocytosed by neighboring cells. Thus, if apoptosis occurs late in the infection, this will allow the completed virus particles to be disseminated with minimum induction of inflammatory and immune response and protected from the

neutralizing antibodies. Our results suggested that HBV appeared to be capable to induce apoptosis, thus it might posses an alternative mechanism of modulating its interaction with the infected host cells.

References

Adams, J. M., and Cory, S. (1998). The Bcl-2 protein family: arbiters of cell survival. Science *281*,1322-1326.

Alexander, G. J. M. (1990). Immunology of hepatitis B virus infection. Br. Med. Bull. *45*, 354-67.

Alshatwi, A. A., Han, C. T., Schoene, N. W., and Lei, K. Y. (2006). Nuclear accumulations of p53 and Mdm2 are accompanied by reductions in c-Abl and p300 in zinc-depleted human hepatoblastoma cells. Exp. Biol. Med. *231*, 611-618.

Antonsson, B., Conti, F., Ciavatta, A., Montessuit, S., Lewis, S., Martinou, I., Bernasconi, L., Bernard, A., Mermod, J.J., Mazzei, G., Maundrell, K., Gambale, F., Sadoul, R., and Martinou, J.C. (1997). Inhibition of Bax channel-forming activity by Bcl-2. Science *277*, 370–372.

Baell, J. B., and Huang, D. C. (2002). Prospects for targeting the Bcl-2 family of proteins to develop novel cytotoxic drugs. Biochem. Pharmacol. *64*, 851-863.

Bakhshi, A., Jensen, J. P., Goldman, P., Wright, J. J., Mcbride, O. W., Epstein, A. L., and Korsmeyer, S. J. (1985). Cloning the chromosomal breakpoint of t (14;18) human lymphomas: clustering around JH on chromosome 14 and near a transcriptional unit on 18. Cell. *41*, 899-906.

Bartenschlager, R., and Schaller, H. (1992). Hepadnaviral assembly is initiated by polymerase binding to the encapsidation signal in the viral RNA genome. EMBO J. *11*, 3413-3420.

Bartenschlager, R., Junker, M., and Schaller, H. (1990). The P gene product of hepatitis B virus is required as a structural component for genomic RNA encapsidation. J. Virol. *64*, 5324-5332.

Bazzoni, F., and Beutler, B. (1996). The tumor necrosis factor ligang and receptor families, New Engl. J. Med. *334*, 1717-1725.

Beckel –Mitchener, A., and Summers, J. (1997). A novel transcriptional element in circular DNA monomers of the duck hepatitis B virus. J. Virol. *71*, 7917-7922.

Benn, J., Su, F., Doria, D., and Schneider, R. J. (1996). Hepatitis B virus HBx protein induces transcription factor AP-1 by activation of extracellular signal-regulated and c-Jun N-terminal mitogen-activated protein kinases. J. Virol. *70*, 4978–4985.

Beutler, B., and van Huffel, C. (1994). Unraveling function in the TNF ligand and

receptor families. Science. *264*, 667-668.

Blum, H. E., Zhang, Z.S., Galun, E., von, W. F., Garner, B., Liang, T.J., and Wands, J.R. (1992). Hepatitis B virus X protein is not central to the viral life cycle in vitro. J. Virol. *66,* 1223-1227.

Blumberg, B. S., Larouze, B., London, W. T., Werner, B., Hesser, J. E., Millman, I., Saimot, G.., and Payet, M. (1975). The relation of infection with the hepatitis B agent to primary hepatic carcinoma. Am. J. Pathol *81*, 669-682.

Bodmer, J. L., Burns, K., Schneider, P., Hofmann, K., Steiner, V., Thone, M., Bornand, T., Hahne, M., Schroter, M., Becker, K., Wilson, A., French, L. E., Browning, J. L., Macdonald, H. R., and Tschopp, J. (1997). TRAMP, a noval apoptosis-mediating receptor with sequence homology to tumor necrosis factor receptor 1 and Fas. Immunity. *6*, 79-88.

Bouchard, M. J., Wang, L. H., and Schneider, R. J. (2001). Calcium signaling by HBx protein in hepatitis B virus DNA replication. Science. *294*, 2376–2378.

Boyd, J. M., Gallo, G. J., Elangovan, B., Houghton, A. B., Malstrom, S., Avery, B. J., Ebb, R. G., Subramanian, T., Chittenden, T., and Lutz, R. J. (1995). Bik, a novel death-inducing protein shares a distinct sequence motif with Bcl-2 family proteins and interacts with viral and cellular survival-promoting proteins. Oncogene *11*, 1921–1928.

Breiner, K. M., and Schaller, H.Cellular (2000). Receptor traffic is essential for productive duck hepatitis B virus infection. J.Virol. *74*, 2203-2209.

Bruin, W. C., Leender, W. P., Kos, T., Hertogs, K., Depla, E., and Yap, S. H. (1994). Hepatitis delta virus attaches to human hepatocytes via human liver endonexin II, a specific HBsAg binding protein. J. Viral. Hepat. *1*, 33-38.

Bruin, W. C., Hertogs, K., Leenders, W. P., Depla, E., and Yap, S. H. (1995). Hepatitis B virus: specific binding and internalization of small HBsAg by human hepatocytes. J. Gen. Virol. *76*, 1047-1050.

Bruss, V., and Ganem, D. (1991). The role of envelope proteins in hepatitis B virus assembly. Proc. Natl. Acad. Sci. USA. *88*, 1059-1063.

Bruss, V., Hagelstein, J., Gerhardt, E., and Galle, P. R. (1996). Myrislation of the large surface protein is required for hepatitis B virus in vitro infectivity. Virology. *218*, 396-409.

Bruss, V., Lu, X., Thomssen, R., and Gerlich, W. H. (1994). Post-translational alterations in transmembrane topology if the hepatitis B virus large envelope protein.

EMBO J. 13, 2273-2279.

Carman, W., Thomas, H., and Domingo, E. (1993). Viral genetic variation: hepatitis B virus as a clinical example. Lancet. *341*, 349-355.

Carman, W. F., Van Deursen, F. J., Minns, L. T. (1997). The prevalence of surface antigen variants of hepatitis B virus in Papua New Guinea, south Africa, and Sardinia. Hepatology. *26*, 1658-66.

Carman, W. F., Zanetti, A. R., and Karayianis, P. (1990).Vaccine-induced escape mutant of hepatitis B virus. Lancet. *336*, 325-329.

Carman, W., Thomas, H., and Domingo, E. (1993). Viral genetic variation: hepatitis B virus as a clinical example. Lancet *341*, 349-353.

Castrilla, A., Prieto, J., and Fausto, N. (1991). Transforming growth factors beta 1 and alpha in chronic liver disease-effect of interferon alpha therapy. New Engl. J. Med. *324*, 933-940.

Chang, C., Zhou, S., Ganem, D., and Standring, D. N. (1994). Phenotypic mixing between different hepadnavirus nucleocapsid proteins reveals C protein dimerization to be *cis* preferential. J. Virol. *68*, 5225-5231.

Chang, L. J., Pryciak, P., Ganem, D., and Varmus, H. E. (1989). Biosynthesis of the reverse transcriptase of hepatitis B viruses invokves de novo translational initiation not ribosomal frameshifting. Nature. *337*, 364-368.

Chen, G. G., Lai, P. B., Chan, P. K., Chak, E. C., Yip, J. H., Ho, R. L., Leung, B. C., and Lau, W. Y. (2001). Decreased expression of Bid in human hepatocellular carcinoma is related to hepatitis B virus X protein. Euro. J. Cancer. *37*, 1695-1702.

Chen, H. S., Kaneko, S., Girones, R., Anderson, R. W., Hornbuckle, W. E., Tennant, B. C., Cote, P. J., and Miller, R. H. (1993). The woodchuck hepatitis virus X gene is important for establishment of virus infection in woodchucks. J.Virol. *67*, 1218-1226.

Chen, W. N., Oon, C. J., Leong, A. L., Koh, S., and Teng, S. W. (2000). Expression of integrated Hepatitis B virus X variants in human hepatocellular carcinomas and its significance. Biochem. Biophys. Res. Commun. *276*, 885-892.

Chervonsky, A. V., Wang, Y., Wong, F. S., Flavell, R. A., Janeway, C. A., and Matis, L. A. (1997). The role of Fas in autoimmune diabetes. Cell. *89*, 17-24.

Chinnaiyan, A. M., O'Rourke, K., Tewari, M., and Dixit, V. M. (1995). FADD, a novel death domain-containing protein, interacts with the death domain of Fas and initiates

apoptosis. Cell. *81*, 505-512.

Chinnaiyan, A. M., O'Rourke, K., Yu, G. L., Lyons, R. H., Garg, M., Duan, D. R., Xing, L., Gents, R., Ni, J., and Dixit, V. M. (1996). Signal transduction by DR3, a death domain-containing receptor related to TNF-R1 and CD95. Science. *274*, 990-992.

Chinnaiyan, A. M., Tepper, C. G., Seldin, M. F., O'Rourke, K., Kischel, F. C., Hellbardt, S., Krammer, P. H., Peter, M. E., and Dixit, V. M. (1996). FADD/MORT1 is a common mediator of CD95 and tumor necrosis factor-induced apoptosis. J. Biol. Chem. *271*, 4961-4965.

Chirillo, P., Pagano, S., Natoli, G., Puri, P. L., Burgio, V. L., Balsano, C., and Levrero, M. (1997). The hepatitis B virus X gene induces p53-mediated programmed cell death. Proc. Natl. Acad. Sci. USA. *94*, 8162-8167.

Chirillo, P., Pagano, S., and Natoli, G. (1997). The hepatitis B virus X gene induces p53-mediated programmed cell death. Proc. Natl. Acad. Sci. USA. *94*, 8162-8167

Chisari, F. V., and Ferrari, C. (1995). Hepatitis B virus immunopathology. Spring Semin Immunopathol. *17*, 261-281.

Chisari, F. V., and Ferrari, C. (1995). Hepatitis B virus immunopathogenesis. Annu. Rev. Immunol. *13*, 29–60.

Chisari, F. V. (1995). Hepatitis B virus transfenic mice: Insights into the virus and disease. Hepatology. *22*, 1316-1325.

Chittenden, T., Flemington, C., Houghton, A. B., Ebb, R. G., Gallo, G. J., Elangovan, B., Chinnadurai, G., and Lutz, R. J. (1995). A conserved domain in Bak, distinct from BH1 and BH2, mediates cell death and protein binding functions. EMBO J. *14*, 5589–5596.

Colgrove, R., Simon, G, and Ganem. D. (1989). Transcriptional activation of homologous and heterologous genes by the hepatitis B virus X gene product in cells permissive for viral replication. J. Virol. *63*, 4019–4026.

Cooper, A., Paran, N., and Shaul, Y. (2003). The earliest steps in hepatitis B virus infection. Biochim. Biophys. Acta. *614*, 89-96.

Cooper, A., Paran, N., and Shaul, Y. (2003). The earliest steps in hepatitis B virus infection. EMBO.J. *13*, 2273-2279.

Cosulich, S. C., Worrall, V., Hedge, P. J., Green, S., and Clarke, P. R. (1997). Regulation of apoptosis by BH3 domains in a cell-free system. Curr. Biol. *7*, 913–920.

Crowther, R. A., Kiselev, N. A., Bottcher, B., Berriman, J. A., Borisova, G. P., Ose, V., and Pumpens, P. (1994). Three-dimentional structure of hepatitis B virus core particles determined by electron cryomocroscopy. Cell. *77*, 943-50.

Dandri, M., Petersen, J., Stockert, R. J., Harris, T. M., and Rogler, C. E. (1998). Metabolic labeling of woodchuck hepatitis B virus X protein in naturally infected hepatocytes reveals a bimodal half-life and association with the nuclear framework. J. Virol. *72*, 9359–9364.

Dandri, M., Schirmacher, P, and Rogler, C. E. (1996). Woodchuck hepatitis virus X protein is present in chronically infected woodchuck liver and woodchuck hepatocellular carcinomas which are permissive for viral replication. J. Virol. *70*, 5246–5254.

Dane, D. S., Cameron, C. H., Briggs, N. M. (1970). Virus-like particles in serum of patients with Australia-antigen-associated hepatitis. Lancet. *1*, 695-698.

Diehl, A., Yin, M., Fleckenstein, J., Yang, S., Lin, H., Brenner, D., Westwick, J., Bagby, G., and Nelson, S. (1994). Tumor necrosis factor-alpha induces c-jun during the regenerative response to liver injury. Am. J. Physiol. *267*, G552–G561.

Douglas, R. G., and John, C. R. (1998). Mitochondria and Apoptosis. Science *281*, 1309-1312.

Ehrmann, J., Galuszkova, D. (2000). Apoptosis-related proteins, Bcl-2 Bax, Fas, Fas-L and PCNA in liver biopsies of patients with chronic hepatitis B cirus infection. Pathol. Oncol. Res. *6*, 130-135.

Eskelinen, E. L. (2005). Doctor Jekyll and Mister Hyde: autophagy can promote both cell survival and cell death. Cell death and Differentiation. *12*, 1468-1472.

Faktor, O., and Shaul, Y. (1990). The identification of hepatitis B virus X gene responsive elements reveals functional similarity of X and HTLV-I tax. Oncogene. *5*, 867–872.

Falco, S., Ruvoletto, M. G., Verdoliva, A., Ruvo, M., Raucci, A., Marino, M., Senatore, S., Cassani, G., Alberti, A., Pontisso, P., and Fassina, G. (2001). Cloning and expression of a novel hepatitis B virus-binding protein from HepG2 cells. J. Biol. Chem. *276*, 36613-36623.

Fang, J. W. S., Sheu, W. W., Meager, A., Lau, J. Y. N. (1996). Activation of the tumor necrosis factor-alpha in the liver in chronic hepatitis B virus infection. A. J. Gastro. *91*, 748-753.

Fang, W. J. S., Gonzalez-Peralta, R. P., Gottschall, J. A., Davis, G. L., Gish, R. G., Mizokami, M., and Lau J. Y. N. (1994). Hepatic exression of c-Fas and apoptosis in chronic hepatitis C virus (HCV) infection . Hepatology. *20*, 24A.

Feiteson, M. A. (1994). Biology of hepatitis B virus variants. Lab. Invest. *71*, 324-349.

Fernholz, D., Galle, P. R., Stemler, M., Brunetto, M., Bonino, F., and Will, H. (1993). Infectious hepatitis B virus variant defective in pre-S2 protein expression in a chronic carrier. Virology. *194*, 137-148.

Ferrari, C., Bertoletti, A., and Penna, A. (1991). Identification of immunodominant T cell epitopes of the hepatitis B virus nucleocapsid antigen. J. Clin. Invest. *88*, 214-222.

Forgues, M., Marrogi, A., Spillare, E., Wu, C. G., Yang, Q., Yoshida, M., and Wang, X. (2001). Interaction of the hepatitis B virus X protein with the Crm1-dependent nuclear export pathway. J. Biol. Chem. *276*, 22797–22803.

Ganem, D., Pollack, J. R., and Tavis, J. (1994). Hepatitis B virus reverse transcriptase and its many roles in hepadnaviral genomic replication. Infect. Agents. Dis. *3*, 85-93.

Ganem, D., and Schneider, R. J. (2001). The molecular biology of the hepatitis B viruses, p. 2923–2970. *In* D. M. Knipe, P. M. Howley, D. E. Griffin, R. A. Lamb, M. A. Martin, B. Roizman, and S. E. Straus, Fields virology, 4th ed, vol. 2. Lippincott Williams & Wilkins, Philadelphia, Pa.

Ganem, D., and Varmus, H.E. (1987). The molecular biology of the hepatitis B viruses. Annu. Rev. Biochem. *56,* 651–693.

Gerlich, W. H, Lu, X., and Heermann, K. H. (1993). Studies on the attachment and penetration of hepatitis B virus. J. Hepatol. *17*, S10-S14.

Giron, M. L., de The, H., and Saib, A. (1998). An evolutionarily conserved splice generates a secreted env-Bet fusion protein during human foamy virus infection. J. Virol. *72*, 4906–4910.

Glebe, D., Aliakbari, M., Krass, P., Knoop, E. V., Valerius, K. P., and Gerlich, W. H. (2003). Pre-S1 antigen-dependent infection of tupaia hepatocyte cultures with human hepatitis B virus. J.Virol. *77*, 9511-9521.

Gripon, P., Diot, C., These, N., Fourel, I., Loreal, O., Brechot, C., and Guguen-Guillouzo, C. (1988). Hepatitis B virus infection of adult human hepatocytes cultured in the presence of dimethylsulfoxide. J.Virol. *62*, 4136-4143.

Gripon, P., Rumin, S., Urban, S., Le Seyec, J., Glaise, D., Cannie, I., Guyomard, C., Lucas, J., Trepo, C., and Guguenguillouzo, C. (2002). Infection of a human hepatoma cell line by hepatitis B virus. Proc. Natl. Acad. Sci. USA. *99*, 15655-15660.

Gripon, P., Le, S. J., Rumin, S., and Guguen, G. C. (1995). Myrisylation of the hepatitis B virus large surface protein is essentialfor viral infectivity. Virology. *213*, 292-299.

Grob, P. (1998). Hepatitis B virus, pathogenesis and treatment. Vaccine. *16*, s11-s16.

Grob, P. (1995). Introduction to epidemiology and risk of hepatitis B. Vaccine. *13*, 514-515.

Guihot, S., Miller, T., Cornman, G., Isom, H. C. (1996). Apoptosis induced by tumor necrosis factor-alpha in rat hepatocyte cell lines expressing hepatitis B virus. AM. J. Pathol. *148*, 801-814.

Günther, S., Sommer, G., Iwanska, A., and Will, H. (1997). Heterogeneity and common features of defective hepatitis B virus genomes derived from spliced pregenomic RNA. Virology. *238*, 363–371.

Guo, J. T., and Pugh, J. C. (1997). The topology of the large envelope protein of duck hepatitis B virus suggests a mechanism for membrane traslocation during particle morphgenesis. J. Virol. *71*, 1107-1114.

Guo, W. T., Wang, J., Tam, g., Yen, T. S, and Ou, J, S. (1991). Leaky transcription termination produces larger and smaller than genome size hepatitis B virus X gene transcripts. Virology. *181*, 630–636.

Hahne, M., Rimoldi, D., Schroter, M., Romero, P., Schreier, M., French, L. E., Schneider, P., Bornand, T., Fontana, A., Lienard, D., Cerottini, J., and Tschopp, J. (1996). Melanoma cell expression of Fas ligand: implication for tumor immune escape. Science. *274*, 1363-1366.

Hamacher-Brady, A., Brady, N. R., Gottlieb, R. A., and Gusstafsson, A. B. (2006). Autophagy as a prospective response to Bnip3-mediated apoptosis signaling in the heart. Autophagy. *2*, 4.

Hantz, O., Baginski, I., Fourel, I., Chemin, I., and Trepo, C. (1992). Viral spliced RNA are produced, encapsidated and reverse transcribed during in vivo woodchuck hepatitis virus infection. Virology. *190*, 193–200.

Hayashi, N., and Mita, E. (1999). Involvement of Fas system-mediated apoptosis in pathogenesisf viral hepatitis. J.Viral. Hepatitis. *6*, 357-365.

Heermann, K. H., Kruse, F., Seifer, M., and Gerlich, W. H. (1987). Immunogenicity of the gene S and Pre-S domains in hepatitis B virions and HBsAg filaments. Intervirology. *28*, 14-25.

Heermann, K. H., Goldmann, U., Schwartz, W., Seyffarth, T., Baumgarten, H., Gerlich, W. H. (1984). Large surface proteins of hepatitis B virus containing the pre-s sequence. J.Virol. *52*, 396-402.

Hegde, R., Srinivasula, S. M., Ahmad, M., Fernandes-Alnemri, T., and Alnemri, E. S. (1998). Blk, a BH3-containing mouse protein that interacts with Bcl-2 and Bcl-xL, is a potent death agonist. J. Biol. Chem. *273*, 7783–7786.

Henkler, F., Hoare, J., Waseem, N., Goldin, R. D, McGarvey, M. J., Koshy, R., and King, I. A. (2001). Intracellular localization of the hepatitis B virus HBx protein. J. Gen. Virol. *82,* 871–882.

Herath, N. I., Leggett, B. A., and MacDonald, G. A. (2006). Review of genetic and epigenetic alterations in hepatocarcinogenesis. J Gastroenterol Hepatol. *21*, 15-21.

Hideaki, K. (2004). Eight Genotypes (A–H) of Hepatitis B Virus Infecting Patients from San francisco and Their Demographic, Clinical, and Virological Characteristics. Journal of Medical Virology. *73*, 516–521.

Higaki, K., Yano, H., and Kojiro, M. (1996). Fas antigen expression and its relationship with apoptosis in human hepatocellular carcinoma and noncanerous tissues. Am. J. Pathol. *149*, 429-437.

Hirsch, R. C., Lavine, J. E., Chang, L. J., Carmus, H. E., and Ganem, D. (1990). Polymerase gene products of hepatitis B virus are required for genomic RNA pachaging as well as for reverse transcription. Nature. *344*, 552-555.

Houvila, A. P., Eder, A. M., and Fuller, S. D. (1992). Hepatitis B surface antigen assembles in a post-ER, pre-Golgi compartment. J. Cell. Biol. *118*, 1305-1320.

Hsu, H., Huang, J., Shu, H. B., Baichwal, V., and Goeddel, D. V. (1996). TNF-depedent recruitment of the protein kinase RIP to the TNF receptor-1 signaling complex. Immunity. *4*, 387-396.

Hu, J., and Seeger, C. (1996). Hsp90 is required for the activity of a hepatitis B virus reverse transcriptase. Proc. Natl. Acad. Sci. USA. *93*, 1060-1064.

Hu, J., Toft, D. O., and Seeger, C. (1997). Hepadnavirus assembly and reverse transcription require a multi-component chaperone complex which is incorporated into nucleocapsids. EMBO J. *16*, 59-68.

Huang, B., Eberstadt, M., Olejniczak, E. T., Meadows, R. P., and Fesik, S. W. (1996). NMR structure and mutagenesis of the Fas(APO-1/CD95) death domain. Nature. *384*, 638-641.

Huang, D. C., and Strasser, A. (2000). BH-3 only proteins-essential initiators of aoptotic cell death. Cell. *103*, 839-842.

Huang, H. L., Jeng, K. S., Hu, C. P., Tsai, C. H., Lo, S. J., and Chang, C. (2000). Identification and characterization of a structural protein of hepatitis B virus: a polymerase and surface fusion protein encoded by a spliced RNA. Virology. *275*, 398–410.

Huang, M., and Summers, J. (1994). *pet*, a small sequence distal to the pregenome cap site, is required for expression of the duck hepatitis B virus pregenome. J. Virol. *68*, 1564-1572.

Hughson, F. M. (1995). Structure characterization of viral fusion proteins. Current. Biology. *5*, 265-274.

Hunter, J. J., Bond, B. L., and Parslow, T. G. (1996). Functional dissection of the human Bc1-2 protein: sequence requirements for inhibition of apoptosis. Mol. Cell. Biol. *16*, 877–883.

Tanaka, Y., Kanai, F., Kawakami, T., Tateishi, K., Ijichi, H., Kawabe, T., Arakawa, Y., Kawakami, T., Nishimura, T., Shirakata, Y., Koike, K., and Omata, M. (2004). Interaction of the hepatitis B virus X protein (HBx) with heat shock protein 60 enhances HBx-mediated apoptosis. Biochem. Biophys. Res. Commun. *318*, 461-469.

Jaeschke, H., Gores, G. J., Cederbaum, A. I., Hinson, J. A, Pessayre, D., and Lemasters, J. J. (2002). Mechanism of hepatotoxicity. Toxicol. Sci. *65*, 166-167.

Jason, B., and Scheller, H. (1997). A fusion of new ideas. Nature. *387*, 133-137.

Jilbert, A. R., Freiman, J. S, Gowans, E. J., Holmes, M., Cossart, Y. E., and Burrell, C. J. (1987). Duck hepatitis B virus DNA in liver, spleen, and pancreas: analysis by in situ and southen blot hybridization. Virology. *158*, 330-338.

Jones, E. Y., Stuart, D. I., and Walker, N. P. (1992). Crystal structure of TNF. Immunol. Ser. *56*, 93-127.

Junke, N. M., Bartenschlager, R., and Schaller, S. (1990). A short cis-acting sequence is required for hepatitis B virus pregenome encapsidation and sufficient for packaging of foreign RNA. EMBO J. *9*, 3389-3396.

Kagi, D., Vignaus, F., Ledermann, B., Burki, K., Depraetere, V., Nagata, S., and Hengartner, H. (1994). Fas and perforin pathways as major mechanisms of T-cell mediated cytotoxicity. Science. *265*, 528-530.

Kann, M., Bischof, A., and Gerlich, W. H. (1997). In vitro model for the nuclear transport of the hepadnavirus genome. J. Virol. *71*, 1310-1316.

Kann, M., Sodeik, B., Vlachou, A., Gerlich, W. H, and Helenius, A. (1999). Phosphoryation-dependent binding of hepatitis B virus particles to the nuclear pore complex. J. Cell. Biol. *145*, 45-55.

Kaplan, P., Greenman, R., Gerin, J., Purell, R., and Robinson, W. (1973). DNA polymerase associated with human hepatitis B antigen. J. Virol. *12,* 995-1005.

Kelekar, A., and Thompson, C. B. (1998). Bcl-2 family proteins: the role of the BH3 domain in apoptosis. Trends in Cell Biol. *8*, 324-330.

Kelekar, A., Chang, B. S., Harlan, J. E., Fesik, S. W., and Thompson, C. B. (1997). Bad is a BH3 domain-containing protein that forms an inactivating dimer with Bcl-XL. Mol. Cell. Biol. *17,* 7040–7046.

Kim, H., Lee, H., and Yun, Y. (1998). X-gene product of hepatitis B virus induces apoptosis in liver cells. J. Biol. Chem. *273*, 381-385.

Kim, K. H., and Seong, B. L. (2003). Pro-apoptotic function of HBV X protein is mediated by interaction with c-FLIP and enhancement of death-inducing signal. EMBO J. *22*, 2104-2116.

Kischkel, F. C., Hellbardt, S., Behrmann, I., Germer, M., Pawlita, M., Krammer, P. H., and Peter, M. E. (1995). Cytotoxicity-dependent APO-1(Fas/CD95)-associated proteins form a death-inducing signaling complex (DISC) with the receptor. EMBO J. *14*, 5579-5588.

Kiss-Laszlo, Z., Blanc, S., and Hohn, T. (1995). Splicing of cauliflower mosaic virus 35S RNA is essential for viral infectivity. EMBO J. *14*, 3552–3562.

Klein, N., and Schneider, R. J. (1997). Activation of Src family kinases by hepatitis B virus HBx protein and coupled signaling to Ras. Mol. Cell. Biol.*17*, 6427–6436.

Kluck, R. M., Bossy-Wetzel, E., Green, D. R., and Newmeyer, D. D. (1997). The release of cytochrome c from mitochondria: a primary site for Bcl-2 regulation of apoptosis. Science. *275*, 1132–1136.

Kondo, T., Suda, T., Fukuyama, H., Adachi, M., and Nagata, S. (1997). Essential roles of the Fas ligand in the development of hepatitis. Nat. Med. *3*, 409-413.

Konig, S., Beterams, G., and Nassal, M. (1998). Mapping of homologous interaction sites in the hepatitis B virus core protein. J. Virol. *72*, 4997-5005.

Kuroki, K., Cheung, P., Marion, L., and Ganem, D. (1994). A cell surface protein that binds avian hepatitis B virus articles. J. Virol. *68*, 2091-2096.

Kuroki, K., Eng, F., Ishikawa, T., Turck, C., Harada, F., and Ganem, D. (1995). gp180, a host cell glycoprotein that binds duck hepatitis B virus particles, is encoded by a member of the carboxypeptidease gene family. J. Biol. Chem. *270*, 15022-15028.

Lambert, V., Chassot, S., Kay, A., Trepo, C., and Cova, L. (1991). In vivo neutralization of duck hepatitis B virus by antibodies specific to the N-terminal portion of pre-S protein. Virology. *185*, 446-450.

Lanford, R. E., Notvall, L., and Beames, B. (1995). Nucleotide priming and reverse transcriptase activity of hepatitis B virus polymerase expressed in insect cells. J. Virol. 69, 4431-4439.

Lara-Pezzi, E., Armessila, A., Majano, P., Redondo, J., and Lopez-Cabrera, M. (1999). The hepatitis B virus X protein activates nuclear factor of activated T cells (NF-AT) by a cyclosporin A-sensitive pathway. EMBO J. *17*, 7066–7077.

Lara-Pezzi, E., Roche, S., Andrisani, A, Sanchez-Madrid, and Lopez-Cabrera, M. (2001). The hepatitis B virus HBx protein induces adherens junction disruption in a src-dependent manner. Oncogene. *20*, 3323–3331.

Lau, J. Y., Xie, X., Lai, M. M., and Wu, P. C. (1998). Apoptosis and viral hepatitis. Sem. Liver. Dis. *18*, 169-176.

Lau, J. Y. N, Sheron, N., Kayhan, K. T., Alexander, G. J. M., and Williams, R. (1991). Increased tumor necrosis factor alpha receptor number in chronic hepatitis B virus infection. Hepatology. *14*, 44-50.

Lau, J. Y. N., and Wright, T. L. (193). Molecular virology and pathogenesis of hepatitis B. Lancet. *342*, 1335-1340.

Lee, J., Shin, J. S., and Choi, I. H. (2006). Human brain astrocytes mediate TRAIL-mediated apoptosis after treatment with IFN-gamma. Yonsei. Med. J. *7*, 354-358.

Lee, W. M. (1997). Hepatitis B virus infection. New. Engl. J. Med. *337*, 1733-1745.

Lee, Y. H., and Yun, Y. (1998). HBx protein of hepatitis B virus activates Jak1-STAT signaling. J. Biol. Chem. *273*, 25510–25515.

Leenders, W. P., Glansbeek, H. L., de Bruin, W. C., and Yap, S. H. (1990). Binding of the major and large HBsAg to human hepatocytes and live plasma membranes: putative external and internal receptors for infection and secretion of hepatitis B virus. Hepatology. *12*, 141-147.

Lenhoff, R. J., Luscombe, C. A, and Summers, J. (1998). Competion in vivo between a cytopathic and a wild-type duck hepatitis B virus. Virology. 251, 85-95.

Levrero, M., Balsano, C., Natoli, G., Avantaggiati, M. L., and Elfassi, E. (1990). Hepatitis B virus X protein transactivates the long terminal repeats of human immunodeficiency virus types 1 and 2. J. Virol. *64*, 3082–3086.

Levrero, M., Jean-Jean, O., Balsano, C., Wills, H., and Perricaudet, M. (1990) Hepatitis B virus (HBV) X gene expression in human cells and anti-HBx antibodies detection in chronic HBV infection. Virology. *174*, 299–304.

Li, J., Tong, S., and Wands, J. R. (1996). Characterization of a 120-kilodalton pre-S binding protein as a candidate duck hepatitis B virus receptor. J. Virol. *70*, 6029-6038.

Li, P., Nijhawan, D., Budihardjo, I., Srinivasula, S. M., Ahmad, M., Alnemri, E. S., and Wang, X. (1997). Cytochrome c and dATP-dependent formation of Apaf-1/caspase-9 complex initiates an apoptotic protease cascade. Cell. *91*, 479–489.

Lien, L. M., Petcu, D. J., Aldrich, C. E., and Mason, W. C. (1987). Initiation and termination of duck hepatitis B virus DNA synthesis during virus maturation. J. Virol. *61*, 3832-3840.

Lin, J., Zhang, Z., Zeng, S., Zhou, S., Liu, B. F., Liu, Q., Yang, J., and Luo, Q. (2006). TRAIL-induced apoptosis proceeding from caspase-3-dependent and -independent pathways in distinct HeLa cells. Biochem. Biophys. Res. Commun. *346*, 1136-1141.

Lowin, B., Hahne, M., Mattmann, C., and Tschopp, J. (1994). Cytolytic T-cell cytotoxicity is mediated through perforin and Fas lytic pathways. Nature. *370*, 650-653.

Lu, X., Block, T., and Gerlich, W. H. (1996). Proteases-induced infectivity of hepatitis virus infectivity for human hepatoma cell line. J. Virol. *70*, 2277-2285.

Lu, X., Hazboun, T., and Block, T. (2001). Limited proteolysis induces woodchuck hepatitis virus infectivity for human HepG2 cells. Virus. Res. *73*, 27-40.

Lucito, R., and Schneider, R. J. (1992). Hepatitis B virus X protein activates transcription factor NF-κB without a requirement for protein kinase C. J. Virol. 66, 983–991.

Magnius, L. O., and Norder, H. (1995). Subtypes, genotypes and molecular epidemiology of the hepatitis B virus as reflected by sequence variability of the s-gene. Intervirology. *38*, 24-34.

Maguire, H. F., Hoeffler, J. P., and Siddiqui, A. (1991). HBV X protein alters the DNA binding specificity of CREB and ATF-2 by protein-protein interactions. Science. 252, 842–844.

Mahe, Y., Mukaida, N., Kuno, K., Akiyama, M., Ikeda, N., Matshushima, K., and Murakami, S. (1991). Hepatitis B virus X protein transactivates human interleukin-8 gene through acting on nuclear factor _B and CCAAT/enhancer-binding protein-like cis elements. J. Biol. Chem. *266*, 13759–13763.

Melegari, M., Scaglioni, P. P., and Wands, J. R. (1998). Cloning and characterization of a novel hepatitis B virus x binding protein that inhibits viral replication. J. Virol. *72*, 1737–1743.

Milich, D. R., Jones, J. E., and Hughes, J. L. (1990). Is a function of the secreted hepatitis B e antigen to induce immunologic tolerance *in utero*? Proc. Natl. Acad. Sci. USA. 87, 6599-6603.

Minn, A. J., Boise, L. H., and Thompson, C. B. (1996). Bcl-x(S) anatagonizes the protective effects of Bcl-x(L). J. Biol. Chem. *271*, 6306-6312.

Minn, A. J., Velez, P., Schendel, S. L., Liang, H., Muchmore, S. W., Fesik, S. W., Fill, M., and Thompson, C. B. (1997). Bcl-x(L) forms an ion channel in synthetic lipid membranes. Nature. *385*, 353–357.

Moraleda, G., Saputelli, J. C., Aldrich, E., Averett, D., Condreay, L., and Mason, W. S. (1997). Lack of effect of antiviral therapy in nondividing hepatocyte cultures on the closed circular DNA of woodchuck hepatitis virus. J. Virol. *71*, 9392-9399.

Motola-Kuba, D., Zamora-Valdes, D., Uribe, M., and Mendez-Sanchez, N. (2006). Hepatocellular carcinoma, an overview. Ann. Hepatol. *5*, 16-24.

Muchmore, S. W., Sattler, M., Liang, H., Meadows, R. P., Harlan, J. E., Yoon, H. S., Nettesheim, D., Chang, B. S., Thompson, C. B., Wong, S. L., Ng, S. L., and Fesik, S. W. (1996). X-ray and NMR structure of human Bcl-xL, an inhibitor of programmed cell death. Nature. *381*, 335–341.

Muzio, M., Chinnaiyan, A. M., Kischkel, F. C., O'Rourke, K., Shevchenko, A., Ni, J., Scaffidi, C., Bretz, J. D., Zhang, M., Gentz, C., Mann, M., Krammer, P. H., Peter, M. E, and Dixit, D. M. (1996). FLICE, a noval FADD-homologous ICE/CED-3-like protease, is recruited to the CD95 (APO-1/Fas) death-inducing signaling complex. Cell. *85*, 817-827.

Muzio, M., Salvesen, G. S., and Dixit, D. M. (1997). FLICE induced apoptosis in a cell-free system. Cleavage of caspase zymogens. J. Biol. Chem. *272*, 2952-2956.

Nakamoto, Y., Guidotti, L. G., Pasquetto, V., Schreiber, R. D., Chisari, F. V. (1997). Different target cell sensitivity to CTL-related death pathways in hepatitis B virus transgenic mice. J. Immunol. *158*, 5692-5697.

Natoli, G., Ianni, A., Costanzo, A., De Petrillo, G., Ilari, I., Chirillo, P., Balsano, C., and Levrero, M. (1995). Resistance to Fas-mediated apoptosis in human hepatoma cells. Oncogene. *11*, 1157-1164.

Neurath, A. R., Kent, S. B., Parker, K., Prince, A. M., Strick, N., Brotman, B., and Sproul, P. (1986). Antibodies to a synthetic peptide from the preS 120-145 region of the hepatitis B virus envelope are virus neutralizing. Vaccine. *4*, 35-37.

Neurath, A. R., Kent, S. B., Strick, N., and Parker, K. (1986). Identification and chemical synthesis of a host cell receptor binding site on Hepatitis B virus. Cell *46*, 429-436

Neurath, A. R., Seto, B., and Strick, N. (1989).Antibodyies to synthetic peptides from the PreS I region of the hepatitis B virus (HBV) envelope (env) protein are virus neutralizing and protective. Vaccine. *7*, 234-236.

Newbold, J. E., Xin, H., Tencza, M., Sherman, G., Dean, J., Bowden, S., and Locarnini, S. (1995). The covalently closed duplex form of the hepadnavirus genome exists in situ as a heterogenerous population of viral minichromosomes. J. Virol. *69*, 3350-3357.

Nguyen, M., Millar, D. G., Yong, V. W., Korsmeyer, S. J., and Shore, G. C. (1993). Targeting of Bcl-2 to the mitochondrial outer membrane by a COOH-terminal signal anchor sequence. J. Biol. Chem. *268*, 25265–25268.

Nijhara, R., Jana, S., Goswami, S., Rana, A., Majumdar, S., Kumar, V., and Sarkar, D. (2001). Sustained activation of mitogen-activated protein kinases and activator protein 1 by the hepatitis B virus X protein in mouse hepatocytes in vivo. J. Virol. *75*, 10348–10358.

Oberhaus, S. M., and Newbold, J. E. (1993). Detection of DNA polymerase activities associated with purified duck hepatitis B virus core particles by using an activity gel

assay. J. Virol. *67*, 6558-6566.

Obert, S., Zachmann-Brand, B., Derndl, E., Tucker, W., Bartenschlager, R., and Schaller, H. (1996). A splice hepadnavirus RNA that is essential for virus replication. EMBO.J. *15*, 2565-2574.

O'Connor, L., Strasser, A., O'Reilly, L. A., Hausmann, G., Adams, J. M., Cory, S., and Huang, D. C. (1998). Bim: a novel member of the Bcl-2 family that promotes apoptosis. EMBO J. *17*, 384–395.

Ogston, C.W., and Razman, D.G. (1992). Spliced RNA of woodchuck hepatitis virus. Virology. *189*, 245–252.

Ou, J. H., Bao, H., Shil, C., and Tahar, S. M. (1990). Preferred translation of human hepatitis B virus polymerase from core protein- but not from precore protein-specific transcript. J. Virol. *64*, 4578-4581.

Pan, G., O'Rourke, K., Chinnaiyan, A. M., Gents, R., and Dixit, V. M. (1997). The receptor for the cytotoxic ligand TRAIL. Science. *277*, 111-113.

Paran, N., Geiger, B., and Shaul, Y. (2001). HBV infection of cell culture: evidence for multivalent and cooperative attachment. EMBO J. *20*, 4443-4453.

Patel, T., and Gores, G. J. (1995). Apoptosis and hepatobiliary diseases. Hepatology. 21, 1725-1741.

Soussan, P., Garreau, F., Zylberberg, H., Ferray, C., Brechot, C., and Kremsdorf, D. (2000). In vivo expression of a new hepatitis B virus protein encoded by a spliced RNA. J. Clin. Invest. *105*, 55-60.

Pattingre, S., and Levine, B. (2006). Bcl-2 inhibition of autophagy: a new route to cancer? Cancer Res. *66*, 2885-2888.

Petit, M. A., Capel, F., Dubanchet, S., and Mabit, H. (1992). PreS1-sepcific binding proteins as potential receptors for hepatitis B virus in human hepatocytes. Virology. *187*, 211-222.

Pollack, J. R., and Ganem, D. (1993). An RNA stem-loop structure derects hepatitis B virus genomic RNA encapsidation. J. Virol. *67*, 3254-3263.

Pollack, J. R., and Ganem, D. (1994). Site-specific RNA binding by a hepatitis B virus reverse transcriptases initiates two distinct reactions: RNA packaging and DNA synthesis. J. Virol. *68*, 5579- 5587.

Pollicino, T., Terradullos, O., Lecoeur, H., Gougeon, M. L.,and Duendia, M. A. (1998). Pro-apoptotic effect of the hepatitis B virus X gene. Biomed Pharmacother. *52*, 363-368.

Pontisso, P., Calabrese, F., Benvegnu, L., Lise, M., Belluco, C., Ruvoletto, M., De Falco, S., Marino, M., Valente, M., Nitti, D., Gatta, A., and Fassina, G. (2005). Overexpression of squamous cell carcinoma antigen variants in hepatocellular carcinoma. Br. J. Cancer. *90*, 833-837.

Pugh, J., Zweidler, A., and Summers, J. (1989). Charactization of the major duck hepatitis B virus core particle protein. J. Virol. *63*, 1371-1376.

Pugh, J. C., and Bassendine, M. F. (1990). Molecular biology of hepadnavirus replication. Br. Med. Bull. 46, 329-353.

Puisieux, A., Ji, L., Guillot, C., Legros, Y., Soussi, T., Isselbacher, K., and Ozturk, M. (1995). p53-mediated cellular response to DNA damage in cells with replicative hepatitis B virus. Proc.Natl.Acad.Sci. USA. 92, 1342-1346.

Purcell, R. H. (1994). Hepatitis viruses: changing patterns of human disease. Proc. Natl. Acad. Sci. USA. *91*, 2041-2046.

Qiao, M., Macnaughton, T. B., and Gowans, E. J. (1994). Adsorption and penetration of hepatitis B virus in a nonpermissive cell line. Virology. *201*, 356-363.

Qiao, M., Scougall, C. A., Duszynski, A., and Burrell, C. J. (1999). Kinetics of early molecular events in duck hepatitis B virus replication in primary duck hepatocytes. J. Gen. Virol. 80, 2127-2135.

Rahmani, Z., Huh, K. W., Lasher, R., and Siddiqui, A. (2000). Hepatitis B virus X protein colocalizes to mitochondria with a human voltage-dependent anion channel, HVDAC3, and alters its transmembrane potential. J. Virol. 74, 2840–2846.

Rakotomahanina, C. K., Hilger, C., Fink, T., Zentgraf, H., and Schroder, C. H. (1994). Biological activities of a putative truncated hepatitis B virus X gene product fused to a polylysin stretch. Oncogene. 9, 2613-2621.

Rao, A., Luo, C., and Hogan, P. (1997). Transcription factors of the NFAT family: regulation and function. Annu. Rev. Immunol. *15*, 707–747.

Rodrigeus-Crespo, I., Nunez, E., Yelamos, B., Gomez-Gutierrez, J., Albar, J. P., Peterson, D. L., and Gavilanes, F. (1999). Fusogenic Activity of Hepadnavirus Peptides Corresponding to Sequences Downstream of the Putative Cleavage Site. Virology. *261*, 133-142.

Rosmorduc, O., Petit, M. A., Pol, S., Capel, F., Bortolotti, F., Berthelot, P., Brechot, C., and Kremsdorf, D. (1995). In vivo and in vitro expression of defective hepatitis B virus particles generated by spliced hepatitis B virus RNA. Hepatology. *22,* 10–19.

Rosse, T., Olivier, R., Monney, L., Rager, M., Conus, S., Fellay, I., Jansen, B., and Borner, C. (1998). Bcl-2 prolongs cell survival after Bax-induced release of cytochrome c. Nature. *391*, 496–499.

Ryo, K., Kamogawa, Y., Ikeda, I., Kmura, T., Miyazono, Y., Shimizu, T., and Nishikawa, M. (1995). Fas and FasL strongly expressed in liver of fulminant hepatitis patients. Hepatology. *22*, 230A.

Ryu, C. J., Gripon, P., Park, H., Park, S., Kim, K., Guguen-guillouzo, C., Yoo, O., and Hong, H. (1997). In Vitro Neutralization of Hepatitis B virus by Monoclonal Antibodies Against the Viral Surface Antigen. J. Med. Virol. *52*, 226-233.

Schek, N., Bartenschlager, R., Kuhn, C., and Schaller, H. (1991). Phosphorylation and rapid turnover of hepatitis B virus X protein expressed in HepG2 cells from a recombinant vaccinia virus. Oncogene. 6, 1735–1744.

Schendel, S. L., Xie, Z., Montal, M. O., Matsuyama, S., Montal, M., and Reed, J. C. (1997). Channel formation by antiapoptotic protein Bcl-2. Proc. Natl. Acad. Sci. U. S. A. *94*, 5113–5118.

Schlesinger, P. H., Gross, A., Yin, X. M., Yamamoto, K., Saito, M., Waksman, G., and Korsmeyer, S. J. (1997). Comparison of the ion channel characteristics of proapoptotic BAX and antiapoptotic BCL-2. Proc. Natl. Acad. Sci. U. S. A. *94*, 11357–11362.

Schulze, O. K., Ferrari, D., Los, M., Wesselborg, S., and Peter, M. E. (1998). Apoptosis signaling by death receptors. Eur. J. Biochem. *254*, 439-459.

Schuster, R., Gerlich, W. H., and Chaefer, S. (2000). Induction of apoptosis by the transactivating domains of the hepatitis B virus X gene leads to suppression of oncogenic transformation of primary rat embryo fibroflasts. Oncogene. *19*, 1173-1180.

Sedlak, T. W., Oltvai, Z. N., Yang, E., Wang, K., Boise, L. H., Thompson, C. B., and Korsmeyer, S. J. (1995). Multiple Bcl-2 family members demonstrate selective dimerizations with Bax. Proc. Natl. Acad. Sci. U. S. A. *92*, 7834–7838.

Seeger, C., Ganem, D., and Varmus, H. E. (1986). Biochemical a nd genetic evidence for the hepatitis B virus replication strategy. Science *232*, 477-484.

Seeger, C., and Mason, W. (2002). Hepatitis B virus biology. Mic. Mol. Biol. Rev. *64*,

51-68.

Sheron, N., Lau, J. Y. N., and Daniel, H. (1991). Increased production of tumor necrosis factor alpha in chronic HBV infection, J. Hepatol. *12*, 241-245.

Shimizu, S., Kanaseki, T., Mizushima, N., Mizuta, T., Arakawa-Kobayashi, S., Thompson, C. B., and Tsujimoto, Y. (2004). Role of Bcl-2 family proteins in a non-apoptotic programmed cell death dependent on autophagy genes. Nat. Cell. Biol. *12*, 1221-1228.

Shin, E. C., Shin, J. S., Park, J. H., Kim, H., and Kim, S. J. (1999). Expression of Fas ligand in human hepatoma cell lines: role of hepatitis B virus X (HBX) in induction of Fas ligand. Int. J. Cancer. *82*, 587-591.

Shin, E. C., Shin, J. S., Park, J. H., Kim, J. J., Kim, H., and Kim, S. (1998). Expression of Fas-related genes in human hepatocellular carcinomas. Cancer Letters. *134*, 155-162.

Smyth, M. J., and Trapani, J. A. (1995). Granzymes: Exogenous proteinases that induce target cell apoptosis. Immunol Today. *16*, 202-206.

Soussan, P., Garreau, F., Zylberberg, H., Ferray, C., Brechot, C., and Kremsdorf, D. (2000). In vivo expression of a new hepatitis B virus protein encoded by a spliced RNA. J. Clin. Invest. *105,* 55-60.

Soussan, P., Tuveri, R., Nalpas, B., Garreau, F., Zavala, F., Masson, A., Pol, S., Brechot, C.,and Kremsdorf, D. (2003). The expression of hepatitis B spliced protein (HBSP) encoded by a spliced hepatitis B virus RNA is associated with viral replication and liver fibrosis. J Hepatol. *38*, 343-348.

.

Stanger, B. Z., Leder, P., Lee, T. H., Kim, E., and Seed, B. (1995). RIP:a noval protein containing a death domain that interacts with fas/APO-1(CD95) in yeast and causes cell death. Cell. *81*, 513-523.

Staprans, S., Loeb, D. D, and Ganem, D. (1991). Mutations affecting hepadnavirus plus-strand DNA synthesis dissociate primer cleavage from translocation and reveal the origin of linear viral DNA. J. Virol. *65*, 1255-1256.

Stibbe, W., and Gerlich, W. H. (1983). Structural relationships between minor and major proteins of Hepatitis B surface antigen. J. Virol. *46*, 626-629.

Su, F., and Schneider, R. J. (1997). Hepatitis B virus HBx protein sensitizes cell to apoptotic killing by tumor necrosis factor. Proc. Natl. Acad. Sci. USA. *94*, 8744-8749.

Sugata, F., Chen, H. S., Kaneko, S., Purcell, R. H., and Miller, R. H. (1994). Analysis

of the X gene promoter of woodchuck hepatitis virus. Virology. *205*, 314–320.

Summers, J., O'Connell, A., and Mullman, I. (1975). Genome of hepatitis B virus: restriction enzyme cleavage and structure of DNA extracted from DNA particles. Proc. Natl. Acad. Sci. USA. *72*, 4597-4601.

Summers, J., and Mason, W. S. (1982). Replication of the genome of a hepatitis B-like virus by reverse transcription of an RNA intermediate. Cell. *29*, 403-415.

Summers, J., Smith, P. M., and Horwich, A. L. (1990). Hepadnavirus envelope proteins regulate covalently closed circular DNA amplification. J. Virol. *64*, 2819-2824.

Summers, J., Smith, P. M., Huang, M. J., and Yu, M. S. (1991). Morphogenetic and regulatory effects of mutations in the envelope proteins of an avian hepadnavirus. J. Virol. *65*, 1310-1317.

Tagawa, M., Robinson, W. S., and Marion, P. L. (1987). Duckhepatitis b virus replicates in the yolk sac of developing embryos. J. Virol. *61*, 2273-2279.

Takada, S., Kaneniwa, N., Tsuchida, N., and Koike, K. (1996). Hepatitis B virus X gene expression is activated by X protein but repressed by p53 tumor suppressor gene product in the transient expression system. Virology. *216*, 80-89.

Takada, S., Shirakata, Y., Kaneniwa, N., and Koike, K. (1999). Association of hepatitis B virus X protein with mitochondria causes mitochondrial aggregation at the nuclear periphery, leading to cell death. Oncogene. *18*, 6965-6973.

Tarn, C., Zou, L., Hullinger, R., and Andrisani, O. (2002). Hepatitis B virus X protein activates the p38 mitogen-activated protein kinase pathway in dedifferentiated hepatocytes. J. Virol. *76*, 9763–9772.

Tarn, C., Lee, S., Hu, Y., Ashendel, C., and Andrisani, O. M. (2001). Hepatitis B virus X protein differentially activates RAS-RAF-MAPK and JNK pathways in X-transforming versus non-transforming AML12 hepatocytes. J. Biol. Chem. *276*, 34671–34680.

Tartaglia, L. A., Weber, R. F., Figari, I. S., Reynolds, C., Palladino, M. A. J., and Geoddel, D. V. (1991). The two different receptors for tumer necrosis factor mediate distinct cellular responses. Proc. Natl. Acad. Sci. USA. *88*, 9292-9296.

Tavis, J. E., and Ganem, D. (1993). Expression of functional hepatitis B virus polymerase in yeast reveals it to be the sole viral protein required for correct initiation of reverse transcription. Proc. Natl. Acad. Sci. USA. *90*, 4107-4111.

Teodoro, J. G., and Branton, P. E. (1997). Regulation of apoptosis by viral gene products. J. Virol. *71*, 1739-1746.

Terradillos, O., de La Coste, A., Pollicino, T., Neuveut, C., Sitterlin, D., Lecoeur, H., Gougeon, M. L., Kahn, A., and Buendia, M. A. (2002). The hepatitis B virus X protein abrogates Bcl-2-mediated protection against Fas apoptosis in the liver. Oncogene. *21*, 377–386.

Terradillos, O., Pollicino, T., Lecoeur, H., Tripodi, M., Gougeon, M. L., Tiollais, P., and Buendia, M. A. (1998). p53-Independent apoptotic effects of the hepatitis B virus HBx protein in vivo and in vitro. Oncogene. *17*, 2115–2123.

Terré, S., Petit, M.A., and Bréchot, C. (1991). Defective hepatitis B virus particles are generated by packaging and reverse transcription of spliced viral RNAs in vivo. J. Virol. *65*, 5539–5543.

Ting, A. T., Pimente, L., Muinos, F. X., and Seed, B. (1996). RIP mediates tumor necrosis factor receptor 1 activation of NF-kB but not Fas/APO-1-initiated apoptosis. EMBO J. *15*, 6189-6196.

Tiollais, P., Charnay, P., and Vyas, G. N. (1981). Biology of hepatitis B virus. Science. 213, 406-411.

Trauth, B. C., Klas, C., Peters, A. M., Matzku, S., Moeller, P., Falk, W., Debatin, K. M., and Krammer, P. H. (1989). Monoclonal antibody-mediated tumor regression by induction of apoptosis. Science. *245*, 301-305.

Treichel, U., Meyer, Z., Buschenfelde, K. H., Dienes, H. P., and Gerken, G.. (1997). Receptor-mediated entry of hepatitis B virus particles into liver cells. Arch. Virol. *142*, 493-498.

Tsujimoto, Y., and Shimizu, S. (2000). Bcl-2 family:Life-or-death switch. FEBS Letters. *466*, 6-10.

Tsujimoto, Y., and Shimizu, S. (2005). Another way to die: autophagic programmed cell death. Cell death and differentiation. *12*, 1528-1534.

Tuttleman, J. S., Pourcel, C., and Summers, J. (1986). Formation of the pool of covlently closed circular viral DNA in hepadnavirus-infected cells. Cell. *47*, 451-460.

Ueda, H., Ullrich, S. J., Gangemi, J. D., Kappel, C. A., Ngo, L., Feitelson, M. A., and Jay, G. (1995). Functional inactivation but not structural mutation of p53 causes liver cancer. Nat. Genet. 9, 41-47.

Urban, S., Hildt, E., Eckerskorn, E., Sirma, H., Kekule, A., and Hofschneider, P. H. (1997). Isolation and molecular characterization of hepatitis B virus X-protein from a baculovirus expression system. Hepatology. *26*, 1045–1053.

Vander Heiden, M. G., Chandel, N. S., Williamson, E. K., Schumacker, P. T., and Thompson, C. B. (1997). Bcl-xL regulates the membrane potential and volume homeostasis of mitochondria. Cell. *91*, 627–637.

Vassalli, P. (1992). The pathophysiology of tumor necrosis factors. Annu. Rev. Immunol. *10*, 411-452.

Verheyen, A. (1998). Influence of age, weight, length, BMI, gender, smoking behaviour, and type of vaccine on the immune response of HB vaccines. Antwerpend: university of antwerpen. Department of Epidemiology and social medicine.In dutch Viral hepatitis prevention board. VHPb recommendations on surveillance of hepatitis B. Viral Hepatitis. *5*, 7-8.

Wang, G. H., and Seeger, C. (1993). Novel mechanism for reverse transcription in hepatitis B viruses. J. Virol. *67*, 6507-6512.

Wang, G. H., and Seeger, C. (1992). The reverse transcriptase of hepatitis B virus acts as a protein primer for viral DNA synthesis. Cell. *71*, 663-670.

Wang, G. H., Zoulim, F., Leber, E. H, Kitson, J., and Seeger, C. (1994). Role of RNA in enzymatic activity of the reverse transcriptase of hepatitis B viruses. J. Virol. *68*, 8437-8442.

Wang, J. C., Hsu, S. L., and Hwang, G. Y. (2004). Inhibition of tumorigenicity of the hepatitis B virus X gene in Chang liver cell line. Virus. Research. *102*, 133-139.

Wang, K., Yin, X. M., Chao, D. T., Milliman, C. L., Korsmeyer, S. J. (1996). BID: a novel BH3 domain-only death agonist. Genes. Dev. *10*, 2859–2869.

Wang, X. W., Gibson, M. K., Vermeulen, W., Yeh, H., Forrester, K., Sturzbecher, H. W., Hoeijmakers, J. H. J., and Harris, C. C. (1995). Abrogation of p53-induced apoptosis by the hepatitis B virus X gene. Cancer Res. 55, 6012-6016.

Weber, M., Bronsema, V., Bartos, H., Bosserhoff, A., Bartenschlager, R., and Schaller, H. (1994). Hepadnavirus P protein utilizes a tyrosine residue in the TP domain to prime reverse transcription. J. Virol. 68, 2994-2999.

Wei, Y., Tavis, J. E., and Ganem, D. (1996). Replication between viral DNA synthesis and virion envelopment in hepatitis B viruses. J. Virol. *70*, 6455- 6458.

White, J. M. (1992). Membrane fusion. Science. 258, 917-924.

Wiley, S. R., Schooley, K., Smolak, P. J., Din, W. S., Huang, C. P., Nicholl, J. K., Sutherland, G. R., Smith, T. D., Rauch, C., and Smith, C. A. (1995). Identification and characterization of a new member of the TNF family that induces apoptosis. Immunity 3, 673-682.

Williams, G. T., and Smith, C. A. (1993). Molecular regulation of apoptosis: Genetic control on cell death. Cell. *74*, 777-779.

Williams, J. S., and Andrisani, O. M. (1995). The hepatitis B virus X protein targets the basic region-leucine zipper domain of CREB. Proc. Natl. Acad. Sci. USA. *92*, 3819–3823.

Wu, H. L., Chen, P. J., Tu, S. J., Lin, M. H., Lai, M. Y., Chen, D. S. (1991). Characterization and genetic analysis of alternatively spliced transcripts of hepatitis B virus in infected human liver tissues and transfected Hep G2 cells. J. Virol. *65*, 1680–1686.

Wu, H. L., Chen, P. J., Lin, M. H., and Chen, D. S. (1991). Temporal aspects of major viral transcript expression in Hep G2 cells transfected with cloned hepatitis B virus DNA: with emphasis on the X transcript. Virology. *185*, 644-51.

Wynne, S. A., Crowther, R. A, and Leslie, A. G. (1999). The crystal structure of the human hepatitis B virus capsid. Mol. Cell. *3*, 771-780.

Xu, Z., Yen, T. S, Wu, L., Madden, C. R., Tan, W., Slagle, B. L., and Ou, J. H. (2002). Enhancement of hepatitis B virus replication by its X protein in transgenic mice. J. Virol. *76*, 2579–2584.

Yaginuma, K., Shirakata, Y., Kobayashi, M., and Koike, K. (1987). Hepatitis B virus (HBV) particles are produced in a cell culture system by transient expression of transfected HBV DNA. Proc. Natl. Acad. Sci. USA. *84*, 2678-2682.

Yang, D., Faris, R., Hixson, D., Affigne, S., and Rogler, C. E. (1996). Insulin-like growth factor II blocks apoptosis of N-Myc2-expressing wood-chuck liver epithelial cells. J. Virol. *70*, 6260-6268.

Yen, T. S. B. (1996). Hepadnaviral X protein: review of recent progress. J. Biomed. Sci. *3*, 20-30.

Yin, X. M., Oltvai, Z. N., Korsmeyer, S. J. (1994). BH1 and BH2 domains of Bcl-2 are required for inhibition of apoptosis and heterodimerization with Bax. Nature. *369*,

321-323.

Yu, M., and Summers, J. (1994). Multiple functions of capsid protein phosphorylation in duck hepatitis B virus replication. J. Virol. *68*, 4341-4348.

Yu, M., and Summers, J. (1994). Phosphorylation of the duck hepatitis B virus capsid rotein associated with conformational changes in the C terminus. J. Virol. *68*, 2965-2969.

Zlotnick, A., Stahl, S. J, Wingfield, P. T, Conway, J. F., Cheng, N., and Steven, A. C. (1998). Shared motifs of the capsid proteins of hepadnaviruses and retroviruses suggest a common evolutionary origin. FEBS lett. *431*, 301-304.

Zoulim, F., and Seeger, C. (1994). Reverse transcription in hepatitis B virus is primed by a tyrosine residue of the polymerase. J. Virol. *68*, 6-13.

Zoulim, F., Saputelli, J., and Seeger, C. (1994). Woodchuck hepatitis virus X protein is required for viral infection in vivo. J. Virol. 68, 2026-2030.

Zuckerman, A. J. (1999). More than third of world's population has been infected with Hepatitis B virus. BMJ *318*, 1213

Available online at www.sciencedirect.com
SCIENCE DIRECT®
ELSEVIER
Biochemical and Biophysical Research Communications 338 (2005) 1551–1556
BBRC
www.elsevier.com/locate/ybbrc

Human hepatitis B virus X protein induces apoptosis in HepG2 cells: Role of BH3 domain

Yi Wei Lu [a], Wei Ning Chen [a,b,*]

[a] School of Biological Sciences, Nanyang Technological University, 60 Nanyang Drive 05N-10, Singapore 637551, Singapore
[b] School of Chemical and Biomedical Engineering, Nanyang Technological University, 16 Nanyang Drive Unit 100, Singapore 637722, Singapore

Received 18 October 2005
Available online 2 November 2005

Abstract

The smallest protein of hepatitis B virus, HBX, has been implicated in the development of liver diseases by interfering with normal cellular processes. Its role in cell proliferation has been unclear as both pro-apoptotic and anti-apoptotic activities have been reported. We showed molecular evidence that HBX induced apoptosis in HepG2 cells. A Bcl-2 Homology Domain 3 was identified in HBX, which interacted with anti-apoptotic but not pro-apoptotic members of the Bcl-2 family of proteins. HBX induced apoptosis when transfected into HepG2 cells, as demonstrated by both flow cytometry and caspase-3 activity. However, HBX protein may not be stable in apoptotic cells triggered by its own expression as only its mRNA or the fusion protein with the glutathione-*S*-transferase was detected in transfected cells. Our results suggested that HBX behaved as a pro-apoptotic protein and was able to induce apoptosis.

Keywords: HBX; BH3; Apoptosis

Hepatitis B virus (HBV) infection leads to a wide range of liver diseases, including viral hepatitis and hepatocellular carcinoma (HCC). Viral hepatitis is characterized by an inflammatory reaction in the infected liver cells and is associated with cell damage and death [1]. On the other hand, inhibition of cell death and uncontrolled cell growth has been observed for HCC. Cell death is therefore a key modulator for the outcome of HBV infection.

One of the typical processes of cell death is apoptosis, commonly known as programmed cell death [2]. Apoptosis is generally considered to be a mechanism of host defense against viral infections [3]. Induction of apoptosis will interrupt viral replication as viral infected cells are eliminated. Apoptosis can be initiated by either external or internal stimuli and two distinct pathways have been defined. These include the death receptor pathway involving the TNF receptor and caspase-8/FLICE activation, and the mitochondrial pathway involving the Bcl-2 family of proteins and caspase-9 activation [3]. To counter the host response, viruses have developed strategies to delay apoptosis such that they can complete their replication process and continue to infect neighboring cells. In the case of HBV infection, a large body of evidence has suggested a role of Fas ligand and HBx protein in the development of apoptosis-related hepatitis [4–7]. Recent reports have also pointed to the involvement of the mitochondria-dependent apoptotic pathway which is governed by the Bcl-2 family of proteins in the development of liver diseases [8,9]. This appears to be supported by the pro-apoptotic role of HBX in the Bcl-2-mediated apoptotic pathway [10–12]. However, little is known on the involvement of HBV viral proteins in this pathway at molecular level. The interest of characterizing the Bcl-2-mediated apoptosis in HBV-related hepatitis lies in the fact that these proteins are able to either delay or induce apoptosis. While the former would ensure prolonged viral replication, it is now known that some viruses are able to induce apoptosis at late stages of infection [13]. This process may result in the dissemination of viral particles with

* Corresponding author. Fax: +65 62259865.
E-mail address: WNChen@ntu.edu.sg (W.N. Chen).

0006-291X/$ - see front matter © 2005 Elsevier Inc. All rights reserved.
doi:10.1016/j.bbrc.2005.10.117

minimum host immune response as well as protecting progeny viral particles from host neutralizing antibodies, since apoptotic cells are usually vacuolized and endocytosed by neighboring cells.

The Bcl-2 family of proteins consists of both suppressors and promoters of programmed cell death (apoptosis). Many of them can interact with each other through a complex network of homodimers and heterodimers. The relative ratios of pro- and anti-apoptotic members of this family determine whether the cell should die and live. Four conserved domains within the Bcl-2 family of proteins have been identified through sequence comparisons, these are named as Bcl-2 homology (BH) domains 1–4 [14]. All members possess at least one of four BH motifs [15]. As opposed to anti-apoptotic members (e.g., Bcl-2 and Bcl-xl) which carry at least BH1 and BH2, some members displaying pro-apoptotic activity (e.g., Bad and Bid) possess only the BH3 domain. Most of these BH3-only pro-apoptotic proteins appear to function essentially as transdominant inhibitors by binding to anti-apoptotic Bcl-2 family proteins and neutralizing their ability to prolong cell survival. In addition to known pro-apoptotic proteins such as Bad, Bid, and EGL-1, BH3-only proteins can also be found in a wide range of cellular proteins. These include Bmf sequestered with myosin [16], Rad9 involved in cell cycle [17], Bbc3 responding to diverse apoptotic stimuli [18], Noxa mediating p53-induced apoptosis [19], an ovarian BH3-only protein BOD [20], and Nbk interacting with human adenovirus protein E1B 19K [21].

Based on previously reported pro-apoptotic activity conferred by HBX, we hypothesize that it may interact with Bcl-2 family of proteins similarly to known interactions between pro- and anti-apoptotic proteins. We show here that HBX contains a BH3 domain and displays apoptotic activity. The implications of our findings in the context of other mechanisms of HBX in cellular apoptosis are also discussed.

Materials and methods

Interaction between HBX and Bcl-2 family of proteins. The coding region of HBX was amplified by PCR and cloned in-frame with a GAL4 DNA binding domain in pBind vector (Promega, USA). The coding regions of six members of Bcl-2 family proteins, including Bcl-2, Bcl-xl, Bad, Bak, Bik, and Bax but excluding their transmembrane region, were amplified from a commercial cDNA library by PCR and cloned in-frame with a VP16 transcription activation domain in pACT vector (Promega, USA). A missense mutation HBX (E125A) was generated by an In-site Direct Mutation kit (Stratagene, USA). Human hepatoma cell line HepG2 was grown in DMEM (Invitrogen, USA) with 10% FBS (Invitrogen, USA). 1.5×10^5 cells were transiently co-transfected with 0.4 μg pBind-HBX, pAct-Bcl-2-related proteins, and pG5luc by using Effectene transfection reagent (Qiagen, Germany). pG5luc contains GAL-4 binding elements upstream of the minimum promoter E1B TATA controlling the firefly luciferase reporter gene. Following 48 h incubation, cells were trypsinized, harvested, and lysed. The lysate was measured for luciferase activities using the Dual-Luciferase Reporter Assay System (Promega, USA) in a Sirius luminometer (Sirius Designs, Germany). Values obtained were normalized with the levels of *Renilla* luciferase absorbance in which pBind acted as an internal control of protein expression.

Apoptotic effect of HBX in HepG2 cells by flow cytometry analysis. The coding region of HBX was amplified by PCR and cloned in pXJ-40 containing a HA tag [22]. pXJ-40-HBX was transiently transfected into 3×10^5 HepG2 cells (Qiagen, Germany). HepG2 cells transfected with empty pXJ-40 and cells treated by 100 μM cisplatin for 16 h were used as negative and positive controls, respectively. Following 48 h incubation, cells were trypsinized, harvested, and analyzed by using ApoAlert Annexin-V kit (BD Biosciences, USA). Cells were rinsed in binding buffer and resuspended in the same buffer. Five microliters of Annexin-V-FITC and 10 μl propidium iodide were added into each sample. Following 30 min incubation in dark, samples were analyzed on FACS station (BD Bioscience, USA).

Apoptotic effect of HBX in HepG2 cells by caspase-3 assay. Two micrograms of pXJ-40-HBx was transiently transfected into 3×10^5 HepG(2) cells in each well of a 6-well plate (Nunc, Den Mark). HepG2 cells transfected with empty pXJ-40 and cells treated by 100 μM cisplatin for 16 h were used as negative and positive controls, respectively. Samples were collected at different post-transfection times and analyzed by using ApoAlert Caspase-3 Fluorescent Assay Kit (BD Bioscience, USA). Cells were lysed in 50 μl lysis buffer for 30 min on ice. After centrifugation, 50 μl supernatant was mixed with 50 μl reaction buffer. Five microliters of caspase-3 substrate DEVE-AFC was added into the mixture and incubated in 37 °C, 5% CO_2 for another 3 h. This mixture was then pipetted into a 96-well plate and analyzed by using microplate fluorescence reader (FL600, Bio-TEK, USA). At an excitation wavelength of 400 nm the cleaved AFC gave out an emission at 505 nm and absorbance was automatically recorded. The caspase-3 activity for each time point was measured in cells transfected with HA-HBX in three independent experiments.

Apoptotic effect of GST-HBX in 293T cells by caspase-3 assay. The coding regions of HBX was amplified by PCR and cloned in-frame with GST in pGEX-5X-1 (Amersham, USA). The coding regions of GST-HBX was amplified by PCR and cloned in-frame with the HA tag in pXJ-40. pXJ-40-GST-HBX was transiently transfected into 5×10^5 293T cells in 60 mm dish (Nunc, Den Mark). 293T cells transfected with the empty pXJ-40-GST and cells treated by 100 μM cisplatin for 16 h were used as negative and positive controls, respectively. Caspase-3 assay was carried out as above mentioned.

Western blot. HA-GST-HBX expressed in 293T cells was detected by primary antibody anti-HA (Santa Cruz, USA) in 1:5000 dilution and secondary antibody anti-mouse conjugated with horseradish peroxidase (Pierce, USA) in 1:5000 dilution. Anti-actin antibody (Sigma, USA) was used to detect actin protein, used as internal control.

Reverse transcription PCR. pXJ-40-HBX was used to transiently transfect HepG2 cells, and transfected cells were collected 24 h later. Total RNA was extracted from HepG2 and HBX-transfected HepG2 cells separately (RNeasy Mini Kit, Qiagen). cDNA used as template for reverse transcription-PCR (with the above-mentioned HBX primers) was generated from the total RNA (TITANIUM One-Step RT-PCR Kit, Clontech).

Results and discussion

HBX contains a BH3 domain

The conserved BH3-like regions of many pro-apoptotic Bcl-2-family of proteins are critical for their induction of cell death and for their interactions with anti-apoptotic proteins including the prototype Bcl-2. To investigate whether any of the HBV viral proteins is directly involved in apoptosis, we screened a BH3 like motif in all HBV viral proteins including HBX. A distantly related BH3 motif was identified in HBX (amino acid 116–130 in an overall 154 residues). A multiple alignment of the BH3 motif in the related Bcl-2 family of proteins is shown in Fig. 1, whereby conserved amino acids are darkly shaded. Although HBX

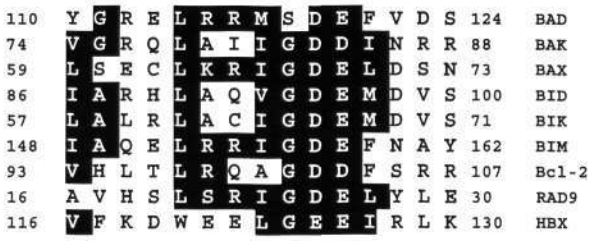

Fig. 1. Alignment of amino acid residues in the BH3-homology regions of Bcl-2 family members and HBX. Comparison of the BH3-like regions in HBx and Bcl-2 family members (HBx GenBank Accession Nos. CAA49453; human BAD, AF021792; human BAK, U23765; human BAXL22474; human BID, CAG30275; human BIK, U34584; human BIM, AF032457; human Bcl-2, P10415; human RAD9, U53174). Amino acids that match the BH3 consensus (Accession No. PS01259) are darkly shaded.

has been reported to be associated with various pathways of apoptosis and possess pro-apoptotic activity, our findings provided a molecular clue on its action.

HBX interacts with anti-apoptotic members of Bcl-2 family proteins

It has been shown that interactions among members of the Bcl-2 family of proteins can be analyzed in the yeast two-hybrid system [23]. To determine the significance of the distantly related BH3 motif identified in HBX, their interaction with Bcl-2 family of proteins was determined in a mammalian cell-based system similar to the yeast two-hybrid. Specifically, the coding region of both full length wild type and mutant (E125A) HBX was amplified by PCR and cloned in-frame with the DNA binding domain of GAL4 in the pBIND plasmid from CheckMate system. On the other hand, the coding region for six members of the Bcl-2 family of proteins, namely Bcl-2 and Bcl-xl (anti-apoptotic), and Bad, Bak, Bik, and Bax (pro-apoptotic), was amplified from commercially available cDNA (Clontech, USA) and cloned in-frame with the GAL4 activation domain in the pACT plasmid. As the luciferase activity results from the gene expression in the nucleus, the interaction between HBX and the Bcl-2-related proteins containing a transmembrane domain (Bcl-2, Bcl-xl, Bax, and Bak) may not be properly reflected using such an assay. For this reason, the coding region of these four Bcl-2-related proteins excluding the transmembrane domain was amplified and cloned in this study.

Transient transfection of HepG2 cells was carried out with an equal amount of the three plasmids, the bait (HBX), prey (Bcl-2-related proteins), and pG5*luc* (encoding the firefly luciferase). The interaction between bait and prey was then measured by the percentage of firefly luciferase as compared with that of *Renilla* luciferase coding on pBIND plasmid, which serves as an internal control of transfection. Results from three independent transfections for each combination are shown in Fig. 2 and indicated that Bad interacted with Bcl-xl (50% of luciferase activity compared with positive control between pBIND-Id and pACT-MyoD) as expected between pro-apoptotic and anti-apoptotic Bcl-2-related proteins. Interestingly, HBX interacted with anti-apoptotic proteins Bcl-2 (30.4%) and Bcl-xl (21.7%), but not with pro-apoptotic proteins such as Bad (8.7%), Bak (4.52%), Bik (4.8%) or Bax (5.2%). The significance of the interaction between HBX and anti-apoptotic Bcl-2-related proteins was further supported by the decrease of luciferase activity between the

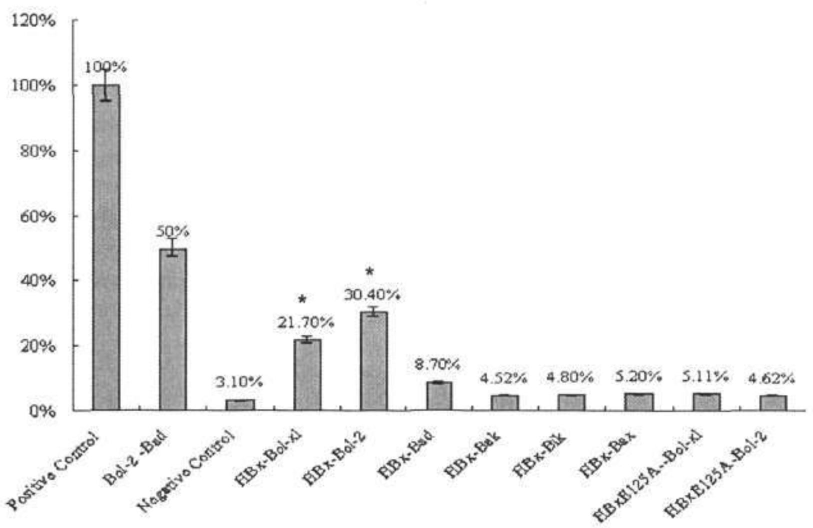

Fig. 2. Interaction of HBX with Bcl-2-related proteins by luciferase activity. The coding region of HBX and the missense mutant HBX (E125A) was amplified and cloned in-frame with a GAL4 DNA binding domain in-pBind vector. The coding regions of six members of Bcl-2 family proteins, including Bcl-2, Bcl-xl, Bad, Bak, Bik, and Bax but excluding their transmembrane region, were amplified and cloned in-frame with a VP16 transcription activation domain in pACT vector. Luciferase activity was measured from HepG2 cells transfected with constructs of HBX and one of the Bcl-2-related genes (see Materials and methods). Values obtained were normalized with the levels of *Renilla* luciferase absorbance in which pBind acted as an internal control of protein expression. The results represent means ± SE from three independent experiments. *Statistically significant at $p < 0.05$ in luciferase activity.

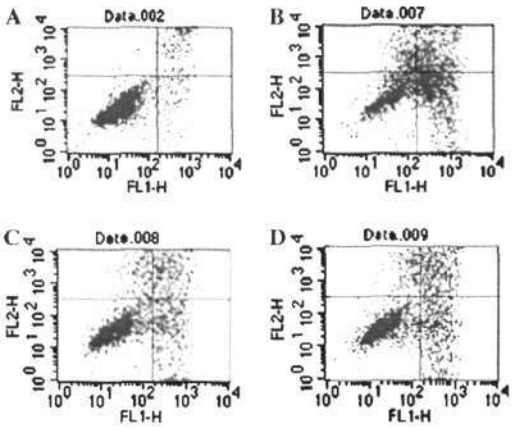

Fig. 3. Apoptotic effect of HBX in HepG2 cells by flow cytometry analysis. HepG2 cells were transfected with either HBX at two different amounts (C,D) or empty pXJ-40 vector (A). Cells treated with cisplatin were used as positive control. The labeling of cells was by Annexin-V-FITC (FL1-H) and propidium iodide (FL2-H) (see Materials and methods). The bottom left square indicates the number of total cells, the bottom right square the number of apoptotic cells, and top right square the number of necrotic cells. The percentage of apoptotic cells was, respectively, 3.53% (empty pXJ-40 as negative control, A), 30.93% (cisplatin treated cells as positive control, B), 12.27% (1.0 μg HA-HBX transfected cells, C), and 15.27% (2.0 μg HA-HBX transfected cells, D).

mutant HBX(E125A) and Bcl-2 (4.62%), as well as between this mutant and Bcl-xl (5.11%).

HBX induces apoptosis in HepG2 cells

To study the apoptotic effects on the cells conferred by HBX, the coding region of HBX was cloned in-frame with the HA tag in mammalian expression vector pXJ-40. HepG2 cells transfected by this HA-HBX construct showed decreased cell viability, in a dose-dependent manner as determined by the MTT assay. Specifically, 49.1% of cells transfected with 1.6 μg HA-HBX construct remained viable two days after transfection.

The apoptotic nature of these dead cells was then analyzed by flow cytometry using the ApoAlert Annexin V Apoptosis kit, based on the observation that apoptotic cells have been shown to translocate the membrane phospholipids phosphatidylserine (PS) from the inner face of the plasma membrane to the cell surface which then becomes detectable by Annexin V [24]. To investigate the effect of HBX in liver cells, HepG2 cells were double-stained with Annexin-V-FITC and propidium iodide (PI) 48 h after transfection with pXJ-40-HBX. Results from flow cytometry indicated there were 12.27% and 15.27% apoptotic cells in cells transfected with 1.0 and 2.0 μg of the pXJ-40-HBX construct, respectively (Figs. 3C and D). This was significantly higher than cells transfected with empty pXJ-40 vector (3.53%, Fig. 3A), but lower than the positive control with cells treated by 100 μM cisplatin for 16 h (30.93%, Fig. 3B). Our results indicated that HBX induced apoptosis when overexpressed in HepG2 cells.

The apoptotic activity of HBX was further examined by measuring the caspase-3 protease activity, a hallmark of apoptosis [25]. To this end, HepG2 cells transfected with 2 μg HA-HBX construct were analyzed at different time points. As shown in Fig. 4, cells transfected with the empty pXJ-40 with a caspase-3 activity (cleavage of DEVE-AFC substrate) at 2254 served as negative control as opposed to those cells treated with cisplatin with a caspase-3 activity at 31766. For cells transfected with HA-HBX construct, the caspase-3 activity was at 1688 (24 h), 1917 (36 h), 4633 (48 h), 7147 (60 h), and 3998 (72 h), respectively (Fig. 4). There was a significant increase of caspase-3 activity in HBX-transfected HepG2 cells from 48 to 72 h, with the peak at 60 h. The decrease of caspase-3 activity as observed at 72 h may be due to the decrease in the

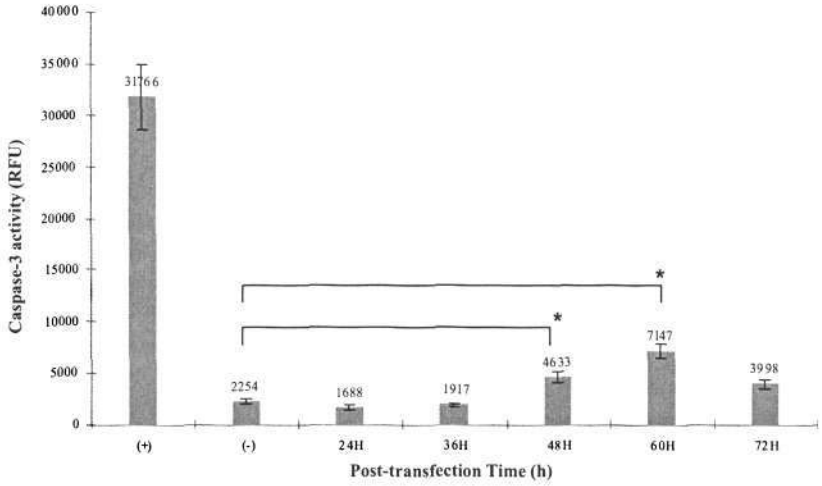

Fig. 4. Apoptotic effects of HBX in HepG2 cells by caspase-3 activity. HepG2 cells were transfected with HA-HBX construct and analyzed for caspase-3 activity at different time points (see Materials and methods). A similar analysis was carried out on cells treated with cisplatin (+) and those transfected with the empty pXJ-40 plasmid (−). The results represent means ± SE from three independent experiments. *Statistically significant at $p < 0.05$ in caspase-3 activity.

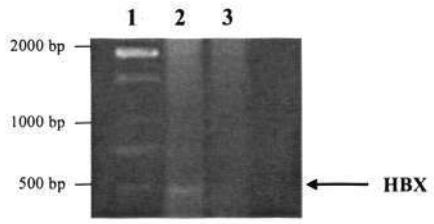

Fig. 5. Expression of HBX mRNA in transfected HepG2 Cells. Total RNA was extracted from HepG2 and HBX transfected HepG2 cells, respectively. Reverse transcription-PCR was carried out using HBX specific primers (see Materials and methods). Lane 1, 100 bp DNA ladder. Lane 2, HBX transfected HepG2 cells. Lane 3, non-transfected HepG2 cells.

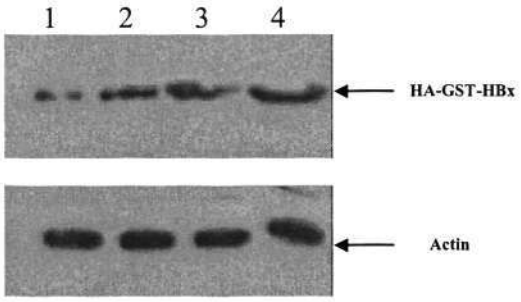

Fig. 6. Western blot analysis of HA-GST-HBX in 293T cells. Cells were transfected with a different amount of the fusion construct HA-GST-HBX, 0.5 μg (lane 1), 1 μg (lane 2), 2 μg (lane 3), and 4 μg (lane 4), respectively. Western blot analysis was carried out on cell extracts using anti-HA and anti-actin antibodies (see Materials and methods).

number of apoptotic cells. Our results further supported the evidence of HBX-induced apoptosis as shown in the flow cytometry analysis described earlier in this study.

Apoptotic effects of HBX may correlate with its half-life

To correlate the expression level of HBX in HepG2 cells with our observed apoptotic effects, Western blot analysis was carried out in HepG2 cells transfected with HA-HBX construct using anti-HA antibody. However, no protein band was observed. This could be due to the fast onset of apoptosis in cells expressing HBX protein, leading to the absence of detectable HBX protein in our Western blot analysis.

To confirm this hypothesis, expression of HBX mRNA in HepG2 transfected with pXJ-40-HBX was examined by reverse transcription PCR. As shown in Fig. 5, the band of expected size for HBX (462 bp) was detected in HBX-transfected HepG2 cells (lane 2) but not in the non-transfected control HepG2 cells (lane 3).

To explore further this possibility, the same HA-HBX construct was transfected into the epithelial cell line 293T which generally yields a higher protein level compared with HepG2 cells (data not shown). No protein band was observed in the 293T cell extract on Western blot analysis. To determine if HBX could be more stable when fused with a different protein as reported by other investigators [26], HBX was cloned in-frame with the glutathione-*S*-transferase (GST) gene together with the HA tag in the same pXJ-40 vector (see Materials and methods). Another cell line, the epithelial 293T cells, was used in the transfection and the subsequent Western blot analysis. Results shown in Fig. 6 indicate that the fusion protein HA-GST-HBX was expressed in 293T cells and as expected in a dose-dependent manner.

However, no apoptotic activity was detected in 293T cells expressing the fusion protein HA-GST-HBX by either flow cytometry or caspase-3 activity (data not shown). Our results were consistent with the hypothesis that HBX protein may not be stable in apoptotic cells triggered by its own expression, while the fusion HA-GST-HBX may be more stable and therefore detectable by Western blot analysis.

In contrast to the widely reported cytoplasmic localization [27], our previous investigation reveals a perinuclear localization of HBX when it was expressed as a fusion protein with the green fluorescent protein (GFP) [28]. It remains possible that the tagging of HBX with the larger GST protein alters the stability of HBX by affecting its subcellular localization, which in turn may abolish the apoptotic activity observed in our study.

While our findings were consistent with recent reports on the pro-apoptotic activity by HBX [29], HBX may be involved in the process apoptosis by other mechanisms including its interaction with tumor suppressor p53 and inhibition of DNA repair [26,30]. The difference in these two distinct mechanisms as reported in this and other studies may be reflective of the expression level of HBX and its stability in transfected cells. Nevertheless, it is possible that HBX may utilize either one of these two, or both, mechanisms to induce apoptosis in infected host cells.

In conclusion, we report the identification of a pro-apoptotic BH3 domain in HBX. Its significance of this BH3 domain was supported by the interactions of HBX with anti-apoptotic members of the Bcl-2 family of proteins, but not with those pro-apoptotic members. The apoptotic activity of HBX was further supported by molecular analyses including flow cytometry and caspase-3 activity. Importantly, our identified BH3 in HBX matches the domain mediating its previously reported pro-apoptotic activity [11]. Our results therefore have provided the first molecular evidence of apoptosis conferred directly by HBX.

Acknowledgments

This work was supported by Grant 03/1/22/18/229 (WN Chen) from the Biomedical Research Council, Agency for Science, Technology and Research, Singapore. Y.W. Lu is a recipient of a graduate research scholarship from Nanyang Technological University, Singapore.

References

[1] J.Y. Lau, X. Xie, M.M. Lai, P.C. Wu, Apoptosis and viral hepatitis, Sem. Liver Dis. 18 (1998) 169–176.

[2] J.M. Adams, S. Cory, The Bcl-2 protein family: arbiters of cell survival, Science 281 (1998) 1322–1326.

[3] J.B. Baell, D.C. Huang, Prospects for targeting the Bcl-2 family of proteins to develop novel cytotoxic drugs, Biochem. Pharmacol. 64 (2002) 851–863.

[4] T. Kondo, T. Suda, H. Fukuyama, et al., Essential roles of the Fas ligand in the development of hepatitis, Nat. Med. 3 (1997) 409–413.

[5] N. Hayashi, E. Mita, Involvement of Fas system-mediated apoptosis in pathogenesis of viral hepatitis, J. Viral Heaptitis 6 (1999) 357–365.

[6] F. Su, R.J. Schneider, Hepatitis B virus HBx protein sensitizes cells to apoptotic killing by tumor necrosis factor a, Proc. Natl. Acad. Sci. USA 94 (1997) 8744–8749.

[7] P. Chirillo, S. Pagano, G. Natoli, et al., The hepatitis B virus X gene induces p53-mediated programmed cell death, Proc. Natl. Acad. Sci. USA 94 (1997) 8162–8167.

[8] G.G. Chen, P.B. Lai, P.K. Chan, E.C. Chak, J.H. Yip, R.L. Ho, B.C. Leung, W.Y. Lau, Decreased expression of Bid in human heaptocellular carcinoma is related to hepatitis B virus X protein, Eur. J. Cancer 37 (2001) 1695–1702.

[9] J. Ehrmann, D. Galuszkova, J. Ehrmann, et al., Apoptosis-related proteins, Bcl-2, Bax, Fas, Fas-L and PCNA in liver biopsies of patients with chronic hepatitis B virus infection, Pathol. Oncol. Res. 6 (2000) 130–135.

[10] S. Tanaka, Y. Shirakata, N. Kaneniwa, K. Koike, Association of hepatitis B virus X protein with mitochondria causes mitochondrial aggregation at the nuclear periphery, leading to cell death, Oncogene 18 (1999) 6965–6973.

[11] R. Schuster, W.H. Gerlich, S. Schaefer, Induction of apoptosis by the transactivating domains of the hepatitis B virus X gene leads to suppression of oncogenic transformation of primary rat embryo fibroblasts, Oncogene 19 (2000) 1173–1180.

[12] T. Pollicino, O. Terradillos, H. Lecoeur, M.L. Gougeon, M.A. Buendia, Pro-apoptotic effect of the hepatitis B virus X gene, Biomed. Pharmacother. 52 (1998) 363–368.

[13] J.G. Teodoro, P.E. Branton, Regulation of apoptosis by viral gene products, J. Virol. 71 (1997) 1739–1746.

[14] A. Kelekar, C.B. Thomson, Bcl-2-family proteins: the role of the BH3 domain in apoptosis, Trends Cell Biol. 8 (1998) 324–329.

[15] D.C. Huang, A. Strasser, BH3-only proteins—essential initiators of apoptotic cell death, Cell 103 (2000) 839–842.

[16] H. Puthalakath, A. Villunger, L.A. O'Reilly, et al., Bmf: a proapoptotic BH3-only protein regulated by interaction with the myosin V actin motor complex, activated by anoikis, Science 293 (2001) 1829–1832.

[17] K. Komatsu, T. Miyashita, H. Hang, et al., Human homologue of *S. pombe* Rad9 interacts with BCL-2/BCL-xl and promotes apoptosis, Nat. Cell Biol. 2 (2000) 1–6.

[18] J. Han, C. Flemington, A.B. Houghton, et al., Expression of bbc3, a pro-apoptotic BH3-only gene, is regulated by diverse cell death and survival signals, Proc. Natl. Acad. Sci. USA 98 (2001) 11318–11323.

[19] E. Oda, R. Ohki, H. Murasawa, et al., Noxa, a BH3-only member of the Bcl-2 family and candidate mediator of p53-induced apoptosis, Science 288 (2000) 1053–1058.

[20] S.Y. Hsu, P. Lin, A.J. Hsueh, BOD is an ovarian BH3 domain-containing proapoptotic Bcl-2 protein capable of dimerization with diverse antiapoptotic Bcl-2 members, Mol. Endocrinol. 12 (1998) 1432–1440.

[21] J. Han, P. Sabbatini, E. White, Induction of apoptosis by human Nbk/Bik, a BH3-containing protein that interacts with E1B 19K, Mol. Cell. Biol. 16 (1996) 5857–5864.

[22] E. Manser, H.Y. Huang, T.H. Loo, et al., Expression of constitutively active alpha-PAK reveals effects of the kinase on actin and focal complexes, Mol. Cell. Biol. 17 (1997) 1129–1143.

[23] T. Sato, M. Hanada, S. Bodrug, et al., Interaction among members of the Bcl-2 protein family analyzed with a yeast two-hybrid system, Proc. Natl. Acad. Sci. USA 91 (1994) 9238–9242.

[24] S.J. Martin, C.P. Reutelingsperger, A.J. McGahon, et al., Early redistribution of plasma membrane phosphatidylserine is a general feature of apoptosis regardless of the initiating stimulus: inhibition by overexpression of Bcl-2 and Abl, J. Exp. Med. 182 (1995) 1545–1556.

[25] K.M. Boatright, G.S. Salvesen, Mechanisms of caspase activation, Curr. Opin. Cell Biol. 15 (2003) 725–731.

[26] A.T. Lee, J.W. Ren, E.T. Wong, et al., The hepatitis B virus X protein sensitizes HepG2 cells to UV light-induced DNA damage, J. Biol. Chem. 280 (2005) 33525–33535.

[27] F. Henkler, J. Hoare, N. Waseem, et al., Intracellular localization of the hepatitis B virus HBX protein, J. Gen. Virol. 82 (2001) 871–882.

[28] W.N. Chen, C.J. Oon, K.S. Goo, Hepatitis B virus X protein in the proteasome of mammalian cells: defining the targeting domain, Mol. Biol. Rep. 28 (2001) 31–34.

[29] N. Lin, H.Y. Chen, D. Li, et al., Apoptosis and its pathway in X gene-transfected HepG2 cells, World J. Gastroenterol 11 (2005) 4326–4331.

[30] S.Y. Kim, J.K. Kim, H.J. Kim, J.K. Ahn, Hepatitis B virus X protein sensitizes UV-induced apoptosis by transcriptional transactivation of Fas ligand gene expression, IUBMB Life 57 (2005) 651–658.

Available online at www.sciencedirect.com
ScienceDirect
Biochemical and Biophysical Research Communications 351 (2006) 64–70
BBRC
www.elsevier.com/locate/ybbrc

The HBSP gene is expressed during HBV replication, and its coded BH3-containing spliced viral protein induces apoptosis in HepG2 cells ☆

Yi Wei Lu [a], Tuan Lin Tan [a], Vincent Chan [b], Wei Ning Chen [b,*]

[a] School of Biological Sciences, College of Engineering, Nanyang Technological University, Singapore 637722, Singapore
[b] School of Chemical and Biomedical Engineering, College of Engineering, Nanyang Technological University, 62 Nanyang Drive, Singapore 637722, Singapore

Received 14 September 2006
Available online 10 October 2006

Abstract

The mechanisms of liver injury in hepatitis B virus (HBV) infection are defined to be due not to the direct cytopathic effects of viruses, but to the host immune response to viral proteins expressed by infected hepatocytes. We showed here that transfection of mammalian cells with a replicative HBV genome causes extensive cytopathic effects, leading to the death of infected cells. While either necrosis or apoptosis or both may contribute to the death of infected cells, results from flow cytometry suggest that apoptosis plays a major role in HBV-induced cell death. Data mining of the four HBV protein sequences reveals the presence of a Bcl-2 homology domain 3 (BH3) in HBSP, a spliced viral protein previously shown to be able to induce apoptosis and associated with HBV pathogenesis. HBSP is expressed at early stage of our cell-based HBV replication. When transfected into HepG2 cells, HBSP causes apoptosis in a caspase dependent manner. Taken together, our results suggested a direct involvement of HBV viral proteins in cellular apoptosis, which may contribute to liver pathogenesis.

Keywords: HBV replication; Apoptosis; HBSP; BH3

Hepatitis B virus (HBV) infection leads to a wide range of liver diseases, including viral hepatitis and hepatocellular carcinoma (HCC). Viral hepatitis is characterized by an inflammatory reaction in the infected liver cell, and is associated with cell damage and death [1]. One of the typical processes of cell death is apoptosis which is generally considered to be a mechanism of host defense against viral infections [2,3]. Apoptosis, or programmed cell death, is a highly conserved, tightly controlled self-destruction process to ablate damaged and neoplastic cells in multicellular organisms. On the other hand, viruses have evolved strategies to counteract and regulate apoptosis in order to maximize the production of virus progeny and promote the spread of virus progeny to neighboring cells. During the course of persistent HBV infection, continuous intrahepatic inflammation maintains a cycle of liver cell destruction and regeneration that often terminates in HCC. While the expression and retention of viral proteins in hepatocytes may influence the severity and progression of liver disease, the mechanisms of liver injury in viral hepatitis are defined to be due not to the direct cytopathic effects of viruses, but to the host immune response to viral proteins expressed by infected hepatocytes [4].

Recent reports have pointed to the involvement of the mitochondria-dependent apoptotic pathway which is governed by Bcl-2 family of proteins in the development of liver diseases [5,6]. However, little is known on the involvement of HBV viral proteins in this pathway at molecular level. The interest of characterizing the Bcl-2 mediated apoptosis in HBV related hepatitis lies in the fact that these proteins are able to either delay or induce apoptosis. While the former would ensure prolonged viral

☆ *Abbreviations:* HBV, hepatitis B virus; HCC, hepatocellular carcinoma; HBSP, HBV spliced variant protein; BH3, Bcl-2 homology domain 3; GST, glutathione- *S*-transferase.

* Corresponding author. Fax: +65 62259865.
E-mail address: WNChen@ntu.edu.sg (W.N. Chen).

0006-291X/$ - see front matter © 2006 Elsevier Inc. All rights reserved.
doi:10.1016/j.bbrc.2006.10.002

replication, it is now known that some viruses are able to induce apoptosis at late stages of infection [7]. This process may result in the dissemination of viral particles with minimum host immune response as well as protecting progeny viral particles from host neutralizing antibodies.

The Bcl-2 family of proteins consists of both suppressors and promoters of apoptosis. Four conserved domains within the Bcl-2 family of proteins have been identified through sequence comparisons, these are named as Bcl-2 homology (BH) domains 1 to 4, with BH3 only proteins being pro-apoptotic [8].

We report in this study evidence of direct involvement of HBV viral protein in apoptosis. HBV replicating HepG2 cells showed characteristics of cellular apoptosis such as detachment from substrate and rounding up, followed by cell death. This observation was supported by FACS analysis and caspase-3 activation assay. Our study further revealed the presence of BH3 domain in HBSP, a spliced HBV protein, which has been reported to induce cellular apoptosis. While its apoptotic effect was confirmed in our study, mutation of the well-conserved residue in the BH3 domain (L25A) significantly reduced the apoptotic effect. The significance of our findings was discussed.

Materials and methods

Cell culture and transfection. HepG2 cells (ATCC, USA) were cultured in Gibco Dulbecco's minimal essential medium (Invitrogen Inc., USA), supplemented with 10% fetal bovine serum (Invitrogen Inc., USA), 1% anti-mycotic (Invitrogen, USA) under 37 °C and 5% CO_2. Effectene transfection reagent (Qiagen, Germany) was the expression system for HBV in HepG2 cells. After adherent HepG2 cells reach 70% confluency, the cells were transfected with 2 μg replicative HBV genome constructed as described previously [9]. Transfected cells were maintained at 37 °C and 5% CO_2 for various times (6, 12, 24, 36, 48, and 60 h) and examined under the microscope.

Cloning of HBSP in pXJ-40 and site-directed mutagenesis. The coding region of HBSP [10] was amplified by PCR, joined in-frame with glutathione- *S*-transferase (GST) gene, and cloned in pXJ-40 containing a HA tag. This resulted in a fusion gene consisting of HA-GST-HBSP on pXJ-40 vector. This construct was used as template for generating mutation (L25A) in HBSP coding region by site-directed mutagenesis (Stratagene, USA). Separately, the coding region of GST alone was also cloned in-frame with the HA tag into pXJ40, resulting in a HA-GST fusion protein.

Reverse transcriptase-PCR. Two microgram of pcDNA3.1 containing the replicative HBV genome was transiently transfected into 3×10^5 HepG2 cells in each well of a 6-well plate. Transfected cells were collected at different time points after transfection (6, 12, 24, 36, 48, and 60 h). mRNA at each time point was extracted using miniRNAse kit (Qiagen, Germany), and served as template for reverse-transcriptase PCR using HBSP specific primers (5′-AT GAATTC ATG CCC CTA TCT TAT CAA-3′ and 5′-TT GCGGCCGC AAG CCC AGG ACG ATG GGA AT-3′). The PCR product using these primers encompassed the coding region of HBSP with an expected size of 279 bp [10]. Positive PCR products were sequenced to confirm their identity as HBSP.

Apoptotic effect of HBV and HBSP in HepG2 cells by flow cytometry analysis. pcDNA3.1 containing the replicative HBV genome and pXJ-40-HA-GST-HBSP were transiently transfected separately into 3×10^5 HepG2 cells. HepG2 cells transfected with empty pXJ-40 and cells treated by 50 μM cisplatin for 16 h were used as negative and positive controls, respectively. Transfected cells were incubated at different time points (6, 12, 24, and 48 h) before being harvested and analyzed by ApoAlert™ Annexin-V kit (BD Biosciences, USA). Cells were rinsed in binding buffer and resuspended in the same buffer. Five microliters of Annexin-V-FITC and 10 μl prodium iodide was added into each sample. Following 30 min incubation in dark, samples was analyzed on FACS station (BD Bioscience, USA).

Apoptotic effect of HBSP in HepG2 cells by caspase-3 assay. Increasing amount of pXJ-40-HA-GST-HBSP (2, 4, 6, and 8 μg) was transiently transfected into 3×10^5 HepG2 cells in each well of a 6-well plate. HepG2 cells transfected with empty pXJ40 and cells treated by 100 μM of cisplatin for 16 h were used as negative and positive controls, respectively. Samples were collected 48 h after transfection and analyzed by using ApoAlert™ Caspase-3 Fluorescent Assay Kit (BD Bioscience, USA). Cells were lysed in 50 μl of lysis buffer for 30 min on ice. After centrifugation, 50 μl

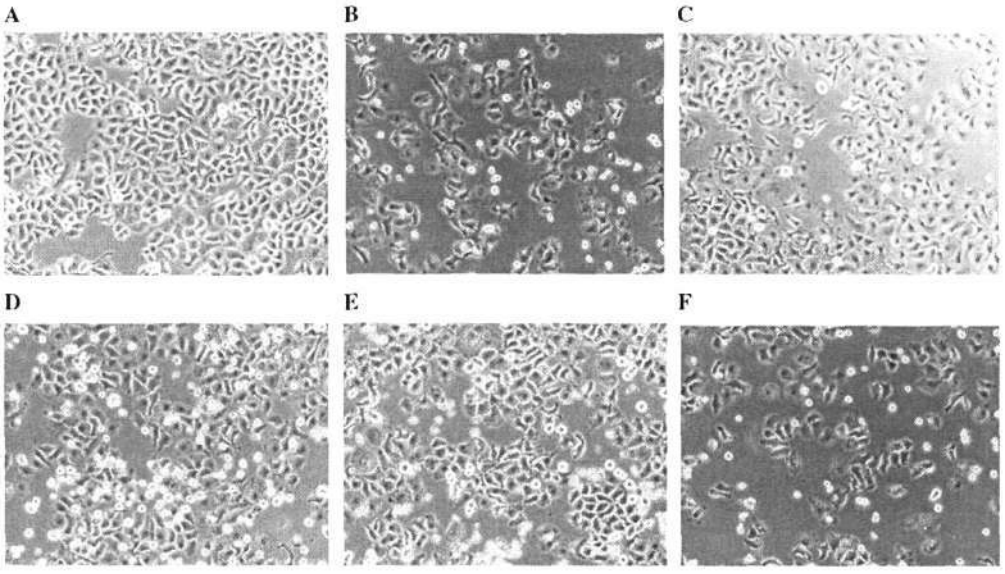

Fig. 1. Analysis of morphology of HBV-replicating HepG2 cells. A series of phase contrast images of HepG2 cell transfected with replicative HBV genome and incubated at 6 h (C), 12 h (D), 24 h (E), and 48 h (F). HepG2 cells transfected with empty vector pXJ40 vector (after 48 h) are shown in (A). Cells treated with cisplatin, an agent inducing apoptosis, are shown in (B). Increasing detachment of cells and their rounding up were observed in (B), and progressively from (C–F). Images were taken using Inverted Microscope (Olympus IX71).

supernatant was mixed with 50 μl of reaction buffer. Five microlitres of caspase-3 substrate DEVE-AFC was added into the mixture and incubated in 37 °C, 5% CO_2 for another 3 h. This mixture was then pipetted into 96-well plate and analyzed by using microplate fluorescence reader (FL600, Bio-TEK, USA). At an excitation wavelength of 400 nm the cleaved AFC gave out an emission at 505 nm and absorbance was automatically recorded. The caspase-3 activity for each time point was measured in cells transfected with pXJ40-HA-GST-HBSP in three independent experiments.

Western blot analysis. HA-GST-HBSP and HA-GST proteins expressed in HepG2 cells were detected by primary anti-HA antibody (Santaclause, USA) in 1:5000 dilution and secondary anti-mouse antibody conjugated with horseradish peroxidase (Pierce, USA) in 1:5000 dilution. Anti-actin antibody (Sigma, USA) was used to detect actin protein as an internal control.

Results and discussion

HBV transfected HepG2 cells show evidence of apoptosis

To generate a cell-based system for HBV replication, a linearized form of HBV genome has been constructed in the mammalian expression vector pcDNA3.1 [9] which has been shown to set viral replication in HepG2 by producing HBV particles in the culture medium [11]. This system was chosen to analyze effects of HBV replication on the cells.

In contrast to the widely accepted non-cytopathic nature of HBV, recent reports suggest a direct role of HBX (the smallest HBV viral proteins) in apoptosis [12,13]. Careful examination of infected cells by light microcopy showed characteristic signs of apoptosis during the infection process. As the incubation time after transfection prolonged, the number of dead cells which were detached from the culture dish increased (6, 12, 24, and 48 h, respectively) (Fig. 1C–F). The morphological anomalies observed in these cells were not detected in HepG2 cells 48 h after they were transfected by the empty plasmid pcDNA3.1 (Fig. 1A). Our data therefore suggested that the observed morphological changes were associated with HBV replication, but not due to transfection process or the empty plasmid. To our understanding, this is the first time that cell death associated with HBV replication has been reported.

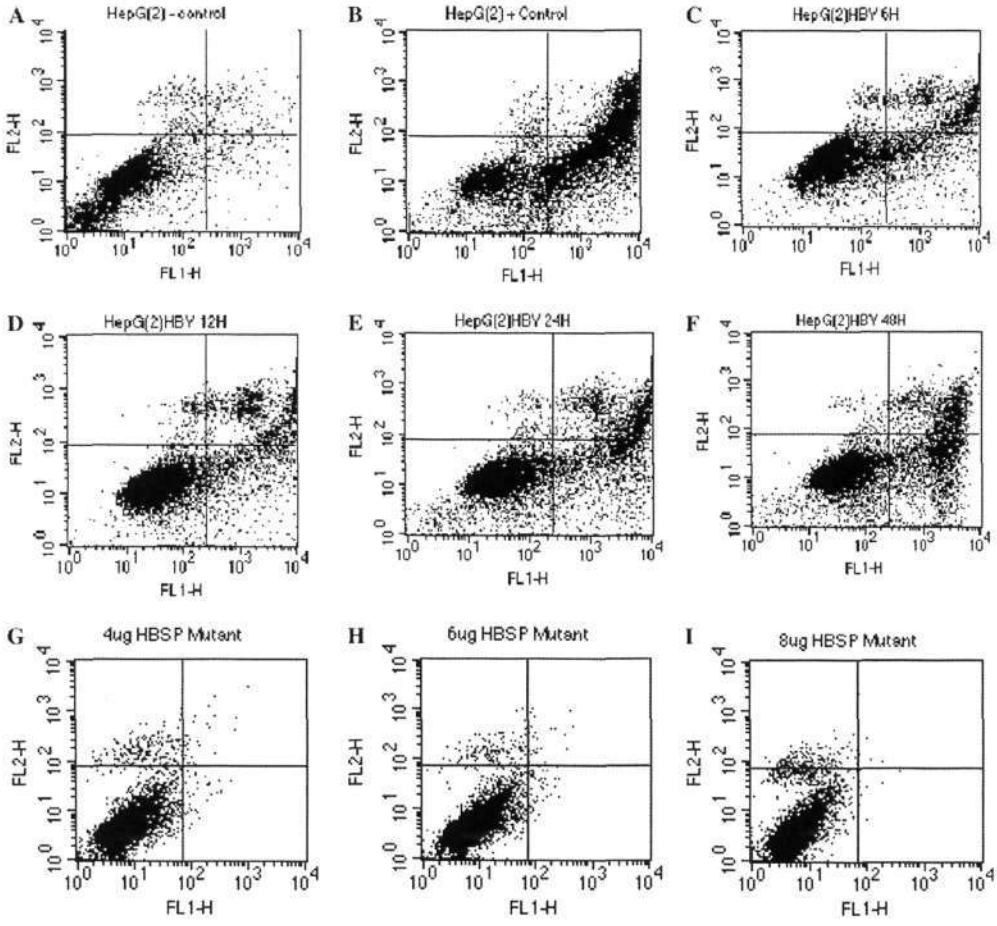

Fig. 2. Flow cytometry analysis of apoptotic effect of HBV replication in HepG2 cells. HepG2 cells were transfected with either pcDNA3.1 carrying the replicative HBV genome and incubated at different time points (12 h (C), 24 h (D), 36 h (E), and 48 h (F)) or empty pcDNA3.1 vector (A). Cells treated with cisplatin were used as positive control (B). The labeling of cells was by Annexin-V-FITC (FL1-H) and prodium iodide (FL2-H). In each panel, the bottom left square indicate the number of cells, the bottom right square the number of apoptotic cells, and top right square the number of necrotic cells. Increasing amount of apoptotic cells is observed from (C–F). (G–I) Represent FACS results on cells transfected with increasing amount (4 μg (G), 6 μg (H), and 8 μg (I)) of pXJ40-HA-GST-HBSP(L25A) mutant protein. There were fewer apoptotic cells which remained unchanged with the increased amount of mutant protein.

The morphological changes in HBV-infected cells at the 48 h time point (Fig. 1F) were similar to those in HepG2 cells treated with cisplatin, a known chemical that causes apoptosis (Fig. 1B).

To investigate if apoptosis was involved in the observed HBV-induced cell death process, flow cytometry (FACS) was used which is based on the observation that apoptotic cells would translocate the membrane phospholipids phosphatidylserine (PS) from the inner face of the plasma membrane to the cell surface which then becomes detectable by Annexin V [14]. Typically, the proportion of apoptotic cells is reflected in the bottom-right square of FACS profile (Fig. 2). In this study, HBV-replicating HepG2 cells were collected at the time points in Fig. 1 and were double-stained with Annexin-V-FITC and propidium iodide (PI) separately. Results shown in Fig. 2 indicated there was an increase in the number of apoptotic cells as the infection time prolonged. Specifically, 10.07% of apoptotic cells were detected 6 h after transfection of HBV genome (Fig. 2C), while the proportion of such cells was at 13.8%, 14.85%, 20.75%, and 28.83% for 12 h (D), 24 h (E), and 48 h (F), respectively. This was significantly higher than HepG2 cells transfected with the empty pcDNA3.1 vector (1.37%, A), but lower than the positive control in which cells were treated by 50 μM cisplatin for 16 h (36.12%, B).

Our data therefore indicated that apoptosis was likely to be the main mechanism of HBV-induced cell death. This is consistent with other viruses capable of inducing cell death [15,16].

HBV spliced protein (HBSP) contains a BH3-like domain

To investigate whether HBV viral proteins were directly involved in the observed apoptosis, we screened amino acid sequences of HBV proteins for pro-apoptotic motif. Results revealed a BH3 domain in the N-terminus of the HBV DNA polymerase, spanning from residue 21 to 35, which included conserved and critical residues found in the BH3 domains of pro-apoptotic Bcl-2 family of proteins (Fig. 3A). The same BH3 domain was also found in HSBP, a spliced variant protein consisting of 46 amino acid residues of the N-terminal part of HBV DNA polymerase, and 47 new amino acid residues [10]. Interestingly, HBSP has been shown to induce apoptosis through a hitherto unknown mechanism [10,17]. The identification of a BH3 domain may therefore provide molecular insights into its apoptotic effect.

HBSP is expressed during HBV replication

Although HBSP has been found in HBV infected liver tissue and anti-HBSP antibodies can be detected in sera of HBV chronic carriers [10], its expression during HBV replication has not been characterized. Results from such an analysis would be particularly relevant to our observed apoptosis following HBV replication in HepG2 cells. To this end, HepG2 cells transfected with pcDNA3.1 carrying

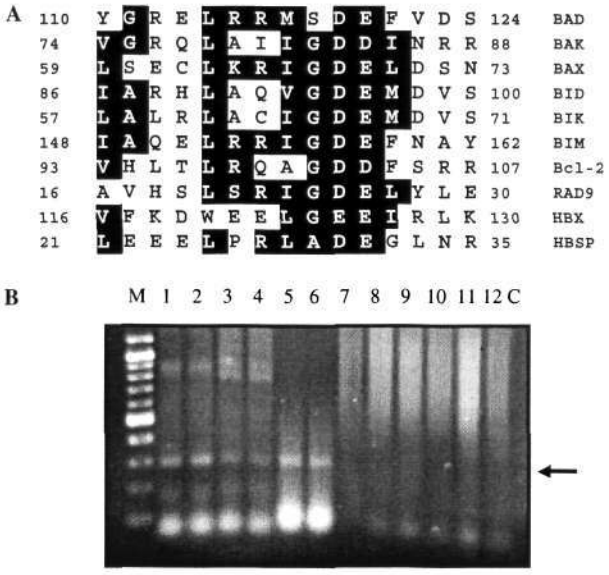

Fig. 3. (A) Alignment of BH3-homology regions of Bcl-2 family members and HBSP. Comparison of the BH3-like regions in HBVPolN and Bcl-2 family members. Conserved amino acids are shaded. (B) Expression of HBSP gene by reverse-transcriptase (RT) PCR analysis. mRNA was extracted from HepG2 cells transfected with replicative HBV genome, and used as template for RT-PCR analysis using primers encompassing the coding region of HBSP. Duplicate samples were analyzed for each of the following time points after transfection: 6 h (lanes 1 and 2), 12 h (lanes 3 and 4), 24 h (lanes 5 and 6), 36 h (lanes 7 and 8), 48 h (lanes 9 and 10), and 60 h (lanes 11 and 12). HBSP expression was detected up to 24 h after transfection (arrow head). Lane M represents 100 bp ladder. Lane C represents negative control for RT-PCR in which no mRNA was added.

the replicative HBV genome were collected at various time points (6, 12, 24, 36, 48, and 60 h). mRNA was extracted from cells at each time point and used as template for reverse-transcriptase PCR. Positive PCR products were confirmed to be HBSP coding region by sequencing. Results shown in Fig. 3B indicated that HBSP gene was expressed in HBV transfected cells at 6, 12, and 24 h, but not thereafter. Our data therefore indicated that HBSP was expressed during HBV replication and may contribute directly to our observed apoptotic effect following HBV replication.

HBSP induces apoptosis in mammalian cells and activates caspase-3 protease

To study the apoptotic effects on the cells conferred by either HBV DNA polymerase or HBSP, their respective coding region of 2526 and 279 bp was cloned in-frame with the GST and HA tag in mammalian expression vector pXJ40. HepG2 cells transfected by either HA-GST-HBV DNA Polymerase or HA-GST-HBSP construct were assessed for their viability. While cells transfected with HA-GST-HBSP showed decreased cell viability in a dose dependent manner as determined by MTT assay, no change of cell viability was observed for those transfected with HA-GST-HBV DNA Polymerase (data not shown).

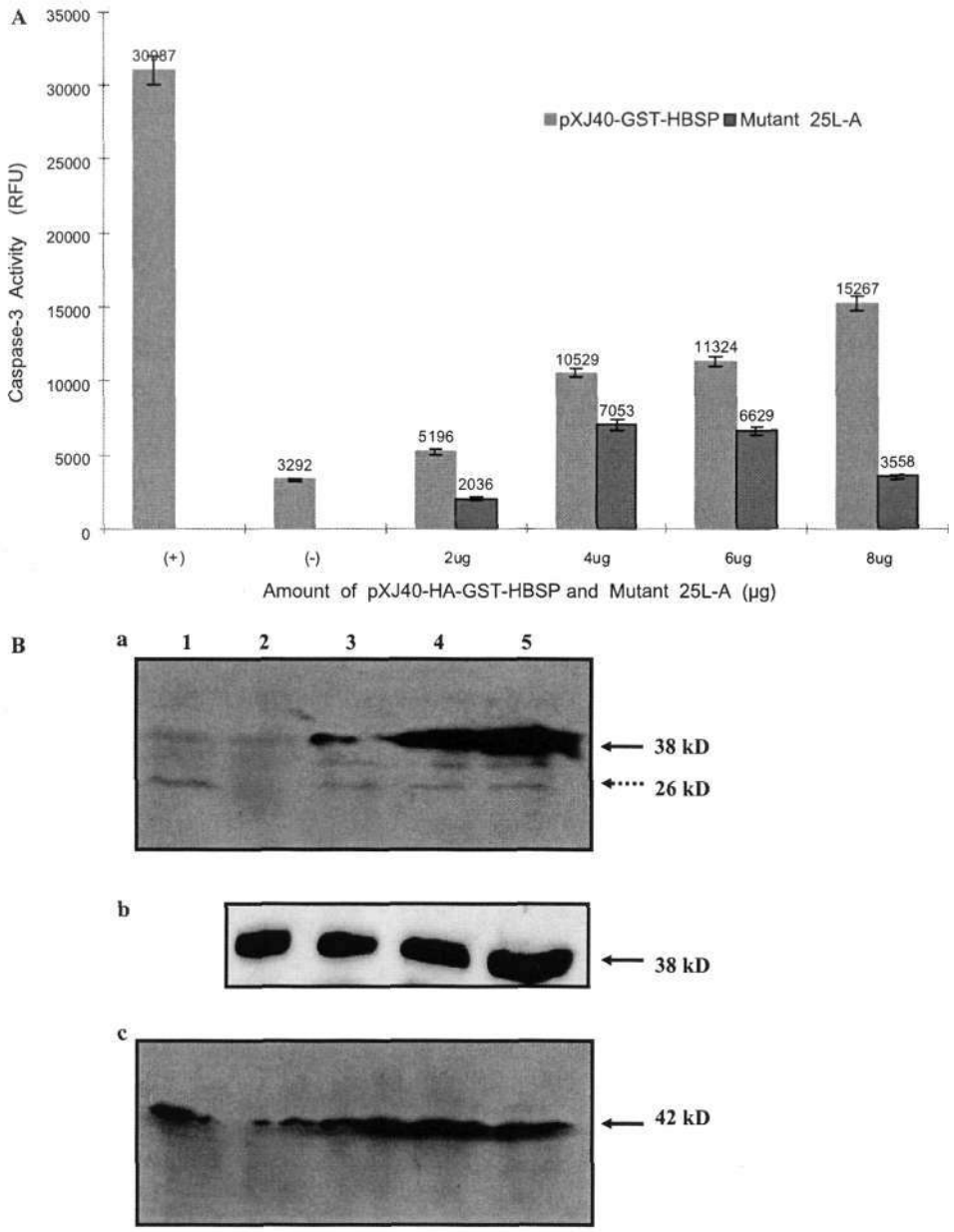

Fig. 4. (A) Apoptotic effects of HBSP in HepG2 cells by caspase-3 activity. HepG2 cells were transfected with increasing amounts of either wild type pXJ40-HA-GST-HBSP or mutant pXJ40-HA-GST-HBSP(L25A) and analyzed for caspase-3 activity (see Materials and methods). Similar analysis was carried out on cells treated with cisplatin (+) and those transfected with pXJ40-HA-GST (−). Caspase-3 activity was measured in three independent transfections for each amount of plasmid used in this study. (B) Western blot analysis of HA-GST-HBSP in HepG2 cells. Cells were transfected with the different amount of either the wild type pXJ40-HA-GST-HBSP (A) or mutant pXJ40-HA-GST-HBSP(L25A) (B) 2 μg (lane 2), 4 μg (lane 3), 6 μg (lane 4), and 8 μg (lane 5), respectively. HepG2 cells transfected with pXJ40-HA-GST were used as negative control (lane 1, a). Endogenous actin was used as an internal control. Antibodies used were anti-HA (a,b) and anti-actin (c), respectively. (a,b), Solid arrowhead indicates the fusion HA-GST-HBSP protein (either wild type or in panel a mutant in panel b) at 38 kD. The discontinued arrowhead indicates the 26 kD GST protein in cells transfected with pXJ40-HA-GST (lane 1, a). (c), Arrowhead indicates the endogenous action protein at 42 kD.

To investigate the molecular basis of HBSP-induced apoptosis, HepG2 cells transfected with pXJ40-HA-GST-HBSP were analyzed by caspase-3 protease assay, a hallmark of apoptosis [18]. To this end, HepG2 cells were transfected with increasing amount of pXJ-HA-GST-HBSP (2, 4, 6, and 8 μg), incubated for 48 h, and analyzed for the caspase-3 protease activity. As shown in Fig. 4A, the caspase-3 activity (cleavage of DEVE-AFC substrate) of 3292 was found in cells transfected with pXJ40-HA-GST (negative control) whereas those cells treated with cisplatin (positive control) had the caspase-3 activity of 30987. In cells transfected with pXJ-HA-GST-HBSP

construct, the caspase-3 activity was at 5196 (2 μg), 10,529 (4 μg), 11,324 (6 μg), and 15,267 (8 μg), respectively. There was therefore a significant increase of caspase-3 activity in HA-GST-HBSP transfected cells, in a dose dependent manner. To correlate the expression level of HBSP in HepG2 cells with our observed caspase-3 activity, Western blot analysis was carried out in HepG2 cells transfected with HA-GST-HBSP construct using anti-HA antibody. Results shown in Fig. 4B indicated that an increase in intensity of the expected molecular weight of HA-GST-HBSP (38 kD, a) was detected, consistent with the increased amount of HA-GST-HBSP used in transfection. On the other hand, only the 26 kD GST protein was detected in cells transfected with pXJ-HA-GST. As an internal control, a constant intensity of the endogenous actin protein (42 kD, c) was observed in cells.

Mutant HBSP(L25A) induces reduced apoptosis

To determine the specificity of HBSP in inducing apoptosis, mutation was generated at the conserved residue (L25A) which has been reported to impact on the pro-apoptotic activity of BH3 containing proteins [19]. HepG2 cells were then transfected, in the same dose dependent manner as for the wild type HBSP, with pXJ40-HA-GST-HBSP(L25A) and the caspase-3 activity determined. Results shown in Fig. 4A indicated a significant reduction in caspase-3 activity for the mutant HBSP (L25 A), particularly in cells transfected with 2 and 8 μg of mutant construct. The moderate decrease in cells transfected with 4 and 6 μg of the same mutant construct suggested that other amino acid residues in the BH3 domain may also be involved in the pro-apoptotic activity. In addition, the HA-GST-HBSP(L25A) detected in each set of the transfected HepG2 cells (panel b, Fig. 4B) further suggested that the observed decrease in caspase-3 activity was due to the mutant HBSP, but not the absence of the mutant protein. Consistent with the analysis of apoptosis induced by HBV replication, HepG2 cells transfected with the increasing amount of pXJ40-HA-GST-HBSP(L25A) (4, 6, and 8 μg) were subjected to FACS analysis. Results shown in Fig. 2G–I, indicated that no significant number of apoptotic cells was detected (below 0.4% for all three panels), and remained unchanged even with the increased amount of plasmid used.

Taken together, our results indicated that HBSP induced apoptosis when overexpressed in HepG2 cells and may have a direct involvement in apoptosis associated with HBV replication. Our findings may also point to a direct involvement of HBV viral proteins in the viral pathogenesis unrelated to the host immune response. Despite a compact genome with overlapping coding regions, evidence of alternative spliced variants has been documented in HBV carriers [10,20,21]. One of these, HBSP which has been shown to induce apoptosis [10] and to be associated with HBV pathogenesis [17], contained a BH3 domain identified in this study. Our results suggest that HBV may possess an alternative mechanism of modulating its interaction with the infected host cells.

Acknowledgments

This work was supported by Grant 03/1/22/18/229 (W.N. Chen) from the Biomedical Research Council, Agency for Science, Technology and Research, Singapore. Lu Y.W. is a recipient of a graduate research scholarship from Nanyang Technological University.

References

[1] J.Y. Lau, X. Xie, M.M. Lai, P.C. Wu, Apoptosis and viral hepatitis, Semin. Liver Dis. 18 (1998) 169–176.
[2] J.M. Adams, S. Cory, The Bcl-2 protein family: arbiters of cell survival, Science 281 (1998) 1322–1326.
[3] J.B. Baell, D.C. Huang, Prospects for targeting the Bcl-2 family of proteins to develop novel cytotoxic drugs, Biochem. Pharmacol. 64 (2002) 851–863.
[4] C. Brechot, Pathogenesis of hepatitis B virus-related hepatocellular carcinoma: old and new paradigms, Gastroenterology 127 (Suppl. 1) (2004) S56–S61.
[5] G.G. Chen, P.B. Lai, P.K. Chan, E.C. Chak, J.H. Yip, R.L. Ho, B.C. Leung, W.Y. Lau, Decreased expression of Bid in human heaptocellular carcinoma is related to hepatitis B virus X protein, Eur. J. Cancer 37 (2001) 1695–1702.
[6] J. Ehrmann, D. Galuszkova, J. Ehrmann, I. Krc, V. Jezdinska, B. Vojtesek, P.G. Murray, Z. Kolao, Apoptosis-related proteins, Bcl-2, Bax, Fas, Fas-L and PCNA in liver biopsies of patients with chronic hepatitis B virus infection, Pathol. Oncol. Res. 6 (2000) 130–135.
[7] J.G. Teodoro, P.E. Branton, Regulation of apoptosis by viral gene products, J. Virol. 71 (1997) 1739–1746.
[8] A. Kelekar, C.B. Thomson, Bcl-2-family proteins: the role of the BH3 domain in apoptosis, Trends Cell Biol. 8 (1998) 324–329.
[9] W.N. Chen, C.J. Oon, I. Toh, Altered antigenicities of hepatitis B virus surface antigen carrying mutations outside the common "a" determinant, Am. J. Gastroenterol. 95 (2000) 1098–1099.
[10] P. Soussan, F. Garreau, H. Zylberberg, C. Ferray, C. Brechot, D. Kremsdorf, In vivo expression of a new hepatitis B virus protein encoded by a spliced RNA, J. Clin. Invest. 105 (2000) 55–60.
[11] C.J. Oon, W.N. Chen, K.T. Goh, S. Mesenas, H.S. Ng, G. Chiang, C. Tan, S. Koh, S.W. Teng, I. Toh, M.C. Moh, K.S. Goo, K. Tan, A.L. Leong, G.S. Tan, Molecular characterization of hepatitis B virus surface antigen mutants in Singapore patients with hepatocellular carcinoma and hepatitis B virus carriers negative for HBsAg but positive for anti-HBs and anti-HBc, J. Gastroenterol. Hepatol. 17 (Suppl.) (2002) S491–S496.
[12] A.T. Lee, J. Ren, E.T. Wong, K.H. Ban, L.A. Lee, C.G. Lee, The hepatitis B virus X protein sensitizes HepG2 cells to UV light-induced DNA damage, J. Biol. Chem. 280 (2005) 33525–33535.
[13] Y.W. Lu, W.N. Chen, Human hepatitis B virus X protein induces apoptosis in HepG2 cells: role of BH3 domain, Biochem. Biophys. Res. Commun. 338 (2005) 1551–1556.
[14] H.L. Huang, K.S. Jeng, C.P. Hu, C.H. Tsai, S.J. Lo, C. Chang, Identification and characterization of a structural protein of hepatitis B virus: a polymerase and surface fusion protein encoded by a spliced RNA, Virology 275 (2000) 398–410.
[15] E.S. Razvi, R.M. Welsh, Apoptosis in viral infections, Adv. Virus. Res. 45 (1995) 1–60.
[16] A. Roulston, R.C. Marcellus, P.E. Branton, Viruses and apoptosis, Annu. Rev. Microbiol. 53 (1999) 577–628.
[17] P. Soussan, R. Tuveri, B. Nalpas, F. Garreau, F. Zavala, A. Masson, S. Pol, C. Brechot, D. Kremsdorf, The expression of hepatitis B

spliced protein (HBSP) encoded by a spliced hepatitis B virus RNA is associated with viral replication and liver fibrosis, J. Hepatol. 38 (2003) 343–348.

[18] K.M. Boatright, G.S. Salvesen, Mechanisms of caspase activation, Curr. Opin. Cell Biol. 15 (2003) 725–731.

[19] M. Sattler, H. Liang, D. Nettesheim, R.P. Meadows, J.E. Harlan, M. Eberstadt, H.S. Yoon, S.B. Shuker, B. Chang, A.J. Minn, C.B. Thompson, S.W. Fesik, Structure of Bcl-xL-Bak peptide complex: recognition between regulators of apoptosis, Science 275 (1997) 983–986.

[20] T.S. Su, C.J. Lai, J.L. Huang, L.H. Lin, Y.K. Yauk, C.M. Chang, S.J. Lo, S.H. Han, Hepatitis B virus transcript produced by RNA splicing, J. Virol. 63 (1989) 4011–4018.

[21] S. Gunther, G. Sommer, A. Iwanska, H. Will, A new class of defective hepatitis B virus genomes with an internal poly(dA) sequence, Virology 24 (1997) 363–371.

Available online at www.sciencedirect.com
ScienceDirect
Biochimica et Biophysica Acta 1762 (2006) 755 – 766
BIOCHIMICA ET BIOPHYSICA ACTA
BBA
www.elsevier.com/locate/bbadis

Adhesion contact kinetics of HepG2 cells during Hepatitis B virus replication: Involvement of SH3-binding motif in HBX

Tuan Lin Tan [b,1], Zhiqin Feng [a,c,1], Yi Wei Lu [b], Vincent Chan [a,*], Wei Ning Chen [a,*]

[a] Center of Biotechnology, School of Chemical and Biomedical Engineering, Nanyang Technological University, Singapore 639798
[b] School of Biological Sciences, Nanyang Technological University, Singapore 637551
[c] School of Mechanical and Aerospace Engineering, Nanyang Technological University, Singapore 639798

Received 17 March 2006; received in revised form 26 May 2006; accepted 12 June 2006
Available online 25 July 2006

Abstract

It has been shown that Hepatitis B virus (HBV) replication directly alters the expression of key cytoskeleton-associated proteins which play key roles in mechanochemical signal transduction. Nevertheless, little is known on the correlation between HBV replication and the subsequent adhesion mechanism of HBV-replicating cells. In this study, it is demonstrated that the lag time of adhesion contact evolution of HepG2 cells with HBV replication is significantly increased by two times compared to that of normal HepG2 cell on collagen coated substrate. During the initial 20 min of cell seeding, only diffuse forms of vinculin was detected in HBV replicating cells while vinculin-associated focal complexes were found in normal and control cells. Similar delay in cell adhesion in HBV-replicating cells was observed in cells transfected with HBX, the smallest HBV protein, suggesting its involvement in this cellular process. In addition, a proline rich region found in many SH3 binding proteins was identified in HBX. HBX was found to interact with the focal adhesion protein, vinexin-β, through the SH3 binding. Furthermore, HepG2 cells with HBV replication showed evidence of cell rounding up, possibly resulting from cytoskeletal reorganizations associated with interaction between HBX and vinexin-β. Taken together, our results suggest that HBX is involved in the cytoskeletal reorganization in response to HBV replication.

Keywords: Cell adhesion; Kinetics; Hepatitis B virus; Extracellular matrix; HBX; Vinexin β; SH3

1. Introduction

Hepatitis B virus (HBV) is a partially double-stranded circular DNA virus belonging to the hepadnaviridae family. HBV infection is associated with the development of major hepatic diseases such as acute liver diseases, chronic liver disease, liver cirrhosis, and hepatocellular carcinoma [1,2]. It is known that HBV attachment is mediated by the specific recognition between the viral surface proteins and membrane-bound receptors of hepatocyte [3,4]. Later on, the fusion of virus with cell membrane and subsequent intracellular release of viral genome lead to viral replication cycle [5]. Generally, The HBV genome contains four genes: *pol*, *env*, *pre-core* and X that encodes the viral DNA-polymerase, envelope protein (HBsAg), core protein (HBcAg) and protein X (HBX), respectively [6,7]. During its replication, HBV makes use of components of host cell to synthesize various viral proteins as mentioned above. For example, the phosphoprotein HBcAg binds to the C-terminal region of actin-binding protein, which may modulate the function of membrane-bound receptor and interfere with the mechanochemical signaling of adherent hepatocytes [8]. Moreover, HBX has been shown to enhance the transcription, translation and secretion of matrix metalloproteinase-9 and metalloproteinase-3 [9,10] which affects cell adhesion and migration of several types of cells [11]. Recent evidence also suggests the role of HBX in cellular apoptosis, a process involving major cytoskeletal disruption [12].

The communication between cell and extracellular matrix (ECM) is mainly mediated by integrin receptor which binds to ECM molecules with its extracellular domain and interacts with cytoskeletal proteins through its intracellular domain. HBV

* Corresponding authors.
E-mail addresses: MVChan@ntu.edu.sg (V. Chan), WNChen@ntu.edu.sg (W.N. Chen).
[1] These authors contributed equally to this work.

0925-4439/$ - see front matter © 2006 Elsevier B.V. All rights reserved.
doi:10.1016/j.bbadis.2006.06.016

infection is known to disrupt the integrin-mediated signaling cascades [13]. For instance, HBX blocks the molecular linkage between the actin filament and cadherin complex and weakens the intercellular adhesion in a Src-dependent manner [14]. Moreover, HBX reduces the expression of α_1 and α_5 subunits of integrin, impairs cell adhesion on fibronectin coated substrate and promotes cell migration [15]. Therefore it is generally expected that the interaction between HBX and actin binding protein contributes to the morphological changes of hepatocytes through the alteration of the cytoskeleton organization. On the other hand, little is known on the effect of HBV replication on the biophysical mechanisms of cell adhesion on ECM.

In this study, the intricate interplay between cell adhesion kinetics, HBV replication and cytoskeletal protein modulation is elucidated with real-time biophysical measurements. The temporal trends of degree of focal adhesion formation and adhesion energy of the cells are found to be perturbed by HBV replication during the initial stage of cell seeding on collagen coated substrates. Most importantly, the biological origin of our observed HBV induced responses is also suggested by the

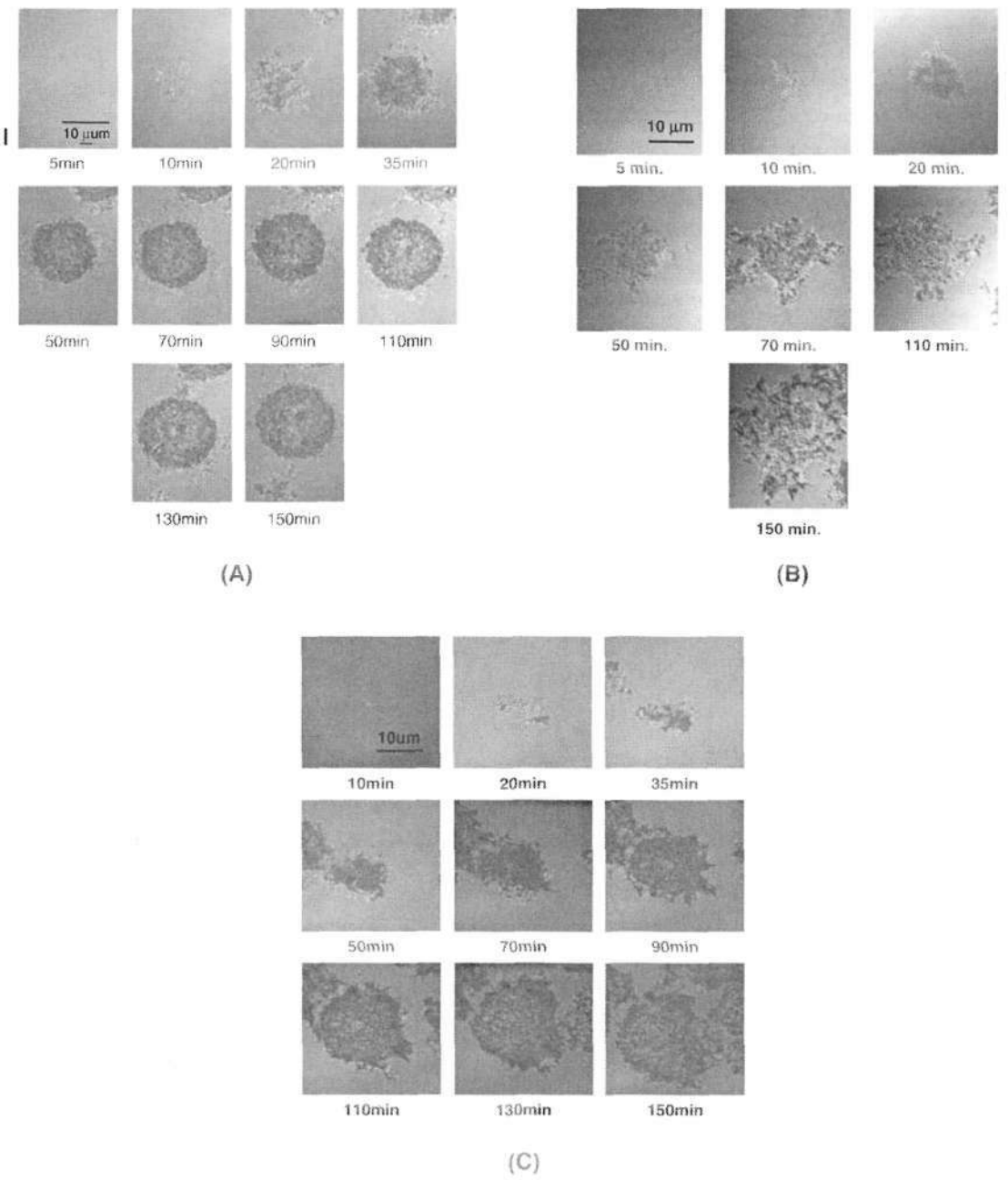

Fig. 1. A series of C-RICM images of normal HepG2 cells (A), HepG2 cells with transfected empty vector (B) and HepG2 cells infected with HBV (C) from 5 to 150 min after seeding on collagen coated glass coverslip at 37 °C. The contact area was determined with the drawing tool of the software which indicates the area of contact between the cell and the substrate.

characterization of interaction between vinexin-β and HBX, via a newly identified SH3-binding motif in the latter.

2. Materials and methods

2.1. Substrate preparations

In brief, 400 μl stock solution of collagen (BD Biosciences Inc., USA) at a concentration of 1 mg/ml in 0.012 N HCl was neutralized by adding 50 μl of 0.1 N NaOH and 50 μl of 10× PBS (final collagen concentration of 0.8 mg/ml). Glass coverslip (Fisher Inc., USA) was cleaned with a mixture of 30% 1 N NaOH and 70% methanol in an ultrasonic bath for 20 min then washed in pure methanol for 15 min, autoclaved and sterilized under UV light for 30 min. The neutralized collagen solution was spread out evenly on the surface of glass coverslip with the use of a cell scraper. After 24 h of collagen incubation at 4 °C, the coverslips were then washed with 1× PBS for three times and dried in air before use.

2.2. Cell culture and transfection

HepG2 cells (ATCC, USA) were maintained in Gibco Dulbecco's Minimal Essential Medium (Invitrogen Inc., USA), supplemented with 10% fetal bovine serum (Invitrogen Inc., USA), 1% anti-mycotic (Invitrogen Inc., USA) under 37 °C and 5% CO_2. They were passaged by trpsinization using 2× Trypsin-EDTA/ PBS pH7.2 (Invitrogen Inc., USA) every other day to maintain their integrity.

Three cell types have been employed for our investigation including: 1. HepG2 cells transfected with a replicative HBV genome cloned in pcDNA3.1 and co-tranfected with pEGFP vector (Invitrogen, USA); 2. HepG2 cells with empty vector (pcDNA3.1) and pEGFP vector; 3. normal HepG2 cells (control experiment). The replicative HBV genome was constructed by cloning a linear form of viral genome into mammalian expression vector pcDNA3.1. The linear genome contains the viral promoter at its 5′ end and the region for termination of transcription at its 3′ end as previously described [16].

Transfection was carried out using Effectene Transfection Reagent (Qiagen) as per manufacturer's instructions. Briefly, 6×10^5 HepG2 cells were seeded and cultured on a 60 mm dish (Nunc Inc., USA) under 37 °C and 5% CO_2 for 24 h before transfection. After adherent HepG2 cells reach 70% confluency, the cells were transfected with 2 μg of pcDNA3.1 plasmid with or without replicative HBV genome (rHBV;genotype A). In brief, the plasmid constructs are mixed with 16 μl of enhancer followed by 60 μl of Effectene transfection reagent. After 2 h of transfection, the medium was removed and rinsed twice with 1× PBS, before addition of fresh medium. Transfected cells were maintained at 37 °C and 5% CO_2 for 48 h to allow HBV replication. The ability of this genome in behaving as a replicative virus was assessed by the amount of HBsAg particles produced in the cell culture medium 2 days after its transfection into HepG2 cells, using ImX semi-quantitative measurement (Abbott Laboratories, USA). Transfected cells are detached by trypsinization as described above, pelleted and resuspended in fresh medium and immediately used for our biophysical studies. To determine the long-term effect of HBV replication, the morphology of HepG2 cells transfected by replicative HBV genome on polystyrene culture plate was determined. HepG2 cells transfected with empty pcDNA3.1 for 48 h was used as negative control to replicative HBV genome. For analysis on cells transfected with HBX, the full length HBX was cloned in pcDNA3.1. This construct was used as template to generate mutations in the proline rich domain (see below). They were then subject to further analysis in this study, including C-RICM and immunostaining for vinculin.

2.3. Vinexin-β and HBX Interaction on SH3 Array

The proline rich domain within HBX, ^{28}RPLPGPLGALP**P^{39}**AS**P^{42}P^{43}**IV**P^{46}**TDHGAHLSLRGL^{58}, identified in our earlier investigation [17] was cloned into pGEX-5X-1 (GE Healthcare) as a fusion protein of Glutathione-*S*-Transferase (GST) with the addition of 6xHis at the C-terminus. The construct pGEX–HBX–SH3 was then expressed in BL21 cells and purified by Glutathione Sepharose 4B (GE Healthcare). It was then used for interaction with SH3 domains spotted on the Panomics SH3 Array II as per manufacturer's instructions. The anti-His antibodies were used to detect interacting proteins with HBX–SH3 protein. Chemiluminescence was then performed using ECL (Amersham Biosciences). To assess the specificity of the binding, the four proline residues in the proline rich region (at position 39, 42 43 and 46 within HBX) were mutated to alanine by site-directed mutagenesis (Stratagene, USA) using the above GST–HBX–SH3 construct as template. The mutant protein HBX–SH3$^{P\text{-}A}$ was then expressed and purified as for the wild type HBX–SH3 protein, and used in the binding assay with the SH3 array for confirmation of the importance of prolines in this interaction.

2.4. In vitro interaction between Vinexin-β and HBX

Human vinexin-β was amplified by PCR using total RNA from HepG2 cells as template. The amplified PCR product 0f 1 kb was cloned into pGEX-5X-1 (GE Healthcare) with a 3′ HA-epitope tag, resulting in a fusion construct pGEX–Vβ–HA. On the other hand, the same PCR product (human vinexin-β) was cloned into a mammalian expression vector pXJ40HA with a HA-epitope tag [17], resulting in the fusion construct pXJ40HA-Vβ. Proper expression of the fusion proteins, either the bacterial GST–Vβ–HA (64 kDa) or the mammalian HA-Vβ (37kD), was assessed by Western blot analysis using anti-HA antibody.

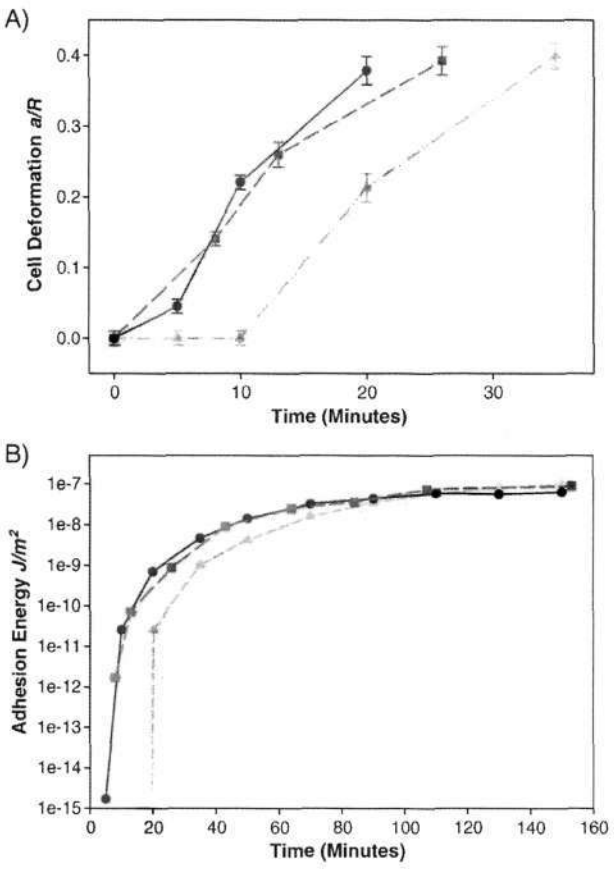

Fig. 2. Adhesion Kinetics of HepG2 Cells Transfected with replicative HBV genome. (A) The average degree of cell deformation *a/R* of HepG2 cells infected with HBV, HepG2 cells with transfected empty vector and normal HepG2 cells on collagen coated substrate against the time of cell seeding. Each error bar represented the standard deviation of the data from at least 60 cells on four identical samples. (B) The average adhesion energy of a population of HepG2 cells infected with HBV, HepG2 cells transfected with empty vector and normal HepG2 cell against time of cell seeding on collagen coated substrate. Data of at least 60 cells on four identical sample sets were used for the calculation of the average adhesion energy.

Due to the low transfection efficiency in HepG2 cells using Effectene transfection reagent (Qiagen), pXJ40HA-Vβ was transfected into 293T cells which showed much higher transfection efficiency using the same reagent (*data not shown*). Briefly, $5x10^6$ 293T (ATCC) cells were seeded overnight prior to transfection. Once the cells reached 50% confluency, 1 μg of pXJ40HA-Vβ plasmid DNA was transfected as per manufacturer's instructions. Two hours after transfection, the transfection media was replaced with fresh media and incubated for 48 h at 37 °C in 5% CO_2. Cells were then pelleted by trypsinization and proteins extracted by sonication. Proteins were then determined by Bradford Assay (Biorad) and 100 μg total protein was used per membrane overlay.

pGEX–Vβ–HA was expressed in *E. coli* strain BL21 in 1 mM IPTG at 37 °C for 4 h. The expressed protein GST–Vβ–HA fusion protein was then purified by microspin GST purification kit (GE Healthcare) using Glutathione Sepharose 4B beads and eluted in elution buffer provided (Supplemented with Complete Proteinase Inhibitor). The concentration of purified protein Vβ-HA was determined by Bradford Assay (Biorad, USA) and 100 μg of protein was used for each membrane overlay assay.

For the membrane overlay assay, the following proteins were expressed as described earlier: GST, pGEX–HBX–SH3, pGEX-HBX and pGEX–HBX–$SH3^{P-A}$. 20 μg of proteins were then separated on 12% SDS-PAGE gel, and transferred to nitrocellulose membrane. The membrane was blocked overnight at 4 °C with 5% milk in PBS, and incubated separately for 4 h with either 100 μg of total mammalian protein extract from pXJ40HA-Vβ transfected cells, or 100 μg of purified GST–Vβ–HA from *E.coli*. The membrane was then incubated with mouse monoclonal anti-HA (Santa Cruz, USA), and subsequently with the goat anti-mouse IgG antibodies (Pierce, USA).

2.5. Immunofluorescent staining of vinculin

Each of the three types of HepG2 cells (HBV-replicating, transfected with pcDNA3.1 or normal cells) was seeded separately on collagen-coated coverslip for 20 or 50 min and washed with pre-warmed PBS and fixed with 1 ml 3% Paraformaldehyde/PBS, followed by another wash with PBS. They were then permeabilized with 0.2% Triton-X100/ PBS, and blocked with 10% FBS/0.1% Triton-X100/ PBS followed by a wash with PBS. Cells were incubated with mouse anti-vinculin (Sigma, USA) at 37 °C for 2 h. After washing with 0.1% Triton-X100/PBS, cells were incubated with anti-mouse secondary antibody for 1 h at room temperature. The coverslip was then mounted with mounting solution and the fluorescence imaging of cell stained with vinculin was performed with a Pascal 5 confocal microscope

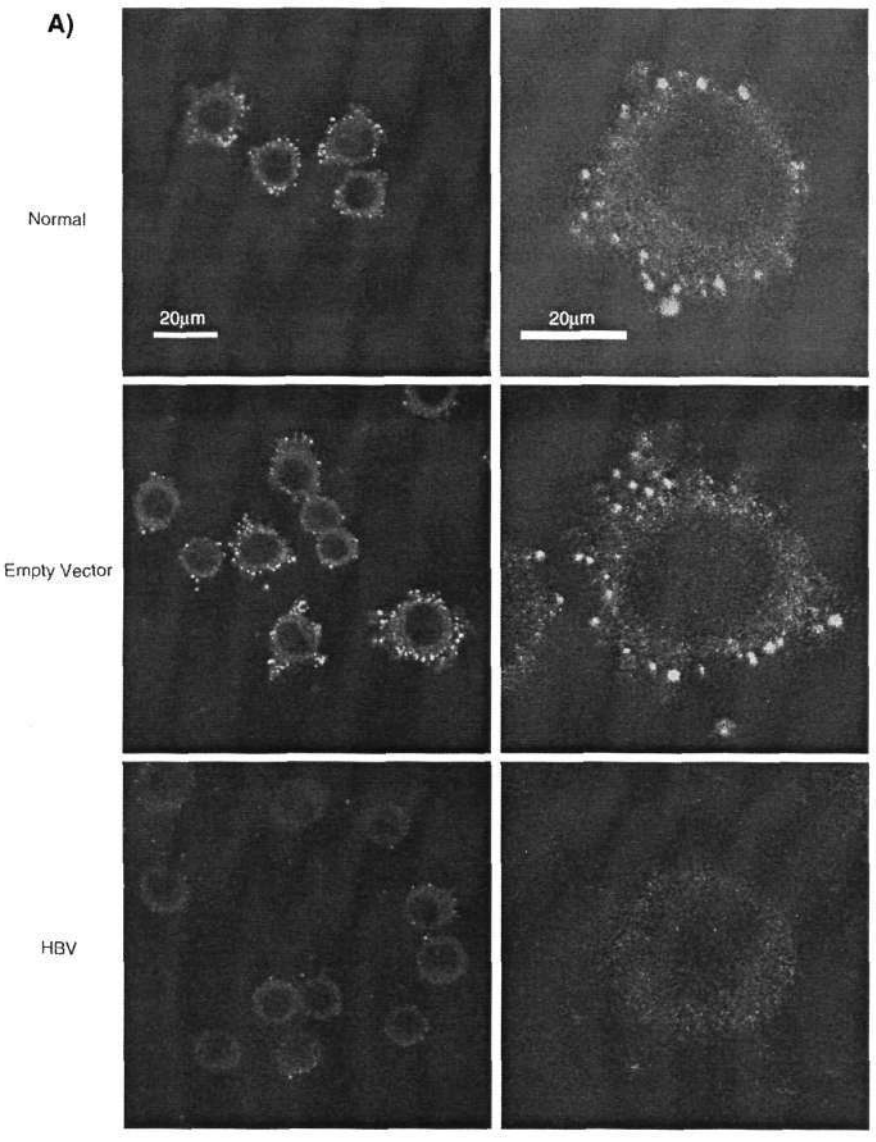

Fig. 3. Immunofluorescence image for vinculin of HepG2 cells infected with HBV, HepG2 cells with transfected empty vector and normal HepG2 cells at (A) 20 min and (B) 90 min post cell seeding (scale bar: 20 μm).

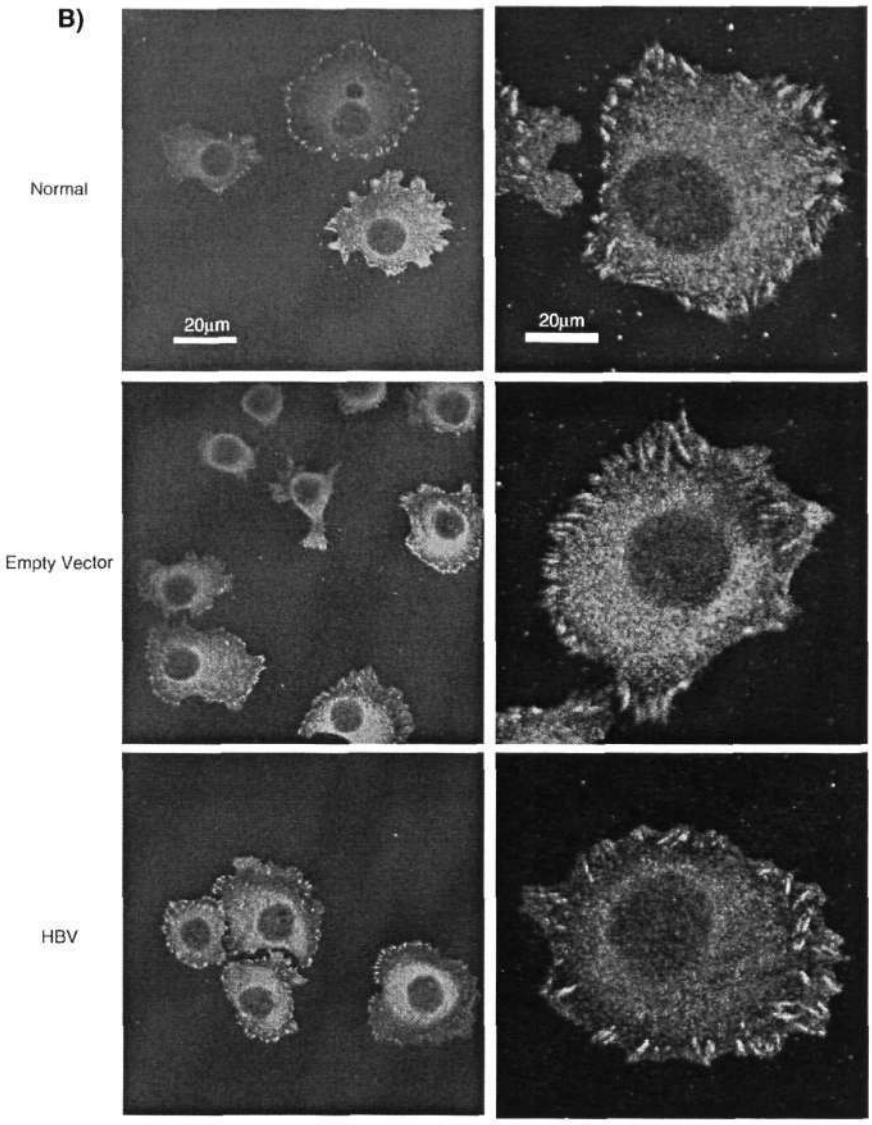

Fig. 3 (*continued*).

(Carl Zeiss, Germany). The sample was excited by an Argon-ion laser with a wavelength of 488 nm and the emitted light was detected with a band-passed filter of 520 nm.

2.6. Confocal Reflection Interference Contrast Microscopy (C-RICM)

The system is based on a laser scanning confocal microscope (Pascal 5, Carl Zeiss, Germany) and is integrated with a temperature/CO_2 control chamber (Carl Zeiss, Germany). The details of the instrument have been described [18]. The illumination source is an Argon-ion laser with a maximum power of 1mW and excitation wavelength of 488 nm. 63× oil immersion objective (Neofluar, NA: 1.25) was used in this study. Immediately following the seeding of HepG2 cells infected with HBV or HepG2 cells with empty vector or normal HepG2 cells on collagen coated coverslip, a series of C-RICM images was taken to investigate the kinetics of adhesion contact area for adherent cells from 0 to 2.5 h. Strong contact zone of the adherent cell appears as dark region on the image ZSM5 software (Carl Zeiss, Germany) and was used for image analysis. The contact area was determined with the drawing tool of the software which indicates the area of contact between the cell and the substrate. The error bar on cell deformation is originated from the standard derivation of at least three sets of experimental data (with at least 60 cells) under each condition.

2.7. Data analysis

Briefly, the equilibrium geometry of a water-filled cell adhering on rigid substrate is modeled as a truncated sphere with a mid-plane radius R [19]. Degree of deformation, $\sin\theta=(a/R)=\alpha$ is an experimentally measurable parameter of cell geometry where a is the contact zone radius and θ is the contact angle. R and a is measured by C-RICM and phase contrast microscopy, respectively. The cell wall is under a uniform equi-biaxial stress, $\sigma=T\varepsilon$. T is the stress equivalent and is equal to $Eh/(1\text{-}\nu)$ in a linear system under small strain where E, h and ν is the elastic modulus, membrane thickness and Poisson's ratio, respectively. We have validated our truncated sphere model [20]. The average biaxial strain, ε, is directly calculated from experimental data including R and α as follows:

$$\varepsilon=\frac{1}{2}\left[\frac{2+2(1-\alpha^2)^{1/2}}{4/R^2-\alpha^2}-1\right] \quad (1)$$

In the absence of external force, it was shown earlier that the adhesion energy, W, is

$$W = (1 - \cos\theta)C\varepsilon + C\varepsilon^2 \quad (2)$$

Based on the experimental measurements of the mid-plane diameter R (phase contrast microscope) and the radius of contact zone, a (C-RICM), W can be found by Eqs. (1) and (2). Elastic modulus E of HepG2 cell is taken as 2000 N/m^2 according to the experimental results obtained from AFM indentation [21].

3. Results and discussions

3.1. Cell adhesion is delayed in HBV replicating cells

It is noticed that hepatocyte cell lines including HepG2 and Huh-7 cells are able to support HBV replication [28] and hence provide a cell-base experimental model for HBV research. Our previous results suggest that the replicative genome delivered through transfection was able to produce significant amount of HBV particles [29]. In this study, the effect of HBV replication on cell adhesion has been explored with our recently developed cell-based HBV replication system in combination with real-time biophysical measurements [16].

Collagen is a common ECM protein which influences cell morphology, survival and proliferation [22]. Cell attachment and spreading are mediated by the interaction between the adhesion receptors on cell surface and biological ligands on ECM [23]. For instance, different variants of integrin mediate the spreading of most anchorage-dependent cells on ECM coated substrates [24,25].

Cell adhesion dynamics is correlated with receptor-mediated signal transduction cascades such as the receptor expressions, ligand affinity, focal adhesion formation and cytoskeleton remodeling, etc [26–28]. In this study, adhesion contact formation for HepG2 cells in response to HBV replication was measured. Fig. 1 showed a series of C-RICM images of a typical normal HepG2 cell (A), HepG2 cell transfected with the empty pcDNA3.1 vector (B) and HepG2 cell transfected with rHBV (C) against time of cell seeding on collagen coated substrate. For transfection with empty vector and rHBV, pGFP plasmid was co-transfected into the cells. The result showed that normal cells and empty vector (pcDNA3.1) transfected cells developed notable adhesion contact at 10 min of cell seeding (cluster-like structures on Fig. 2A and B) while similar adhesion contact formation was seen in cells transfected with rHBV 20 min after cell seeding (Fig. 2C). At 20 min after cell seeding, the adhesion contact area of normal cell and cell transfected by rHBV reached 173 μm^2 (50% of the steady-state value) and 48 μm^2 (9% of the steady-state value), respectively. The result supported that the extent of adhesion contact formation was significantly lower in HBV transfected cells during initial cell seeding. In addition, the adhesion contact area of the normal HepG2 cell reached steady-state level of around 271 μm^2 at around 70 min. In contrast, 46% longer time was needed for HBV-replicating cells to reach the same steady state. The fact that cell transfected with the empty vector developed significant adhesion contact with an areas of 175 μm^2 (43% of the steady-state value) at 20 min after cell seeding (Fig. 2C), supported that the observed adhesion contact evolution was not due to the transfection or the plasmid, but more likely related to the HBV replication.

The degree of cell deformation (a/R) is a key biophysical parameter which collectively reflects the simultaneous spreading and contact formation of adherent cells on a planar substrate. In this study, it may be used as a geometry index for elucidating the influence of HBV replication on the responses of adherent cells. Fig. 2 showed the a/R of normal HepG2 cells (●), HepG2 cells transfected with the empty vector (■) and HepG2 cells transfected with rHBV (▲) on collagen-coated substrate. Each error bar represented the standard deviation of the data from at least 60 cells on four sample sets. Generally, a/R of normal HepG2 cells rapidly increased against time during the initial 5 min of cell seeding (Fig. 2A). Similar trend was observed in cells transfected with the empty vector. In contrast, a/R of HepG2 cells transfected with rHBV showed detectable level 10 min after cell seeding. The initial cell deformation rate for normal HepG2 cell and cell transfected with empty vector is 0.019 and 0.018 min^{-1}, respectively. In contrast, the initial cell deformation rate of cells transfected with rHBV (calculated from 10 min onward) was at 0.013 min^{-1}. Our results supported that the kinetics of cell deformation is dependent on HBV replication.

Cell adhesion to ECM or biomaterials is a highly dynamic process [33]. The complex dynamical response of the adhesion energy between cell and ECM or biomaterial has been measured [25,34]. Contact mechanics model of adherent cell has been successfully used to determined adhesion energy of HepG2 cells [18,25]. Fig. 2B showed the averaged adhesion energy of a population for normal HepG2 cells (●), HepG2 cells transfected with the empty vector (■) and HepG2 cells transfected with rHBV (▲) against time of cell seeding on collagen coated substrate. The averaged adhesion energy of all types of cells spanned several orders of magnitude. The results indicated that normal HepG2 cells rapidly achieved a notable adhesion energy of 1.7×10^{-15} J/m^2 at 5 min after seeding on collagen coated substrate. In contrast, the averaged adhesion energy of HBV-replicating HepG2 cells was negligible during the initial period of 19 min and was two orders of magnitude lower than that of normal HepG2 cells and cells transfected with empty vector at 20 min after cell seeding. Significant reduction in adhesion energy induced by HBV replication as discussed above remained after 90 min post cell seeding. Moreover, normal HepG2 cells and cells transfected with empty vector required 70 min to reach steady state in adhesion energy. HBV-replicating HepG2 cells take longest time of about 130 min in reaching a steady state of adhesion energy compared with the other two cell types. At steady state, the adhesion energy of all three types of cells approached the same level of around 1.2×10^{-7} J/cm^2. It is possible that our observation was caused by the cytoskeleton alteration upon HBV replication which led to the change in the mechanochemical responses on ECM [15]. Our hypothesis was supported by the interaction between key cytoskeletal proteins and HBV associated proteins. Furthermore, our findings on the delayed cell adhesion in HBV-replicating HepG2 cells have provided new insights on the mechanism of development of hepatocellular carcinoma, consistent with the observation that inhibition of cell adhesion

is implicated in intrahepatic metastasis of human hepatocellular carcinoma [36].

3.2. Focal complex formation is delayed in HBV replicating cells

The link between cytoskeleton reorganization, the reduction of adhesion rate and HBV replication was not clearly understood. It is widely known that integrin-mediated cell adhesion triggers the formation of focal adhesion complex through the association with actin cytoskeleton and subsequent clustering. In detail, focal adhesion sites compose of cytoskeletal proteins such as vinculin, talin, and α-actinin, and signaling molecules, including FAK, Src, and paxillin. The focal adhesion formation plays a critical role in the cell adhesion by serving as structural links between the cytoskeleton and ECM. Fig. 3A showed the confocal fluorescence images of normal HepG2 cells, HepG2 cells transfected with rHBV and HepG2 cells transfected with the empty plasmid immuno-stained with anti-vinculin at 20 min after cell seeding. The result showed that significant expression of vinculin was detected in a typical group of normal HepG2 cells (top panel) while vinculin was barely detected in the group of HBV-replicating cells (bottom panel). Specifically, dot-like structures of vinculin which have a diameter ranging from 0.5 to 1.5 μm emerged at the lamellipodium of normal HepG2 cells (Fig. 3A: single-cell image in top panel). The dot-like structures composed of vinculin are known as focal complexes which served as precursor of focal adhesion [37]. In contrast, only diffused vinculin instead of clusters was detected in the cytoplasm of HepG2 cells transfected by HBV (single-cell image in bottom panel Fig. 3A). As a control, HepG2 cells transfected by empty vector also demonstrated the expression of similar focal complexes found in normal HepG2 cells (single-cell image in middle panel Fig. 3A). The result strongly supported that HBV replication delayed the formation of focal adhesion complexes during initial cell seeding. This delay of focal complex evolution coincides with the reduction of initial cell deformation rate and adhesion energy during the first 20 min of cell seeding. In particular, the formation of focal complexes serves as a traction base for cell movement, anchor point at the cell–cell connection, and as cement during morphogenesis [31].

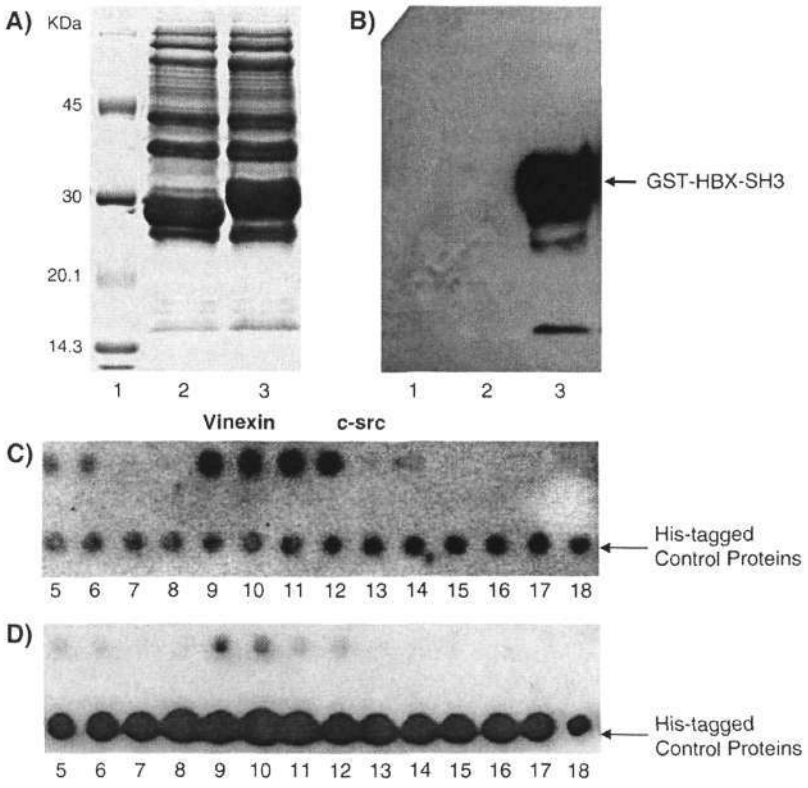

Fig. 4. Proline rich region of HBX interacts with SH3-containing cellular proteins.The proline rich region of HBX was cloned as a fusion protein with GST with an additional His tag. Panel A, a Coomassie blue stained SDS-PAGE gel showing expression of proteins. The 32 kDa fusion protein was expressed in *E. coli* (lane 3) while the 26 kDa GST protein was separately expressed (lane 2). Molecular weight markers were indicated in lane 1. Panel B, Western blot analysis using anti-His antibody. Identical samples in panel A were transferred to nitrocellulose membrane and subjected to Western blot analysis. Only GST-HBX fusion protein with a His-tag was recognized by the antibody. Sepharose 4B (Amersham Biosciences) were used for the purification of the fusion protein for use as protein probes on Panomics SH3 arrays. Panel C, interaction between purified wild type GST-HBX and SH3 array as detected by anti-His antibody. In the upper row, Spots 9 and 10 corresponds to vinexin SH3 domain while spots 11 and 12 contained c-Src. Negative controls provided by manufacturer were included in spots 13 to 18 in the upper row (spots 13 and 14 is empty GST while spots 15 to 18 are not spotted). Positive controls (proteins with His-tag) were included in the bottom row. Panel D, interaction between mutant HBX (proline to alanine) and SH3 array. Position and identity of spots were identical to panel C.

Towards 90 min of adhesion, the dot-like focal adhesion complexes in normal HepG2 cells and cells transfected by empty vector were transformed to dense patches at cell periphery (Fig. 3B). The elongated and oval vinculin containing structure had an averaged length of 4 μm, generally known as focal adhesion (zoom-in view on the right of all panels). Interestingly, vinculin patches also emerged at cell periphery of HBV-replicating HepG2 cells after 90 min of cell seeding. At the same time, all cell types demonstrated high level of diffuse vinculin in the cytosol. The formation of focal adhesion in HBV-replicating HepG2 cells may be caused by the integrin-collagen recognition and the subsequent cytoskeletal reorganization. The results further supported the transient effect of HBV replication on the adhesion energy and degree of deformation during the initial 20–30 min of cell seeding on ECM.

3.3. Cytoskeletal protein vinexin-β interacts with HBX through SH3 binding

One direct interaction between HBV viral proteins and cellular cytoskeleton may be through specific domain interaction. In our earlier investigation, a proline rich region (characteristic of SH3-binding motif) has been revealed at the N-terminal region of HBX, ^{28}RPLPGPLGALPP^{39}ASP^{42}P^{43}IVP^{46}TDHGAHLSLRGL^{58} [17]. Such proline rich domains are typically found in cellular proteins capable of binding to SH3 domain [32] To analyse its potential in interacting with SH3 containing proteins, the proline rich region of 30 amino acids was cloned in pGEX-5X-1 plasmid with a His tag, expressed and purified in *E. coli* as a GST fusion protein with an inclusion of His tag. Results shown in Fig. 4 indicate that the 32 kDa GST–HBX–SH3 fusion protein was successfully expressed (lane 3, panel A). The correct in-frame fusion with GST was further supported by the Western blot analysis using anti-His antibody (lane 3, panel B). As a control, the GST protein alone expressed in *E. coli* (lane 2, panel A) was not recognized by the anti-His antibody (lane 2, panel B). The purified GST–HBX–SH3 fusion protein was then used to incubate with SH3 array containing various SH3 domains of cellular proteins that contain such domains. Results shown in panel C indicated that both vinexin β and c-src interacted with GST–HBX–SH3 protein. While the interaction with c-src had been previously reported [33], our data revealed for the first time the interaction between vinexin β and HBX. Vinexin-β is an adaptor protein that is involved in the process of actin polymerization [34]. In a recent study, it had been shown that the SH3 domain of vinexin-β binds

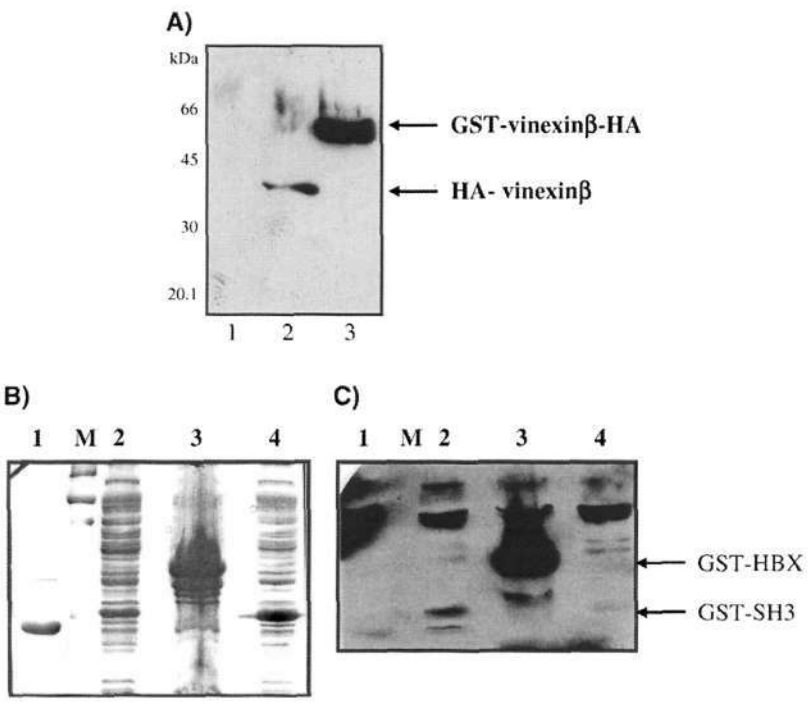

Fig. 5. In vitro interaction between vinexin-β and HBX. (A) Expression of bacterial GST–Vβ–HA (64 kDa) or mammalian HA-Vβ (37 kDa) by Western blot analysis using anti-HA antibody. Lane 1, protein lysates from 293T cells transfected with the empty pXJ40HA. No band was observed Lane 2, protein lysates from 293T cells transfected with pXJ40HA-vinexinβ construct. The expected 37 kDa HA-Vβ protein was seen. Lane 3, bacterial protein lysates from BL21 cells expressing pGEX-vinexinβ-HA protein. The expected 64 kDa fusion protein GST–Vβ–HA was detected. (B) In vitro interaction between vinexin-β and HBX (full length or SH3 binding domain). Total lysates (both soluble and insoluble) from bacterial cells containing four individual plasmids were separated on SDS-PAGE gel. Lane 1, purified GST protein coded by pGEX-5X-1 plasmid. Lane 2, lysates containing GST–HBX–SH3 protein coded by pGEX–HBX–SH3 plasmid. Lane 3, lysates containing the insoluble GST-HBX full length protein coded by pGEX-HBX plasmid. Lane 4, lysates containing GST–HBX–SH3$^{P\text{-}A}$ mutant protein coded by pGEX–HBX–SH3$^{P\text{-}A}$ plasmid. Lane M, protein molecular weight marker. The membrane containing these proteins was incubated with the mammalian protein extracts containing HA-vinexin-β (panel A) followed by Western blot using anti-HA antibody. Interaction was detected between HA-vinexin-β and wild type GST–HBX–SH3 (lane 1), and between HA-vinexin-β and full length HBX (lane 2).

to the hinge region of vinculin and vinexin localized with vinculin at the focal adhesion [39]. Moreover, the expression of vinexin-β was found to enhance the formation of focal adhesion and cell spreading in 3T3 fibroblasts [40]. Therefore the interaction of HBX with vinexin following HBV replication could significantly reduce vinculin self-assembly necessary for focal complex formation. To assess the specificity of the interaction between vinexin β and HBX, four proline residues in the proline rich region (P^{39},P^{42}, $P^{43}$and P^{46}) known to be involved in SH3 binding [32] were mutated to alanine residues and the mutant fusion protein GST–HBX–$SH3^{P\text{-}A}$ expressed and purified as described for the wild type protein. Binding assay with SH3 array indicated that interaction between mutated HBX and either c-src or vinexin β decreased significantly (panel D, Fig. 4). In the case of binding assay between mutant GST–HBX–$SH3^{P\text{-}A}$, the positive control proteins with His tag, serving as internal control for the anti-His antibody, showed significantly stronger intensity. This suggested that the signal intensity between mutant GST–HBX–$SH3^{P\text{-}A}$ and vinexin-β was much weaker than panel D, further supporting that this praline rich domain in HBX was likely to be involved in the interaction with vinexin-β via SH3 binding.

To further investigate the interaction between vinexin-β and HBX, *in vitro* analysis was carried out. Consistently with earlier investigation [17], our attempt in expressing either HBX or GST-HBX fusion protein was not successful as both were insoluble. This in turn made conventional *in vitro* analyses, such as immunoprecipitation or GST-pull down, not feasible. To overcome this limitation, a membrane overlay assay was developed in this study. First, vinexin-β was expressed as a HA fusion protein in 293T cells which had much higher transfection efficiency compared with HepG2 cells. The correct expression of the soluble HA-vinexinβ protein of 37 kDa was shown by Western blot analysis (lane 2, panel A, Fig. 5). Second, four different proteins were expressed (GST, GST–HBX–SH3, full length GST-HBX, and mutant GST–HBX–$SH3^{P\text{-}A}$). Among these four proteins, the full length GST-HBX protein was found only in the insoluble fraction. Total protein extracts containing these four proteins were separated on SDS-PAGE gel (panel B, Fig. 5), transferred to nitrocellulose membrane which was incubated with the mammalian protein extract containing HA-vinexinβ protein. Western blot using anti-HA antibody which recognized HA-vinexinβ protein indicated that vinexin-β interacted with the wild type SH3 binding domain of HBX (lane 2, panel C, Fig. 5). Similar interaction was also seen with the full length albeit insoluble HBX protein. Much weaker interaction was seen between vinexin-β and mutant $SH3^{P\text{-}A}$ protein (lane 4, panel C, Fig. 5), as well as with GST protein (lane 1, panel C, Fig. 5). Our membrane overlay assay therefore provided further support, using full length vinexin-β in addition to the panomic array containing only SH3 domains, on the interaction between vinexin-β and HBX.

3.4. Delay in cell adhesion is mediated by SH3-binding domain in HBX

To investigate the impact of interaction between vinexin-β and HBX on cell adhesion process, HepG2 cells were transfected with either the wild type HBX or mutant HBX. The mutant HBX contained four proline to alanine mutations (P^{39}, P^{42}, $P^{43}$and P^{46}) in the SH3-ding domain. Cell adhesion analysis, similar to that carried out in this study on HBV-replicating cells, was then carried out.

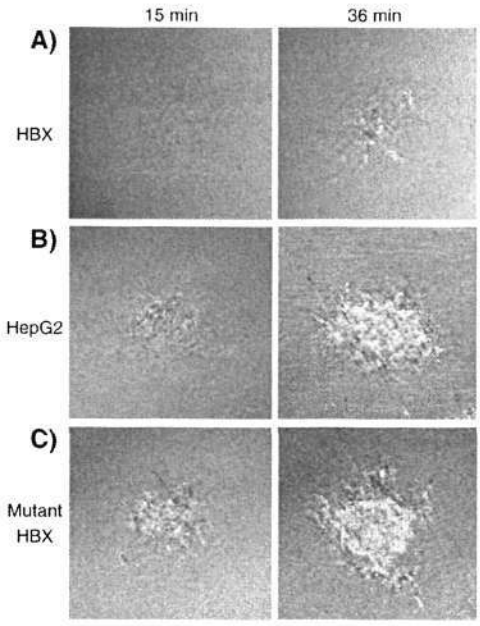

Fig. 6. C-RICM images of HepG2 cell transfected with wild type HBX (A), normal HepG2 cell (B) and HepG2 cell transfected by mutant HBX (C) during the initial stage of cell seeding on collagen coated coverglass.

Fig. 6 showed the C-RICM images of HepG2 cell transfected by HBX, normal HepG2 cell and HepG2 cell transfected by mutant HBX during the initial stage of cell seeding on collagen coated coverglass. The result indicated that the normal HepG2 cell and HepG2 cell transfected with mutant HBX develops an adhesion contact of 30.1 and 50.2 μm^2, respectively, after 15 min of seeding. Interestingly, HepG2 cell transfected by wild type HBX failed to develop any strong adhesion contact during the initial 30 min of cell adhesion. After 36 min of seeding, the adhesion contact area of normal HepG2 cell and HepG2 cell transfected with mutant HBX reaches 122.4 and 142.7 μm^2, respectively. In contrast, the adhesion contact area of the HepG2 transfected with wild type HBX at 36 min is approximately 80% smaller than (30 μm^2) that of normal HepG2 cell and HepG2 cell transfected with mutant HBX.

The observed delay in adhesion in cells transfected with the wild type HBX was similar to that observed in cells transfected with replicative genome. Significantly, the importance of HBX protein in this cellular process was further indicated by the fact that mutations in the proline rich domain of HBX, identified in this study, resulted in the restoration of normal cell adhesion. Perhaps more importantly, our results suggested a direct involvement of interaction between HBX and vinexin-β via SH3 binding, as mutations at proline residues which have been known to be involved in SH3 binding abolished the delay in cell adhesion.

Similarly to HepG2 cells transfected with rHBV, the average degree of deformation (a/R) for HepG2 cell transfected by HBX

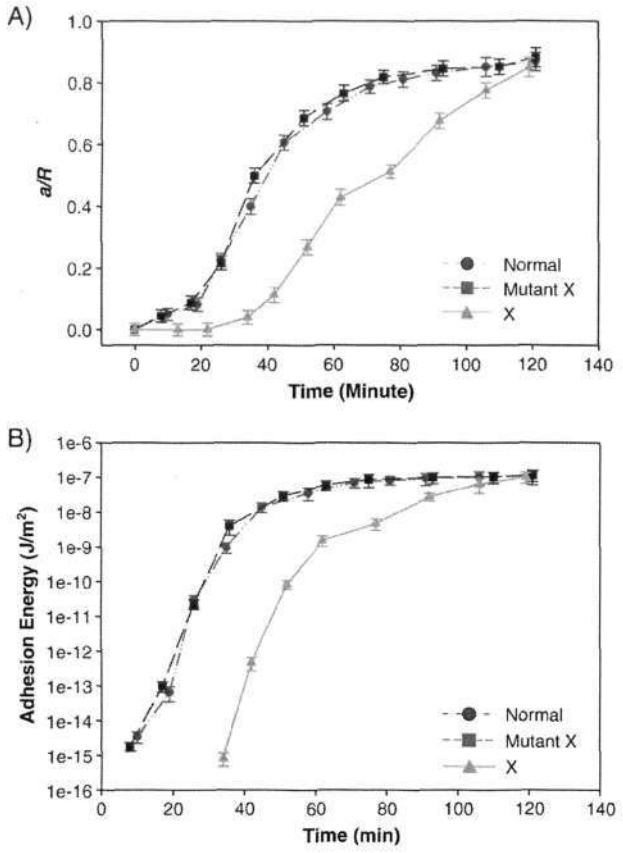

Fig. 7. Adhesion Kinetics of HepG2 Cells Transfected with HBX. (A) The average degree of deformation (*a/R*) for HepG2 cell transfected by HBX, normal HepG2 cell and HepG2 cell transfected by mutant HBX against the time of cell seeding on collagen coated coverglass. (B) The average adhesion energy for HepG2 cell transfected by HBX, normal HepG2 cell and HepG2 cell transfected by mutant HBX against the time of cell seeding on collagen coated coverglass.

was shown in Fig. 7A. The error bar of each data point represented the standard deviation of 60 cells on three samples. The result showed that *a/R* of both normal HepG2 cell and HepG2 cell transfected by HBX rapidly rose during the initial 30 min of seeding. On the other hand, *a/R* for HepG2 cell transfected with mutant HBX was undetectable until 36 min of seeding and remained lower than the value for both normal HepG2 cell and HepG2 cell transfected with HBX from 36 to 120 min of seeding. After 80 min of seeding, *a/R* of both normal HepG2 cell and HepG2 cell transfected by wild type HBX reached 0.83. Fig. 7B showed the average adhesion energy for HepG2 cell transfected by HBX, normal HepG2 cell and HepG2 cell transfected by mutant HBX against the time of cell seeding on collagen coated coverglass. The result showed that adhesion energy of both normal HepG2 cell and HepG2 cell transfected with wild type HBX spanned eight orders of magnitude between 8 min and 2 h of seeding. In contrast, the adhesion energy of HepG2 cell transfected by wild type HBX was not detectable until 36 min of seeding and was seven orders of magnitude lower than that of normal HepG2 cell and HepG2 cell transfect by mutant HBX.

Taken together, our results indicated that the expression of wild type HBX significantly dampened the kinetic of adhesion contact evolution. Such a delay in cell adhesion was reversed by specific mutations in the SH3 binding domain of HBX. It is likely that our identified interaction between vinexin-β and HBX played a direct role in the cell adhesion process in the context of HBV replication.

To investigate the impact of the observed changes in cell adhesion kinetics as a result of HBV replication, HepG2 cells transfected with replicative HBV genome or empty pcDNA3.1 vector were incubated for 48 h on polystyrene tissue culture plate and observed under phase contrast microscope. The use of polystyrene dish eliminated the complication brought by the collagen-integrin signaling in interpreting the main effect of HBV replication on the cell phenotypes. Moreover, these cells originally adhering on polystyrene dish were subsequently trypsinized for our biophysical measurements. Results shown in Fig. 8 indicated that HBV-replicating cells (panel B) were on the verge of detachment from the substrate and showed the round-up shape compared with cells transfected the empty pcDNA3.1 vector (panel A, Fig. 8). This result indicates that the phenotype induced by HBV replication immediately before our biophysical measurement has led to the changes of cell adhesion kinetics and the cytoskeletal protein organization during initial period of cell seeding. Consistently, it was also observed that HBX transfected cells detached approximately 2-fold faster compared to HBX mutant or empty vector pcDNA3.1 transfected cells (*data not shown*) via trypsinization. The significance of such cell

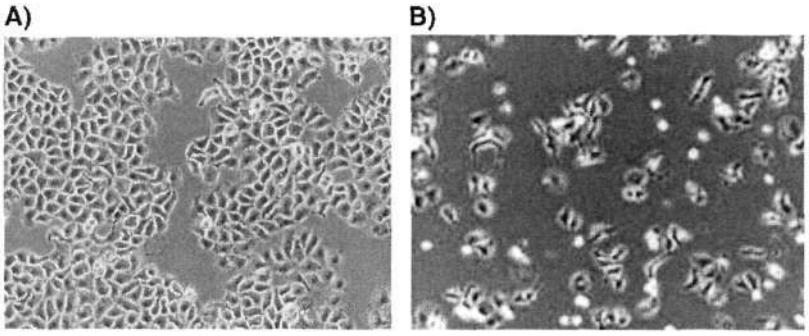

Fig. 8. HBV-replicating HepG2 cells undergo phenotypic changes observed under phase contrast microscope. Panel A, cells were transfected with empty pcDNA3.1 vector. Panel B, cells transfected with the replicative HBV genome cloned in pcDNA3.1 and observed after 48 h incubation.

detachment in relation to apoptosis [12] or adopting an invasive phenotype as reported for HBX [42] should warrant further investigations.

In conclusion, we have successfully combined biophysical techniques based on confocal microscopy with transfection technique to investigate the effect of HBV replication on the adhesion contact dynamics of HepG2 cell on model ECM. Overall, intricate interplay between HBV replication, adhesion contact kinetics, and adhesion energy dynamics has been revealed herein. Our results indicate that HBV replication directly tunes the adhesion contact kinetics of normal HepG2 cells on collagen coated substrates. The close interplay between HBV replication and cellular cytoskeleton was further supported by the interaction between vinexin-β and HBX through SH3 binding. The significance of our finding in the context of HBV replication has been supported by the onset of phenotypic changes in HBV-replicating cells before seeding on collagen.

Acknowledgements

This work was supported by grant 03/1/22/18/229 (WN Chen) from the Biomedical Research Council, Agency for Science, Technology and Research, Singapore. TL Tan and YW Lu are recipients of graduate research scholarship from Nanyang Technological University, Singapore.

References

[1] A. Castilla, J. Prieto, N. Fausto, Fibrogenesis in chronic viral hepatitis and cirrhosis: effects of lymphoblastoid α-interferon therapy, in: F.B. Hollinge, S.M. Lemon, H.S. Margolis (Eds.), Viral Hepatitis and Liver Disease, Williams Sunamb Williams, Philadelphia, 1991, pp. 690–694.
[2] N.C. Foo, B.Y. Ahn, X. Ma, W. Hyun, T.S. Yen, Cellular vacuolization and apoptosis induced by hepatitis B virus large surface protein, Hepatology 36 (2002) 1400–1407.
[3] K. Lonberg-Holm, L. Philipson, Virus receptor: part2-animal viruses, in: K. Lonberg-Holm, L. Philipson (Eds.), Receptors and Recognition Series B, vol. 8, Champamn and Hall, London, 1981, pp. 85–211.
[4] J. LeSeyec, P. Chouteau, I. Cannie, C. Guguen-Guillouzo, P. Gripon, Infection process of the hepatitis B virus depends on the presence of a defined sequence in the pre-S1 domain, J. Virol. 73 (1999) 2052–2057.
[5] M. Debra, A. Eckert, S. Peter, Mechanism of viral membrane fusion and its inhibition, Annu. Rev. Biochem. 70 (2001) 777–810.
[6] D. Ganem, Hepadnaviridae and their replication, in: B.N. Fields, D. M. Knipe (Eds.), Fields Virology, Raven Press, New York, NY, 1996, pp. 2703–2738.
[7] D. Ganem, H.E. Varmus, The molecular biology of the hepatitis B viruses, Annu. Rev. Biochem. 56 (1987) 651–693.
[8] C.J. Juang, Y.H. Chen, L.P. Ting, Heptitis B virus core protein interacts with the C-terminal region of actin binding protein, J. Biomed. Sci. 7 (2000) 160–168.
[9] T.W. Chung, S.K. Moon, Y.C. Lee, J.G. Kim, J.H. Ko, C.H. Kim, Enhanced expression of matrix metalloproteinase-9 by hepatits B virus infection in liver cells, Arch. Biochem. Biophys. 08 (2002) 147–154.
[10] F.L. Yu, H.J. Liu, J.W. Lee, M.H. Liao, W.L. Shih, Hepatitis B virus X protein promotes cell migration by inducing matrix metalloproteinase-3, J. Hepatol. 42 (2005) 520–527.
[11] E. Lara-Pezzi, M.V. Gómez-Gaviro, B.G. Gálvez, E. Mira, M.A. Iñiguez, M. Fresno, A.C. Martínez, A.G. Arroyo, M. López-Cabrera, The hepatitis B virus X protein promotes tumor cell invasion by inducing membrane-type matrix metalloproteinase-1 and cyclooxygenase-2 expression, J. Clin. Invest. 110 (2002) 1831–1838.
[12] Y.W. Lu, W.N. Chen, Molecular mechanism of pro-apoptotic activity by human hepatitis B virus X protein: the role of the BH3 domain, Biochem. Biophys. Res. Commun. 338 (2005) 1551–1556.
[13] C.T. Yeh, Hepatitis B virus X protein: serching for a role in hepatocarcinogensis, J. Gastroenterol. Hepatol. 15 (2000) 339–341.
[14] E. Laza-Pezzi, S. Roche, O.M. Andrisani, F. Sanchez-Madrid, M. Lopez-Cabrera, The hepatitis B virus HBx protein induces adherens junction disruption in a src-dependent manner, Oncogene 20 (2001) 3323–3331.
[15] E. Laza-Pezzi, P.L. Majano, M. Yanez-Mo, M. Gomez-Gonzalo, M. Carretero, R. Moreno-Otero, F. Sanchez-Madrid, M. Lopex-Cabrera, Effect of the hepatitis B virus HBx protein on integrin-mediated adhesion to migration on extracellular matrix, J. Hepatol. 34 (2001) 409–415.
[16] W.N. Chen, C.J. Oon, I. Toh, Altered antigenicities of hepatitis B virus surface antigen carrying mutations outside the common 'a' determinant, Am. J. Gastroenterol. 95 (2000) 1098–1099.
[17] T.L. Tan, W.N. Chen, A proteomics analysis of cellular proteins associated with HBV genotype specific HBX: potential in identification of early diagnostic markers for HCC, J. Clin. Virol. 33 (2005) 293–298.
[18] C. Yin, K. Liao, H.Q. Mao, K.W. Leong, R.X. Zhou, V. Chan, Adhesion contact dynamics of HepG2 cells on galactose-immobilized substrates, Biomaterials 4 (2003) 837–850.
[19] K.T. Wan, K.K. Lui, Contact mechenics of a thin-walled capsule adhered onto a rigid planar substrate, Med. Biol. Eng. Comput. 39 (2001) 605–608.
[20] N. Fang, V. Chan, K.T. Wan, H.Q. Mao, K.W. Leong, Colloidal adhesion of phospholipids vescles: high-resolution reflection interference contrast microscope and theory, Colloids Surf., B Biointerfaces 253 (2002) 347–362.
[21] A.B. Mathur, A.M. Collinsworth, W.M. Reichert, W.E. Kraus, G.A. Truskey, Endothelial, cardiac muscle and skeletal muscle exhibit different viscous and elastic properties as determined by atomic force microscopy, J. Biomech. 34 (2000) 1545–1553.
[22] C.D.W. Wilkinson, D.M. Riehle, M. Wood, J. Gallagher, A.S.G. Curtis, The use of materials patterned on a nano- and micro-metric scale in cellular engineering, Mat. Sci. Eng. C-Biol. 19 (2002) 263–269.
[23] T. Shibutani, H. Iwanaga, K. Imai, M. Kitago, Y. Doi, Y. Iwayama, Use of glass slides coated with apatite–collagen complexes for measurement of osteoclastic resporption activity, J. Biomed. Mater. Res. 50 (2000) 153–159.
[24] L. Koivisto, K. Larjava, L. Hakkinen, V.J. Uitto, J. Heino, H. Larjava, Different integrins mediate cell spreading, haptotaxis and lateral migration of HaCaT keratinocytes on fibronectin, Cell Adhes. Commun. 7 (3) (1997) 245–257.
[25] Z.Q. Feng, W.N. Chen, P.V.S. Lee, K. Liao, V. Chan, The influence of GFP-actin expression on the adhesion dynamics of HepG2 cells on a model extracellular matrix, Biomaterials 2626 (2005) 5348–5358.
[26] C. Gauet, W.A. Marganski, S. Kim, C.T. Brown, V. Gunderia, M.J. Dembo, J.Y. Wong, Influence of type I collegan surface density on fibroblast spreading, motibility, and contractility, Biophys. J. 85 (2003) 3329–3335.
[27] S.P. Palecek, J.C. Loftus, M.H. Ginsberg, D.A. Lauffenburger, A.F. Horwitz, Integrin-ligand binding properties govern cell migration speed through cell-substratum adhesiveness, Nature 385 (1997) 537–540.
[28] N. Paran, B. Geiger, Y. Shaul, HBV infection of cell culture: evidence for multivalent and cooperative attachment, EMBO J. 20 (2001) 4443–4453.
[29] Q.C. Toh, T.L. Tan, W.Q. Teo, C.Y. Ho, S. Parida, W.N. Chen, Identification of cellular membrane proteins interacting with Hepatitis B surface antigen using yeast split-ubiquitin system, Int. J. Med. Sci. 2 (2005) 114–117.
[31] M. Cohen, D. Joester, B. Geiger, A. Lia, Spatial and temporal squence of events in cell adhesion: from molecular recognition to focal adhesion assembly, ChemBioChem 5 (2004) 1393–1399.
[32] S.S. Li, Specificity and versatility of SH3 and other proline-recognition domains: structural basis and implications for cellular signal transduction, Biochem. J. 390 (2005) 641–653.
[33] N.P. Klein, R.J. Schneider, Activation of Src family kinases by hepatitis B

virus HBx protein and coupled signaling to Ras. Mol. Cell. Biol. 17 (1997) 6427–6436.

[34] N. Kioka, K. Ueda, T. Amachi, Vinexin, CAP/ponsin, ArgBP2: a novel adaptor protein family regulating cytoskeletal organization and signal transduction, Cell. Struct. Funct. 27 (2002) 1–7.

[36] W.J. Tan, G.P. Teo, K. Liao, K.W. Leong, H.Q. Mao, V. Chan, Adhesion contact dynamics of primary heptocytes on poly(ethylene terephthalate) surface, Biomaterials 26 (2005) 891–898.

[37] T. Genda, M. Sakamoto, T. Ichida, H. Asakura, S. Hirohashi, Loss of cell–cell contact is induced by integrin-mediated cell-substratum adhesion in highly-motile and highly-metastatic hepatocellular carcinoma cells, Lab. Invest. 80 (2000) 387–394.

[39] H. Chen, D.M. Cohen, D.M. Choudhury, N. Kioka, S.W. Craig, Spatial distribution and functional significance of activated vinculin in living cells, J. Cell Biol. 169 (2005) 459–470.

[40] N. Kioka, S. Sakata, T. Kawauchi, T. Amachi, S.K. Akiyama, K. Okazaki, C. Yaen, K.M. Yamada, S. Aota, Vinexin: a novel vinculin-binding protein with multiple SH3 domains enhances actin cytoskeletal organization, J. Cell Biol. 144 (1999) 59–69.

[42] E. Lara-Pezzi, J.M. Serrador, M.C. Montoya, D. Zamora, M. Yanez-Mo, M. Carretero, H. Furthmayr, F. Sanchez-Madrid, M. Lopez-Cabrera, The hepatitis B virus X protein (HBx) induces a migratory phenotype in a CD44-dependent manner: possible role of HBx in invasion and metastasis, Hepatology 33 (2001) 1270–1281.

J_ID: Z8H Customer A_ID: 30864 Cadmus Art: JBMB30864 Date: 19-APRIL-07 Stage: I Page: 1

Osteoblast Interactions With Various Hydroxyapatite Based Biomaterials Consolidated Using a Spark Plasma Sintering Technique

J. L. Xu,[1] K. A. Khor,[1] Y. W. Lu,[2] W. N. Chen,[2] R. Kumar[3]

[1] School of Mechanical and Aerospace Engineering, Nanyang Technological University, 50 Nanyang Avenue, Singapore 639798

[2] School of Chemical and Biomedical Engineering, Nanyang Technological University, 50 Nanyang Avenue, Singapore 639798

[3] Department of Environmental Engineering, Montana Tech of the University of Montana, 1300 West Park Street Butte, Montana 59701

Received 18 July 2006; revised 13 February 2007; accepted 23 March 2007
Published online 00 Month 2007 in Wiley InterScience (www.interscience.wiley.com). DOI: 10.1002/jbm.b.30864

Abstract: This study investigated the osteoblast behaviors on various hydroxyapatite based biomaterials that were consolidated at 1100°C for 3 min by a spark plasma sintering technique. The osteoblasts from human fetal osteoblast cell line were cultured in the medium on the various biomaterials surfaces (HA, RF21, 1SiHA, and 5SiHA) to assess the cell morphology and proliferation as well as cell differentiation (alkaline phosphatase activity). Moreover, the bone γ-carboxyglutamic protein or osteocalcin in the medium were determined at different periods of culture. The present results indicated that the amount of osteocalcin in the medium decreased during the periods of culture. The highest osteocalcin production obtained from the biomaterial 5SiHA after cell culture for 2 days demonstrated that the presence of silica in the biomaterials enhanced the cell differentiation by the rapid release of silicate and calcium ions. © 2007 Wiley Periodicals, Inc. J Biomed Mater Res Part B: Appl Biomater 00B: 000–000, 2007

Keywords: biomaterial; osteoblast; proliferation; differentiation; osteocalcin

INTRODUCTION

In vitro and *in vivo* studies indicate that a biological apatite might deposit on the surface of Ca-containing implants.[1,2] This apatite layer will serve as a substrate for subsequent protein adsorption and bone cell attachment. The formation of apatite layers depends on direct interactions of bone matrix and osteoblasts (bone matrix forming cells) with biomaterials. The proteins (cell receptors) adsorb to the material surface (cell ligands), resulting in cell attachment on the material surface. Once attached to the surface, osteoblasts will proliferate and subsequently differentiate. Bone osteocalcin constitutes about 15 wt % of the noncollagenous bone matrix proteins, and it is produced exclusively in osteoblasts and its dental counterpart. Because of this tissue-specific expression, the level of osteocalcin could be considered as an indicator of the overall activity of cells operating in bone formation. Thus it could be suggested that when there is increased bone formation, the serum osteocalcin concentration will also be increased. Alkaline phosphatase (AKP) activity is another widely recognized biochemical marker for osteoblast activity. It is commonly studied to assess osteoblast differentiation. AKP catalyses the hydrolysis of phosphate esters at an alkaline pH and is believed to play a role in skeletal mineralization.[3] The *in vitro* biocompatibility of the material component has already been assessed by a cell line to test cytotoxicity of the materials.[4] The surface chemistry and physical factors, such as crystallinity, particle size, porosity, topography, and surface energy, would directly influence cell attachment, proliferation, and differentiation of the cells.[5] It is reported that osteoblasts appear to be very sensitive to minor variations in surface composition and topography.[1] The evaluation of cell-material interactions is of main importance when developing new materials for biomedical application.

Bioceramic structures made of hydroxyapatite (HA) are capable of inducing bone growth. The main limitation of HA is however its poor mechanical properties, which

Correspondence to: J. L. Xu (e-mail: jlxu@ntu.edu.sg)
Contract grant sponsors: Nanoscience Innovation and Nanyang Technological University (NSI–NTU joint project)

ID: srinivasanv Date: 19/4/07 Time: 18:38 Path: J:/Production/JBMB/Vol00000/070086/3B2/C2JBMB070086

J_ID: Z8H Customer A_ID: 30864 Cadmus Art: JBMB30864 Date: 19-APRIL-07 Stage: I Page: 2

include low fracture toughness and poor strength. Spheroidized HA powder obtained through RF plasma spraying has been densified using a spark plasma sintering (SPS) technique with the aim of enhancing its mechanical properties.[6] Previous study[6] showed that a biological apatite layer was formed when SPS sample was soaked in the simulated body fluid for some period.

However, despite its importance in the bioceramic field, there remained a need to correlate the chemical and physical composition of HA with cellular interaction. In addition, there is evidence that natural bone contained other calcium phosphate species and subtle, but significant, chemical elements such as magnesium, carbonate, and silicate. These elements help natural bone exhibit a higher bioactivity and mechanical properties compared with the synthetic HA. Silicon deficiency may result in abnormal bone formation. Evidence of silicon's influence on bone mineralization, metabolism, collagen synthesis, and cross-linking is compelling. In this study, we studied the cellular activities of bone cells on various HA based ceramic samples consolidated through SPS, including HA doped with amorphous silica precipitation. The SPS ceramic were seeded with human fetal osteoblast cell line to investigate the responses of bone-forming cells on the surfaces of these various HA-based materials. The cell morphology was assessed using a scanning electron microscope (SEM). The cell proliferation and differentiation was assessed using biochemical techniques.

EXPERIMENTAL AND CHARACTERIZATION

A starting HA slurry was prepared for synthesis of powder according to previous study.[6] Amorphous precipitated silica as preset weight (0, 1, and 5 wt %) was added into the HA slurry and the slurry was stirred for 4 h before transportation into a spray dryer (Ohkawara LT-8, Japan) to get spray dried HA doped with various amount of silica. The powder feedstock used for SPS were spray dried HA (ceramic: HA), RF plasma sprayed calcium phosphate prepared at a power level of 21 kW (ceramic: RF21),[6] and spray dried HA doped with 1 wt % (ceramic: 1SiHA) and 5 wt % of silica (ceramic: 5SiHA).

A SPS system (Sumitomo Coal Mining SPS system, Dr. Sinter Modal 1050, Japan) was used to prepare the consolidated compacts. The sintering temperature was 1100°C with a heating rate of 100°C/min and a cooling rate of 100°C/min. The sintering duration was 3 min. Three samples were prepared from each kind of powder feedstock. The obtained ceramic samples were ground till Grit P 2400 for the following characterization. The phases present were analyzed by X-ray diffraction (XRD) that was carried out utilizing CuK_α Ni filtered radiation at 30 kV and 20 mA on a Philips MPD 1880 diffractometer (The Netherlands). The chemical state of silicon in the SPS consolidated HA doped with silica was determined by X-ray photoelectron spectroscopy, (XPS, Kratos spectrometer, Japan) which was operated using Al Kα (1486.6 eV) monochromatic X-ray source. The XPS pressure was about 10^{-9} Pa. The binding energy of Si 2p was charge referenced to the P 2p line of apatite at a binding energy of 133.6 eV.

After the samples were sterilized via autoclaving, hFOB 1.19 (ATCC, CRL-11372) osteoblast cells were cultured in a 1:1 mixture of Ham's F12 medium and Dulbecco's Modified Eagle Medium containing 2.5 m*M* L-glutamine and 0.3 mg/mL G418 and supplemented with 10% of fetal bovine serum and 5 vol % of antibiotics. The osteoblast were seeded with an initial cell density of $2 \times 10^4/cm^2$ onto the samples and polystyrene as controls in a 24-well culture tray and incubated at 37°C in a 5% CO_2 atmosphere for up to 2 weeks. The culture medium was replaced with an equal volume of fresh one every third day.

The cell attachment was observed under SEM (JEOL JSM-5600 LV, Japan) after cell culture for 24 h. The cells on the bioceramic surfaces were fixed in 2.5% glutaraldehyde buffered in 0.1*M* sodium cacodylate (pH 7.3–7.4) for 1 h at 4°C followed by 30 min treatment in 1% tannic acid in 0.1*M* sodium cacodylate at 4°C. The post fixation was processed with 1% OsO_4 buffered in 0.1*M* sodium cacodylate for 30 min at 4°C. Following post fixation, the samples were rinsed with distilled water for 10 min and dehydrated in a graded series of ethanol for 5–10 min at room temperature. Finally the samples were immersed in increasing concentrations of hexamethyldisilazane (HMDS), which was a mixture of HMDS and ethanol, for critical point drying. After removing the HMDS solution and drying the sample in the dryer, they were gold sputtered for 120 s at 10 mA to allow observation under the SEM.

A methyl thiazole tetrazodium (MTT) test was employed to determine the proliferation of the cells. The cells cultured on the sterile plastic Petri dish were used as a control group. Two hundred microliters of MTT solution (5 mg/mL in phosphate buffer) and 800 μL of medium were added to each sample and incubated at 37°C for 2 h. After the supernatant had been discarded, the dark blue crystal of formazan was dissolved by adding 200 μL of DMSO and quantified spectrophotometrically at 490 nm on a microplate reader machine (Benchmark Plus, Bio-Rad Laboratories Inc.). The number of the cells was determined according to a plot of absorbance against the standard numbers of cells. For the MTT tests, three of each kind of the sample were employed and three separate experiments have been carried.

The amount of osteocalcin production in the conditioned medium was determined by a Gla-OC ELSIA Kit, which utilized a novel set of monoclonal antibodies highly reactive to the osteocalcin. The microplate reader was used for the measurement of absorbance at 450 nm wavelength. The osteocalcin expression level by the cells was determined based on an osteocalcin standard curve prepared according to the kit protocol. Three replicates of each analysis were measured. The data represent the mean value of three independent experiments.

ID: srinivasanv Date: 19/4/07 Time: 18:38 Path: J:/Production/JBMB/Vol00000/070086/3B2/C2JBMB070086

J_ID: Z8H Customer A_ID: 30864 Cadmus Art: JBMB30864 Date: 19-APRIL-07 Stage: I Page: 3

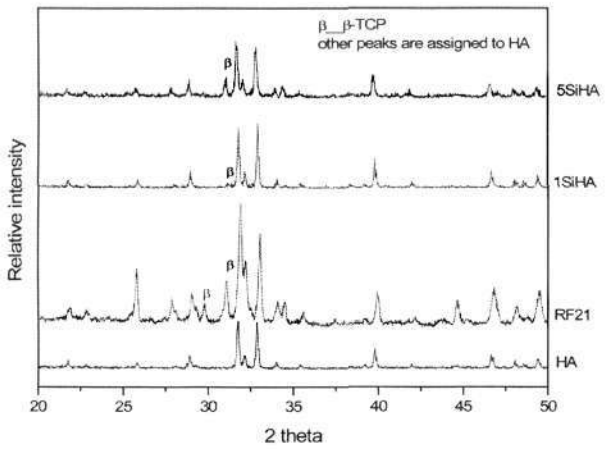

Figure 1. XRD patterns of various SPS HA based ceramics. [Color figure can be viewed in the online issue, which is available at www.interscience.wiley.com.]

An AKP reporter gene assay kit was employed to determine the secretion of AKP of osteoblast into the culture medium after 2 days and 4 days of cell culture, respectively. At harvest, the cell layer lysates on the various ceramic samples were also collected to determine AKP activity. Fifty microliters of cell lysis buffer (BD Bioscience) was added to lyse each cell layer. Twenty microliters aliquots were used to estimate the AKP activity. A cell layer lysate from the polystyrene substrate was prepared as positive control group. A microplate fluorescence reader (FL600, Bio-TEK) with an excitation of 360 nm wavelength and an emission of 440 nm wavelength was used to measure the absorbance intensities. The absorbance was directly converted to AKP activity level based on a protein standard curve. Three replicates of each analysis were measured. The data represent the mean value of five independent experiments.

RESULTS

Surface Analysis

F1 The XRD results presented in Figure 1 show that HA was the main phase in all of the consolidated ceramic samples. Beta tricaclium phosphate (β-TCP) was also observed in the samples RF21, 1SiHA, and 5SiHA. Referring to the relative peak intensities compared with the peak intensities of HA, there were higher amount of β-TCP in the RF21 samples. The presence of β-TCP in the sample RF 21 has been discussed in Ref. 6. The presence of β-TCP in the consolidated pellets doped with silica might attribute to the amorphous silica precipitation that resulted in the HA becoming AQ2 less stable at the sintering temperature of 1100°C. In addition, the impact of spark plasma caused a localized increase in temperature and introduced some liquid phase of silica, which did not form a strong chemical bond with apatite, and therefore the presence of liquid phase reduced interfacial energy and promoted the transformation of apatite phase to β-TCP phase during sintering. Similar detection was reported by Ruys[7] that the introduction of silica would lead to the decomposition of HA into secondary calcium phosphate phases such as TCP.

Figure 2 showed Si 2p binding energies in the ceramic F2 5SiHA after etching for various seconds in the XPS. The binding energies lay between 99.6 and 102.4 eV. There was a slight decrease in Si 2p binding energies with increasing etching time, indicating silicate depolymerization, as observed for crystalline silicates.[8] The variations in binding energies reflected the differences in the electronic environment of the Si element, and the sharper peaks might indicate the more ordered structure. Some broadening of the Si 2p peaks may be because of the presence of amorphous silica. Therefore, we assumed that the polymerization of Si in the SPS consolidated 5SiHA pellets was not uniform, rather that there was a mixture of different silicate arrangements, namely containing both crystalline silicate and amorphous silica. Based on the minor increase in peak width (full width at half maximum) of Si 2p with an increasing etching time, we inferred that there was more amorphous silica in the inner part when compared with the surface part of the 5SiHA pellets. This might attribute to that effect of skin current on the consolidated pellets at the initial stage of SPS.

The silicate depolymerization might lead to increased numbers of Ca—O—Si units and fewer Si—O—Si units, which might result in the formation of calcium silicate. Thus it was assumed that HA decomposed into TCP and calcium oxide (CaO) that could react with silica to form calcium silicate. However, no calcium silicate could be observed from the XRD patterns, which was because of either too small amount or silicate substituted into apatite structure. Both possibilities would cause the decomposition of HA into TCP. Detailed study of the chemical state

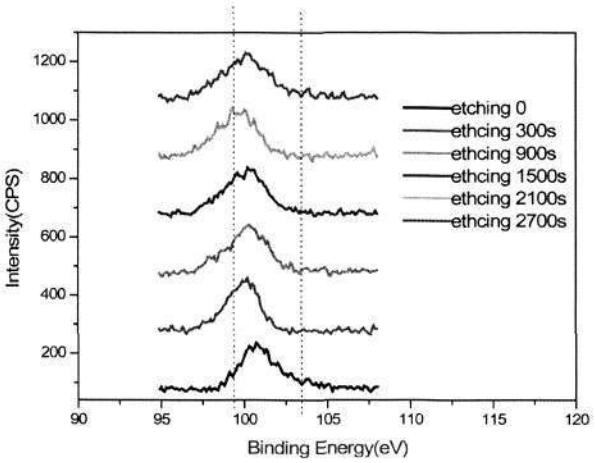

Figure 2. Si 2p spectra of the SPS consolidated HA doped with 5 wt % of silica after etching for various seconds from the surface. [Color figure can be viewed in the online issue, which is available at www.interscience.wiley.com.]

ID: srinivasanv Date: 19/4/07 Time: 18:38 Path: J:/Production/JBMB/Vol00000/070086/3B2/C2JBMB070086

J_ID: Z8H Customer A_ID: 30864 Cadmus Art: JBMB30864 Date: 19-APRIL-07 Stage: I Page: 4

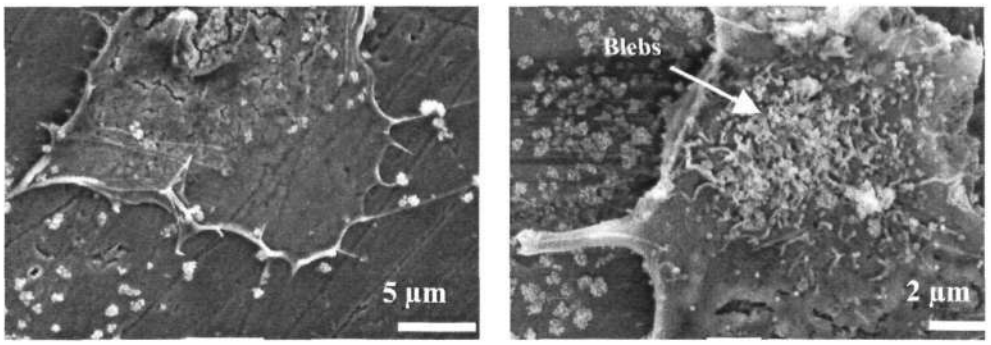

Figure 3. SEM images of human osteoblast-like cells on the SPS ceramic 5SiHA.

silicon in the SPS consolidated HA pellets are under proceeding using XPS and Raman spectrometer.

Morphology of Osteoblasts

The typical osteoblast morphologies under SEM were exhibited in Figure 3 after fixation. It was found that the cells had attached on the sample surface after 2 days of cell culture. No apparent differences in the cell morphology on any of the ceramic surfaces were found. The majority of the cells had a flattened appearance with a predominantly polygonal morphology. A rough texture was observed because of the presence of numerous blebs on the surface of the cells. The cells were attached to the biomaterials exhibiting filopodia-like, with various lengths, and lamelliapodia-like extensions. Close contact between the cells and the substrate was established through extending filopodia, which initiated the cellular anchorage on the substrate. This result indicated that the SPS sample surfaces provided preferential sites for cell attachment and in return, would recruit proteins and other growth factors to enhance the cellular activity.

Cell Proliferation and Differentiation

The data from MTT assay reflected the ability of cell proliferation and cytotoxicity on the ceramic surfaces. The higher the MTT results, the more the viable cells. Therefore, as presented in Figure 4, the RF plasma processing samples indicated the highest cell viabilities when compared with the other samples after 2 days and 4 days of cell culture.

In addition, the MTT results provided the evidence of increased osteoblast viability on the silica doped ceramic. It was found that the osteoblast viability values on these ceramic surfaces were slightly higher than the control group cultured in the polystyrene Petri dish whose density was $8.3 \times 10^3/cm^2$ after cell culturing for 2 days, while after 4 days of culture, the value of $2.6 \times 10^4/cm^2$ obtained from the sample 1SiHA was lower than the result of $3 \times 10^4/cm^2$ obtained from the control group.

As shown in Figure 5, it was found that the amount of osteocalcin in the conditioned medium was time and surface composition dependent, though it was comparable among the various samples. The level of osteocalcin production in the medium decreased during the periods of culture. The highest concentration of osteocalcin detected in conditioned medium after culturing for 2 days was obtained

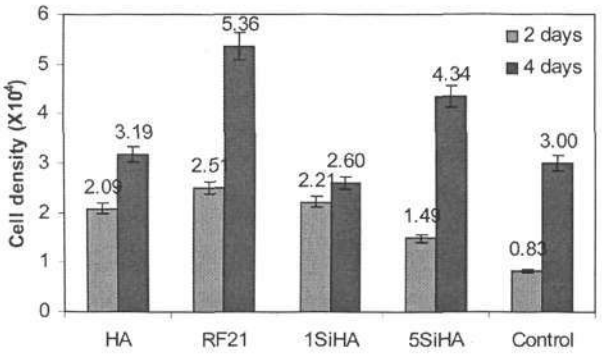

Figure 4. Cell densities (number/cm^2) on the various SPS ceramic samples obtained after culture for 2 and 4 days.

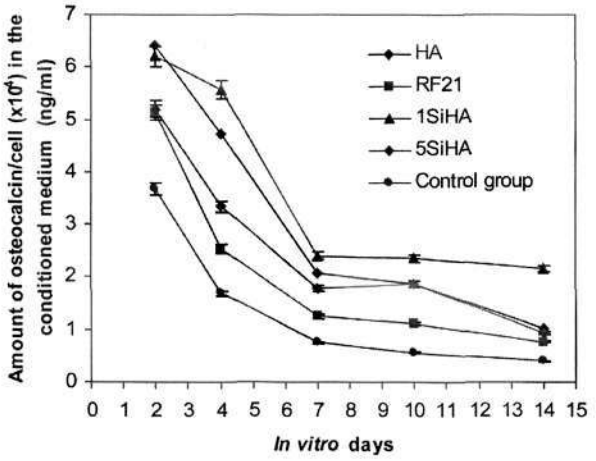

Figure 5. Effect of various HA based ceramic samples on osteocalcin production by osteoblasts at different culture periods. [Color figure can be viewed in the online issue, which is available at www.interscience.wiley.com.]

ID: srinivasanv Date: 19/4/07 Time: 18:38 Path: J:/Production/JBMB/Vol00000/070086/3B2/C2JBMB070086

J_ID: Z8H Customer A_ID: 30864 Cadmus Art: JBMB30864 Date: 19-APRIL-07 Stage: I Page: 5

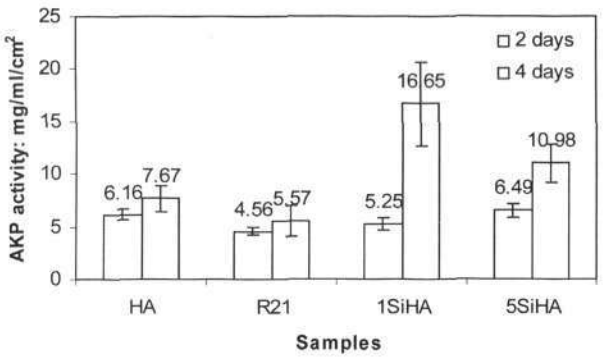

Figure 6. AKP activity is secreted into the culture medium by osteoblasts on various HA based ceramic samples at different culture periods. [Color figure can be viewed in the online issue, which is available at www.interscience.wiley.com.]

in the supernate after culturing for 2 days. Moreover, it was found that osteoblast differentiation is enhanced when compared with osteoblasts grown on the polystyrene surfaces. In addition, the osteocalcin production was slightly higher after culturing on the ceramic 1SiHA when compared with the results obtained from the other samples.

F6 Figure 6 shows the secretion of AKP into the culture medium from the various samples after culture for 2 and 4

F7 days. Figure 7 displays the influence of various samples on the AKP activity from the cell lysates. Similar amount of AKP on the various samples was secreted in the medium after culture for 2 days, as presented in Figure 6. It was observed that the AKP activity of the cells after 4 days of culture was higher than those of 2 days of culture. The highest AKP secretion after 4 days of culture was detected in the 1SiHA sample. As shown in Figure 7, significant difference in AKP activity was observed between HA and the culture plates. Moreover, the results from sample R21, 1SiHA, and 5SiHA showed relatively higher values when compared with the results from HA and the culture plate.

DISCUSSION

Osteoblasts are anchorage-dependent cells, and their morphology was determined by the properties of the substrates. The flattened appearances in the present study indicated a high affinity to the substrate surfaces. The more flattened cells would produce more collagen than those less flattened cells.

The initial point of contact between the cell and the substrate has been shown to be a random process that was largely determined by the distribution of adhesion proteins adsorbed onto the surface of the biomaterials.[9] Serum was known to contain the glycoproteins fibronectin and vitronectin, and these were known to adsorb onto the surfaces of biomaterials.[10] Furthermore, exclusion of these proteins from cell culture has been shown to cause a decrease in the total number of cellular attachments on biomaterials.[11] Cells used these proteins as anchoring points, which enabled them to attach to the substrate through extending filopodia, followed by the ''zipping-up'' of the cytoplasm between the filopodia to form flattened regions. Depending on the cell types, the filopodia developed from lamelliapodia would also provide cells a more defined direction to migrate.[12]

Cells interacted with the adsorbed proteins through membrane integral proteins (integrins) localized at the region of focal contacts. Integrins acted as signal transducers linking the extracellular matrix to the intracellular protein, in particular cytoskeleton actin (a protein in muscle) filaments forming stress fibers, which in return regulated cellular morphology and gene expression.

The recruitment of osteoblastic cells played a crucial role in osteogenesis (bone growth),[4] since the bone formation was mainly dependent on the number of osteoblastic cells rather than the osteoblast activity according to Marie.[13]

Though AKP is very sensitive and may display a high standard deviation, an increase of AKP expression was obviously obtained as the culturing period increased from 2 to 4 days, and relatively high AKP activity was obtained from the samples doped with silica, suggesting that the processed HA ceramic materials improved the functional activity of the bone-derived cells. However, the various HA-based biomaterials profoundly inhibited the osteocalcin expression. It is known that the type of substrate and the physicochemical features of the ceramic surfaced can determine which integrins and extracellular matrix proteins are expressed by osteoblasts providing information on how implant materials may affect osteoblast differentiation. It has been demonstrated that osteoblast-like cell behavior, such as cell attachment efficiency, spreading as well as cell migration, was also dependent on the material surface chemistry[10] and the concentration of Ca ions in the culturing medium.[14] Along with this postulation, the different level of ionic release observed would affect the cellular responses, such as the cell proliferation and differentiation.

The instability of β-TCP and even minor tetracaclium phosphate (TTCP), amorphous calcium phosphate phase

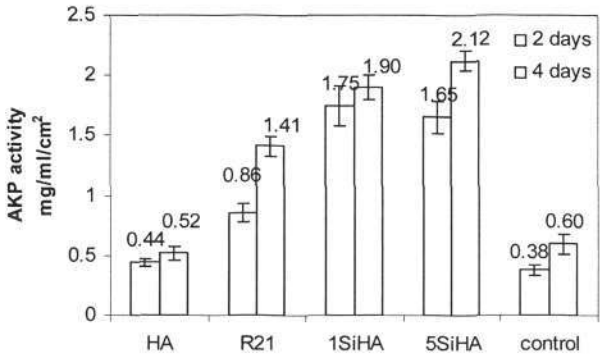

Figure 7. AKP activity is expressed by osteoblast cell layers on various HA based ceramic samples at different culture periods.

ID: srinivasanv Date: 19/4/07 Time: 18:38 Path: J:/Production/JBMB/Vol00000/070086/3B2/C2JBMB070086

J_ID: Z8H Customer A_ID: 30864 Cadmus Art: JBMB30864 Date: 19-APRIL-07 Stage: I Page: 6

(ACP), and CaO in the RF21 ceramic samples[6] was thought to be a factor that accelerated osteoconductivity and improved the chemical affinity and connectivity with the bone tissue *in vivo*.[14] Referred to the peaks intensities in XRD patterns, as shown in Figure 1, there were large amounts of β-TCP in RF21 samples. Also, β-TCP was detected in the silica doped apatite samples. The comparative dissolution behavior[15] of TTCP, HA, β-TCP, and ACP in increasing order is shown below:

$$\text{HA} < \beta\text{-TCP} < \text{CaO} < \text{TTCP} << \text{ACP}$$

In the present study, the dissolution of Ca ions from the ceramic surfaces resulted in an interfacial supersaturated condition with the already present Ca ions in the medium. The super-saturation of Ca ions consequently stimulated the proliferation of osteoblast[16] compared with the sample HA. The increased cell proliferation is often associated with enhanced differentiation through additional mechanism.[17]

However, excessively high solubility and reactivity of bioceramic surfaces may result in damage to adherent cells, which may correspondingly stimulate inflammatory responses in surrounding tissues.[14] It was showed that the proliferation and AKP activity of porcine osteoblasts *in vitro* were inhibited at a concentration higher than 7 m*M*.[18] The high solubility of the TTCP and TCP was found to be the dominant factor. They would decrease the viability of the cells by causing their rupture during initial anchoring phase. The failure of the initial attachment between the surrounding tissues and the implant materials might cause acute inflammation, and thus delay wound repair.

It has been reported that nucleation of bioacitve apatite around silicate-substituted HA was enhanced by increased dissolution of calcium and phosphate ions from the implant.[19] It was also important to emphasize the effect of silica on cell behaviors on these SPS biomaterials substrates. The presence of silicon played an important role during the bone mineralization processes.[20] It was a fundamental constituent of collagen and thus being an essential element in the formation the formation of collagen. The effects of orthosilicic acid on collagen type I synthesis have demonstrated the enhanced differentiation of osteoblastic cell lines exposed to orthosilicic acid. Other study has elaborated the role of silicon or silica in osteoblast function.[21] According to Sahai et al., at the near-neutral pH range of blood plasma, the planar Si three-ring was the active surface site on silica bioceramic.[22] The dissolution products from the silica bioceramic in the body fluid might be composed of hydrated silicon and calcium ions. The hydrated soluble silicon would enhance the proliferation of osteoblasts and active cellular production of transforming growth factors.[23,24] Thian et al.[23] reported that the released Si could have bound with oxygen, forming a silicate network structure on the surface, which might be capable of holding elements of the proteins together in an organized fashion, thus contributing to the architecture of connective tissue. It was possible that these proteins were adsorbed onto the bound silicate network, thus promoting better cell differentiation via the interaction with the intergrins on the osteoblast cells. Hing et al.[25] suggested recently that incorporation of silicate ions into the lattice of apatite may influence surface charge and wettability and highlighted the importance of surface chemistry on the interaction between proteins and cells with bioceramic surfaces at the early time points. Therefore, relatively high AKP activity and osteoclain expression was observed at the initial period of culturing. However, the exact ionic concentrations for the optimal cellular responses, especially the decreased osteocalcin expression over time is still unclear depending on cells used, culturing conditions, and ceramic structure, in terms of pore size and blend composition. In addition, the topography of the samples may also induce specific adsorption of proteins, which influenced cell interaction.[26] It is hypothesized that differences in various calcium phosphates in the ceramic samples lead to altered surface chemistries that are sensed by osteoblasts. At least by the greater degree of Ca^{2+} ion release from the biomaterials, the cellular responses are considered to be significantly affected. Thus a decrease of osteocalcin expression over time was detected by our studies, when compared to the increased AKP activity at the initial cell culture periods.

CONCLUSIONS

The osteoblast behaviors on the various HA based ceramic were investigated. The results of the flattened appearances of the cells indicated a high affinity of osteoblasts to the various substrate surfaces. Furthermore, our findings suggested that osteoblasts differentiated on all these HA based biomaterials, which was consistent with the ability of HA to support osteoblast attachment and promote bone formation within implants. It was also confirmed that osteoblast differentiation was enhanced when compared with the control group whose cells were directly cultured on the polystyrene surfaces. In addition, the presence of trace levels of silicon has helped to enhance the cell differentiation according to the AKP activity analysis. Possible reasons for this finding were mainly contributed to the combined effects of various calcium phosphate phases and silicate structures in the final SPS consolidated pellets.

REFERENCES

1. Loty C, Sautier JM, Boulekbache H, Kokubo T, Kim HM, Forest N. In vitro bone formation on a bone-like apatite layer prepared by a biomimetic process on a bioactive glass-ceramic. J Biomed Mater Res 2000;49:423–434.
2. Kikuchi M, Itoh S, Ichinose S, Shinomiya K, Tanaka J. Self-organization mechanism in a bone-like hydroxyapatite/collagen nanocomposite synthesized in vitro and its biological reaction in vivo. Biomaterials 2001;22:1705–1711.
3. Rea SM, Brooks RA, Best SM, Kokubo T, Bonfield W. Proliferation and differentiation of osteoblast-like cells on

ID: srinivasanv Date: 19/4/07 Time: 18:38 Path: J:/Production/JBMB/Vol00000/070086/3B2/C2JBMB070086

J_ID: Z8H Customer A_ID: 30864 Cadmus Art: JBMB30864 Date: 19-APRIL-07 Stage: I Page: 7

apatite-wollastonite/polyethylene composites. Biomaterials 2004; 25:4503–4512.
4. Hott M, Noel B, Didier BA, Rey C, Marie PJ. Proliferation and differentiation of human trabecular osteoblastic cells on hydroxyapatite. J Biomed Mater Res 1997;37:508–516.
5. Feng B, Weng J, Yang BC, Qu SX, Zhang XD. Characterization of titanium surfaces with calcium and phosphate and osteoblast adhesion. Biomaterials 2004;25:3421–3428.
6. Xu JL, Khor KA, Gu YW, Kumar R, Cheang P. Radio frequency (rf) plasma spheroidized HA powders: Powder characterization and spark plasma sintering behavior. Biomaterials 2005;26:2197–2207.
7. Ruys AJ. Silicon-doped hydroxyapatite. J Aust Ceram Soc 1993;29:71–80.
8. Black L, Garbev K, Beuchle G, Stemmermann P, Schild D. X-ray photoelectron spectroscopic investigation of nanocrystalline calcium silicate hydrates synthesized by reactive milling. Cem Concr Res 2006;36:1023–1031.
9. Annaz B, Hing KA, Kayser M, Buckland T, Disilvio L. Porosity variation in hydroxyapatite and osteoblast morphology: A scanning electron microscopy study. J Microsc 2004;215: 100–110.
10. Steele JG, Dalton BA, Underwood PA. The role of serum vitronectin and fibronectin in adhesion of fibroblasts following seeding on tissue culture polystyrene. J Biomed Mater Res 1992;26:861–884.
11. Howlette CR, Evans MD, Walsh WR, Johnson G, Steel JG. Mechanism of initial attachment of cells derived from human bone to commonly used prosthetic materials during cell culture. Biomaterials 1994;15:213–222.
12. Zhao Z, Rivkees SA. Rho-associated kinases play a role in endocardial cell differentiation and migration. Dev Biol 2004;275:183–191.
13. Marie PJ. Human endosteal osteoblastic cells: Relationship with bone formation. Calcif Tissue Int 1995;56:13–16.
14. Suzuki T, Hukkanen M, Ohashi R, Yokogawa Y, Nishizawa K, Nagata F, Lee B, Polak J. Growth and adhesion of osteoblast-like cells derived from neonatal rat calvaria on calcium phosphate ceramics. J Biosci Bioeng 2000;89:18–26.
15. Redey SA, Nardin M, Assolant DB, Rey C, Delannoy P, Sedel L, Marie PJ. Behavior of human osteoblastic cells on stoichiometric hydroxyapatite and type A carbonate apatite: Role of surface energy. J Biomed Mater Res 2000;50:353–364.
16. Gross KA, Berndt CC. Thermal processing of hydroxyapatite for coating production. J Biomed Mater Res 1998;39:580–587.
17. Shu R, McMullen R, Baumann MJ, McCabe LR. Hydroxyapatite accelerates differentiatin and suppresses growth of MC3T3-E1 osteoblasts. J Biomed mater Res A 2003;67: 1196–1204.
18. Eklou-Kalonji E, Denis I, Lieberherr M, Pointillart A. Effect of extracellular calcium on the proliferation and differentiation of porcine osteoblasts in vitro. Cell Tissue Res 1998;292:163–171.
19. Porter AE, Patel N, Skepper JN, Best SM, Bonfield W. Effect of sintered silicate-substituted hydroxyapatite on remodeling processes at the bone-implant interface. Biomaterials 2004;25: 3303–3314.
20. Carlisle EM. Silicon: An essential element for the chick. Science 1970;167:279–280.
21. Keeting PE, Oursler MJ, Wiegand KE, Bonde SK, Spelsberg TC, Riggs BL. Zeolite A increase proliferation, differentiation, and transforming growth factor b production in normal adult human osteoblast-like cells in vitro. J Bone Mineral Res 1992;7:1281–1289.
22. Sahai N, Tossell JA. Molecular orbital study of apatite ($Ca_5(PO_4)_3OH$) nucleation at silica bioceramic surfaces. J Phys Chem B 2000;104:4322–4341.
23. Thian ES, Huang J, Best SM, Barber ZH, Brooks RA, Rushton N, Bonfield W. The response of osteoblasts to nanocrystalline silicon-substituted hydroxyapatite thin films. Biomaterials 2006;27:2692–2698.
24. Kim HW, Kim HE, Salih V. Stimulation of osteoblast responses to biomimetic nanocomposites of gelatin-hydroxyapatite for tissue engineering scaffolds. Biomaterials 2005;26: 5221–5230.
25. Hing KA, Revell PA, Smith N, Buckland T. Effect of silicon level on rate, quality and progression of bone healing within silicate-substituted porous hydroxyapatite scaffolds. Biomaterials 2006;27:5014–5026.
26. Deligianni DD, Katsala ND, Koutsoukos PG, Missirlis YF. Effect of surface roughness of hydroxyapatite on human bone marrow cell adhesion, proliferation, differentiation and detachment strength. Biomaterials 2001;22:87–96.

ID: srinivasanv Date: 19/4/07 Time: 18:38 Path: J:/Production/JBMB/Vol00000/070086/3B2/C2JBMB070086

AQ1: Kindly check whether the short title is OK as given.

AQ2: Kindly check whether the edited sentence conveys the intended meaning.